Using Hi-Spots to investigate *in vitro* network dysfunction in Cysteine String Protein α knockout mice

Joanne Louise Bailey BSc (Hons)

A thesis presented for the degree of Doctor of Philosophy of the University of Southampton in the Faculty of Medicine, Health and Life Sciences School of Biological Sciences

September 2010

University of Southampton

Abstract

Faculty of Medicine, Health and Life Sciences
School of Biological Sciences

Doctor of Philosophy

Using Hi-Spots to investigate *in vitro* network dysfunction in Cysteine String Protein α knockout mice

Hi-Spot are highly re-aggregated neural cultures grown on PTFE membrane at the liquid-air interface. The Hi-Spot protocol was developed by scientists at Capsant Neurotechnologies using embryonic neural tissue. We characterised Hi-Spots made using existing protocols to confirm they represented a maturing neural network with molecular, cellular and functional signatures. We have additionally modified existing protocols to allow use of postnatal tissue as the source for dissociation and re-aggregation. Hi-Spots made from postnatal day zero (P0) rats self organised into a complex 3D tissue-like structure containing anatomically synaptically-interconnected neurons, astroglia and microglia. This CNS analogue of brain tissue provides for the emergence of a co-ordinated excitatory and inhibitory network, demonstrating a maturing pattern of activity involving single spikes developing into bursting behaviour driven by intrinsic synaptic activity. This activity can be represented as frequency or averaged amplitude (RMS), increases with time in culture and is blocked by glutamate receptor antagonists and stimulated by the inhibitory receptor antagonist bicuculline. The validity of its more *in vivo*-like organization, not observed in more conventional dissociated cultures, is evidenced by a glutamate toxicity resistance in the Hi-Spot cultures.

Further, the thesis describes the optimisations to the Hi-Spot protocol to allow viable high density re-aggregated cultures to be made from individual rather than pooled brain dissociations. Modifications to the protocol included dissociation of the mouse tissue using a protease papain kit and cell plating at an increased cell density.

Using this as a platform we have gone on to investigate the neuronal dysfunction occurring in Cysteine String Protein (CSP)α-/- mice. CSPα is a presynaptic protein thought to have co-chaperone like functions, mice lacking CSPα are born alive but show progressive weakness and neuronal degeneration soon after birth (Fernandez-Chacon, Wolfel et al. 2004). Hi-Spots formed from CSPα -/- tissue did not show overt neurodegenerative characteristics compared to +/+ controls and functional analysis demonstrated that at ~*DIV14* CSPα +/+ and -/- mice displayed equal levels of basal spontaneous network activity. Addition of bicuculline (50μM) to +/+ cultures lead to a significantly increased frequency and RMS value. However, in -/- cultures there was no increase induced by bicuculline. This may be due to an inability of CSPα -/- cultures to sustain high frequency synaptic transmission that is associated with bursting activity, or a selective degeneration of a sub-population of inhibitory neurons and a homeostatic network plasticity. The data suggest CSPα may act to protect the ability of neurons for high frequency synaptic transmission and/ or protect inhibitory neurons from degeneration.

Contents

List of figures

List of Tables

Acknowledgments

I would firstly like to thank my supervisors Vincent O Connor, John Chad, Thelma Biggs, and Hugh Perry and everyone at Capsant Neurotechnologies for their continuous support help and guidance.

I would like to acknowledge Lindsay Hewlett and Matthew Hannah for help with processing the electron microscopy samples, without their help the images would not have been such good quality. I would like to thank Katya Malfa for help processing the Arc:Arg 3.1 RTPCR and Matthew Findlay for writing the Matlab MEA analysis program. I would also like to thank John Chad for writing the Yorick MEA analysis program and test files, and scientists at Capsant Neurotechnologies for help feeding Hi-Spot cultures.

I would also like to thank Dr Shmma Quraishe who befriended me when I first started working in the lab and has been a continuous source of support ever since.

I would like to acknowledge Dr Deji Asuni, his passion for neuroscience was as much inspiring as it was overwhelming. Lastly I would like to thank my family who have always been helpful, understanding and supportive and I know my Dad would be very proud to see me finish my PhD.

Abbreviations

αGDP,	αGDP-dissociation inhibitor
2D,	Two Dimensional
3D,	Three Dimensional
AAA,	ATPase associated with different cellular activity protein
ACSF,	Artificial Cerebrospinal Fluid
ALS,	Amyloid Lateral Sclerosis
AMPA,	α- amino-3-hydroxy-5-methyl-4-isoxazole propionic acid
APS,	Ammonium Persulphate
Arc,	Activity Regulated Cytoskeleton Associated Protein
Arg 3.1,	Activity-Regulated Gene 3.1
BWSV,	Black Widow Spider Venom
CNQX,	6-Cyano-7-Nitroquinoxaline-2,3-Dione
CNS,	Central Nervous System
CSP,	Cysteine String Protein
D-APV,	D-amino-phosphovaleric acid
DC,	Direct Current
DG,	Dentate Gyrus
DIV,	Days In Vitro
E,	Embryonic
ECM,	Extracellular Matrix
EPSP,	Excitatory Postsynaptic Potential
FGF,	Fibroblast Growth Factor
GABA,	γ-Amino butyric acid
GAD,	Glutamate Decarboxylase
GC,	Granule Cell
GFAP,	Glial Fibriallary Acidic Protein
GPCR,	G-Protein Coupled Receptor
GRIP-1,	Glutamate-Receptor-Interacting- Protein-1
HPF,	High Pressure Freezing
Hsc70,	Heat Shock Cognate Protein 70kDa
HSP70,	Heat Shock Protein 70kDa
IEG,	Immediate-Early Gene
IHC,	Immunohistochemistry
MEA,	Multielectrode Array
mEPSC,	Miniature Excitatory Postsynaptic Potential
MF,	Mossy Fibres
mIPSC,	Miniature Inhibitory Postsynaptic Potential

MK801, (+)-5-methyl-10,11- dihydro-5*H*-dibenzo[*a*,*d*]cyclohepten-5,10-imine maleate
ML, Moleculare Layer
MNTB, Medial Nucleus of the Trapezoid Body
MP, Mulitphoton
NMDA, N-methyl-$_D$-aspartate
NMJ, Neuromuscular Junction
NR1, NMDA Receptor Subunit 1
NSF, N-ethylmaleimide- sensitive factor
O-LM, Oriens-Lacunosum Moleculare Cell
P, Postnatal
PBS, Phosphate Buffered Saline
PC, Pyramidal cell
PC, Pyramidal
PCR, Polymerase Chain Reaction
PFA Paraformaldehyde
PI, Propidium Iodine
PSD-95, Postsynaptic Density Protein 95kDa
RMS, Root Mean Squared
ROS, Reactive Oxygen Species
SDS, Sodium Dodecyl Sulphate
SEM, Standard Error Mean
SF, Serum Free
SGT, Small Glutamine-Rich Tetratricopeptide Repeat- Containing Protein
SL, Stratum Lacunosum
SLM, Stratum Lacunosum Moleculare
SM, sec-1p/Munc-18-1
SNAP-25, Synaptosomal-Associated Protein 25kDa
SNARE, Soluble NSF Attachment Protein Receptor
SO, Stratum Oriens
SR, Stratum Radiatum
TBS, Tris Buffered Saline
TC, Time Course
TEMED, N,N,N′,N′-Tetramethylethylenediamine
TGF-β1, Transforming Growth Factor- beta
UDV, User Defined Variable
V-ATPase, Vacuolar H+ ATPase
VCN, Ventral Cochlea Nucleas
VGAT, Vesicular GABA Transporter
VGLUT, Vesicular Glutamate Transporter

Declaration of Authorship

I, Joanne Louise Bailey declare that this thesis entitled "Using Hi-Spots to investigate *in vitro* network dysfunction in Cysteine String Protein α knockout mice" and the work presented in this thesis are my own, and have been generated by me as the result of my own original research. I confirm that:

- This work was done wholly or mainly while in candidate for a research degree at this University;
- Where any part of this thesis has previously been submitted for a degree or any other qualification at this University or any other institution, this has been clearly stated;
- Where I have consulted the published work of others, the source is always given. With the exception of such quotations, this thesis is my own work;
- I have acknowledged all main sources of help;
- Where the thesis is based on work done by myself jointly with other, I have made clear exactly what was done by others and what I have contributed myself;

Signed: …Joanne Louise Bailey.....

Date:……

1 - General Introduction

The brain is a complex organ. It is made up of anatomical regions that are precise three dimensional organisations of interconnected neuronal networks. Networks are made up of many cell-cell interactions. The neural cells that form the brain in higher and simpler organisms are highly organised in their localisation and function and made up of specialised neuronal cell subtypes (Tsien, Chen et al. 1996; Bargmann 1998). The nervous system allows coordinated responses to changes in the environment and controls an organism's behaviour (Chiel and Beer 1997; Markram, Toledo-Rodriguez et al. 2004).

Neuronal cells can be broadly divided into those with excitatory and inhibitory functions which co-operate in circuits to produce brain activity. Within this broad classification there are many different subtypes of neuronal cells which form intricate neuronal networks, and use their distinct functions to produce integrated activity (Freund and Buzsaki 1996; Somogyi and Klausberger 2005; Sterling and Matthews 2005). In particular the spatial and temporal organizations of their activity are key facets in producing integrated and complex neuronal signalling (Freund and Buzsaki 1996; Somogyi and Klausberger 2005; Bartos, Vida et al. 2007; Klausberger and Somogyi 2008).

Figure 1.1 depicts the different levels of brain organisation encompassing a complex structure containing many different anatomically defined regions, to a specific network formed of microcircuits. This depends on ensembles of cell-cell interactions mediated by the chemical signalling between synapses. Neuronal cells and synapses express specialisations of function; this can be seen at the gross level between excitatory and inhibitory synapses and at individual specialisations of different synapses. These specialisations in synaptic signalling impart an important sub-cellular refinement of neuronal control.

Synapses are formed of presynaptic and postsynaptic regions and are the structures at which neuronal cells communicate through the release of chemical neurotransmitters from the presynaptic compartment (Figure 1.4). There is a growing awareness that synaptic dysfunction and degeneration represent early events in neurodegenerative diseases such as Alzheimer's disease, Prion disease and Amyloid Lateral Sclerosis (ALS) (Frey, Schneider et al. 2000; Jeffrey, Halliday et al. 2000; Selkoe 2002; Cunningham, Deacon et al. 2003; Gutierrez, Hung et al. 2009). Further, neuronal dysfunction has been shown to be disrupted

in microcircuit and systems outputs which underpin pathology associated with major psychiatric diseases (Lewis, Hashimoto et al. 2005).

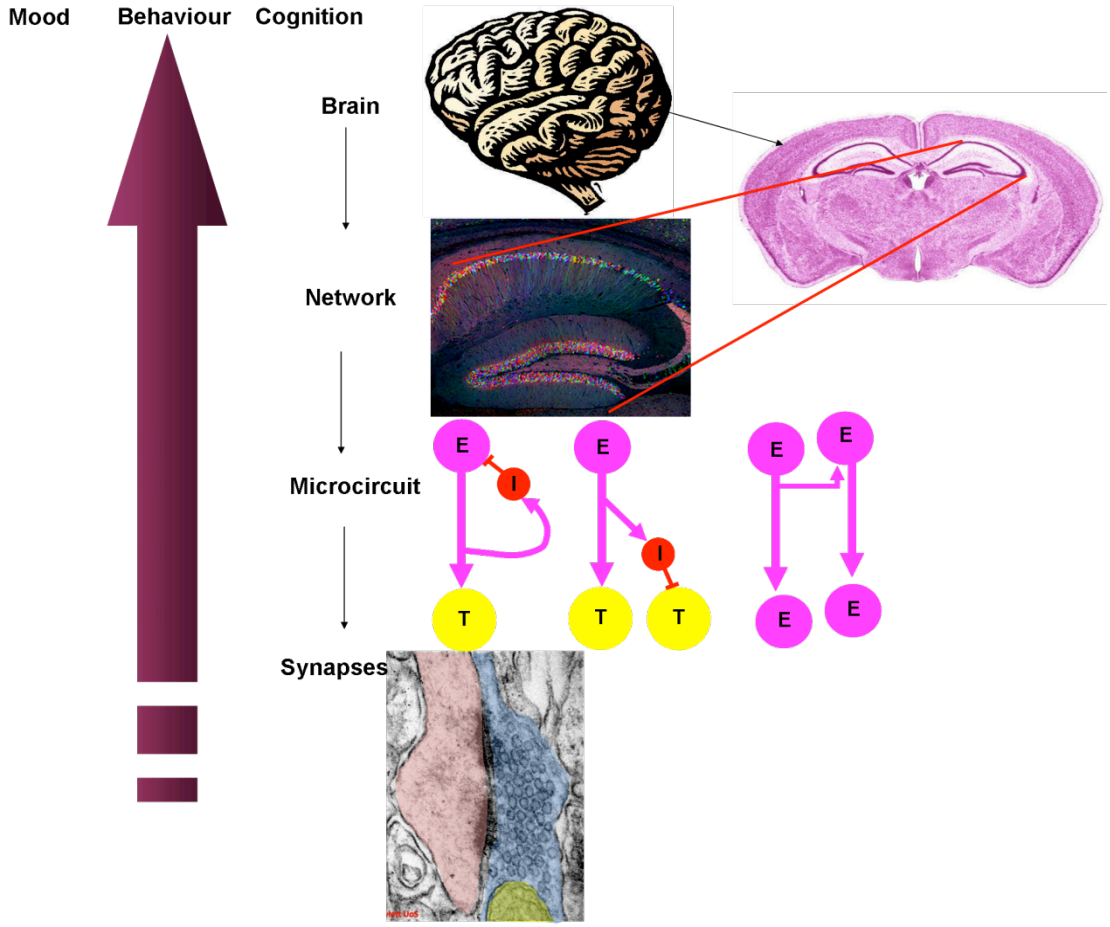

Figure 1.1: From the brain to the synapse
The brain is formed of different anatomical regions, such as the hippocampus. The distinct neuronal cell body layers of the hippocampus are shown in the transverse section of a mouse brain (Brainbow (Livet, Weissman et al. 2007)), and the anatomical location is shown in the cell body stained mouse brain (from mouse brain atlas). Distinct anatomical regions use common, core principles, of excitatory and inhibitory synapses forming distinct neuronal networks. In the case of the hippocampus, excitatory neurons connect the different sub-regions of the hippocampus (the dentate gyrus, CA3, CA2, and CA1), which are modulated by inhibitory interneurons (E-Excitatory neuron, T-Target neuron, I- inhibitory neuron). The schematics show feedback, feedforward and recurrent excitation. The neurons communicate with one another at synapses, which possess particular functional specialisations depending on the neuronal cell. The synapse is formed of a presynaptic (blue) and postsynaptic region (pink). The presynaptic region contains synaptic vesicles and an electron dense region, where vesicles fuse, the active zone. The postsynaptic synapse contains a postsynaptic density marked by the electron dense region. This region contains the acceptor receptors for the neurotransmitter released from the presynaptic synaptic vesicles. The neuronal heterogeneity of the brain produces complex regulation of the neuronal microcircuit and network which controls the brains activity and thus the behaviour of the organism.

1.1 Neurons

In the mammalian CNS excitatory neuronal cells mainly communicate using the neurotransmitter glutamate and inhibitory cells mainly use γ-Amino butyric acid (GABA). Inhibitory cells interact with other inhibitory and excitatory neurons to control neuronal activity and shape network activity in ways shown in figure 1.1. In the hippocampus at least 16 different types of inhibitory cells have been identified according to their, target innervation sites, electrophysiological properties and expression of specific marker proteins (Freund and Buzsaki 1996; Somogyi and Klausberger 2005; Klausberger and Somogyi 2008; Klausberger 2009) (Table 1.1). There are also many different types of glutamatergic excitatory neuronal cells with intrinsic functional specialisations in key aspects of their core function, consisting of Ca^{2+} stimulated vesicle exocytosis, retrieval of the synaptic vesicle proteins and membrane lipids by endocytosis, and post synaptic detection and downstream signalling (Stevens and Williams 2000; Wang, Lu et al. 2003; Sudhof 2004; Rodriguez-Contreras, van Hoeve et al. 2008; Jarsky, Tian et al. 2010). Subtypes of neuronal cells are seen in the simplest organisms but manifest with increasing complexity in higher organisms (Hall and Russell 1991; Schuske, Beg et al. 2004; Klausberger and Somogyi 2008). Examples of neuronal subtypes which permit fast, slow, and tonic activity and their associated specialisations will be reviewed in subsequent sections (Section 1.6).

1.1.1 Inhibitory neuron diversity

GABAergic neurons constitute a morphologically highly heterogeneous population of neuronal cells this is exemplified by neocortical cells (Somogyi and Klausberger 2005; Klausberger and Somogyi 2008). Table 1.1 lists examples of interneurons and their innervation sites on their target cells and the protein or peptide markers that have been used to distinguish these cells. Figure 1.2 depicts the axonal innervation regions and dendritic projections of the basket cells, bistratified cells and O-LM cells in relation to the glutamatergic excitatory pyramidal cell in the CA1 (for review see Freund (1996) and Klausberger (2009), (Freund and Buzsaki 1996; Klausberger 2009).

Name	Innervation site	Marker
Basket cells	Soma (perisomatic region)	PV or CCK
Chandelier or axo-axonic cells	Axon initial segment	PV
Bistratified cells	Dendrites	PV, SOM. NPY
O-LM	Stratum Lacunosum-moleculare	SOM
Trilaminar	Dendrites	CB- negative
Shaffer collateral associated cell	Apical Dendrites	CCK CB

Table 1.1: Different interneurons, innervation sites and marker proteins
Different interneurons innervate different target areas of the postsynaptic neuron. The diversity of inhibitory neurons likely contributes to distinct functions in the regulation of network activity.
PV= Parvalbumin, SOM=Somatostatin, NPY= Neuropeptide Y, CB= Calbindin, CCK= Cholecystokinin. Adapted from Peter Somogyi et al 2005 (Somogyi and Klausberger 2005)

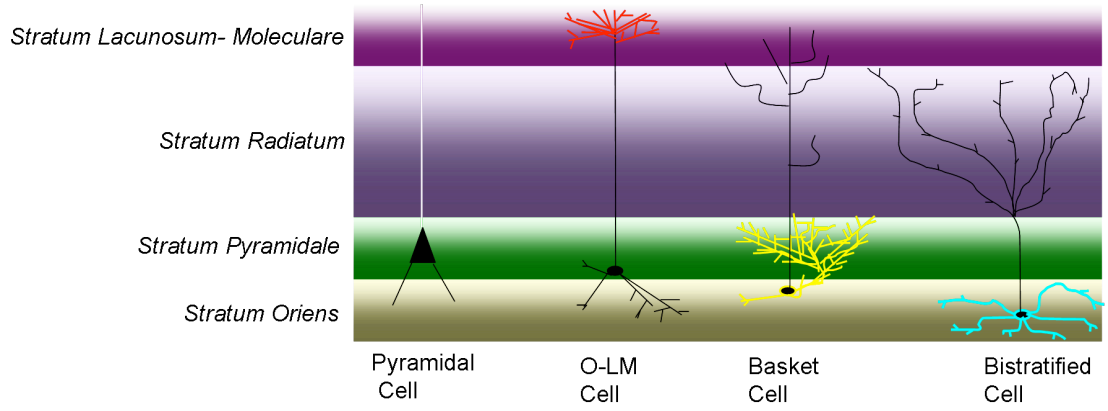

Figure 1.2: Interneuron innervation sites in the CA1 of the hippocampus
The axonal projections of the interneurons are coloured red, yellow and blue. The dendritic processes are coloured black. The diagram shows the innervation sites of the interneurons onto the excitatory pyramidal cell. Adapted from: (McBain and Fisahn 2001; Somogyi and Klausberger 2005; Klausberger and Somogyi 2008; Klausberger 2009)

Neuropeptides have been shown to act as important regulators of neuronal activity and modulate the core function of synaptic transmission via activation of G-protein coupled receptors (GPCR) (reviewed in (Baraban and Tallent 2004; Salio, Lossi et al. 2006). Interneurons inhibit target cells by hyperpolarizing the membrane of target cells controlling the discharge rate and timing of action potentials, which can modulate the number of cells that participate in population activity (Miles, Toth et al. 1996). Interneurons have a pivotal role in the microcircuitry participating in feedforward and

feedback inhibitory mechanisms. These properties coordinate the outputs of ensembles of neurons to generate oscillatory network rhythms. These rhythms occur at different frequencies and distinct types are associated with different behaviours including sleep rapid eye movement and exploratory behaviour (Table 1.2). Altered interneuronal heterogeneity has been shown to be a common mechanism contributing to various neurological and psychiatric disorders (Levitt, Eagleson et al. 2004; Santhakumar and Soltesz 2004; Takahashi, Brasnjevic et al. 2010) (Section1.9).

Rhythm	Frequency Hz	Associated Behaviour	Reference
Theta	3-8	• Exploratory activity, and REM	(Buzsaki 2002; Cantero, Atienza et al. 2003; Csicsvari, Jamieson et al. 2003)
Beta	12-30	• Exploration of novel environments	(Berke, Hetrick et al. 2008)
Gamma	30-80	• Exploratory activity, and REM • Work and episodic memory task	(Csicsvari, Jamieson et al. 2003; Fuchs, Zivkovic et al. 2007)

Table 1.2: Oscillatory activity in the hippocampus
REM- rapid eye movement sleep

1.2 Glial cells

Neuronal cells in the brain are supported by glial cells. Glial cells such as astrocytes and microglial have been shown to respond to changes in the neuron network activity and health, and maintain homeostasis of the extracellular environment.

1.2.1 Astrocytes

Astrocytes are the most numerous cells in the Central Nervous System (CNS) (Ullian, Christopherson et al. 2004). An important aspect of their function is the interaction with the presynaptic and postsynaptic compartment to form a tripartite synaptic structure (Araque, Parpura et al. 1999; Barres 2008; Perea, Navarrete et al. 2009). Astrocytes are important for neuronal health and serve many house keeping functions from maintenance of the extracellular environment to regulating the development and stabilisation of cell-cell communications in the CNS (Figure 1.3) (Ullian, Sapperstein et al. 2001; Ullian, Christopherson et al. 2004).

In the mature nervous system, astrocytes modulate neuronal activity by both uptake of extracellular glutamate (Rothstein, Van Kammen et al. 1995; Rothstein, Dykes-Hoberg et al. 1996; Tanaka, Watase et al. 1997) and by release of gliotransmitters, such as ATP and glutamate (Araque, Li et al. 2000; Newman 2003; Jourdain, Bergersen et al. 2007). Intimate cell-cell interactions between neuronal and glial cells are needed to maintain neuronal viability during high levels of extracellular glutamate (Choi, Maulucci-Gedde et al. 1987; Rosenberg and Aizenman 1989).

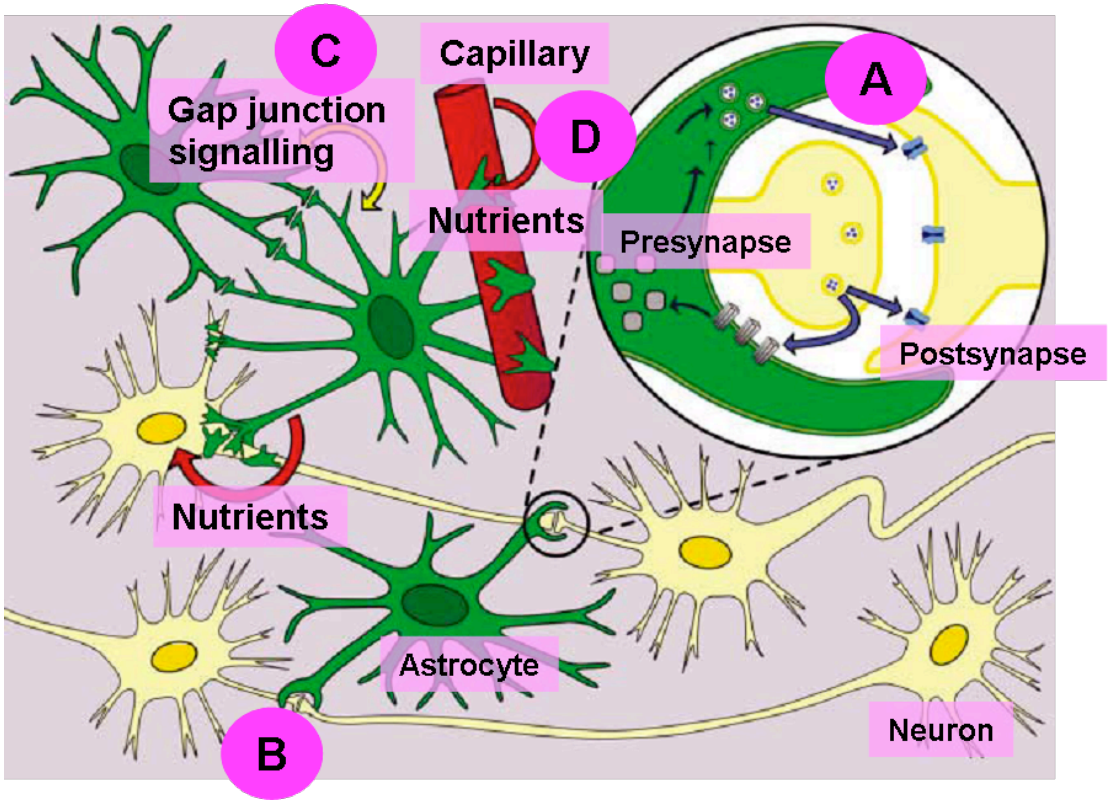

Figure 1.3: Astrocyte functions
Astrocytes make contacts with neurons (A) and capillaries (D) and shuttle nutrients between the blood supply and the active neuronal cells. A single astrocyte can contact many neuronal cells (B). A tripartite structure is formed between astrocyte processes and the neuronal synapse (A), the astrocytes are intimately associated with the neuronal synapse and can take up and release neuronal neurotransmitters. Astrocytes communicate together in a network formed by gap junction links (C). Astrocytes green, Neurons yellow. Adapted from:(Kurosinski and Gotz 2002)

In addition to directly modulating the signalling that underpins neuronal activity astrocytes form networks connected together by gap junctions. These allow the non-neuronal networks to direct communication through the propagation of intracellular calcium waves

(Salter and Hicks 1995) and have been implicated to function in mature brain oscillatory activity (Verderio, Bacci et al. 1999; Parri and Crunelli 2001).

1.2.2 Microglial cells

Microglial cells are the resident macrophages of the CNS and one of the main functions of the microglial cells is to monitor the health of the neuronal population (Butovsky, Talpalar et al. 2005; Lalancette-Hebert, Gowing et al. 2007). Neuronal and microglial cells are able to communicate with one another using expression of certain neuronal membrane proteins which have complementary receptors on microglial membranes (Hoek, Ruuls et al. 2000; Honda, Sasaki et al. 2001; Cardona, Pioro et al. 2006). Neurons release neurotransmitter and secrete chemokines and cytokines can also act to stimulate either pro-inflammatory or anti-inflammatory microglial cell responses and can lead to microglial chemotaxis towards the signalling neuronal cells (Rappert, Bechmann et al. 2004).

1.2.3 Oligodendrocytes

Oligodendrocytes are specialised glial cells that ensheath axons in the white matter of the Central Nervous System (CNS) and spinal cord to aid rapid salutatory impulse propagation. Oligodendrocytes also maintain long-term functional integrity of neuronal axons and are necessary for the functional clustering of sodium channels at nodes of ranvier along the axon (Dupree, Mason et al. 2004; Kassmann and Nave 2008). The importance of oligodendrocytes can be seen by the numerous human neurological diseases that are caused primarily by dysfunction of myelinating glial cells in the CNS (reviewed in (McTigue and Tripathi 2008) and (Nave and Trapp 2008).

1.2.4 Reactive response of glial cells

Astrocytes and microglial cells also respond to injury in the central nervous system. The astrocytic response to injury is referred to as an astrogliosis and changes in the intermediate filament protein, glial fibrillary acid protein (GFAP) are used as a marker for astrogliosis (Kunkler and Kraig 1997).

The functions of astrogliosis can be both beneficial and deleterious to neuronal cells (Barres 2008). The breakdown or dysfunction of key astrocyte functions such as

maintaining extracellular K^+ homeostasis, glutamate uptake from the synaptic clefts and astrocyte contribution to the glutamine shuttle can result in neuronal dysfunction (Janigro, Gasparini et al. 1997; Bacci, Sancini et al. 2002). In Amyotrophic Lateral Sclerosis (ALS) decreased expression of the astrocytic glutamate transporter GLT-1 is thought to contribute to a glutamate induced neurotoxicity that contributes to motor neuron loss (Rothstein, Van Kammen et al. 1995; Maragakis and Rothstein 2006).

Microglial cells have been shown to be activated in response to brain injury. Upon activation the microglia change their morphology to become more rounded, which is described as amoeboid (Giordana, Attanasio et al. 1994). As discussed above, microglial cells can release pro-and anti-inflammatory mediators depending on the stimulus. Microglia cells may contribute to neuronal cell damage by releasing reactive oxygen species (ROS) (Qin, Liu et al. 2002; Mander and Brown 2005).

1.3 Neuronal communication

All neuronal cells communicate using the same core mechanism; electrical action potential stimulation leads to transmitter release and transmission of the signal to neuronal cells. The transmission of the chemical signals occurs at sub-compartments called synapses. The release of neurotransmitters from nerve endings is highly complex and tightly regulated, involving specific and sequential interactions of a large number of neuronal proteins (Fernandez-Chacon and Sudhof 1999; Sudhof 2004; Jahn and Scheller 2006; Rizo and Rosenmund 2008). However, despite the complexities involved in exocytosis neurotransmitter release can occur within less than 100μs of the nerve terminal depolarisation and calcium entry (Burgoyne and Morgan 1995).

Synapses are modified tight junction- like structures that appear as two juxtaposed functional components, the presynaptic terminal and the postsynaptic terminal in electron microscopy. Figure 1.4 shows electron microscopic images of presynaptic and postsynaptic specialisations from excitatory and inhibitory neuronal synapses in the murine hippocampus.

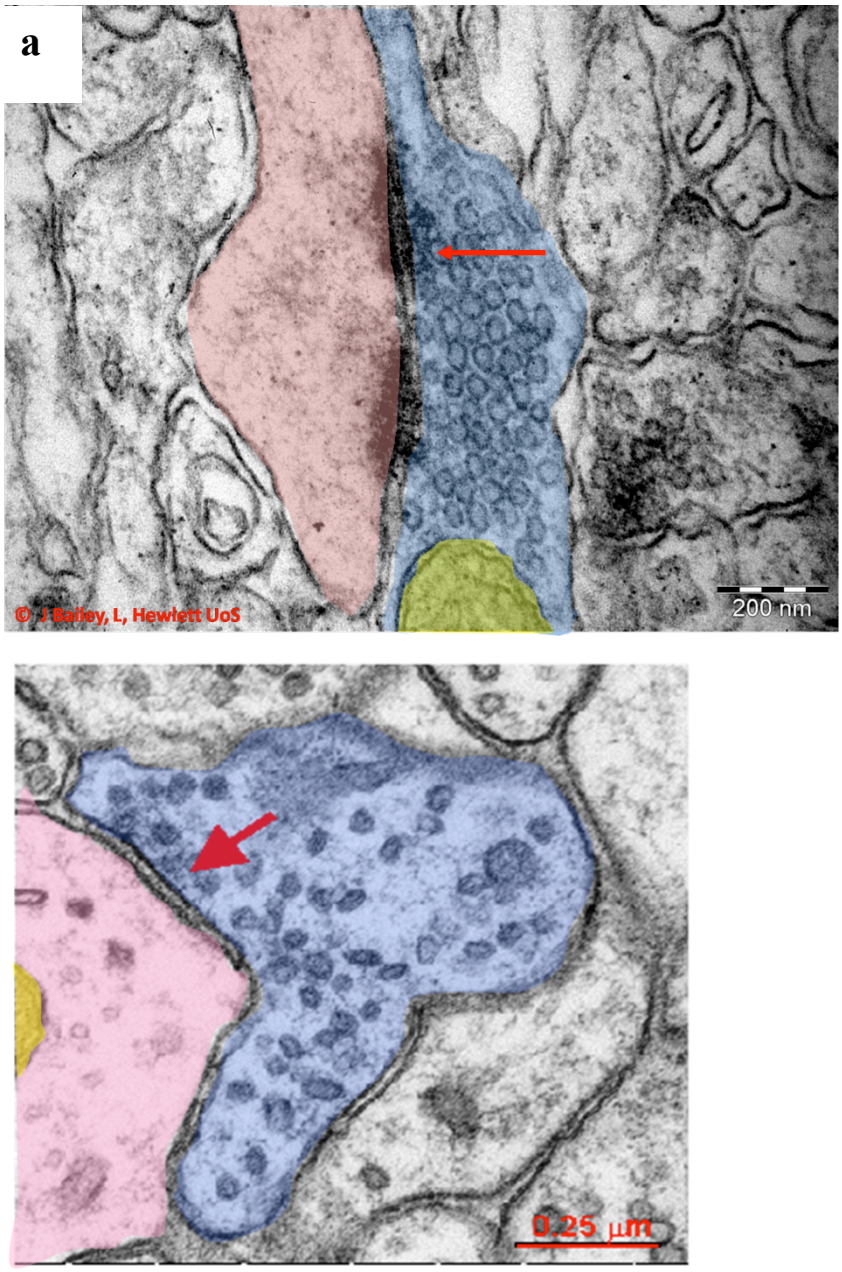

1.4: Excitatory and inhibitory synapses can be distinguished structurally
n asymmetric glutamatergic excitatory synapse
symmetric GABAergic inhibitory synapse

In both images the presynaptic compartment is shaded blue and the arrow marks the active zone. The presynaptic compartment contains synaptic vesicles (approx 50nm diameter) and mitochondria shaded yellow. The postsynaptic compartment is shaded pink and contains an electron dense region, the postsynaptic density**.**
In the excitatory synapse (a) the postsynaptic density appears as a highly electron dense structure opposite regularly shaped vesicles positioned close to the active zone in the presynaptic compartment. In the inhibitory synapse (b) the electron dense region in the postsynaptic density is less pronounced and the postsynaptic membrane parallels the presynaptic active zone. In the presynaptic compartment the synaptic vesicles appear flattened. Symmetric synapse picture is taken from a image on 'synapse web' http://synapses.clm.utexas.edu/

The excitatory asymmetrical synapse can be distinguished from the inhibitory symmetrical synapse due to the differential electron dense proteinacous region which harbours the array of molecular components that make the presynaptic and postsynaptic specialisations, the active zone and postsynaptic density, respectively. Fusion of transmitter filled vesicles presynaptically at the active zone leads to neurotransmitter release into the synaptic cleft (~20nm) and its diffusion to the postsynaptic site. After exocytosis the synaptic vesicles undergo endocytosis, recycling and are refilled with neurotransmitter so that vesicle stores can be replenished (Sudhof 2004).

The postsynaptic compartment contains the effector receptors complementary to the released neurotransmitter. These core features of vesicle fusion and postsynaptic reception are reiterated at each type of synapse but there are striking degrees of specialisation. In the case of excitatory and inhibitory synapses these modified specialisations are observable at the microscopic level (Figure 1.4). Aspects of these specialisations and their relation to function are discussed in section 1.6.

1.3.1 Presynaptic compartment and exocytosis

The presynaptic compartment is the site of neurotransmitter exocytosis from synaptic vesicles. Synaptic vesicles are specialised organelles that store neurotransmitters and release their contents in quantal packets into the synaptic cleft (Katz 1971). In response to membrane depolarisation the Ca^{2+} channels which selectively accumulate in the presynaptic active zone provide a localized influx of Ca^{2+}. This increased intracellular calcium concentration triggers synaptic vesicles to fuse with the presynaptic active zone. Regulated neurotransmitter release is accomplished by coupling nerve activity and exocytosis on a sub-millisecond time scale dependent on the highly organized voltage activated calcium channels. As these open, the increase in intracellular calcium increases to 10-100μM in a limited sub-domain initially described as a microdomain (Chad and Eckert 1984), but in some synapses exists as more discrete nanodomains (Bucurenciu, Kulik et al. 2008)

1.3.2 Synaptic vesicles

Synaptic vesicles are highly specialised organelles, at least nine classes of transmembrane proteins are localised to synaptic vesicles (Sudhof 2004; Chua, Kindler et al. 2010). These

proteins are involved in, neurotransmitter loading, and storage, and synaptic vesicle trafficking. Neurotransmitter loading in glutamatergic synapses requires the vesicular glutamate transporters (VGLUTs) (Wojcik, Rhee et al. 2004), and the vesicular GABA transporter (VGAT) in inhibitory synapses (Chaudhry, Reimer et al. 1998; Jin, Wu et al. 2003). The transporters require an electrochemical proton gradient maintained by the vacuolar H^+ ATPase (V-ATPase) (Step 9 Figure 1.5). Trafficking proteins include the soluble NSF attachment protein receptor (SNARE) synaptobrevin and synaptotagmin. Synaptic vesicles also contain the transmembrane protein synaptophysin and synaptic vesicle protein 2 (SV2) (Abraham, Hutter et al. 2006; Yao, Nowack et al. 2010).

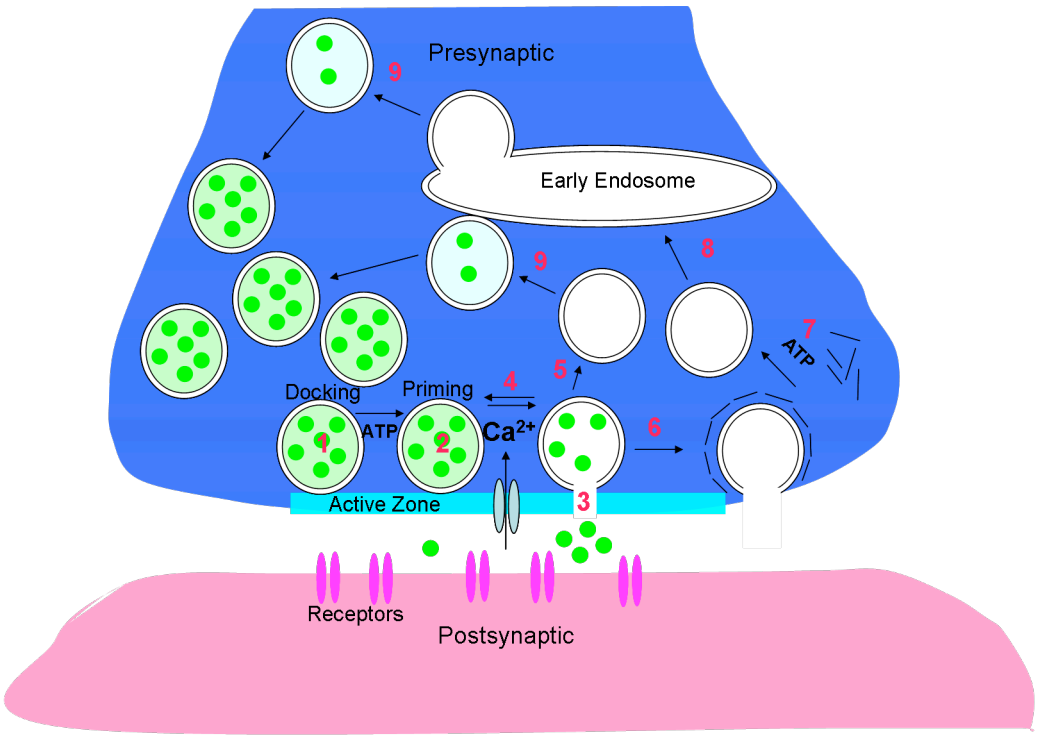

Figure 1.5: The synaptic vesicle cycle
The synaptic vesicle cycle is depicted as a series of steps from vesicle docking to reloading of the vesicles with neurotransmitter. Step 1, vesicle docks with the presynaptic membrane at the active zone, Step 2, vesicle is primed to a fusion ready state, Step 3, vesicle membrane fusion with the plasma membrane. The vesicle can then be reused for multiple rounds of endocytosis, this is proposed to occur by at least 3 different mechanism, Step 4, Kiss and stay, the vesicles remains at the active zone and is reloaded with neurotransmitter and re-primed for fusion, Step 5, kiss and run, the vesicle does not loss its lipid identity and does not fully fuse with the plasma membrane, and is reloaded with neurotransmitter away from the plasma membrane. Step 6, full vesicle fusion, and clathrin mediated endocytosis, Step 7, which follows clathrin mediated endocytosis, is clathrin uncoating, the vesicle can then either be directly re-loaded with neurotransmitter (Step 9) or Step 8, pass through an early endosome intermediate. Adapted from Sudhof 2004.

To explain the function of synaptic vesicles and the protein-protein interactions involved it is easiest to start with synaptic vesicle membrane fusion, as many of the protein-protein interactions are centred around this step. Figure 1.5 shows the steps of vesicle exocytosis in order from docking to reloading the vesicle with neurotransmitter. The figure greatly simplifies the cycle, and does not show any of the complex protein-protein interactions that occur.

1.3.3 Synaptic vesicle fusion with the plasma membrane

The final step of vesicle exocytosis is vesicle membrane fusion with the plasma membrane (Step 3 in Figure 1.5). Fusion of the two membranes occurs within microseconds of calcium entry into the synaptic cleft and is mediated by a set of highly conserved proteins the SNARES. The SNARE complex at the synapses is made of a collection of four α-helices, one of the α-helices is contributed by the vesicle SNARE protein synaptobrevin and the other three α-helices are contributed by the t-SNAREs, SNAP25 (synaptosomal-associated protein of 25kDa) and syntaxin, of which SNAP25 donates two α-helices and syntaxin donates one (Rizo and Rosenmund 2008)(Lonart and Sudhof 2000). These α-helical regions are called the SNARE domains and their membrane localisations are depicted in figure 1.6.

The four α-helical SNARE domains have two conformations, *trans* and *cis*. The α-helical *trans* configuration of the SNARE proteins results in the close association of the vesicle and plasma membrane (Figure.1.6) (Sutton, Fasshauer et al. 1998). Upon vesicle fusion the SNARE conformation changes to *cis* configuration and the SNARE proteins appear in the same membrane as the vesicle membrane and the plasma membrane fuse.

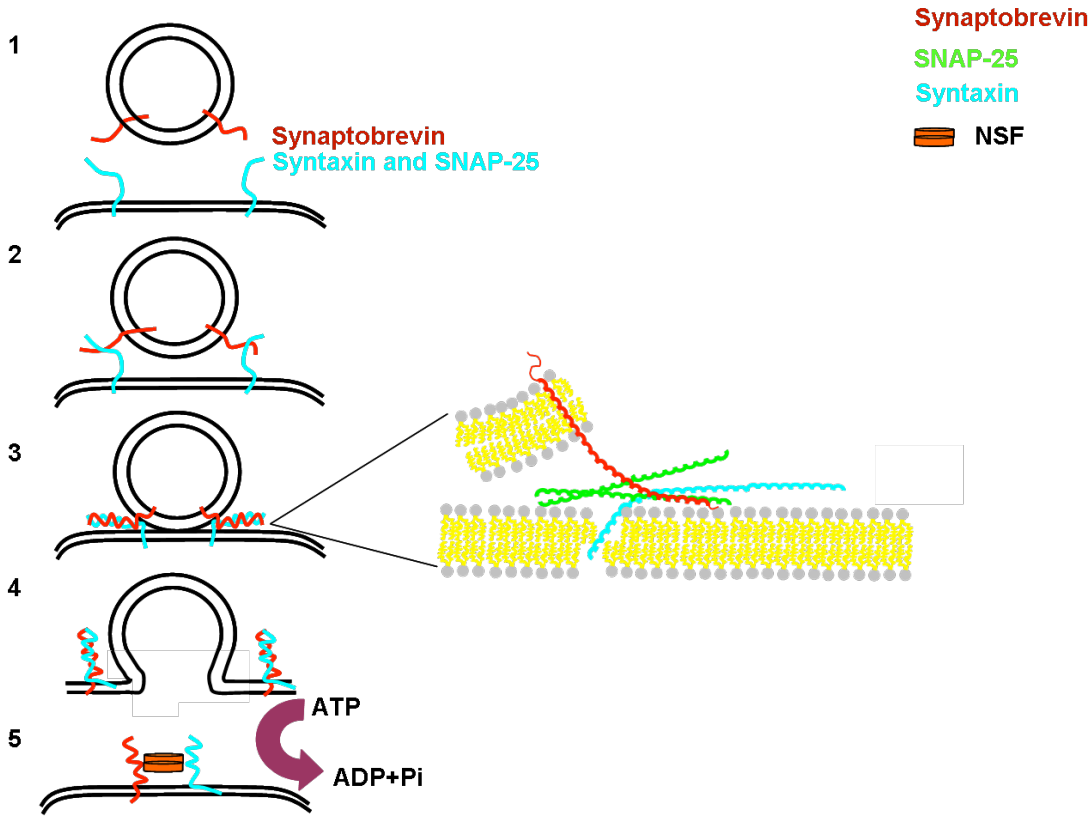

Figure 1.6: Vesicle fusion and neurotransmitter exocytosis
The synaptic vesicle SNARE protein synaptobrevin comes together with the plasma membrane SNARE proteins, syntaxin and SNAP-25, to aid the energetically unfavourable fusion of the vesicle and plasma membrane lipid bilayers (Rizo and Rosenmund 2008). After vesicle exocytosis the SNARE proteins require unfolding so that they can undergo multiple rounds of exocytosis. SNARE unfolding is catalysed by the ATPase activity of NSF.

The selective targeting of these proteins by the protease activity of clostridial neurotoxins has proved their importance for neurotransmitter release (Chen, Scales et al. 1999; Chen, Scales et al. 2001). However, the rate of SNARE only mediated fusion *in vitro* is very low compared to the rate of vesicle fusion at the synapse (Weber, Zemelman et al. 1998), suggesting that other protein-protein interactions co-operate to facilitate the fusion (Sabatini and Regehr 1996). Protein-protein interactions between the t-SNAREs syntaxin and SNAP25 and the presynaptic protein synaptotagmin have been shown (Chapman, Hanson et al. 1995; Schiavo, Stenbeck et al. 1997; Gerona, Larsen et al. 2000; Fernandez-Chacon, Konigstorfer et al. 2001; Zhang, Kim-Miller et al. 2002). Calcium has been shown to increase these interactions (Tucker, Weber et al. 2004).

Synaptotagmin proteins have an N terminal region, a variable linker region and two C-terminal C2 domains, C2A and C2B, which bind calcium and phospholipids (Ubach, Zhang et al. 1998; Zhang, Rizo et al. 1998; Davis, Bai et al. 1999). Support for synaptotagmin's role in calcium sensing and facilitation of vesicle fusion have been shown by mutations that result in incremental changes in the affinity of synaptotagmin for calcium, which parallel the incremental change in calcium dependence of release (Fernandez-Chacon, Konigstorfer et al. 2001). It has been proposed that synaptotagmin facilitates synaptic vesicle fusion in a calcium dependent manner by promoting SNARE α-helical domain zippering to form the 4 α- helix bundle.

Other proteins have been proposed to function as calcium sensors in promoting SNARE α-helical zippering. These include Rim, Rabphilin and Complexin which is proposed to interact with SNARE complexes and align SNARE complex for efficient fusion (Shirataki, Kaibuchi et al. 1993; Wang, Okamoto et al. 1997). This is supported by investigations on Complexin knockout mice which demonstrated reduced neurotransmitter release efficiency paralleled with reduced calcium sensitivity (Reim, Mansour et al. 2001), (discussed further below).

1.3.4 Priming of synaptic vesicles at the presynaptic membrane

The short latency between the presynaptic nerve terminal calcium entry and neurotransmitter release suggests that there is a population of synaptic vesicles at the presynaptic active zone 'primed' for fusion (Figure 1.5 Step 2). Vesicle priming events are thought to be ATP-dependent steps that render vesicles competent for calcium triggered-fusion (Verhage and Sorensen 2008). At the molecular level vesicle priming is thought to occur through interactions of the SNARE proteins in the *trans* confirmation (Lonart and Sudhof 2000; Rizo and Rosenmund 2008). This is supported by increases in SNARE complexes in the '*trans'* confirmation increasing the number of primed fusion capable vesicles (Lonart and Sudhof 2000).

The regulation of synaptic vesicle priming and release has been shown to be dependent on more than the SNARE proteins and synaptotagmin. Munc-18-1 is a hydrophilic arc shaped protein, initially identified due to its strong binding to syntaxin (Hata, Slaughter et al. 1993). Munc18-1 was shown to bind strongly to syntaxin in its 'closed' formation (Misura,

Scheller et al. 2000). In addition to syntaxins SNARE domain, characteristic of all SNARE proteins, syntaxin has an N-terminal 3 helix bundle called the Habc domain, which folds back onto the SNARE motif and intramolecularly occludes the SNARE domain needed to form the SNARE complex with synaptobrevin and SNAP25. The closed formation of syntaxin is likely to be important for preventing re-assembly of the SNARE complex after disassembly by NSF and SNAP (Rizo and Rosenmund 2008). The interaction between Munc18 and 'closed' syntaxin was originally believed to function to block SNARE complex assembly but knockout studies revealed that Munc18 is essential for vesicle fusion (Weimer, Richmond et al. 2003).

Munc18 was later shown to also bind-to, and interact with, the assembling SNARE complex, containing syntaxin and SNAP25 heterodimers (Dulubova, Khvotchev et al. 2007; Guan, Dai et al. 2008; Weninger, Bowen et al. 2008) leading to the hypothesis that the Munc18- syntaxin complex is an intermediary in the pathway to SNARE complex assembly and the docking and stable association of the vesicle with the plasma membrane (de Wit 2010). A pathway in which Munc 18 is able to bind to the 'closed' and 'open' form of syntaxin, and release of the SNARE motif from the 'closed' syntaxin to bind SNAP25 (likely assisted by Munc13, discussed below), results in the formation of a acceptor complex for the vesicle SNARE protein synaptobrevin. The role of Munc18 is also likely to prevent unwanted interactions between the promiscuous SNARE motifs of syntaxin and SNAP25 (Pobbati, Stein et al. 2006; Sorensen, Wiederhold et al. 2006; Rizo and Rosenmund 2008; Burgoyne, Barclay et al. 2009; Deak, Xu et al. 2009).

1.3.5 Complexin and synaptotagmin

Complexin is a small soluble protein which inserts an antiparrallel α- helix into the groove of the four helix bundle of the SNARE complex (Chen, Tomchick et al. 2002). In mice deletion of Complexin has been shown to impair fast Ca^{2+} stimulated exocytosis but not vesicle fusion in general, having no effect on spontaneous release (Reim, Mansour et al. 2001). Addition of excess Complexins has also been shown to inhibit exocytosis (Giraudo, Eng et al. 2006; Schaub, Lu et al. 2006), leading to the idea that Complexin functioned as a fusion clamp, but this did not support the mouse knockout studies showing that Complexins are facilitators of fast Ca^{2+} dependent vesicle exocytosis (Reim, Mansour et al. 2001). A more recent investigation provides a unifying explanation for these two

observations and suggests that Complexin and synaptotagmin compete for binding to SNARE complexes. Synatotagmin is 40 fold more potent at displacing Complexin from the SNARE complexes than Complexin is at displacing synaptotagmin. The hypothesis follows that Complexins are able to activate synaptic vesicle and plasma membrane SNARES into a primed state, whilst inhibiting full SNARE complex formation and vesicle fusion. Upon nerve terminal depolarisation and Ca^{2+} influx synaptotagmin binds Ca^{2+} and binds the SNARE complex and the plasma membrane displacing Complexin and promoting vesicle fusion. Thus Complexin still acts as a fusion clamp but only on formed (activated) SNARE complexes (Tang, Maximov et al. 2006; Rizo and Rosenmund 2008).

1.3.6 Docking of synaptic vesicles at the presynaptic membrane

Docking is the stable association of the vesicle with the plasma membrane (Figure 1.5 Step 1). The spatial specificity of docking at the presynaptic active site suggests that it is regulated by mechanisms that mediate attachment of the vesicles to this region. Of all the steps in synaptic vesicle exocytosis the protein-protein interactions that mediate docking of the synaptic vesicles are the least well defined. Munc 13 has been shown to be essential for synaptic vesicle fusion, as synapses lacking Munc 13 are entirely devoid of fusion competent vesicles and are complete unable to execute spontaneous or evoked synaptic vesicle fusion (Varoqueaux, Sigler et al. 2002). Initial electron microscopy studies showed no loss of docked synaptic vesicles at the active zone (Varoqueaux, Sigler et al. 2002), which led to the conclusion that the function of Munc 13 was downstream of vesicle docking. However, recent studies which do not employ aldehydes for electron microscopy fixation but use high pressure freezing (HPF) have revealed a docking deficit in Munc 13 mutants and in syntaxin mutants, suggesting that Munc 13 and the SNARE protein syntaxin are important for vesicle docking (Weimer, Gracheva et al. 2006; Hammarlund, Palfreyman et al. 2007; Siksou, Varoqueaux et al. 2009).

The protein Munc 18 has been implicated in docking (Weimer, Richmond et al. 2003), but conflicting results have been shown in CNS synapses and chromaffin cells of Munc 18 null mice (Voets, Toonen et al. 2001). In neocortical slice cultures from embryonic Munc18 KO mice the number of docked vesicles does not differ from wild type mice (Gerber, Rah et al. 2008), however in chromaffin cells from the same mice a deficit in synaptic vesicle

docking was observed (Voets, Toonen et al. 2001), however, this could be due to synaptic phenotypes being harder to resolve with aldehyde based fixatives (Sorensen 2009).

1.3.7 Calcium influx via voltage gated calcium channels

Several subtypes of Ca^{2+} channel are known to mediate Ca^{2+} influx in response to a nerve terminal action potential, these include the N, P/Q and R type Ca^{2+} channels (Iwasaki and Takahashi 1998; Westenbroek, Hoskins et al. 1998; Dietrich, Kirschstein et al. 2003). Among these the N ($Ca_V2.2$) and P/Q ($Ca_V2.1$) type Ca^{2+} channels are most important for mediating fast synaptic transmission. This has been shown by inhibiting N and P/Q type Ca^{2+} channels to reveal near complete block of synaptic transmission (Takahashi and Momiyama 1993; Iwasaki and Takahashi 1998).

The Ca^{2+} influx through these channels triggers two forms of release, a fast synchronous phasic component which is induced rapidly (Sabatini and Regehr 1996) and a slower asynchronous release, which continues for more than 1 second as an increase in the rate of spontaneous release after the action potential (Goda and Stevens 1994; Atluri and Regehr 1998).

Synchronised release of neurotransmitter from synaptic vesicles is thought to occur due to short lived, micro- or nanodomains of elevated calcium which build up and decay rapidly around the voltage dependent Ca^{2+} channels (Bucurenciu, Kulik et al. 2008). Asynchronous release is thought to be sustained by residual Ca^{2+} in the presynaptic nerve terminal and is enhanced during conditions that elevate intracellular Ca^{2+}, as observed after repetitive stimulation (Goda and Stevens 1994; Hagler and Goda 2001). The amount of asynchronous release primarily activated during or following high frequency stimulus trains, also varies in a synapse specific manner (Hefft and Jonas 2005). The molecular basis for this remains unclear but the diversity could be in part due to different isoforms of synaptotagmin (Xu, Mashimo et al. 2007) or other C2 domain proteins.

1.3.8 Ca^{2+} Domains

The transient rises in cytoplasmic calcium concentration serve as second messenger signals for a host of neuronal functions (Kater and Mills 1991; Hardingham, Fukunaga et al. 2002). Therefore in order for calcium to be able to trigger different neuronal actions the

temporal and spatial localisation of the calcium signal must be tightly controlled (Chad and Eckert 1984). A key feature of the active zone is the concentration of Ca^{2+} channels which trigger vesicle exocytosis. Additionally variations in these core processes are expanding an understanding of the differential nature of release at distinct synapses (Jonas, Racca et al. 1994; Sun, Wu et al. 2002; Hefft and Jonas 2005; Hayashi, Raimondi et al. 2008).

The diffusion of calcium after influx into the presynaptic terminal is limited by cytoplasmic buffers and membrane pumps and carriers, which affect the time course and magnitude of the calcium signal (Juhaszova, Church et al. 2000; Collin, Chat et al. 2005). Additionally, although there is evidence for the regulation of neurotransmitter release by calcium released from intracellular stores (Liang, Yuan et al. 2002), the primary source of the calcium signal is the influx from voltage gated calcium channels, which results in vesicle fusion and neurotransmitter release from vesicles in close proximity or docked with the active site in the readily releasable pool (RRP).

The expression and localisation of different calcium channels can affect the coupling of the vesicle neurotransmitter release to the calcium signal. In certain central neuronal synapses the expression and localisation of calcium channels is developmentally controlled and results in a developmental increase in the coupling efficiency of calcium influx to vesicle release (Iwasaki, Momiyama et al. 2000).

1.3.9 Ca^{2+} channels and Ca^{2+} sensing

Biochemical data indicates that calcium channels and synaptotagmin interact with each other (Charvin, L'Eveque et al. 1997; Zamponi 2003), which can be due to either a direct interaction between the two or due to calcium channel binding to SNARE proteins (Sheng, Rettig et al. 1994; Kim and Catterall 1997). This is supported by investigations which show that the local interaction between synaptotagmin and calcium channels is important for local calcium signalling and transmitter release (Mochida, Yokoyama et al. 1998; Cohen, Elferink et al. 2003). Additionally, the isoforms of synaptotagmin expressed at the synapses can affect the mechanism of vesicle release.

1.3.10 Synaptotagmin isoforms

There are thought to be at least 16 synaptotagmin isoforms and distinct subtypes impart differential control of release kinetics. Although many aspects will control the determinants of release the use and expression of distinct Ca^{2+} sensors is now appreciated as important in imparting distinct function, synaptotagmin 1 and 2 are good examples.

Synaptotagmin 1, 2, 3, 5, 6, 7, 9, and 10 are expressed in the brain and bind calcium (synaptotagmin 4 does not bind calcium (Dai, Shin et al. 2004)). Synaptotagmin 1, 2 and 9 have been associated with fast synchronised release, but even though synaptotagmin 1 and 2 are substantially more alike than they are to synaptotagmin 9, they also exhibit significant differences in their transmitter release kinetics. Release triggered by synaptotagmin 2 has been shown to be nearly 30% faster than release triggered by synaptotagmin 1 (Xu, Mashimo et al. 2007).

1.3.11 SNARE protein unfolding-'re-charging'

To be reused in multiple rounds of fusion the SNARE proteins need to be re-activated by disassembly of the '*cis*' complex. This is mediated by the hexameric ATPase N-ethylmaleimide- sensitive factor (NSF), a member of the ATPase associated with different cellular activity protein (AAA) superfamily.

NSF uses energy from ATP hydrolysis to dissociate the SNARE complexes after membrane fusion (Littleton, Barnard et al. 2001; May, Whiteheart et al. 2001). However, NSF does not bind directly to the SNARE complex but indirectly by binding to alpha soluble NSF attachment protein (α-SNAP). The co-factors SNAPs exist in mammals in three different isoforms α- SNAP, β- SNAP, γ- SNAP (Clary, Griff et al. 1990). α- SNAP interacts directly with the SNARE complex and ATP- bound NSF to form the '20 S particle' and, NSF-ATP hydrolysis results in SNARE dissociation (Sollner, Bennett et al. 1993; Fasshauer 2003).

Loss of NSF or α-SNAP leads to accumulation of SNARE complexes and eventual cell death (Littleton, Barnard et al. 2001) and increased intracellular concentration of NSF and α-SNAP results in increased fusion (Xu, Xu et al. 2002). Several studies have also shown that α-SNAP may not only function in SNARE protein disassembly but also in SNARE

complex formation and the regulation of membrane fusion. Increasing the dosage of α-SNAP in *Drosophila* diminished exocytosis and lead to the accumulation of SNARE proteins, and increasing the NSF concentration was shown to be able to overcome the inhibition (Babcock, Macleod et al. 2004) This indicates a second role for α-SNAP in the regulation of membrane fusion which may occur by the binding of α-SNAP to syntaxin and inhibiting SNARE complex formation (Barszczewski, Chua et al. 2008).

After vesicle exocytosis and neurotransmitter release into the synaptic cleft the vesicle stores in the presynaptic neuronal compartment need to be replenished so that multiple rounds of exocytosis can occur. This is achieved by vesicle endocytosis and results in the rescue of the vesicle proteins from the plasma membrane and refilling of the presynaptic compartment with fusion competent synaptic vesicles.

1.4 Vesicle endocytosis

Synaptic terminals contain from dozens to hundreds to thousands of vesicles, hippocampal excitatory synapses have been measured to have ~200 vesicles/ bouton and ~10 docked vesicles at the active site (Schikorski and Stevens 1997), compared to the rod ribbon synapses which have been quantified to contain 130 docked vesicles, and 640 reserve vesicles (Sterling and Matthews 2005). Additionally, not all of these vesicles have an equal probability of undergoing exocytosis upon nerve terminal stimulation. A subset of vesicles termed the rapidly releasable pool is thought to recycle locally (Figure 1.5). As long as the recycling of the vesicles can keep up with demand, neurotransmitter release is maintained (Kuromi and Kidokoro 1998). The reserve (Figure. 1.5) vesicles are thought to be recruited when the demand exceeds the capacity of the rapidly recycling cohort.

After neurotransmitter exocytosis vesicles can undergo different types of endocytosis; these include kiss-and-stay, kiss-and-run and clathrin mediated endocytosis (Figure 1.5). During fast endocytosis vesicles may preserve their identity and recycle locally at the active zone, this form of endocytosis is called ‘kiss-and-run’ (Stevens and Williams 2000) (Figure 1.5). During slow endocytosis vesicles may be recycled from areas outside the active zone and be taken up by clathrin-coated pits (Brodin, Low et al. 2000) (Figure 1.5). Evidence suggests that the mode of vesicle endocytosis functioning to maintain vesicle supplies depends on the type of synapse (Paillart, Li et al. 2003; Rea, Li et al. 2004;

Hayashi, Raimondi et al. 2008) and the activity demand imposed on the synapse (Sun, Wu et al. 2002).

There is also fourth pathway of endocytosis, called bulk membrane endocytosis. This form of endocytosis has been shown to occur at a subset of synapses that do not employ clathrin-coated endocytosis (Paillart, Li et al. 2003). The in-foldings of the plasma membrane pinch off to form large endosomes, which give rise to new synaptic vesicles (Paillart, Li et al. 2003).

1.4.1 Clathrin-mediated endocytosis and vesicle uncoating

Clathrin coats are composed of heavy and light chains of clathrin and bind to the adaptor proteins AP-2 and AP-180. The adaptor proteins are thought to facilitate the targeting of proteins destined for internalisation into synaptic vesicles (Ricotta, Conner et al. 2002). The breaking away of the synaptic vesicle membrane from the plasma membrane is catalysed by dynamin a GTPase. Dynamin forms a ring around the neck of the budding vesicle and upon GTP hydrolysis a conformational change in dynamin results in constriction of the neck causing the vesicle to break away (Yamashita, Hige et al. 2005; Hayashi, Raimondi et al. 2008) (Figure 1.7).

Once in the cytosol the vesicles are uncoated from their clathrin shell in an ATP dependent manner by Hsc70 and its partner Dna J protein auxilin. Hsc70 functions as a molecular chaperone mediating biological processes such as folding/ refolding of proteins, formation and dissociation of protein complexes and translocation of proteins across membranes (Schmid, Baici et al. 1994; Ungewickell, Ungewickell et al. 1995; Voisine, Craig et al. 1999; Jiang, Gao et al. 2000).

The ATPase cycle can be modulated by co-chaperones of the J domain family. J domain proteins are able to target Hsc70 to their substrates and can localise Hsc70 proteins to specific sub-compartments of the cell to carry out a particular function. J domain proteins can also couple the action of several chaperones, such as Hsc70 and Hsp90 (Sakisaka, Meerlo et al. 2002).

1.4.2 Chaperone- co-chaperone actions in clathrin uncoating

Auxilin is a 100kDa co-chaperone protein containing a J domain and capable of stimulating the ATPase activity of Hsc70 by upto 5 fold (Jiang, Greener et al. 1997). Neuronal auxilin contains a central clathrin binding domain and a J domain at the C terminus. *In vitro* studies have shown that the clathrin binding domain first assembles onto clathrin cages, before the J domain stimulates free Hsc70 to hydrolyse ATP. The ADP containing Hsc70 binds tightly to clathrin; this binding distorts the conformation of the clathrin leading to disassembly of the cage (Holstein, Ungewickell et al. 1996).

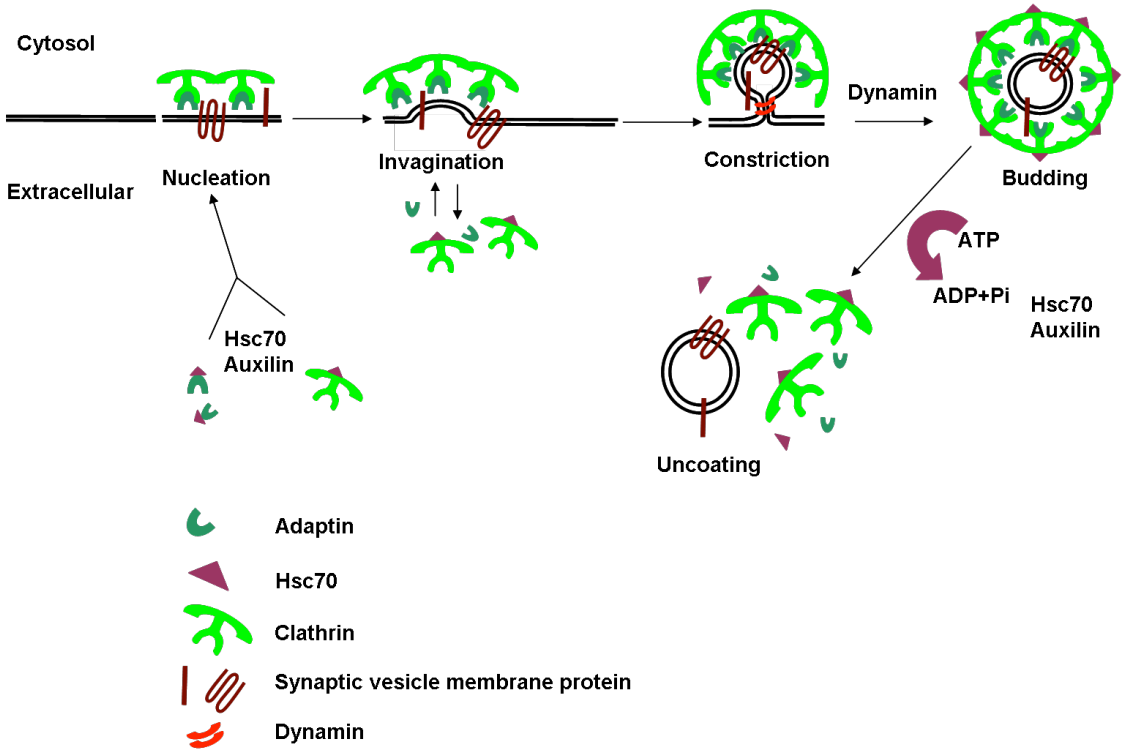

Figure 1.7: Clathrin coating and uncoating
Clathrin mediated endocytosis occurs outside of the active zone and involves the retrieval of synaptic vesicle lipids and proteins into a synaptic vesicle coated with clathrin triskelions. In order for the vesicle to function in subsequent rounds of exocytosis the clathrin coat must be removed from the vesicle. This function is performed by the chaperone protein Hsc70 and its J domain co-chaperone protein, auxilin. Auxilin stimulates the ATPase activity of Hsc70 leading to Hsc70 binding and release of clathrin and the conformational change in the clathrin coat facilitate vesicle uncoating. Hsc70 may also act to sustain clathrin in an unpolymerised form in the cytosol so that it is ready to conduct another round of clathrin mediated endocytosis.

In the cytosol Hsc70 continuously releases and rebinds clathrin, and together with clathrin assembly proteins including AP180 acts to stabilise clathrin for re-assembly into clathrin baskets for future rounds of clathrin mediated endocytosis (Jiang, Gao et al. 2000).

1.4.3 Hsc70 co-chaperone Cysteine string protein

Additionally, just as the J domain protein auxilin mediates recruitment of Hsc70 for endocytosis, the J domain containing synaptic vesicle protein Cysteine String Protein (CSP) may recruit Hsc70 to facilitate late steps in exocytosis. CSP contains a J domain similar to auxilin which binds Hsc70 and stimulates its intrinsic ATPase activity *in vitro*. Additionally, investigations in *Drosophila* and mice have demonstrated that CSP is critical for regulated neurotransmitter exocytosis (Dawson-Scully, Bronk et al. 2000; Ruiz, Casanas et al. 2008).

CSP localises to the synaptic vesicles membrane via palmitoylation. The exact mechanism of CSP activity is still unresolved (Section 1.10). CSP has been shown to interact with some of the neuronal SNARE proteins (Leveque, Pupier et al. 1998; Nie, Ranjan et al. 1999; Wu, Fergestad et al. 1999; Evans, Wilkinson et al. 2001; Evans and Morgan 2002) and Hsc70 which maybe recruited to the vesicle by CSP and has been proposed to stabilize unstructured monomeric SNAREs before formation of the fusion-active heter-oligomeric SNARE complex (Chandra, Gallardo et al. 2005).

1.4.4 Postsynaptic specialisation

In mammalian glutamatergic synapses the postsynaptic density contains approximately 374 different proteins (Peng, Kim et al. 2004) largely involved in positioning neurotransmitter receptors opposite the active zone. This is achieved by receptor associated scaffold proteins such as PSD-95 and cytoskeleton elements. Adhesion molecules help to hold these two membranes parallel. The cadherin, immunoglobulin superfamily (Uchida, Honjo et al. 1996), integrins, neurexins and their binding partners the neuroligins contribute to membrane anchoring at synaptic locations (Song, Ichtchenko et al. 1999; Iida, Hirabayashi et al. 2004). The adhesion proteins such as the presynaptic neurexins and the postsynaptically located neuroligins are anchored to the active zone and postsynaptic density by protein-protein interactions with scaffolding proteins. In the presynaptic membrane the scaffolding proteins Bassoon and RIM (Schoch, Castillo et al. 2002) link to the adhesion proteins and PDZ containing proteins PSD-95 and GRIP bind to adhesion proteins in the postsynaptic density (Iida, Hirabayashi et al. 2004). The scaffolding proteins make up the postsynaptic density and can be observed with electron microscopy as the electron dense region opposing the presynaptic active zone (Figure 1.4).

The postsynaptic density is specialised for signal transduction and permits the dynamic regulation of surface neurotransmitter receptors and their subunit compositions, phosphorylation and degradation. This integrated signalling is essential for maintaining synaptic function and for allowing modulation of signal transduction that leads to strengthening or weakening of synaptic transmission (Esteban, Shi et al. 2003; Shepherd, Rumbaugh et al. 2006) reviewed by Malinow and Malenka (Malinow and Malenka 2002).

1.5 Neurotransmitter receptors

Glutamate is the main excitatory neurotransmitter in the vertebrate CNS and three classes of ionotropic neurotransmitter receptors mediate its action; α- amino-3-hydroxy-5-methyl-4-isoxazole propionic acid (AMPA) and N-methyl-$_D$-aspartate (NMDA) and kainate receptors. AMPA, NMDA and kainate receptors bind glutamate released from the presynaptic terminal and produce depolarisation of the postsynaptic membrane (reviewed (Ozawa, Kamiya et al. 1998). Although all three primarily respond to glutamate, the roles played by each of the receptors are very different.

AMPA receptors mediate the majority of fast synaptic transmission (Lerma, Morales et al. 1997). Kainate receptors contribute to the postsynaptic response at excitatory synapses and can also modulate presynaptic neurotransmitter release at some synapses (Cossart, Tyzio et al. 2001). NMDA receptors play an important role in calcium signal transduction into the postsynaptic cell (Hardingham, Arnold et al. 2001).

Activation of ionotropic AMPA receptors (Section 1.5.1), by glutamate, leads to the flow of Na^+ and K^+ across the postsynaptic membrane, the ions flow towards their reversal potentials (the membrane potential at which there is no net flow of ions from one side of the membrane to the other), leading to a depolarised synaptic potential. The excitatory postsynaptic potential increases the probability that the postsynaptic neuron will fire an action potential, defining the synapse as an excitatory synapse.

$GABA_A$ receptors are activated by GABA (Section 1.5.4) and lead to Cl^- ion fluxes across the membrane through the pentameric receptor. Cl^- ions flow down their electrochemical gradient towards the reversal potential, which in mature neurons leads efflux of Cl^- and

hyperpolarisation of the membrane, because the reversal potential of Cl^- is more negative than the resting membrane potential and action potential threshold. Hyperpolarisation thereby reduces the probability that the neuron will fire an action potential. Thus the probability of a neuron firing an action potential is a summation of the excitatory and inhibitory inputs onto individual postsynaptic spines on the neuron.

1.5.1 AMPA Receptors subtypes

AMPA receptors are heteroligomeric tetramers containing different combinations of four homologous subunits GluR 1-4 (A-D). The receptors of differing subunit stoichiometries form receptor subtypes with distinct functional properties. The distinct AMPA receptor subtypes are differentially expressed in distinct cells and confer varied postsynaptic responses (Geiger, Melcher et al. 1995).

Each subunit has a large extracellular N –terminus, three transmembrane domains and a C-terminal cytoplasmic domain, although the N-terminus and transmembrane domains of the different AMPA receptor subunits are very similar. Their intracellular C-terminus are very distinct and contribute to localization and trafficking.

Through their C-terminal tails each subunit interacts with specific cytoplasmic proteins, consisting of scaffolding and trafficking proteins that make up the postsynaptic density corresponding to the electron dense region observed under the electron microscope (Figure 1.4). Most of the AMPA receptor interacting proteins identified interact with AMPA receptors via well characterised PDZ protein-protein interactions (Leonard, Davare et al. 1998; Dong, Zhang et al. 1999; Sala, Piech et al. 2001). AMPA receptors interaction with PDZ containing scaffolding proteins such as glutamate-receptor-interacting- protein-1 (GRIP-1), localises AMPA receptors to synaptic regions opposite the presynaptic active zone and ensures efficient synaptic transmission (Hanley and Henley 2010).

Splicing imparts an important diversity and the intracellular domain is a functionally important site of splicing (Bredt and Nicoll 2003). The four AMPA receptor subunits have two alternatively spliced versions, Flip and Flop (Monyer, Seeburg et al. 1991) that modify the extracellular ligand binding domains of the receptor. The Flip variant predominates before birth whereas the Flop forms are upregulated after birth. Flip and Flop subunit

versions differ in their responses to agonist binding, with Flop versions desensitising much more rapidly than the Flip forms (Mosbacher, Schoepfer et al. 1994; Bredt and Nicoll 2003).

In the case of the GluR2 AMPA receptor subunit its RNA is also post-transcriptionally modified by RNA-editing, which leads to single amino acid changes in the M2 pore region (Kwak, Hideyama et al. 2010). In the transcript of the GluR2 subunit a glutamine codon in the M2 domain encoded by CAG can be edited to an arginine encoded by CIG, at what is called the Q/R site. When an arginine is encoded in the Q/R site the receptor subunit is referred to as 'edited'. Edited versions of GluR2 leads to decreased Ca^{2+} permeability (Hume, Dingledine et al. 1991) and low single channel conductance (Swanson, Feldmeyer et al. 1996). When a glutamine resides at the Q/R region the subunit is referred to as 'unedited' and the receptor is Ca^{2+} permeable. Therefore, if an AMPA receptor does not contain GluR2 or contains an unedited form of GluR2 the heteromeric AMPA receptor will be Ca^{2+} permeable. After embryonic day 14, most rat GluR2 subunits (>99%) are edited, containing an arginine at the Q/R site and the vigorous editing of the GluR2 subunit has been shown to be vital for survival (Brusa, Zimmermann et al. 1995).

1.5.2 Kainate Receptors

Kainate receptors are tetramers made of 5 kainate receptor subunits, GluR5, GluR6, GluR7, KA1 and KA2. There are also additional isoforms generated from alternative splicing (Jaskolski, Coussen et al. 2004). The subunits GluR5-7 are able to form homomeric channels, but KA1 and KA2 only form channels when co-assembled with other kainate receptor subunit (Lerma 2006).

Kainate receptors also undergo RNA–editing which affects their calcium permeability (Vissel, Royle et al. 2001). mRNA editing occurs in the GluR5 and GluR6 subunits but not the GluR7, KA1 or KA2 subunits. The GluR5 and GluR6 subunit editing involves a posttranscriptional modification in the M2 pore forming segment of the channel at the glutamine/arginine (Q/R) site (Egebjerg and Heinemann 1993; Vissel, Royle et al. 2001).

Kainate receptors have been shown to modulate both presynaptic and postsynaptic functions (Chittajallu, Vignes et al. 1996) and function at excitatory and inhibitory

neuronal cells to modulate neuronal activity, and have been shown to be activated by glutamate release from astrocytes (Castillo, Malenka et al. 1997; Clarke, Ballyk et al. 1997; Liu, Xu et al. 2004) .

1.5.3 NMDA Receptors

NMDA receptors are ionotropic receptors permeable to calcium. Upon binding of glutamate and its co-agonist glycine the NMDA receptor is opened. However passage of ions through the channel pore is not permitted until the Mg^{2+} block of the ion channel has been removed by coincident membrane depolarization and co-agonist binding (Mori, Masaki et al. 1992).

NMDA receptors are tetrameric receptors normally composed of at least two NR1 subunits co-assembled with the various NR2 or NR3 subunits. NR1 has also been shown to combine with the NR3 subunit to form a glycine only activated excitatory receptor (Chatterton, Awobuluyi et al. 2002; Cavara and Hollmann 2008). There are eight different isoforms of NR1 that arise through three alternative splicing sites. Four different NR2 subunits exist named A, B, C and D. The different NR2 subunits (A-D) are expressed differentially throughout development; NR2B containing NMDA receptors predominate in the neonatal brain and during development are exchanged for NR2A containing NMDA receptors and in some parts of the brain by NR2C (e.g. cerebellum) (Flint, Maisch et al. 1997; Liu, Murray et al. 2004).

The different NR2 subunits confer distinct pharmacological and kinetic properties on the NMDA receptors. NR2B containing receptors have slower kinetics and are sensitive to the antagonist Ifenprodil, whereas NR2A containing receptors display faster kinetics and are relatively insensitive to Ifenprodil (Kim, Dunah et al. 2005). In mature neuronal cells NR1/ NR2A containing receptors are mainly localised at synaptic locations opposing the presynaptic active site, and NR2B containing receptors are mainly located at extrasynaptic sites (Li, Chen et al. 2002) and have been shown to be linked to different intracellular signalling cascades (Hardingham, Arnold et al. 2001; Hardingham and Bading 2010).

1.5.3.1 NMDA Receptor Antagonism

NMDA receptor antagonists are widely used in scientific research to assess the neuronal network activity associated with NMDA receptor activity and to block cell death (Hardingham, Fukunaga et al. 2002). MK801 is a glutamate receptor antagonist: on activation of glutamate receptors MK801 is able to bind inside the receptor channel to block ion flow and hence the activity of the receptor (Foster and Wong 1987; Wong, Knight et al. 1988). The ability of MK801 to antagonise the NMDA receptor is use-dependent, meaning that the degree of blockage is greatly enhanced by the presence of NMDA receptor agonists, glutamate and glycine (Wong, Kemp et al. 1986; Foster and Wong 1987; Reynolds and Miller 1988). MK801 has also been shown to antagonise the nicotinic receptor α7 nAChR, which like the NMDA receptors are highly calcium permeable (Briggs and McKenna 1996).

Other NMDA receptor antagonists such as Ifenprodil and NVP have NMDA receptor subunit specific blocking effect, Ifenprodil blocks NR2B containing NMDA Receptors and NVP blocks NR2A containing NMDA Receptors (Williams 1993; Kinney, Davis et al. 2006). The NMDA Receptor antagonist Memantine is an uncompetitive blocker and is in clinical trials as a treatment for Alzheimer's Disease (Danysz and Parsons 2003; Gauthier, Wirth et al. 2005).

1.5.4 GABAergic Receptors

Most inhibitory synapses in the mammalian brain have GABA as their transmitter. Synaptically released GABA acts via two main receptor types: the ionotropic $GABA_A$ receptor and the metabotropic $GABA_B$ receptors. $GABA_A$ receptors allow Cl^- fluxes. They perform two distinct types of inhibition (Figure 1.8). Receptors that are clustered at synaptic release sites are able to conduct with fast rise and decay kinetics and mediate phasic inhibition (Brickley, Cull-Candy et al. 1999). $GABA_A$ receptors are also expressed at extra-synaptic sites (Brickley, Cull-Candy et al. 1996). These receptors are sensitive to ambient levels of GABA and give rise to tonic inhibitory conductances (Nusser, Sieghart et al. 1998; Banks and Pearce 2000; Semyanov, Walker et al. 2004) (Figure 1.8). $GABA_B$ receptors are located pre- and postsynaptically and have a major role regulating transmitter

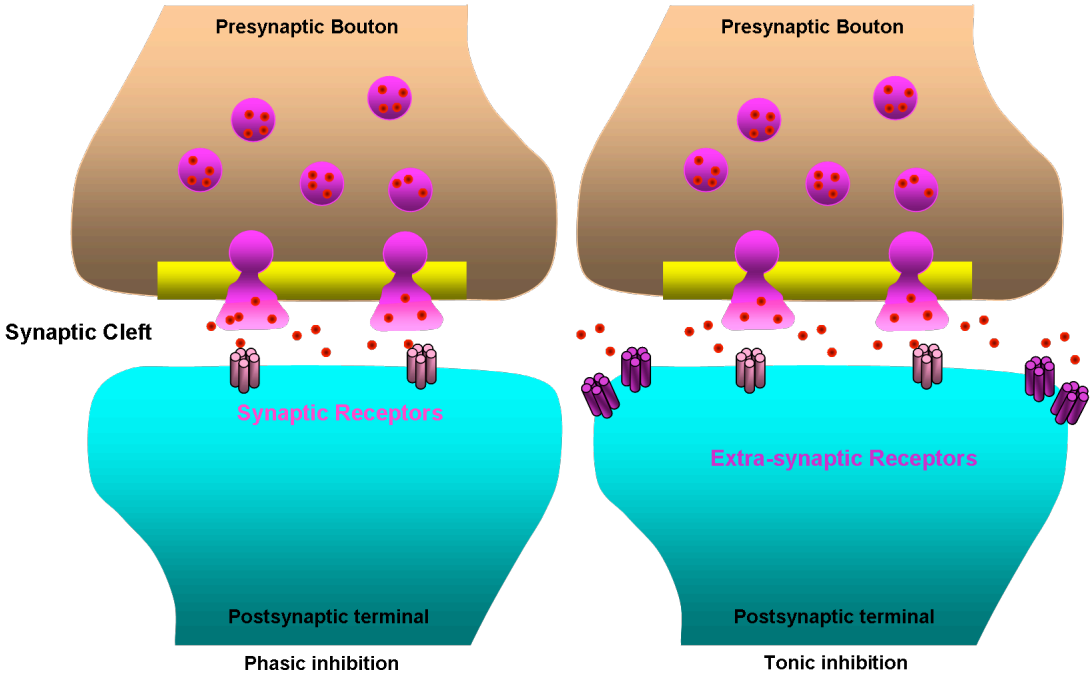

Figure 1.8: Phasic and tonic inhibition of $GABA_A$ receptors
Phasic $GABA_A$ receptors are located synaptically and respond with fast kinetics to synaptically released GABA. Extrasynaptic receptors respond to ambient levels of GABA and provide tonic inhibition**.** The synaptic and extrasynaptic $GABA_A$ receptors are made of different $GABA_A$ receptor subunits which convey different molecular properties, including affinity for GABA (Wei, Zhang et al. 2003; Cope, Hughes et al. 2005).

release and excitability by modulating Ca^{2+} and K^+ channels (Mintz and Bean 1993; Thompson, Capogna et al. 1993; Sakaba and Neher 2003; Ulrich and Bettler 2007).

There is considerable diversity of functional GABA receptors resulting from different subunit combinations. Ionotrophic GABA receptors consist of 5 protein subunits arranged around a central pore which makes the ion channel. There are 16 different types of subunit comprising the $GABA_A$ receptor family, α 1-6, β 1-3, γ 1-3, δ, ε, π and θ, of which some subunits also have additional splice variants (Quinlan, Firestone et al. 2000; Mohler 2006). The major combinations, their region and neuronal localisation are listed in table 1.3.

Furthermore, different subunit compositions confer different deactivation kinetics (Lavoie, Tingey et al. 1997). $GABA_A$ receptors containing the α_2 subunit have slower deactivation kinetics than those expressing the α_1 subunit, and GABAergic neurons which employ fast spiking kinetics have been shown to undergo a developmental switch from α_2 subunit to α_1 subunit containing $GABA_A$ receptors (Laurie, Wisden et al. 1992; Klausberger, Roberts et al. 2002; Doischer, Hosp et al. 2008).

Composition	**Neuronal location**	**Abundance**
$\alpha_1\ \beta_{2/3}\ \gamma_2$	Soma and Dendrites and extrasynaptic in all neurons with high expression. Fast deactivation kinetics.	Major subtype (60% of all $GABA_A$ receptors)
$\alpha_2\ \beta_3\ \gamma_2$	Mainly synaptic, enriched in axon initial segment or cortical and hippocampal pyramidal cells. Slow deactivation kinetics.	Minor subtype (15-20%)
$\alpha_3\ \beta_3\ \gamma_2$	Mainly synaptic, some axon initial segments.	Minor subtype (15-20%)

Table 1.3: Composition and regional localisation of the major $GABA_A$ receptors in the brain. Adapted from (Mohler 2006)

1.6 Distinct Neuronal modality through specialisation in core synaptic mechanism

Neuronal cells are adapted in their core function to allow specialisations that increase complexity. These adaptations in neuronal cells include different firing properties, protein expression, or structural modification(s) (Freund and Buzsaki 1996; Somogyi and Klausberger 2005; Bartos, Vida et al. 2007). The synaptic compartment is an important locus for bringing about adapted core mechanism to impart discrete specialisation of neuron function. Table 1.4 is focuses on Ca^{2+} coupling to vesicle release and different modes of endocytosis and draws its examples from important classes of excitatory glutamatergic and GABAergic neurons, which exhibit fast, slow and tonic signalling and

highlight important adaptations of these the core mechanisms (Section. 1.3). The table also highlights the importance of these adaptations in the presynaptic and postsynaptic compartments to the overriding neuronal and microcircuit output. These distinct neuronal subtypes, which are introduced in more detail below, are introduced to exemplar functional specialisation. Furthermore, despite clear differences in their structural and physiological properties, as discussed later, they express a shared susceptibility to dysfunction and degeneration through a common lesion namely genetic removal of CSP and its associated function (Section 1.10).

1.6.1 Parvalbumin positive interneuron

The parvalbumin positive GABAergic basket cell is an example of a fast spiking inhibitory cell, the CCK positive basket cell is an example of a slow spiking inhibitory neuron (Kawaguchi and Kondo 2002) and the hippocampal pyramidal cell synapse is an example of a slow spiking glutamatergic synapse (Csicsvari, Hirase et al. 1999). The parvalbumin

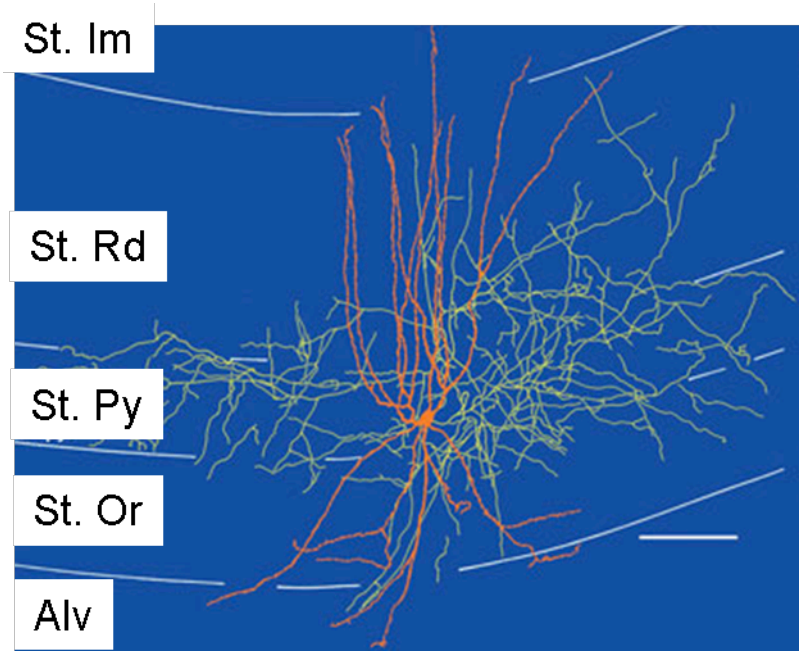

Figure 1.9: Parvalbumin positive basket cell.
The cell body of the basket cell lays in the St. Py. The dendrites from the parvalbumin positive basket cell are labelled orange and the axonal projections are green. The basket cell axons innervate the perisomatic region. The synapses formed by the parvalbumin positive basket cells are symmetric synapses as seen in figure 1.4. Alv- Alveus, St. Im- Stratum Lacunosum Moleculare, St.Or- Stratum Oriens, St. Py- Stratum Pyramidale, St. Ra- Stratum Radiatum. Scale bar 20µm. Image adapted from: (Klausberger, Magill et al. 2003)

positive interneurons provide perisomatic inhibition to the pyramidal neurons. Figure 1.9

shows the cell body location, axon collaterals and dendritic processes of a parvalbumin positive basket cell in the CA1 of the hippocampus.

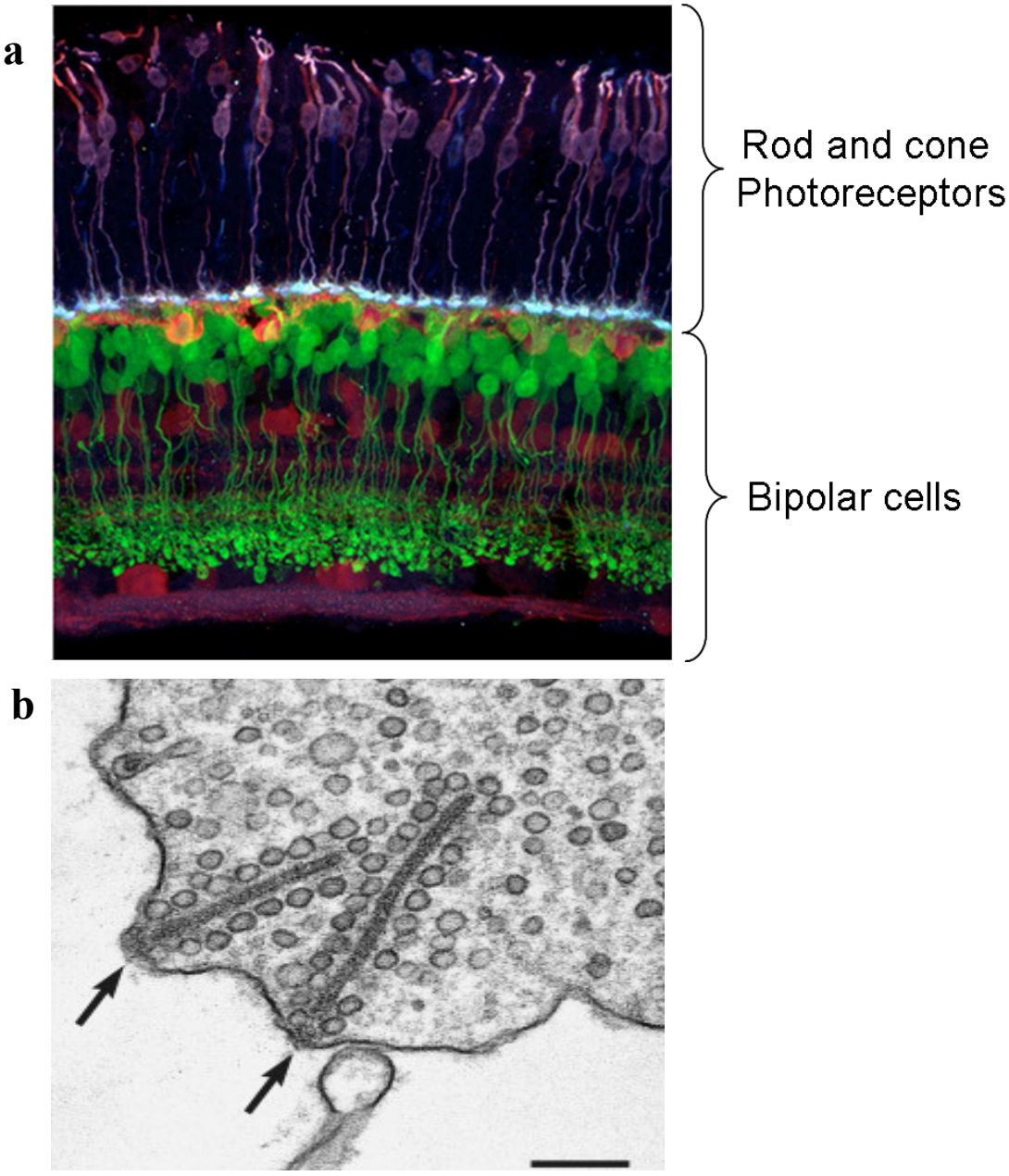

Figure 1.10: Photoreceptors and ribbon synapse in the retina

a) Cross-section of an immunostained mouse retina, the bipolar cells are green, the photoreceptors are purple, and the amacrine and ganglion cells are red. The light blue ends on the purple photoreceptors mark the synapses containing the synaptic ribbons. Adapted from http://wonglab.biostr.washington.edu/Research.html.

b) The arrows mark a synaptic ribbons in a photoreceptor, with vesicles tethered to it. Vesicles tethered to the ribbon are thought to be primed for release and respond quickly to nerve terminal excitation. Vesicles surrounding, un-tethered to the ribbon make up the reserve pool of vesicles. The ribbon structure may aid the tonic and efficient release of vesicles from the photoreceptors. Adapted from (Thoreson, Rabl et al. 2004).

1.6.2 Ribbon synapse of the photoreceptors

The ribbon synapse of the rod and cone photoreceptors is an example of a tonically active synapse. Ribbon synapses occur in sensory neurons including the photoreceptors, bipolar cells of the vertebrate retina and in the mechanosensory hair cells of the inner ear (Moser and Beutner 2000; Dick, tom Dieck et al. 2003). Synaptic ribbons are named because of their electron microscopy appearance (Figure 1.10). The synaptic ribbon is thought to act as a conveyer belt that funnels vesicles towards fusion sites at the active zone, allowing them to respond to single photons of light (Rao-Mirotznik, Buchsbaum et al. 1998), which are directly opposite the postsynaptic receptors.

1.6.3 Calyx of Held synapse

The calyx of Held is an example of a fast firing glutamatergic synapse (Hermann, Pecka et al. 2007). A large number of studies investigating vesicle release upon nerve terminal stimulation have used the calyx of Held preparation. The calyx of Held preparation has been shown to accurately model all the properties of release such as the Ca^{2+} influx (Meinrenken, Borst et al. 2002) and Ca^{2+} triggering of vesicle release (Bollmann, Sakmann et al. 2000; Meinrenken, Borst et al. 2002), (reviewed in (Meinrenken, Borst et al. 2003) .

The calyx of Held is a large glutamatergic synaptic terminal innervating principal neurons of the medial nucleus of the trapezoid body (MNTB) and is capable of high frequency firing of >600Hz (Hermann, Pecka et al. 2007). The calyx forms a large nerve terminal (~15μm in diameter), which envelops the soma of the postsynaptic membrane (Figure 1.11). The calyx terminal makes approximately 500-600 synaptic contacts with the postsynaptic cell and receives a large number of synaptic contacts. A single action potential has been shown to trigger release at ~200 synaptic contacts (Satzler, Sohl et al. 2002). This results in strong coupling between the calyx and the postsynaptic cell by hundreds of parallel synapses. This reliability in presynaptic and postsynaptic coupling is important because the calyx is part of the auditory pathway central to fast synaptic transmission (Hermann, Pecka et al. 2007) and sound localisation.

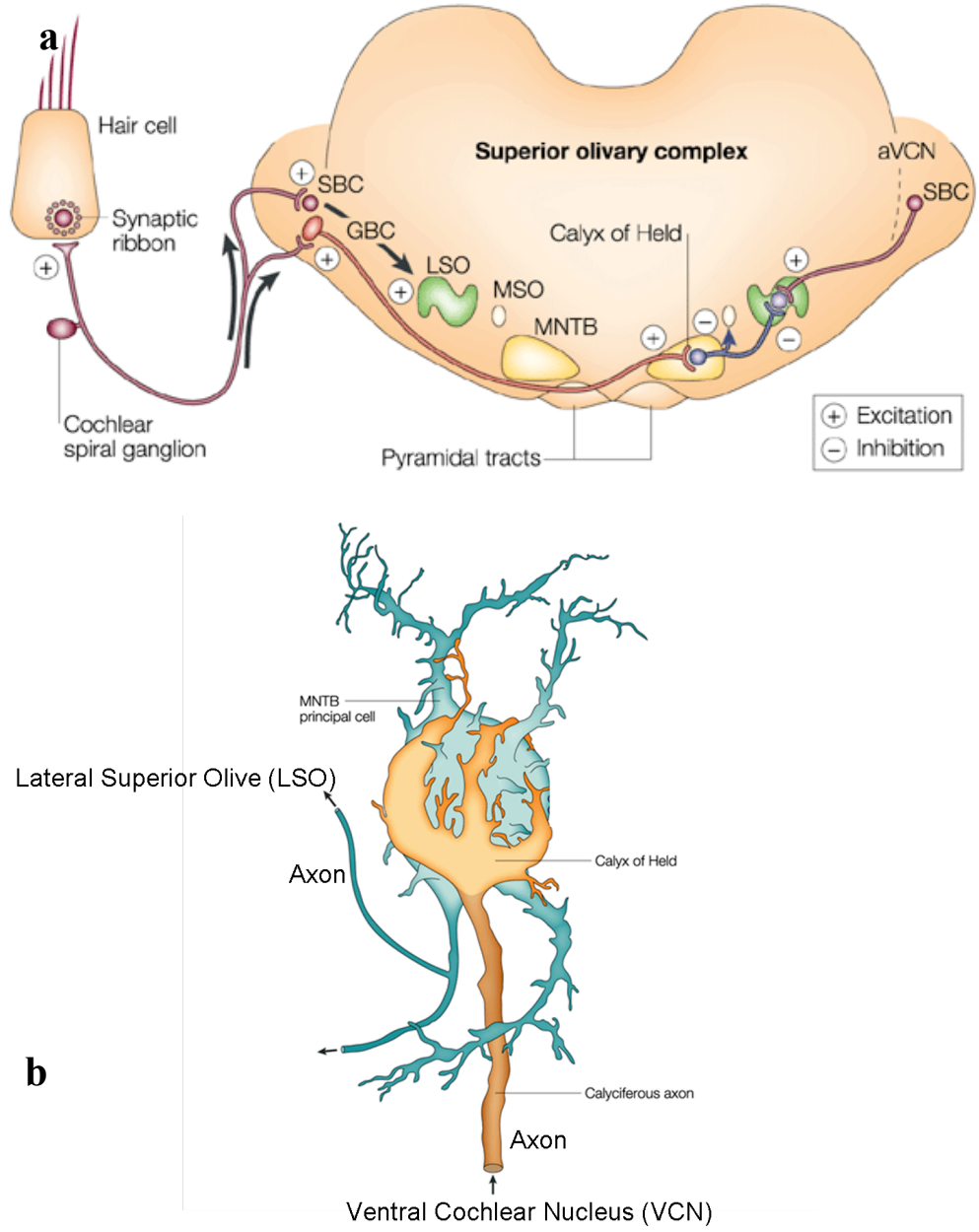

Figure 1.11: The Calyx synapse

a) The signals arriving at the cochlea are transmitted to the ipsilateral anterior ventral cochlea nuclear (VCN) by excitatory synapses onto the globular bushy cells (GBC) and the spherical bushy cells (SBC). The GBC from the VCN send axons to the contralateral medial nucleus of the trapezoid body (MNTB) where they synapse using the calyx of Held synapses onto the MNTB principal cells. The principal cells then project their axons to the lateral superior olive, where they inhibit postsynaptic neurons. This synaptic pathway is required for high frequency sound localisation.

b) The calyx of Held synapse (orange) wrapped around the MNTB principal cell (blue). Adapted from:(von Gersdorff and Borst 2002).

Neuron/cell	Synapse	Function	Adaptation for function presynaptic/ postsynaptic
Parvalbumin positive interneuron basket cell	Inhibitory GABAergic	Fast spiking cell >100Hz	• Nanodomain coupling between calcium entry and calcium sensor for vesicle fusion and release [1] • Higher dependence of clathrin-coat mediated endocytosis [5] • Expression of α_1 GABAergic receptor subunit in postsynaptic target cell [10] • AMPA receptors with fast deactivation desensitisation kinetics (GluR1/4) [11]
CCK positive interneuron Basket cell	Inhibitory GABAergic	Slow spiking	• Microdomain coupling between calcium entry and calcium sensor for vesicle fusion and release [1, 2] • Expression of α_2 GABAergic receptor subunit in postsynaptic target cell [10]
Ventral Cochlear Nucleus	Calyx of Held Glutamatergic	Fast Spiking >100Hz	• Nanodomain coupling between calcium entry and calcium sensor for vesicle fusion and release [9] • AMPA receptors with fast deactivation desensitisation kinetics (GluR1/4) [11]
Hippocampal/ Layer 5 neocortical Pyramidal cell	Glutamatergic	Slow Spiking ~1Hz	• Microdomain coupling between calcium entry and calcium sensor for vesicle fusion and release [3] • Less dependent on clathrin-coat mediated endocytosis [5, 12] • AMPA receptor with slow deactivation and desensitisation kinetics (GluR1/2 and 2/3) [11]
Photoreceptors, Rods and Cones	Ribbon Synapse Glutamatergic	Tonic release	• Nanodomain coupling between calcium entry and calcium sensor for vesicle fusion and release [4] • Synaptic ribbon structure, acts as conveyer belt to localise and regulate synaptic vesicles [8] • Large vesicle pools [7] • Use constant clathrin-coat mediated endocytosis to maintain vesicle supplies [6]

Table 1.4: Synaptic adaptations from the core mechanisms of neurotransmission.
Detailed are fast frequency spiking, slow frequency spiking and tonically active synapses.
The table highlights some the presynaptic (green) and postsynaptic (red) adaptations observed in these synapses which permit them to function as either fast, slow or tonically active synapses.
1= (Bucurenciu, Kulik et al. 2008) 2= (Hefft and Jonas 2005) 3= (Ohana and Sakmann 1998) 4= (Jarsky, Tian et al. 2010), 5= (Hayashi, Raimondi et al. 2008), 6= (Rea, Li et al. 2004) 7= (von Gersdorff, Vardi et al. 1996) 8= (Sterling and Matthews 2005) 9=(Fedchyshyn and Wang 2005) 10= (Klausberger, Roberts et al. 2002) 11=(Geiger, Melcher et al. 1995) 12=(Gandhi and Stevens 2003)

These anatomically and functionally different synapses share a common susceptibility to neuronal degeneration in the absence of CSPα (discussed in section 1.10), but each synapse is adapted to its specific function. Some of these adaptations are discussed below and summarised in table 1.4.

1.6.4 Calcium domain differences

Due to differences in the organization of Ca^{2+} channels and neurotransmitter release mechanisms, different neuronal synapses display distinct functions with respect to active zone Ca^{2+} signals. These are described as either micrometer (μm) or nanometer (nm) range Ca^{2+} domains. Some synapses which rely on fast synaptic transmission have been shown to employ 'nanodomain' localisation of Ca^{2+} coupling to release, where as slower or immature neuronal synapses have been shown to have 'micrometer' calcium domains (Bucurenciu, Kulik et al. 2008).

At the calyx of Held and the neuromuscular junction (nmj) synapses there is a developmental switch from N type to P/Q type Ca^{2+}channels as the synapses mature. The switch from N to P/Q type calcium channels is thought to result in more mature 'nanodomain' coupling of the mature calyx (Chuhma and Ohmori 1998; Fedchyshyn and Wang 2005). The developmental time frame between loose 'microdomain' and tight 'nanodomain' coupling also correlates with the opening of the auditory canal at postnatal day 10 (So, Chen et al. 2010). This contrasts with the loose microdomain coupling of the slow spiking glutamatergic pyramidal cell neurons (Ohana and Sakmann 1998).

Presynaptic tight coupling in the nanometer range (Ca^{2+} 'nanodomain') has also been reported between the Ca^{2+}channels and sensor in parvalbumin positive basket cells (Bucurenciu, Kulik et al. 2008) and the ribbon synapses (Jarsky, Tian et al. 2010), compared to the loose Ca^{2+} 'microdomain' coupling N type Ca^{2+} expressing slow spiking CCK positive interneurons (Hefft and Jonas 2005). This is paralleled with different postsynaptic expression of $GABA_A$ receptor subunits which ensure that the fast frequency firing of the parvalbumin positive basket cell is relayed to the postsynaptic target (Klausberger, Roberts et al. 2002).

1.6.5 SNARE and synaptotagmin isoforms differences

The tighter coupling in synapses of fast spiking cells has been suggested to be due to expression of different SNARE proteins (Bucurenciu, Kulik et al. 2008). As described in section 1.3.10, 16 different isoforms of synaptotagmin have been found, and because synaptotagmin is thought to act as the Ca^{2+} sensor for Ca^{2+} stimulated release and has been shown to interact with Ca^{2+} channels (Charvin, L'Eveque et al. 1997), different isoform expression in different synapses could account of the differences in calcium- sensor coupling and vesicle release.

Faster firing neuronal synapses have been shown to express synaptotagmin 2 (Pang, Sun et al. 2006; Fox and Sanes 2007; Xu, Mashimo et al. 2007; Kerr, Reisinger et al. 2008) and release triggered by synaptotagmin 2 has been described to be nearly 30% faster than release triggered by synaptotagmin 1 (Xu, Mashimo et al. 2007). This data fits well with differential synaptotagmin isoforms expression at least partly explaining the difference in coupling in fast and slow firing synapses.

SNAP 25 was proposed to be expressed in glutamatergic neurons but not in GABAergic interneurons (Verderio, Pozzi et al. 2004; Frassoni, Inverardi et al. 2005). GABAergic neurons were instead shown to express the SNAP 25 homologue SNAP-23 (Frassoni, Inverardi et al. 2005) and were shown to have a higher calcium responsiveness to depolarisation, indicated by a significant increase in mIPSC frequency in response to increased extracellular calcium (Verderio, Pozzi et al. 2004). This difference in SNARE isoform expression could also explain the difference in coupling between fast and slow synapses. However, further research has failed to confirm these results and has instead shown that both SNAP-23 and SNAP-25 are expressed in both Glutamatergic and GABAergic neurons, and that stimulus evoked transmission was abolished in GABAergic neurons from $Snap25^{-/-}$ mice (Tafoya, Mameli et al. 2006).

The differential expression of SNAP 23 and SNAP25 isoforms has been proposed as another possible link between the slow coupling of vesicles release in glutamatergic and fast coupling in GABAergic neurons (Bucurenciu, Kulik et al. 2008). However, differences in Ca^{2+}channel types and calcium binding proteins are also likely to be an important determinant (Hefft and Jonas 2005; Bucurenciu, Kulik et al. 2008).

1.6.6 Vesicle pool and mode endocytosis differences

The mammalian rod ribbon synapse is predicted to release ~100 synaptic vesicles in response to 1 photon of light (Rao-Mirotznik, Buchsbaum et al. 1998). To maintain this release, endocytosis and vesicle recycling need to constantly replenish the vesicle pool (Section 1.4). This is also likely to be the case for the highly active fast firing synapses which transmit fast spike trains with high temporal precision, such as the calyx and the parvalbumin interneurons (Llobet, Cooke et al. 2003; Zenisek, Davila et al. 2003) (Section 1.4, Figure 1.7).

An advantage of 'kiss-and-run' or 'kiss-and-stay' pathways is that vesicle components do not need to be sorted from the plasma membrane because the vesicle membrane does not mix with the plasma membrane (Section 1.4). However, because the synaptic vesicle endocytosis via either 'kiss-and-run' or 'kiss-and-stay' are sorted at the active zone, they occupy a limited space in the active zone with a non-functional vesicle. For a synapse with a low frequency of release, or during low frequency stimulation, this may not be limiting to further vesicle exocytosis at the active zone. However, in synapses with continuous or high frequency release blockage of the active zone with non-functional vesicles may be limiting. Thus, although counter intuitive the more efficient retrieval mechanism may not be an advantage for the relatively continuous transmission utilized at ribbon synapses. Modes of endocytosis which occur outside the active zone such as clathrin mediated endocytosis and bulk membrane endocytosis may be more efficient (Matthews 2004).

Support that highly active neurons use modes of endocytosis that do not compromise the active zone space comes from investigations of cone photoreceptors ribbon synapses which release neurotransmitter continuously and have been shown to employ constant rounds of clathrin-mediated endocytosis to replenish vesicle supplies (Llobet, Cooke et al. 2003; Zenisek, Davila et al. 2003; Rea, Li et al. 2004). This contrasts to the dominant mode of 'kiss-and-run' observed at hippocampal synapses (Gandhi and Stevens 2003), and parallels the differential use of either fast vesicle endocytosis or clathrin-mediated endocytosis when the calyx of Held synapse is stimulated with either low or high frequency stimulation protocols respectively (Sun, Wu et al. 2002).

1.6.7 AMPA receptor subunit differences

Most AMPA receptors contain the GluR2 subunit; the GluR2 subunit confers the properties of Ca^{2+} impermeability (Section 1.5.1). However, the subtype composition of AMPA receptors varies between cell types and brain regions. The majority of AMPA receptors in the hippocampal pyramidal cells are composed of GluR1:GluR2, and GluR2:GluR3 heteromers, whereas heteromers of GluR1:GluR4 have been shown to predominate at GABAergic interneuronal synapses, and at the mouse glutamatergic synapses of the calyx of Held (Joshi, Shokralla et al. 2004). Therefore, these AMPA receptors would confer Ca^{2+} permeability. The GluR2 subunit was not found to be absent in the calyx synapses in rat tissue, suggesting that the Ca^{2+} permeability due to lack of GluR2 could be murine specific (Koike-Tani, Saitoh et al. 2005)

In hippocampal neocortical pyramidal neurons the AMPA receptors expressed have been shown to have both low permeability to Ca^{2+} and slow deactivation, whereas postsynaptic sites of GABAergic and calyx (MNTB principal cell) synapses have faster AMPA receptor deactivation and higher Ca^{2+} permeability (Yin, Turetsky et al. 1994; Geiger, Melcher et al. 1995; Leranth, Szeidemann et al. 1996; Moga, Hof et al. 2002). These functional differences were shown to correlate with different AMPA receptor subunit expressions. Expression of faster gated AMPA receptors in interneurons and the calyx synapses on the MNTB neurons could serve to decrease the rise time of the excitatory postsynaptic potential (EPSC) and reduce the time interval between the EPSP and the postsynaptic action potential (Geiger, Lubke et al. 1997) (Joshi, Shokralla et al. 2004).

Table 1.4 and section 1.6 highlight the functional adaptations and differences between neuronal subtypes. These functional differences allow for regulated brain network activity and demonstrate how different brain regions are adapted to perform different functions. Section 1.7 discusses formation of neuronal networks and the importance of a neuronal excitatory: inhibitory balance to maintain healthy neuronal network function.

1.7 Neurons develop intricate microcircuits to form a complex neuronal network

1.7.1 Network formation

The assembly of neurons into microcircuits requires the precise timing of cell migration and differentiation and during maturation of the brain neuronal networks transform from a group of cells with sparse non-synaptic spontaneous activity to an assembly of neuronal microcircuits communicating via synapses to generate complex network oscillations (Section. 1.8). Emerging brain networks engage in a sequential maturation demonstrating co-ordinated activity that is believed to control the formation of synaptic connections (Ben-Ari, Khazipov et al. 1997; Rheims, Minlebaev et al. 2008).

Studying this in the intact brain is more feasible now than in the past however reduced systems often provide tractable solutions to such investigation. For example hippocampal slice cultures removed from mice as they develop from embryonic day 19 to postnatal day 14 have shown that the emergent activity is formed from sporadic calcium spikes corresponding with calcium influx through L type calcium channels. This activity develops in the form of calcium spikes that are temporally correlated between different cells through gap junction connections (Crepel, Aronov et al. 2007). After birth the neuronal cells become synaptically linked and early network oscillations are driven through the immature excitatory actions of GABA (Ben-Ari 2001; Payne, Rivera et al. 2003).

At early stages GABA is thought to be released from postmitotic neuroblasts and tonically activate $GABA_A$ receptors ($GABA_AR$) on neural progenitor cells. This controls transition from cell proliferation to neuronal differentiation (Antonopoulos, Pappas et al. 1997). GABA has also been shown to have similar trophic effects on progenitor cells in the adult brain (Tozuka, Fukuda et al. 2005).

At early stages of development $GABA_A$ receptor activation depolarises the membrane as a result of immature expression patterns of the chloride transporter proteins NKCC1 and KCC2. NKCC1 is a sodium potassium chloride co-transporter and is expressed relatively early in development in neuronal cells and leads to an accumulation of intracellular chloride (Wang, Shimizu-Okabe et al. 2002). KCC2 is a potassium chloride co-transporter and is expressed later in development in mature neurons and transports chloride out of the

cell (Wang, Shimizu-Okabe et al. 2002). In immature neurons the activation of $GABA_A$ receptors leads to chloride efflux out of the cell and membrane depolarisation (Ben-Ari, Gaiarsa et al. 2007; Tyzio, Holmes et al. 2007).

1.7.2 Excitatory and inhibitory balance

Before becoming a chemical synapse, a physical contact is formed between an axon and the dendritic shaft (Ahmari, Buchanan et al. 2000). The initial contact is followed by temporally controlled changes in morphology and molecular content to form mature synapses with an active zone and synaptic vesicles in close opposition to a receptor studded postsynaptic density. The transformation from a filopodia-dendrite contact site to a synapse involves recruitment and stabilisation of both pre-synaptic and postsynaptic elements (Washbourne, Bennett et al. 2002). Adhesion molecules have been shown to be important in synapse formation and stabilisation (Fu, Washbourne et al. 2003), and have been shown to regulate excitatory and inhibitory balance in neurons (Prange, Wong et al. 2004).

Name	Function	Reference
NCAM	• Homophilic and heterophilic interactions • Maturation and strength of excitatory synaptic connections	(Sytnyk 2002) (Dityatev 2000)
Neuroligin-1	• β-neurexin recruits synaptic vesicles • Neuroligin-1 binds PSD-95 and promotes recruitment of NMDA receptors • Neuroligin 1 localised to excitatory synapses • Neuroligin-1 over-expression increases excitatory synaptic responses and potentiates NMDA and AMPA receptor ratios	(Dean 2003) (Fu 2003) (Song 1999) (Prange 2004)
Neuroligin-2	• Neuroligin-2 localised to inhibitory synapses • Over-expression increases inhibitory synaptic response	(Varoqueaux 2006) (Chih 2005)
PSD-95	• PSD-95 overexpression enhanced excitatory synapse size, and reduced number of inhibitory synapses.	(Prange 2004)
SynCAM	• Induces formation of presynaptic terminals • Homophilic interactions • Over-expression promotes excitatory synaptic transmission	(Fu 2003) (Biederer 2002)

Table 1.5: Cell adhesion and scaffold proteins involved in synapse formation
Table compiled from:(Song, Ichtchenko et al. 1999; Dityatev, Dityateva et al. 2000; Biederer, Sara et al. 2002; Sytnyk, Leshchyns'ka et al. 2002; Dean, Scholl et al. 2003; Fu, Washbourne et al. 2003; Prange, Wong et al. 2004; Chih, Engelman et al. 2005; Varoqueaux, Aramuni et al. 2006)

The number of excitatory versus inhibitory contacts that a single neuron receives dictates neuronal excitability and function (Schummers, Marino et al. 2002). This means that a precise control system must be established in each neuron to maintain the appropriate number of excitatory and inhibitory inputs. The interplay between excitation and inhibition seems to play an important role in moulding of synapse formation and studies have begun to identify proteins that are important in differential stabilisation of glutamatergic and GABAergic synapses and the determinants of the late stages of synapse formation. These molecules are listed in table 1.5. They include several classes of important trans-synaptic signalling molecules well placed to provide molecular interactions that mature synapse stabilization.

1.7.3 Neurexin-Neuroligin

Interactions between presynaptic β neurexins and postsynaptic neuroligins have been shown to promote synapse formation (Scheiffele, Fan et al. 2000; Prange, Wong et al. 2004). Furthermore, different neuroligin isoforms have also been shown to preferentially affect the formation of either excitatory or inhibitory synapses by co-ordinating the assembly of the relevant presynaptic and postsynaptic machinery (Futai, Kim et al. 2007). The trans-synaptic signalling proteins may therefore be able to translate the developmental patterns of synaptic activity into circuit formation.

Neuroligins 1-4 are active early in development and in a calcium dependent manner the extracellular domains of neuroligins bind to the extracellular domain of neurexin (Rao, Harms et al. 2000; Dean, Scholl et al. 2003)

During synapse development there is evidence that the postsynaptic cell may be 'instructive' to the presynaptic cell. Support for this notion comes from research showing that the postsynaptic cell can signal retrogradely to the presynaptic cell to affect vesicle number and release probability (Prange, Wong et al. 2004; Futai, Kim et al. 2007; Gottmann 2008; Kang, Zhang et al. 2008).

In vitro studies have shown that the expression of individual neuroligins is sufficient to alter the density of excitatory and inhibitory synapses. Specifically Neuroligin 1 has been shown to affect excitatory synapses and neuroligin 2 influences inhibitory synapses (Chubykin, Atasoy et al. 2007). Over expression of neuroligin 1 in hippocampal neurons increases excitatory neuronal synapses and excitatory activity was not enhanced by the $GABA_A$ receptor blocker bicuculline as it was in wild type neuronal cells. This was suggested to be due to a greater excitatory input at activated synapses, and therefore removing inhibition had less of an effect (Dahlhaus, Hines et al. 2010).

Neuronal network formation, development and maturation of both excitatory and inhibitory neuronal cells have been shown to be important for the generation of synchronized network activity both *in vivo* and *in vitro* (Voigt, Opitz et al. 2001; Sohal, Zhang et al. 2009). Section 1.8 highlights the importance of excitatory and inhibitory

neuronal development and the types of microcircuit interactions occurring to regulate neuronal network activity in the brain.

1.8 Mature network activity is formed of co-ordinated network oscillations

The brain cognitive functions rely on the co-ordination of large numbers of neurons that are distributed across functionally specialised brain areas. The synchronization of neuronal discharges has been proposed as a possible mechanism to dynamically connect together widely distributed sets of neurons into neuronal ensembles (Buzsaki and Chrobak 1995). Neuronal synchrony is also likely to be important for the large scale interactions between cortical cells in different areas (Brecht, Singer et al. 1998).

1.8.1 Hippocampus as an example of a cortical specialisation

Neurons in the cortical areas, including the hippocampus, can be divided into two major classes: principal (pyramidal, mossy and granule) cells and non- principal cells or interneurons. Principal cells comprise the majority (~80%) of the neuronal population; they are glutamatergic excitatory neurons and send axonal collaterals to other brain regions. GABAergic inhibitory cells are generally characterised by dense local axonal arbors which allows them to control and co-ordinate the activity of large populations of locally active neurons (Kawaguchi and Kondo 2002).

The hippocampus is one of the best studied microcircuits in the brain; it can be subdivided into the dentate gryrus, CA3, CA2 and CA1 regions and forms a well characterised tri-synaptic excitatory loop (Figure 1.12). Excitatory to excitatory (E-E) connections transmit the information processed by the dentate gyrus (DG) to the CA3 pyramidal cells via mossy fibres and the principal cells in the CA3 then project their output to the CA1 principal cells via the Schaffer collateral pathway. However, the tri-synaptic pathway has many divisions of excitatory to inhibitory (E-I), inhibitory to excitatory (E-I), excitatory to excitatory (E-E) and inhibitory to inhibitory (I-I) connections (Figure 1.13). These are listed in table 1.6 and illustrate the increased complexity that underpins the out-puts of the hippocampal circuit. These principles apply in the other microcircuits and systems that make up the brain.

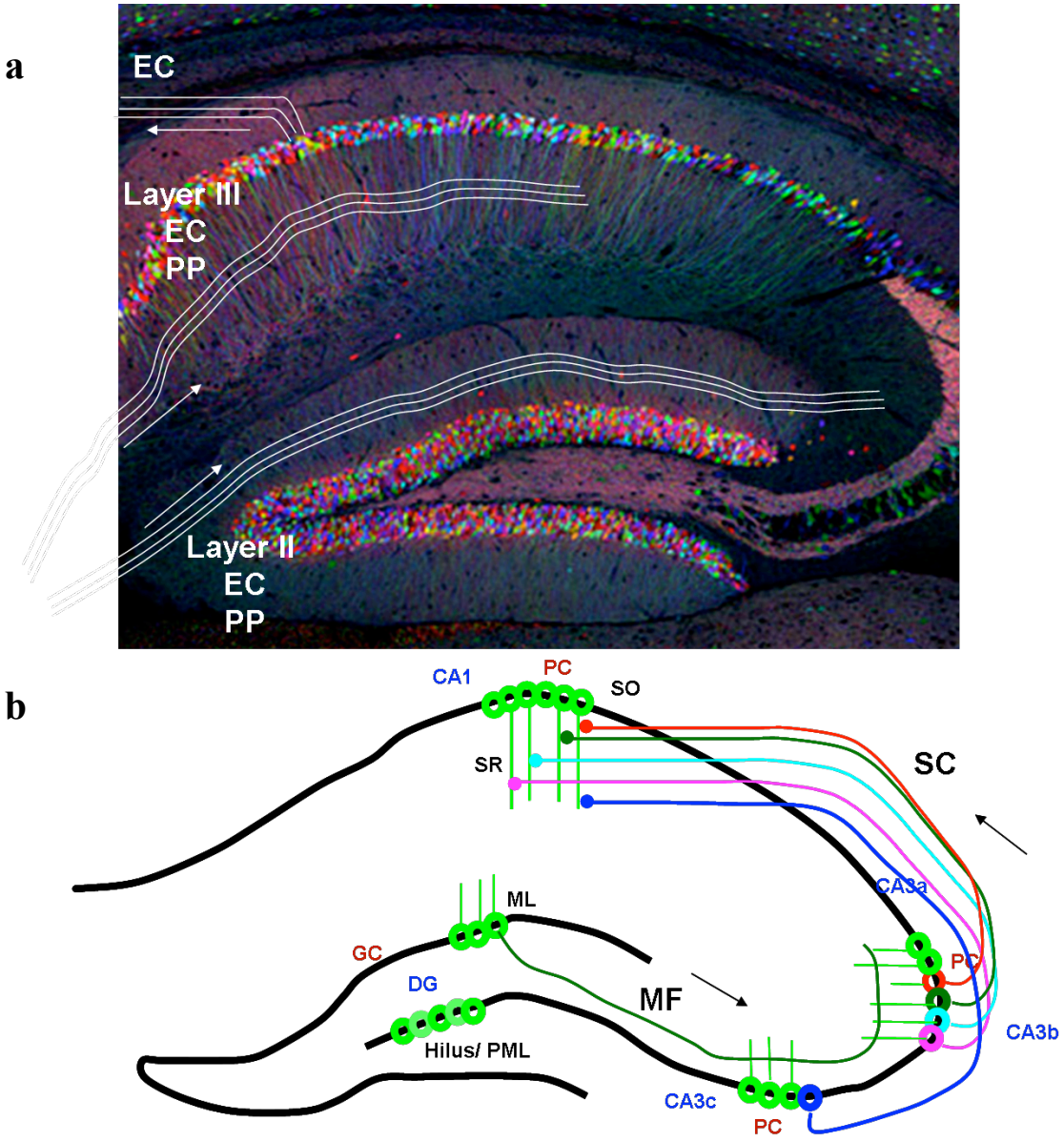

Figure 1.12: The Hippocampal formation

a) Layer II of the entorhinal cortex (EC) projects to the Granule cells (GC) and the CA3 Pyramidal cells (PCs) via the perforant pathway (PP). Layer III pyramidal cells from the entorhinal cortex also innervate the CA1. CA1 pyramidal cells send afferent outputs back to the entorhinal cortex. Adapted from (Livet, Weissman et al. 2007).

b) The granule cells in the dentate gyrus send axon collaterals to the CA3 (mossy fibres (MF). CA3 pyramidal cells are strongly interconnected by recurrent axon collaterals and innervate the CA1 via the Shaffer collateral pathway. Pyramidal Cells in the CA3a innervate the Stratum radiatum and oriens and have a bias for adjacent segments of CA1. CA3b cells terminate mainly in stratum radiatum and predominantly terminate in the intermediate areas of CA1. CA3c innervate the stratum radiatum with a preference for the distal segments. (Freund and Buzsaki 1996)

Connection	Location/ Cell type	Reference
I-I	• Between basket cell	1
E-E	• DG granule cells to CA3 PC via mossy fibres • CA3 PC to CA1 PC via Shaffer collaterals	7 8
Feedback inhibition	• CA1 PC innervation of O-LM interneurons, EPSC in O-LM cell feeds-back to inhibit PC in distal dendrites of SLM.	2 3 4
Feedfoward inhibition	• PP innervation of CA1 PC at the same time as innervating interneurons in SLM layer, interneurons subsequently inhibit CA1 PCs	2 3 4 5
Excitatory recurrent collateral	• Between CA3 PCs	6

Table 1.6: Examples of microcircuit synaptic connections in the hippocampus
PC- Pyramidal cells, O-LM-oriens lacunosum moleculare interneurons, EPSP- Excitatory postsynaptic potential, SLM- stratum lacunosum-moleculare
1=(Bartos, Vida et al. 2001) 2= (Sloviter 1991) 3=(Elfant, Pal et al. 2008) 4=(Somogyi and Klausberger 2005) 5=(Remondes and Schuman 2002) 6=(Bains, Longacher et al. 1999) 7=(Christie and Jahr 2006) 8=(Chicurel and Harris 1992)

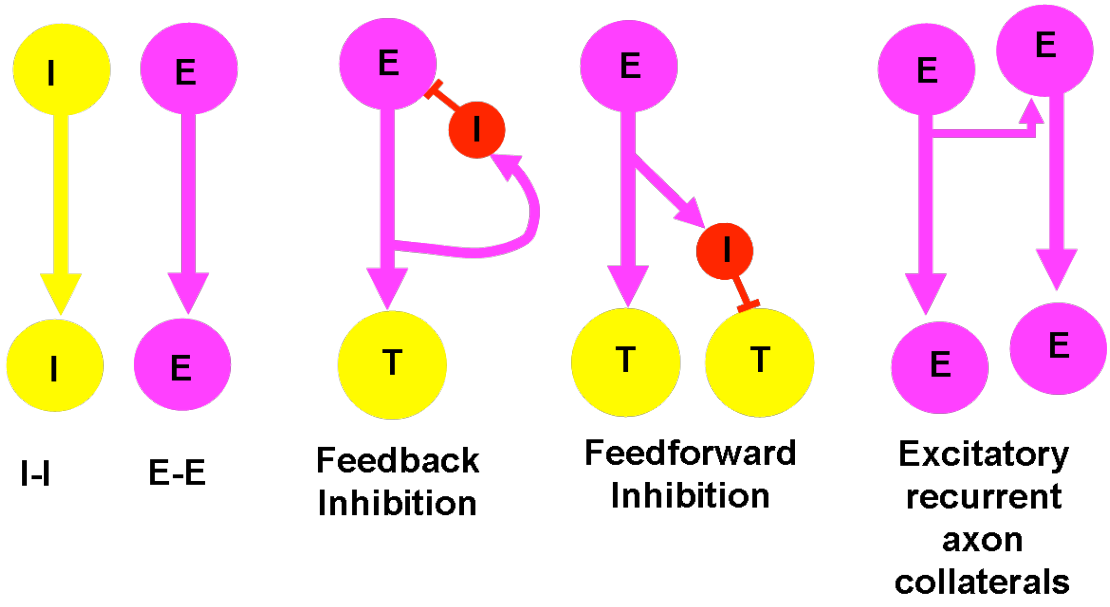

Figure 1.13: Microcircuit connections
Neuronal microcircuits are underpinned by interactions between conventional excitatory and inhibitory connections. Inhibitory neurons synapse onto other inhibitory neurons, inhibitory cells also communicate with one another via gap junctions which are important in generating network oscillations (Fukuda and Kosaka 2000). Excitatory to excitatory connections are for example found in the hippocampal CA3 pyramidal cells to the CA1 pyramidal cell via the Schaffer collateral excitatory input. Feedback and feedforward inhibition also occur between excitatory and inhibitory neurons to control excitation onto target (T) cells. Excitatory recurrent collaterals like those seen in the CA3 region of the hippocampus are depicted and these recurrent collaterals are thought to aid the generation of oscillatory activity before it is transferred to the CA1.

Intrinsic E-E are formed in the CA3 by recurrent axonal projections and connections between the CA3 to CA1 are highly divergent, with one CA3 PC contacting ~30,000 sites mainly in the CA1 (Li, Somogyi et al. 1994). The high degree of divergence from CA3 to CA1 favours the rapid synchronization of the CA1 principal cells population (Csicsvari, Hirase et al. 2000). Further complexity in the CA3 region occurs because the principal cells are not homogenous, axon collaterals in the CA3a and b give rise to extensive recurrent collaterals confined to the CA3, whereas CA3c principal cells mostly project to the CA1 via shaffer collateral axons. The recurrent activity in sub-regions of the CA3 has been proposed to allow gamma oscillations to emerge in the recurrent collaterals of the CA3a and b principal cells which can then subsequently recruit the CA3c region which in turn can entrain the CA1 region (Csicsvari, Jamieson et al. 2003).

1.8.2 Oscillatory activity in the hippocampus

The hippocampal microcircuits are able to generate oscillating rhythms of activity which co-ordinate large groups of neurons to fire in a precise temporal pattern. Oscillating rhythms are also described for the spinal cord and other cortical circuits (Sanchez-Vives and McCormick 2000; Bartos, Vida et al. 2002; Demir, Gao et al. 2002; Bartos, Vida et al. 2007). Oscillations in cortical structures like the hippocampus are believed to provide temporal windows to correlate coherently co-operating neuronal assemblies for the processing, storage, and retrieval of information (Sederberg, Schulze-Bonhage et al. 2007). The hippocampus is able to generate different types of rhythmic synchronized activity at a range of frequencies, Theta (4-12Hz), Beta (15-30 Hz), gamma (30-80 Hz) and ultra fast oscillations (90-200 Hz) (Ylinen, Soltesz et al. 1995; Buhl, Harris et al. 2003; Maier, Nimmrich et al. 2003).

Gamma oscillations have received a lot of attention because of their relationship to higher brain functions and are particularly important for the storage and recall of information (Sederberg, Kahana et al. 2003). Disruption of gamma oscillations has been shown to occur in some psychiatric disorders such as schizophrenia (Spencer, Nestor et al. 2003; Gonzalez-Burgos, Hashimoto et al. 2010; Jones 2010) and GABAergic neurons have been shown to be highly important for the generation of gamma oscillatory activity (Traub, Kopell et al. 2001; Bartos, Vida et al. 2002).

Parvalbumin positive fast spiking interneurons (Section 1.1.1) have been shown to play an important role in gamma oscillatory activity (Fuchs, Zivkovic et al. 2007; Sohal, Zhang et al. 2009), because of their perisomatic inhibition, fast firing kinetics (~100Hz) (Ylinen, Bragin et al. 1995) and intricate electrical connections through gap-junctions to other basket cells. The gap junction connections enable the basket cells to interact with one another and efficiently entrain the principal cells (Hormuzdi, Pais et al. 2001). Selective knockout of the predominant AMPA receptor (GluR4(D)) in parvalbumin neurons or using GluR1(A)$^{PVCre-/-}$ in mice has shown that parvalbumin positive interneurons play a critical role in the output timing of pyramidal cells. These mice demonstrated reduced power of gamma band oscillations, showing the effect of insufficient recruitment of fast spiking cells in network activity (Fuchs, Zivkovic et al. 2007).

In the preceding introduction I have highlighted how molecular and cellular components are used to organize excitation and inhibition in the nervous system and the significance of these sub-systems for network activity. I have also described the core mechanism of synaptic communication through the exocytosis of synaptic vesicles, and the different modes of endocytosis required to replenish vesicle stores. Using this as a platform I have then detailed how this core mechanism varies in subtypes of neuronal cells which adapts them for their distinct functions. In the following sections I will discuss what happens when network activity is disrupted and how molecular lesions of synaptic proteins can lead to neuronal dysfunction and degeneration.

1.9 Network and synaptic dysfunction

As the mechanisms involved in synapse formation and neuronal network function are revealed the causes of neuronal dysfunction in neurodegenerative diseases such as Alzheimer's disease are being tracked back to, or associated with, molecular and synaptic changes. Neurodegeneration is no longer seen only to manifest as a consequence of cell death but can be related to a host of synaptic, glial, and neuronal network changes that occur before the neuronal cells are lost. *In vitro* culture models and genetically manipulated mouse models of neurodegenerative diseases have played an important role in developing the understanding that supports the concept of dysfunction preceding neuronal loss or leading to network activity changes (Cepeda, Hurst et al. 2003; Gutierrez, Hung et al. 2009).

1.9.1 Synapse loss

Support for an early synapse loss in neurodegenerative disease comes from a host of pathologies (Table 1.7). Synapse loss in Alzheimer's disease patients has also been shown to correlate better with cognitive changes than plaque and tangle formation (Terry, Masliah et al. 1991; Coleman and Yao 2003). Synapse loss and protein alterations have also been shown to occur in Prion disease, Huntington's disease and Amyotrophic Lateral Sclerosis (Sze, Troncoso et al. 1997; Larson, Lynch et al. 1999; Sze, Bi et al. 2000; Cepeda, Hurst et al. 2003; Cunningham, Deacon et al. 2003; Siskova, Page et al. 2009) .

Model	Synaptic dysfunction	Reference
Prion disease	• Early synapse loss • Spine loss	(Cunningham et al 2001) (Fuhrmann, Mitteregger et al. 2007) (Siskova, Page et al. 2009)
Alzheimer's disease	• Cognitive changes • Synapse loss • Defect in plasticity/ synaptic transmission	(Coleman et al 2003) (Terry et al 1991) (Sze 1997) (Sze 2000) (Koffie, Meyer-Luehmann et al. 2009)
Huntington's disease	• Early loss of synaptophysin and PSD-95 • Reduction in Complexin II • Abnormal phosphorlaytion of synapsin • Alterations in exocytosis and endocytosis	(Cepeda 2003) (Morton and Edwardson 2001) (Lievens, Woodman 2003) (Li, Plomann 2003)
Amyotrophic Lateral Sclerosis	• Selective early loss of fast-fatigable neuromuscular junction synapses	(Frey, Schneider et al. 2000)

Table 1.7: Synaptic loss as an early dysfunction before neuronal loss in neurodegenerative diseases

Network changes have also been shown to occur in some of the neurodegenerative diseases outlined above, which in some cases have been suggested to occur due to loss of specific subtypes of neuronal cells (Palop, Chin et al. 2007). Neuronal network dysfunction has also been shown to occur in developmental disorders such as Schizophrenia and Autism (Zhang and Reynolds 2002; Lewis, Hashimoto et al. 2005).

1.9.2 Network dysfunction

Selective alterations in interneuron diversity have been reported in human brains from patients who suffered from psychiatric disorders. Investigations of the frontal cortex of schizophrenic patients demonstrated a deficit in the GABAergic interneurons, which was due to a selective decrease of a subtype of inhibitory neuron the parvalbumin positive cells (Zhang, Sun et al. 2002; Lewis, Hashimoto et al. 2005).

Current studies investigating the network dysfunction in autism suggest that the dysfunction may be due to decreased neural synchrony and an imbalance between excitation and inhibition, which leads to hyperexcitability and unstable cortical networks (Hussman 2001; Rubenstein and Merzenich 2003; Gutierrez, Hung et al. 2009).

1.10 Cysteine String Knock Out paradigm: A mouse a model to study synaptically driven network dysfunction

Cysteine string protein alpha (CSPα) is a presynaptic protein which is thought to have chaperone-like functions in the synaptic vesicle cycle regardless of transmitter type. It has been shown to be important in maintaining synaptic function in synapses with high activity levels (Fernandez-Chacon, Wolfel et al. 2004; Schmitz, Tabares et al. 2006; Garcia-Junco-Clemente, Cantero et al. 2010). Selective vulnerability of more active synapses has been shown in motor neuron disease (Frey, Schneider et al. 2000), and in other genetically altered mice which lack proteins associated with the core function of the presynaptic nerve terminal (Hayashi, Raimondi et al. 2008; Gibson, Huber et al. 2009). Hence CSPα -/- mice may present a model to study network activity and investigate if network changes due to synapse dysfunction in more active neurons leads to network changes.

CSP was originally discovered in *Drosophila* in 1990 (Zinsmaier, Hofbauer et al. 1990), it is an evolutionarily conserved synaptic vesicle membrane protein. Three CSP isoforms have been identified in mice, α, β, and γ. CSPα has been shown to be synaptically expressed, whereas the expression of CSPβ and γ is thought to be mainly testicular (Fernandez-Chacon, Wolfel et al. 2004). Analysis of the proteins sequence of CSP has revealed three distinct regions, an N-terminal J-domain, a central Cysteine rich region containing a high density of cysteine residues and a Linker (L) domain (Figure 1.14).

The J Domain contains a Dna J domain which has highly conserved identity between species. A number of proteins containing J-domains have been shown to bind to and regulate members of the heat-shock protein 70kDa (Hsp70) chaperone family, which amongst other functions is involved in protein folding in vesicle endocytosis and recycling (Jiang, Gao et al. 2000) (Section 1.4).

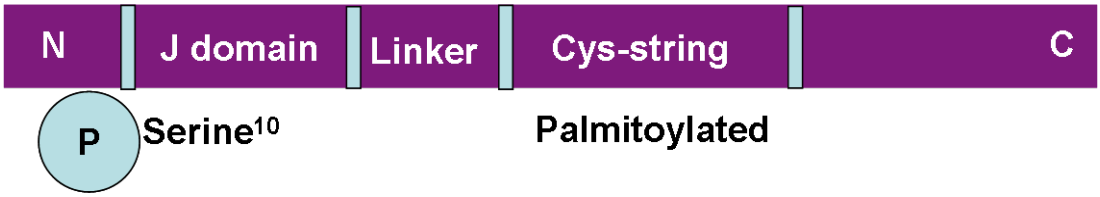

Figure 1.14: The domains of cysteine string protein α
Schematic of the domains of CSPα, showing the Phosphorylation site at Serine 10 which reduces binding to syntaxin and synaptotagmin (Evans, Wilkinson et al. 2001; Evans and Morgan 2002), and palmitoylated cysteine string domain.

CSP is associated with synaptic vesicles in neurons and makes up approximately 1% of total vesicle protein (~8 monomers/ vesicle) (Mastrogiacomo, Parsons et al. 1994; Chua, Kindler et al. 2010). CSP is also present on secretory granules in non-neuronal cells (Brown, Larsson et al. 1998; Zhang, Kelley et al. 1999).

Genetic studies of the single copy of CSP in *Drosophila* and CSPα in mice revealed that CSP is important for regulated neurotransmitter release and sustained synaptic function, as in the absence of this protein neurons exhibit presynaptic degeneration (Zinsmaier, Eberle et al. 1994; Fernandez-Chacon, Wolfel et al. 2004; Schmitz, Tabares et al. 2006; Garcia-Junco-Clemente, Cantero et al. 2010).

1.10.1 Neuronal dysfunction in CSP null *Drosphila*

CSP null flies die as larvae or within 4-5 days of adulthood. The flies that survive to adulthood (4%) are characterised by a temperature sensitive paralysis, sluggishness, spasmic jumping, shaking, and a shortened life span (Zinsmaier, Eberle et al. 1994). Presynaptic defects include: a marked deficit in release, a reduced ability to maintain normal presynaptic calcium levels, and a reduction in the number of synaptic boutons at

the neuromuscular junction (Umbach, Zinsmaier et al. 1994; Dawson-Scully, Bronk et al. 2000; Dawson-Scully, Lin et al. 2007).

1.10.2 Neuronal dysfunction in CSPα-/- mice

Mice lacking CSPα die within 3 months of birth and degeneration has been observed in a number of synaptic structures. Deficits in growth and movement appear after 2-3 weeks when the mice begin to suffer from progressive weakness and stop gaining weight (Fernandez-Chacon, Wolfel et al. 2004). Neuronal degeneration of the nmj, Calyx of Held, ribbon synapses of the photoreceptors, and the parvalbumin positive interneurons has been described (Fernandez-Chacon, Wolfel et al. 2004; Chandra, Gallardo et al. 2005; Schmitz, Tabares et al. 2006; Garcia-Junco-Clemente, Cantero et al. 2010).

1.10.3 Functions of Cysteine String Protein

The molecular role of CSP is likely to be due to its biochemical function as a co-chaperone of Hsc70, these functions are summarised in table 1.8. CSP has a conserved J domain with which it is able to bind and stimulate the ATPase activity (Tobaben, Thakur et al. 2001; Tobaben, Varoqueaux et al. 2003). In a complex with small glutamine-rich tetratricopeptide repeat-containing protein (SGT) and Hsc70, CSP has been shown to stimulate the ATPase activity of Hsc70 19 fold (Tobaben, Thakur et al. 2001; Tobaben, Varoqueaux et al. 2003). SGT alone is also able to stimulate the ATPase activity of Hsc70, but only by 3 fold (Tobaben, Varoqueaux et al. 2003). CSP also contains a cysteine rich domain, which is heavily palmitoylated, and localises CSP to the vesicular membrane (Chamberlain and Burgoyne 1998). The localisation of CSP may act to recruit the SGT and Hsc70 chaperone complex for regulation of vesicle release.

Consistent with a role in vesicle mediated transmitter release CSP and Hsc70 are required for regulated neurotransmitter release at synaptic terminals. Studies in *Drosophila* have shown that CSP null mutants have impaired nmj evoked release (Heckmann, Adelsberger et al. 1997; Umbach and Gundersen 1997; Dawson-Scully, Bronk et al. 2000; Dawson-Scully, Lin et al. 2007). Vesicle run-down due to mis-localisation of Hsc70 from the vesicle membrane and dysfunction in vesicle recycling would be plausible considering the role of Hsc70 in vesicle endocytosis (Section1.4.1), however, this does not seem to be the case (Umbach and Gundersen 1997; Ranjan, Bronk et al. 1998). Instead evidence suggests

the chaperone complex regulates exocytosis downstream of calcium entry and aids coupling of calcium influx to the exocytotic machinery (Dawson-Scully, Bronk et al. 2000; Dawson-Scully, Lin et al. 2007; Ruiz, Casanas et al. 2008).

1.10.4 CSP and Ca^{2+} secretion coupling

Vesicle mediated release is rescued by increasing the extracellular calcium concentration at both the fly and mouse nmjs (Dawson-Scully, Bronk et al. 2000; Ruiz, Casanas et al. 2008). A rightward shift in the calcium dependence of evoked release suggests that the CSP activities modulate the calcium sensitivity of release. These studies are further supported by an investigation in PC12 cells, which demonstrated that over-expression of CSP in these cells increased calcium stimulated exocytosis (Chamberlain and Burgoyne 1998).

Interestingly, stimulation using depolarisation independent release mechanism, black widow spider venom (bwsv) or calcium ionophores, did not prevent evoked release. This further suggests that the vesicles are capable of exocytosis but a defect in excitation-secretion coupling in the absence of CSP leads to malfunction of evoked exocytosis (Ranjan, Bronk et al. 1998).

Further support for the CSP chaperone complex in regulating the calcium sensitivity of evoked release comes from mutational studies showing that mutations in *Drosophila* Hsc4 have the same impairment in exocytosis as CSP null *Drosphila (Bronk, Wenniger et al. 2001)*. Hsc4 is the closest homologue to Hsc70 in *Drosophila*, and mutation of this protein leads to thermo-intolerant loss of evoked but not spontaneous release, decreased calcium sensitivity of evoked release, increased facilitation of neurotransmitter release and rescue of evoked release by increasing the extracellular calcium concentration (Bronk, Wenniger et al. 2001). All of these defects have also been reported for CSP null *Drosophila* and in some cases CSP null mice (Dawson-Scully, Bronk et al. 2000; Ruiz, Casanas et al. 2008). This suggests that the two proteins, Hsc70 and CSP function in the same signalling pathway and together function to increase or sustain the calcium sensitivity of calcium triggered vesicle fusion (Bronk, Wenniger et al. 2001).

1.10.5 CSP, SNARES and Synaptotagmin

Further support for CSP's function in calcium triggered vesicle release comes from studies demonstrating the binding of CSP to synaptotagmin, the calcium sensor in the presynaptic terminal (Section 1.3.10) and the SNARE proteins (Section 1.3.3) involved in vesicle fusion and neurotransmitter release (Nie, Ranjan et al. 1999; Evans, Wilkinson et al. 2001; Evans and Morgan 2002; Boal, Laguerre et al. 2010). CSP has also been shown to interact with the 'synprint' site on the P/Q calcium channel to regulate calcium influx (Leveque, Pupier et al. 1998) and modulate calcium channel activity through G-Proteins (Magga, Jarvis et al. 2000). The regulation becomes quite complex when one considers that syntaxin has also been shown to modulate calcium channel activity by binding to the same site as CSP (Swayne, Beck et al. 2006) and that the interaction between CSP and synaptotagmin and syntaxin is regulated by phosphorylation of CSP on Serine 10 by PKA (Figure 1.14) (Evans, Wilkinson et al. 2001; Evans and Morgan 2002).

1.10.6 CSP and vesicle targeting

CSP has also been suggested to localise the Rab-specific αGDP-dissociation inhibitor (αGDP) to synaptic vesicles through its binding to Hsc70 and Hsp90 to CSP. Rab3A is a small GTPase which facilitates the targeting and fusion of vesicles with their target membrane (Sakisaka, Meerlo et al. 2002). αGDI binds the Rab-GDP and dissociates the protein from the vesicle membrane so that it can undergo multiple rounds of vesicle targeting. Lack of CSP on the vesicle membrane may lead to a dysfunction in the Rab mediated vesicle targeting to the active zone. However, Dawson-Scully et al found that there was no impairment in the number of docked or clustered vesicles at the active zone nmj synapse *Drosophila* larvae (Dawson-Scully, Lin et al. 2007).

1.10.7 CSP and Neurotransmitter loading

Additionally through a mutual interaction with Hsc70, CSP has been implicated in the regulation of GABA uptake into synaptic vesicles. Hsc70s binds directly with the synthesising enzyme glutamate decarboxylase (GAD), therefore CSP could act to tether the Hsc70-GAD complex to the synaptic vesicle surface promoting vesicular uptake of GABA (Jin, Wu et al. 2003). These functions are summarised in table 1.8.

1.10.8 Use dependent degeneration of synapses in CSPα-/- mice

In CSPα -/-mice the degeneration of the nmj, calyx of Held, ribbon synapses of the photoreceptors and the parvalbumin positive interneurons has been shown to occur in the absence of degeneration of the less active slower firing glutamatergic pyramidal cells of the hippocampus, and also the tonically active ribbon synapses of the bipolar cells, and the ribbon synapses of the inner hair cells (Fernandez-Chacon, Wolfel et al. 2004; Schmitz, Tabares et al. 2006; Garcia-Junco-Clemente, Cantero et al. 2010).

The calyx synapses (Section 1.5.4), parvalbumin-positive interneurons, and the basket cells, fire at frequencies over 100Hz (Ylinen, Bragin et al. 1995; Hermann, Pecka et al. 2007). The ribbon synapses and the nmj are also highly active synapses, and together the degeneration of these synapses led to the hypothesis that in the absence of CSPα neuronal synapses which have high use-dependent stresses are susceptible to degeneration without the chaperoning function of CSPα (Fernandez-Chacon, Wolfel et al. 2004).

Use-dependent degeneration CSPα-/- mice is supported by the lack of degenerative changes in the glutamatergic hippocampal pyramidal synapses which trigger action potentials at much lower frequency (1Hz) (Csicsvari, Hirase et al. 1999; Frerking, Schulte et al. 2005). Functional redundancy between CSPβ, which is expressed in the hair cells, and CSPα was suggested to compensate for the loss of CSPα in the hair cells and was able to protect them from neurodegeneration (Schmitz, Tabares et al. 2006).

Lack of CSPα and the subsequent degeneration of the rod and cone photoreceptors have been suggested to occur in isolation to the bipolar cells because degeneration of the photoreceptors would subsequently lead to loss of synaptic input, and therefore less use-dependent stress in the bipolar cells (Schmitz, Tabares et al. 2006).

Function	Method	Reference
Prevention of neuronal degeneration	Mice, and hippocampal dissociated cultures	25,26,27,28
Co-chaperone function activating Hsc70 ATPase activity	Luciferase refolding assay Synaptosomes- rabbit brain Yeast two-hybrid screen	1, 2, 3, 4
Interaction with P/Q calcium channels via 'synprint' site	Rabbit brain GST fusion proteins	5
Interaction with Syntaxin	PC12, Chromaffin cells, *Drosophila*	14, 19, 20
Interaction with synaptobrevin	Rabbit brain GST fusion proteins	5, 30
Interaction with synaptotagmin		18, 29
Activation of G-protein mediated N type calcium channel inhibition	HEK cells GST fusion proteins	6, 7
Guanine nucleotide exchange factor specific for $G\alpha_s$	HEK cells	16
Regulation of exocytosis downstream of calcium entry- calcium sensitivity of release	*Drosophila*-nmj Mouse-nmj	9, 10, 11, 12, 13
Coupling GABA synthesis to synaptic vesicles	Complex purified on a anti GAD_{65} affinity column	17
Rab vesicle recycling		21
Effects exocytosis, without regulation of calcium channels	Insulin secreting β-cell, PC12 cells	22, 23, 24

Table 1.8: Functions of Cysteine String Protein

CSP has been shown to be crucial for neurotransmitter release and preventing neuronal degeneration. The best characterised molecular function of CSP relate to its J-domain and its ability to activate the ATPase activity of Hsc70 (1, 2, 3, 4, 8,). The CSP molecular chaperone complex has been suggested to function in the late stages of exocytosis upstream of calcium entry (9, 10, 11, 12, and 13). CSP has been shown to interact with many synaptic proteins including the SNARE proteins (14,19,20,5), N and P/Q type calcium channel, to modulate calcium channel activity either directly or by G-protein modulation (5,6,7). However, studies in permeabilised cells have suggested that the exocytosis dysfunction is not due to calcium channel deregulation but a dysfunction in the late stages of exocytosis itself (22, 23, and 24). This is supported by lack of evidence for calcium channel dysfunction in CSP mutant mice (28), and a lack of deregulation in calcium channels in mutant *Drosophila* peptidergic terminals (8). CSP has also been suggested to localise the GABA synthesising enzyme GAD_{65} and αGDI a Rab specific dissociation inhibitor to synaptic vesicles through interactions with Hsc70 (17, 21). CSP has also been shown to act as a Guanidine exchange factor for $G\alpha_s$ the only known GEF for $G\alpha_s$, and suggests that the CSP chaperone complex may also regulate exocytosis through cAMP and PKA activation (16). Several studies have also identified a role for the L (linker) domain in exocytosis and binding to the SNARE synaptobrevin (30) and calcium sensor synaptotagmin-9 (29).

1= (Chamberlain and Burgoyne 1997), 2= (Tobaben, Thakur et al. 2001), 3= (Tobaben, Varoqueaux et al. 2003), 4= (Braun, Wilbanks et al. 1996), 5= (Leveque, Pupier et al. 1998), 6= (Miller, Swayne et al. 2003), 7= (Magga, Jarvis et al. 2000), 8= (Morales, Ferrus et al. 1999), 9= (Ruiz, Casanas et al. 2008), 10= (Dawson-Scully, Lin et al. 2007), 11= (Dawson-Scully, Bronk et al. 2000), 12= (Ranjan, Bronk et al. 1998), 13= (Umbach and Gundersen 1997), 14= (Evans, Wilkinson et al. 2001), 16= (Natochin, Campbell et al. 2005), 17= (Jin, Wu et al. 2003), 18= (Evans and Morgan 2002), 19= (Nie, Ranjan et al. 1999), 20= (Wu, Fergestad et al. 1999), 21= (Sakisaka, Meerlo et al. 2002), 22= (Brown, Larsson et al. 1998), 23= (Zhang, Kelley et al. 1998), 24= (Zhang, Kelley et al. 1999), 25= (Chandra, Gallardo et al. 2005), 26= (Schmitz, Tabares et al. 2006), 27= (Garcia-Junco-Clemente, Cantero et al. 2010), 28= (Fernandez-Chacon, Wolfel et al. 2004), 29=(Boal, Laguerre et al. 2010), 30=(Boal, Zhang et al. 2004)

Further support for the concept that high synaptic activity is a major factor in increased nerve terminal vulnerability in the absence of CSPα comes from the fact that inhibiting excitatory neuronal network activity prevents *in vitro* degeneration of the fast spiking parvalbumin positive interneurons (Garcia-Junco-Clemente, Cantero et al. 2010).

Investigations of the network dysfunction in the CSPα-/- mouse may provide insight into the changes that occur in the neuronal network due to loss of cells capable of firing at high frequencies. The loss of such a cell type leading to reduced neuronal functional heterogeneity, particularly if they are minor cell types, might be best manifested in network-wide effects. Loss of the fast firing inhibitory neuronal cells, in a neuronal network in which the output of excitatory cells is finely controlled is important for network activity (Fuchs, Zivkovic et al. 2007) and the health of the animal (Powell, Campbell et al. 2003; Cobos, Calcagnotto et al. 2005).

In this thesis I will describe investigations which have established methods to allow investigation of function and dysfunction in an *in vitro* mimic (the Hi-Spot) of neural function encompassing a range of cell types. The work will include optimisation of this culture method for both rat and mouse tissue. The technical approaches here established with a view to testing if discrete molecular lesions can inform on the core mechanism of neuronal function and how it can be modified to achieve discrete changes in neuronal function. The experimental focus will develop the recent understanding of the role of CSP mediated synaptic dysfunction in the context of neuronal dys-regulation in an artificial but complex *in vitro* neural circuit.

1.11 Aims

- To firstly build on the work of Van Vliet et al 2007 by making Hi-Spot cultures from embryonic rat brain tissue and characterising their development and maturation of the neuronal and glia cells in the cultures.
- Secondly to produce Hi-Spots from postnatal rat tissue and assess if the same culturing protocol used to produce Hi-Spots from embryonic tissue can be used to produce Hi-Spots from postnatal tissue. Additionally to assess if postnatal Hi-Spots contain a maturing population of neuronal and glial cells.
- Aggregated cultures from embryonic tissue have previously been shown to develop spontaneous network activity, which was measured on a multielectrode array (van Vliet, Stoppini et al. 2007). In order to use the postnatal Hi-Spot cultures as an *in vitro* model of the brain the neuronal network formed must be functional. Therefore, the third aim is to investigate the development of the spontaneous network activity in postnatal Hi-Spots using extracellular multielectrode array recordings.
- The fourth aim is to progress the use of the Hi-Spot system from rat tissue to mouse tissue. Production of Hi-Spots from mouse tissue would have the added benefit of allowing Hi-Spots to be produced from different mouse mutants where specific synaptic proteins have been genetically ablated and their function in synaptic activity can be investigated.
- The last aim is to use the Hi-Spot culturing method adapted for mouse tissue to investigate the network changes occurring in cultures made from CSPα-/- mice using multielectrode array recordings and pharmacological intervention.

2 - General Methodologies

2.1 Hi-Spot Culture

Rats were time mated and plug checked to estimate the time of gestation. After 17 days post plug the dam was sacrificed and embryos extracted (E17), the embryos were killed using procedures in accordance with schedule one of the 1966 animal rights act. Whole brains were dissected from the rat brains and the cerebellum removed. The brains minus the cerebellum were then mechanically dissociated in Earle's Balanced Salt Solution. Debris was removed using a cell strainer (100μm mesh) and the viable cell number estimated using the trypan blue exclusion assay.

The mesh filtered cell suspension was centrifuged at 200g for 5 minutes and the cell rich pellet re-suspended in growth medium (Ham's F12 10% (Sigma), Foetal Bovine Serum 20% (Hyclone), Horse Serum 5% (GibcoBRL), Hepes 10mM (GibcoBRL), Glutamine 2mM (Sigma), Penicillin: streptomycin 50U/0.5mg (Sigma), DMEM high Glucose (15.6mmol/L) (Sigma) at a concentration of 50,000 live cells/μl (Figure 2.1 a).

Re-aggregated cell spots (Hi-Spots) were formed by pipetting 5μl of the cell suspension onto 6mm diameter PTFE (Teflon) membrane discs (Biocell-interface, SA) giving an estimated 250,000 live cells per Hi-Spot (Figure 2.1 a). PTFE discs had a pore size of 0.4μm and a thickness of ~30μm. The discs were placed onto the membranes of Millicell CM inserts in 6 well culture plates with 1000μl of growth medium per well, and incubated at 37°C in air with 5% CO2.

The Hi-Spot arrangement in the 6 well culture plate on top of a semi-permeable membrane insert is illustrated in Figure 2.1b. The suspension of neural tissue when spotted onto PTFE self-aggregates into a compact disc (Figure 2.1b). Western blot, immunohistochemistry and multielectrode array recordings (see sections 2.2, 2.6, 2.9) were conducted on cultures between *1* to *>28* Days in Vitro (*DIV)* as indicated in text and figure legends. Growth media was changed twice a week, never on the same day as electrophysiology recordings.

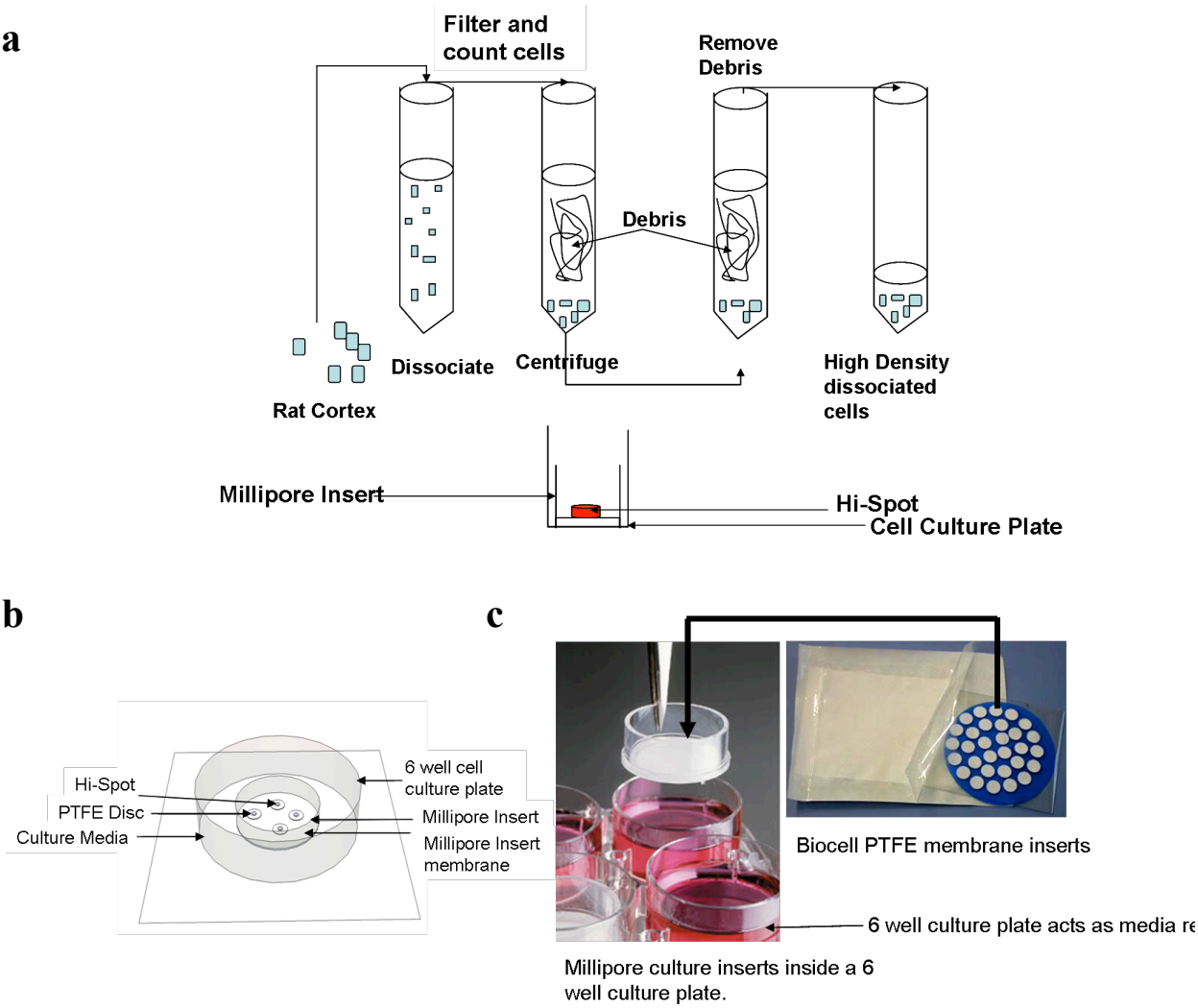

Figure 2.1: Hi-Spot protocol

a) Cortices dissociated to a single cell suspension were centrifuged to remove debris, re-aggregated and cells plated at high density with 250,000 live cells/ Hi-Spot. The Hi-Spots were plated at the liquid air interface onto a PTFE disc (diam ~6mm).

b) The layout of the Hi-Spots in a 6 well culture plate. Up to 5 Hi-Spots can be placed in a well. Hi-Spots sit on the moveable PTFE membrane, the PTFE membrane sits on a semi permeable Millipore culture insert. The Millipore culture insert sits in a well of a 6 well plate which acts as the media reservoir. Hi-Spots can be moved by picking up the PTFE membrane with fine forceps.

c) Photographic image of a 6 well culture plate with red culture media inside with a Millipore membrane insert held by forecepts. The 6 well culture plate acts as the media reservoir. The biocell PTFE membrane is places on top of the Millipore culture insert and allows the Hi-Spot to be cultured at the liquid- air interface.

2.2 Western Blot

Growth media was removed from culture wells and samples were harvested by lifting the Hi-Spots on the PTFE supports and putting them into homogenisation buffer at stated *DIV*. Homogenisation buffer was made using; SDS (2%w/v); Sodium Chloride (100mM) (Sigma); Hepes (20mM) (Sigma); Protease Complete Inhibitor (DAKO); pH 7.4.

2.2.1 Extraction of proteins

Hi-Spots were separated from the PTFE membrane disc by freeze/thaw and centrifugation (2 minutes; 200g) in homogenisation buffer. The PTFE membrane was removed and samples were centrifuged at 14,000rpm 4°C for 30 minutes before homogenisation in homogenisation buffer to extract proteins. Samples were stored at -20°C.

2.2.2 Poly- Acrylamide gel Electrophoresis

The BioRad mini protein II gel system was used for casting and running SDS- Poly-Acrylamide gel electrophoresis (PAGE) gels. All gels were run with a resolving and stacking layer. The resolving gel composition is listed in Table 2.1 and gel used indicate in figure legends. The resolving gels were poured carefully and overlaid with isopropanol until the acrylamide had polymerised.

% Gel	Acrylamide (30%)	3M TRIS (pH 8.8)	SDS (10%)	APS (10%)	Water (ddH_20)	TEMED
12.5	4.2ml	1.25ml	100µl	50 µl	Up to 10 mls	10µl
10	3.3ml	1.25ml	100µl	50 µl		10µl

Table 2.1: The method for mixing a resolving gel layer for SDS-PAGE gels
All percentages correspond to individual volumes within the final solution.
Acrylamide- 29:1, SDS- Sodium Dodecyl Sulphate, APS- Ammonium Persulphate, TEMED- N,N,N',N'-tetramethylethylenediamine

The isopropanol was then removed before addition of the stacking gel. A stock solution of stacking layer was made by combining 15% v/v of 30% Acrylamide (BioRad), 37.5% v/v 0.25M Tris (pH6.8) and 0.1% SDS in distilled water. Working solution of the stacking solution was made by combing 5ml of the stock solution with 0.01% v/v of 10% Ammonium persulfate (APS) and 0.02% v/v *N*,*N*,*N*′,*N*′-Tetramethylethylenediamine (TEMED). The stacking layer was poured over the polymerised resolving gel and a 10-well comb inserted until the gel set. BioRad short plates and back plates where used to cast the gels producing a gel thickness of 1.5mm.

To prepare cultures for SDS-PAGE, a stock solution of 5x sample buffer was made containing 312.5mM TRIS (pH6.8) 10% w/v SDS, 50% glycerol, 25% v/v β mercaptoethanol and 0.005% v/v bromophenol blue dye. Sample buffer was added to the Hi-Spot samples to produce a 1x sample buffer solution. The positive control, adult rat cortex and freshly dissociated sample were combined with water and sample buffer to produce a final protein concentration of 0.35mg/ml, and 12µg of these samples was loaded onto the gel. The samples were boiled at 95°C for 5 minutes and centrifuged for 1 minute at 300g before vortex and gel loading of the supernatant.
The gel was placed in a chamber surrounded by 1x Laemilli buffer (0.25M TRIS, 1.92M glycine, 10% w/v SDS). Gels were run at 30mA continuous current whilst the proteins migrated through the stacker gel and then the current was increased to 50mA for protein migration through the resolving gel.

2.2.3 Normalisation of Hi-Spot protein samples

Preliminary experiments showed that Hi-Spots could not be washed before transfer into homogenisation buffer as re-aggregated cells became disrupted prior to homogenisation steps. This means that all samples have a sera background.

Control experiment where PTFE inserts were placed on semi-permeable PTFE membrane inserts inside a six well culture dish containing media and were incubated overnight without Hi-Spot addition show the amount of background. In these control experiments the PTFE membranes were removed and placed into homogenisation buffer. Sample buffer was added to the solution as detailed below in section 2.2.2 and samples loaded and run on a SDS 10% PAGE in parallel to cultures.

Figure 2.2a shows the Coomassie protein stained gel. There is a very distinct band at 65kDa, which corresponds to albumin in the culture media. Therefore, to normalise loading Hi-Spots were placed into equivalent volumes of Homogenisation buffer (i.e. four Hi-Spots into 100µl). Figure 2.2b shows the protein profile of homogenate extracted from Hi-Spots in homogenisation buffer, showing that although the protein contamination from the media produces a prominent band, appreciable amounts of additional protein are derived from extracted cultures.

To produce positive controls for Western blot antigens (see table 2.2 for Western blot antibodies used), cortex from a mature adult rat was also homogenized, quantified for protein content (see section 2.4) and 12μg of sample loaded into each gel (labelled C). Additionally, the samples of freshly dissociated rodent tissue used for Hi-Spot production were also homogenized, protein quantified and 12μg was loaded into each gel to give a zero time in culture control (labelled D).

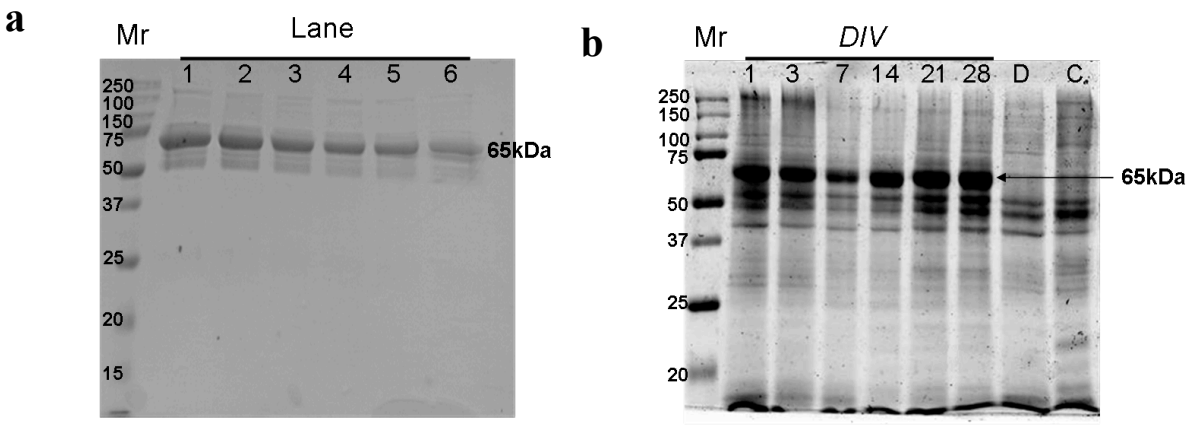

Figure 2.2: Protein contamination from the culture media.

a) Protein contamination from media soaked into PTFE membranes:
PTFE membranes were incubated over night with cell culture media. The media was removed and PTFE membranes placed in to homogenisation buffer 4 discs/ 100µl. The homogenate (35 %) of was resolved by SDS PAGE 10%. The gel was stained with colloidal coomassie to visualise the protein contamination from the media soaked PTFE discs. A prominent band of 65kDa (albumin) is a protein contamination from the media.

b) Proteins extracted from Hi-Spots:
Four Hi-Spots on PTFE at the *DIVs* indicated were placed into 100µl homogenisation buffer. Hi-Spot proteins were extracted from PTFE discs. 35 % of the extracted proteins were resolved on a 10% PAGE gel. The gel was stained with colloidal coomassie A prominent band at 65kDa corresponding to the media contamination can be seen but additional proteins extracted from the Hi-Spots are also clearly evident.

2.2.4 Protein transfer

To transfer proteins from SDS-PAGE gels to a nitrocellulose membrane (Amersham), a sandwich was constructed consisting of a sponge pre-soaked in 1xLaemlli buffer containing 20% v/v methanol, 2 sheets of filter paper (Whatman, 3mm chromatography paper) (pre-soaked as above), the gel, a sheet of pre-soaked nitrocellulose, 2 filter paper sheets and another pre-soaked sponge (depicted in Figure 2.3). This was placed into a mini blotting tank with the gel on the side of the cathode and the nitrocellulose membrane nearest the anode. Proteins were electro-transferred at 4°C overnight in transfer buffer (1x Laemilli buffer containing 20% v/v methanol) with continuous stirring using a magnetic flea. A voltage of 30V was applied overnight for 17 hours. Protein transfer was verified by

staining the nitrocellulose membrane for 10mins with 0.2%w/v solution of Ponceau Red (BDH,UK).

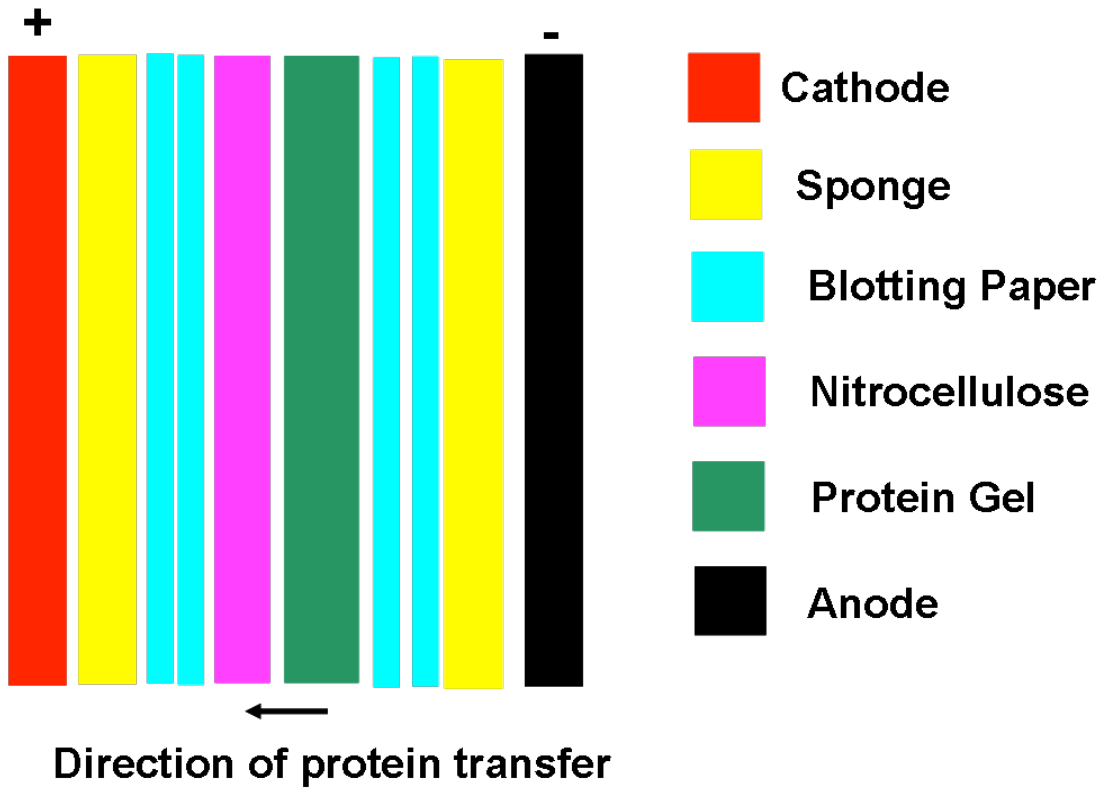

Figure 2.3: Protein transfer onto nitrocellulose membrane
After the SDS PAGE the protein gel is place between the nitrocellulose membrane and blotting paper in the arrangement depicted above. Proteins are transfer onto nitrocellulose membrane towards to cathode.

2.2.5 Antibody labelling of transferred proteins

After transfer nitrocellulose membranes were rinsed with distilled water. Nitrocellulose membranes were then blocked with TBS/ Tween (pH 6.8) (NaCl 0.15M, TRIS 10mM containing 0.005% v/v Tween) / low fat milk powder (4% w/v) (Tesco) for 1 hour at room temperature. Membranes were then incubated with primary antibodies under optimised conditions (Table 2.2). Antibodies were diluted in TBS/ Tween/ low fat milk powder (2.5% w/v) and incubated with nitrocellulose membrane with constant shaking. The membranes were subsequently washed for 3x5minutes (TBS/Tween), and then incubated with the appropriate secondary antibody conjugated to a fluorophore (Alexa Fluor-680 or 800nm, Invitrogen Molecular Probes) at a dilution of 1:10,000 for 1 hour in the dark at room temperature.

The membranes were washed in the dark for 3x5 minutes (TBS/Tween). Fluorescence from secondary antibody labelling was visualised with an Odyssey Infrared Scanner (Licor) at 700nm and 800nm at a fixed intensity setting of 4.0 throughout work described in the thesis.

Antibody	Source	Primary Ab Incubation	Detection	Dilution
Synaptobrevin 1, 2, 3	Synaptic Systems Mouse monoclonal 104 001 Clone C1 10.1	O/N 4°C	Fluorescence	1:1000
Syntaxin	Autogen Bioclear Mouse monoclonal 619-0269	1 hr RT	Fluorescence	1:1000
PSD-95	Millipore Mouse monoclonal MAB1596	1 hr RT	Fluorescence	1:1000
β III Tubulin	Covance Mouse monoclonal MMS-435P	1 hr RT	Fluorescence	1:1000
NR1	Santa Cruz Goat Polyclonal Sc-1467	O/N 4°C	Fluorescence	1:1000
GFAP	DAKO Rabbit Polyclonal Nr. Z 0334	1 hr RT	Fluorescence	1:5000
CSP	Abcam Rabbit polyconal ab24560	1 hr RT	Fluorescence	1:1000

Table 2.2: Antibodies and incubation conditions for Western Blot. RT- Room Temperature**,** O/N- Over Night

For electrochemilluminescence (ECL) detection of antibody binding, HRP conjugated secondary antibody was used at 1:10,000 diluted in TBS/Tween/ low fat milk power (2.5% w/v) for 1 hour with shaking. Membranes were washed with TBS/Tween 3x5 minutes and immunoreactivity detected by ECL (SuperSignal West Pico) as per manufacturers guidelines and X-ray film was exposed. Exposed film was fixed and developed using a Xograph.

Western blots figures presented are composits of several nitrocellulose blots from different nitrocellulose membranes. In general one nitrocellulolose membrane was cut and immuno detection preformed for Syntaxin (35kDa) and PSD-95 (95kDa), and one nitrocelluose membrane was cut and immuno detection preformed for GFAP (45kDa) and NR1

(115kDa). The other antibody immuno detections were preformed on single blots without cutting.

2.3 Colloidal Coomassie Gel Staining

After electrophoresis the acrylamide gel was fixed for 1 hour in a solution containing 7% glacial acetic acid/ 40% methanol (final concentration). A staining solution was made by diluting colloidal Coomassie concentrate (BioRad) 4:1 with de-ionized water. This was mixed thoroughly and then methanol was added at 1:4 to the diluted colloidal Coomassie to make the active staining solution. The fixed gel was incubated in the active staining solution overnight at room temperature with shaking. The gel was de-stained with 10% acetic acid/ 25% methanol for 60 seconds and then rinsed in 25% methanol until gel was de-stained before being scanned at 700nm on an Odyssey scanner (Licore). Scan setting did not need not to be changed between gels, an offset value of 0.75 and intensity value of 4.0 was always used.

2.4 Protein Assay for the Control Sample from Adult Cortical Tissue

Assays for protein quantification were conducted using the D_c protein assay method (BioRad), as described in the manufacturer's instructions. Quantification of protein content was determined against a bovine serum albumin (BSA) standard curve (2mg/ml-0.03mg/ml), diluted with the same buffer as the Hi-Spot samples. A background control sample consisted of homogenization buffer only. All samples were tested in duplicate on a 96 well microtitre plate, incubated for 5 minutes at room temperature and then absorbance read at 630nm.

2.5 Bright field Microscopy

Analysis of culture morphology was conducted by bright field microscopy on an upright light microscope. Hi-Spots were assessed over *DIV 1-24* for their morphological appearance. Hi-Spots were imaged using leica software and the whole Hi-Spot was viewed using a 5 x objection lens.

2.6 Processing Hi-Spot Cultures for Immunohistochemistry

Hi-Spots were removed from their culture wells using forceps to hold the PTFE membrane, and placed in a 96 well ELISA plate. Hi-Spots were washed with Phosphate Buffered

Saline (PBS) 3 times before fixation in 4% Para-Formaldehyde (PFA), see table 2.3 for optimised fixation conditions for different antigens. After fixation, cultures were removed from PFA and washed 3x 5 minutes in wash buffer (PBS Tween 0.001%). Samples were blocked with 5% serum for 30 minutes at RT. Primary Antibodies were incubated overnight at 4°C and samples were washed in wash buffer 3x 5minutes before addition of secondary antibodies. The primary antibody concentrations used are shown in table 2.3. Secondary antibodies (Alexa 488nm or 568nm) were used at 1:500 and were incubated at room temperature for 45 minutes

Antibody	Source	PFA Fixation	Dilution
β III Tubulin	Covance Mouse monoclonal MMS-435P	4°C O/N	1:200
GFAP	DAKO Rabbit Polyclonal Nr. Z 0334	4°C O/N	1:200
NeuN	Chemicon Mouse monoclonal MAB377	4°C O/N	1:200
Synaptophysin	Chemicon Mouse monoclonal MAB368	10 mins RT	1:50
PSD-95	Millipore Mouse monoclonal MAB1596	10 mins RT	1:100
VGAT	Synaptic Systems Rabbit Polyclonal 131 002	10 mins RT	1:100
VGLUT1	Synaptic Systems Mouse Monoclonal 135 311	10 mins RT	1:100
ED1 (CD68)	Serotec Mouse monoclonal MCA341R	4°C O/N	1:200
Synaptobrevin 1, 2, 3	Synaptic Systems Mouse monoclonal 104 001 Clone C1 10.1	10 mins RT	1:100
CSP	Abcam Rabbit polyconal Ab24560	10 mins RT	1:100
Parvalbumin	Abcam Mouse monoclonal ab50338	Formalin	1:800

Table 2.3: Antibodies and fixation conditions for Immunohistochemistry staining. RT- Room Temperature**,** O/N- Over Night

Samples were then washed for 5minutes in wash buffer, the second wash contained Hoechst 33342 (5µl/ml) (Sigma), the third wash was wash buffer only. The Hi-Spots were then mounted onto glass slides with mounting solution (Sigma) and covered with a glass cover slip and sealed with nail varnish.

2.7 Production and Processing of Coronal Brain Sections for Immunohistochemistry (IHC)

2.7.1 Perfusion, Fixation and Tissue Processing

All procedures were conducted according to the animal license and animal rights act 1966. Animals were terminally anaesthetised with Sodium Pentobarbital and the thoracic cavity opened to expose the heart. A butterfly needle (27-gauge, Venisystems, Eire) was inserted into the left ventricle, and the right atrium was cut. Animals were perfused with heparin saline (0.9% saline containing 5000U/L heparin) until the perfusate ran clear. Animals were perfusion fixed with formalin. Once fixed the brain was removed and placed into fresh formalin fixative. The brain was then stored in the formalin fixative at 4°C for at least one night to ensure adequate fixation. The brain tissue was dehydrated through an increasing alcohol series and immersed in Histoclear in a Leica-TP 1020 tissue processor:

70% ethanol	2 hours
70% ethanol	2 hours
80% ethanol	1 hour
90% ethanol	1 hour
Absolute ethanol I	1 hour
Absolute ethanol II	1 hour
Absolute ethanol III	2 hours
Histoclear 2 I	4 hours
Histoclear 2 II	2 hours
Histoclear 2 III	overnight

The brains were submerged in paraffin wax (Polywax, UK) at 40°C, embedded in fresh wax and allowed to cool. The wax blocks were stored at room temperature. 10µm sections were cut on a Leica RM2255 rotary microtome and floated on dH_2O at 40°C (tissue floatation bath, LAMB). Sections were mounted on SuperFrost Plus (Fischer) microscope slides and dried overnight at 37°C. Slides were stored at room temperature.

2.7.2 Antigen Retrieval and IHC of Wax Sections

Wax sections mounted on glass slides in a rack were wrapped in paper and heated at 60°C for 30minutes to remove the wax. De-waxing was continued by incubating the slides in xylene for 10 minutes followed by a second clean xylene incubation for 10 minutes at room temperature. Slides were then re-hydrated through graded ethanol concentrations from 100% to 70%. The following ethanol incubations were used; 100% 5 minutes, clean 100% 5 minutes, 95% 5 minutes, 80% 5 minutes, 70% 5 minutes, PBS 5 minutes.

Sections were permeabilised using PBS/Tween (0.05%) for 5 minutes. After permeabilisation sections were micro-waved in citrate buffer (pH6) for 3 minutes before being cooled for 5 minutes in water and repeating the citrate microwaving step. After further cooling in water the sections were washed in PBS/ Tween (0.05%) for 5 minutes at room temperatures.

Sections were isolated using a hydrophobic wax pen and unspecific antibody binding was blocked by incubating each section with 5% Bovine Serum Albumin (BSA)/ PBS for one hour at room temperature. After blocking, the sections were washed three times with PBS/ Tween.

Primary antibodies were centrifuged for 1 minute in a bench top centrifuge before pippetting them into a buffer containing BSA 0.25% (Sigma) and Triton X 100 0.2% (Sigma). The sections with primary antibodies were incubated overnight at 4°C in a water saturated container.

The primary antibody was washed off using PBS/ Tween and the sections were incubated with the appropriate secondary antibody (Alexa Fluor-488; Alexa Fluor-546, Molecular Probes) in a buffer containing BSA 0.25% and Triton X100 0.2% for 1 hour at room temperature. After the secondary antibody incubation the sections were washed 3 times for 5 minutes in PBS/ Tween. After the final wash the sections were covered with a small amount of DAPI Vector Shield Hard Set mount and cover slips laid over the top.

All control and test tissue were treated in parallel. All images were taken using a Leica CM5000 microscope. LAS-AF software was used for fluorescence microscopy and for paired comparisons exposure times, offset and intensity values were kept the same.

2.8 Confocal Microscopy

Hi-Spots were imaged with a Leica TCS SP2 TCS MP microscope and confocal images for excitations at 488 and 568 were scanned sequentially to eliminate fluorophore cross talk. Hoechst 33342 was visualised using multi-photon excitation at 780nm.

Settings were determined using test Hi-Spots consisting of young (*DIV 1-7*) and old Hi-Spots (*DIV 21-35*) stained for the antigens in table 2.3. Young and old Hi-Spots were used to account for increases and decrease in antigen immunoreactivity during Hi-Spot development so that over or under exposure did not occur as the Hi-Spots aged and matured. These settings were used as the standard settings for all further experiments.

To obtain a representative image of each Hi-Spot two random images were taken with the 40X objective. 12 z-sections were taken through each sample at a resolution of 2048x2048 and scan speed of 400Hz. The gain, offset, expansion, pinhole and laser power were setup for each wavelength and kept constant for all samples imaged (Table 2.4). To produce images representative of the whole Hi-Spot, the data in the twelve z-section images was compressed into a single image where the data value at each xy location is the maximum value detected in any z-plane. Effectively this produces an image with infinite depth-of-field and is described as a maximum projection image.

WaveLength	488nm	568nm	780nm [MP]
Number of z Sections	12	12	12
Resolution	2048x2048	2048x2048	2048x2048
Scan Speed Hz	400	400	400
Pin Hole µm	40.96	40.96	600.00
Gain	500	627.8	500
Offset	1%	0.8%	1%
Expansion	3	3	1
Averages/ Scan	6	6	6

Table 2.4: Confocal settings for visualisation of Immunohistochemistry stained Hi-Spots. MP- Multi Photon

2.9 Multi- Electrode Array (MEA) Recording

The MEA (Biocell- Interface SA) consists of a plastic chamber in which 40 electrodes are mounted as a 500μm by 800μm grid, on a membrane dividing the chamber horizontally. Each electrode has a diameter of 100μm with an inter-electrode distance of 250μm (Figure 2.4a).

Initially, the MEA lower chamber is filled with Artifical Cerebral Spinal Fluid (ACSF) (see below) and then the Hi-Spot is placed in contact with the electrodes on the other side, which is in air. The ACSF is able to reach the Hi-Spot due to pores in the MEA membrane around the electrodes. The MEA assembly is then placed into the recording system where it is maintained at 37°C and allowed ~30min for recovery from the transfer (Figure 2.4d).

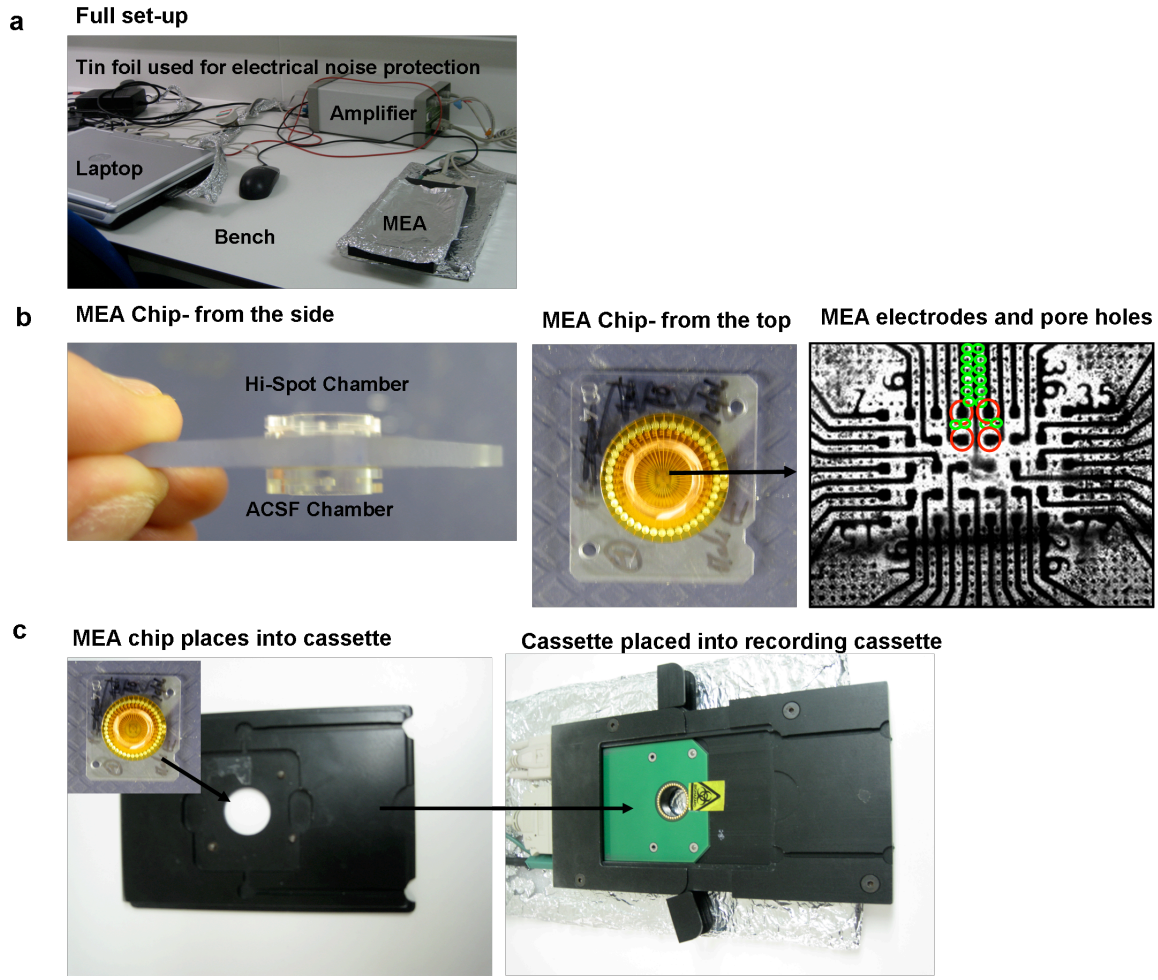

Figure 2.4: Multi- Electrode Array Apparatus:

a) The whole set-up including the lap top used to record the MEA data in labview software, MEA recording cassette and amplifier. Tin foil was used to protect from electrical 50Hz noise.
b) The Multielectrode array chip. The Hi-Spot culture is picked up using forecepts on the PTFE membrane is placed over the MEA electrodes in the top chamber which is sealed with a lid and the ACSF solution is placed in the bottom chamber. The MEA gold electrodes are 100µm in diameter and 150µm apart (red circles) and are surrounded by pores (green circles) which allow the perfusion of the ACSF to the Hi-Spot.
c) The MEA chip is placed into the cassette which is inturn places into the recording cassette. The recording cassette is maintained at 37°C.

The system allows recordings to be taken from any 8 of the 40 electrodes at any one time. Sampling frequency was set at 1kHz, which allows detection of both spontaneous bursts and single spiking activity. Labview software was used to control data recording (BioCell Interface).

Drugs were made up to the required concentrations in ACSF and perfused into the chamber when required, reaching the Hi-Spot through the pores in the MEA membrane. After ~30 minutes recovery from transfer onto the MEA Hi-Spot basal activity was recorded for 5-15 minutes. ACSF was then removed from the lower chamber not in contact with the Hi-Spot and replaced with an ASCF drug containing solution. Drugs were incubated with the Hi-Spots for 15 minutes to allow adequate time for equilibration before Hi-Spot activity was subsequently recorded for 5-30 minutes.

ACSF consisted of: Sodium Chloride (124mM), Potassium Chloride (1.6mM), Sodium Bicarbonate (24mM) Potassium dihydrogen phosphate (1.2mM), Glucose (10mM) Magnesium Chloride (0.15mM) and Calcium Chloride (0.25mM). The solution was maintained at 37°C and aerated with 95% O2/ 5% CO2.

MEAs last about 1 month with continuous use. MEAs were discarded when they became non-perfusable, due to contamination of the porous membrane. When the MEA become non-perfusable the ACSF can not perfuse through to the Hi-Spot and the PTFE membrane dries out and becomes opaque. This was important to be aware of, ACSF and drug perfusion would have been directly impaired if MEA pores had become blocked. MEAs were washed after every use with distilled water and 70% Ethanol. After 2 weeks MEAs were soaked in a low concentration of bleach solution for ~10 minutes.

2.9.1 MEA Data Analysis

Custom software written in Yorick (http://yorick.sourceforge.net/) and MatLab (Mathworks USA) was used for off-line analysis (Figure 2.5). Data analysis involved correction of voltage offset on each channel, and removal of heater switching artefacts (>0.5mV, values set to zero). Heater spikes were easily distinguished from biological spikes as heater spikes usually had a much higher positive amplitude 1-3mV and resulted in large spikes simultaneously across all channels (Figure 2.6,3b). Estimates of electrical noise were made from non-spiking portions of recordings. All recordings were examined and any with artefacts (drop outs, DC offsets, and large amounts of 50Hz electrical noise) were discarded. Spike activity was specified as voltage signals that exceeded an operator set threshold (usually ±0.03mV; Figure 2.6,5) based on viewing a magnified window of non-spiking activity showing the level of electrical non-biological noise.

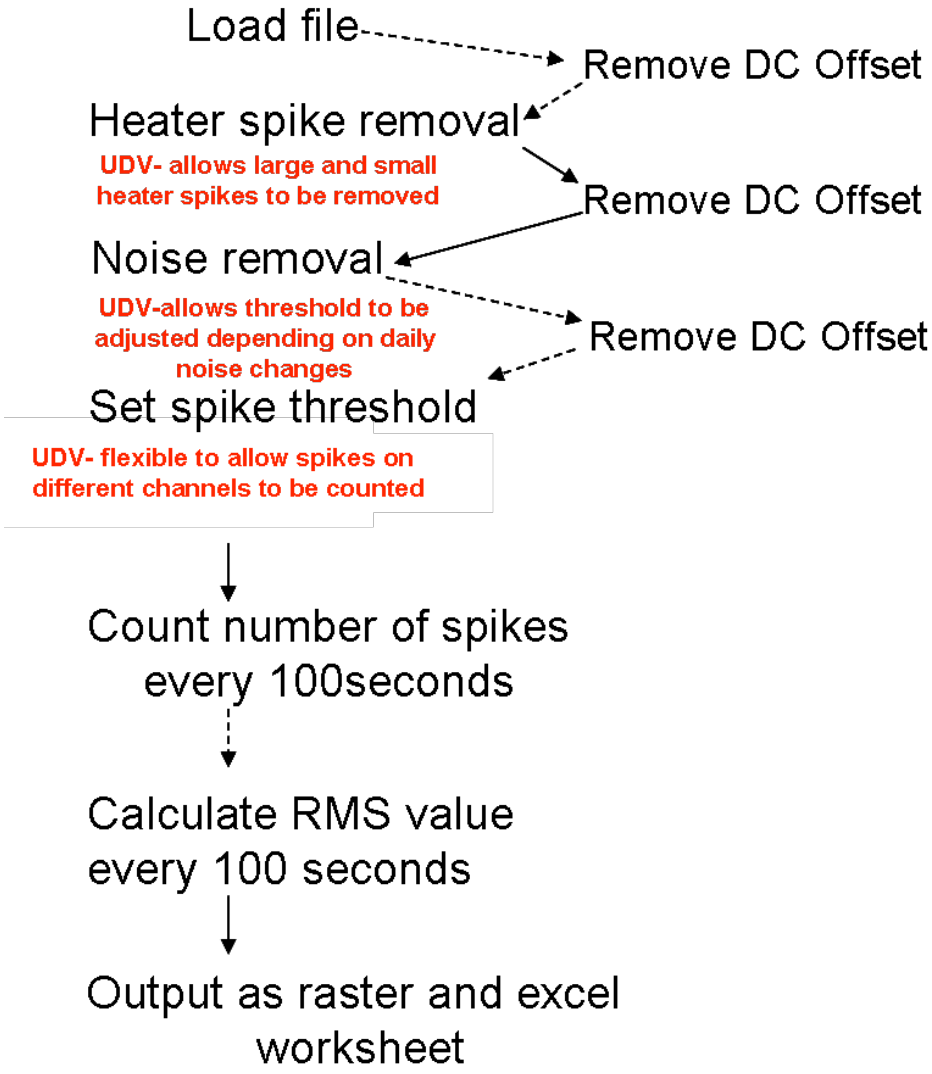

Figure 2.5: Multi Electrode Array Spike and RMS Program Routine
The program algorithm: the flow chart shows each step of the routine. Each step can be visualised as the program updates the graph in the viewing window. The heater spike threshold, noise filter, spike filter and bin length are all set by the user. UDV= user defined variable**.** Individual channels can also be removed or processed independently to remove noise and non-biological spikes

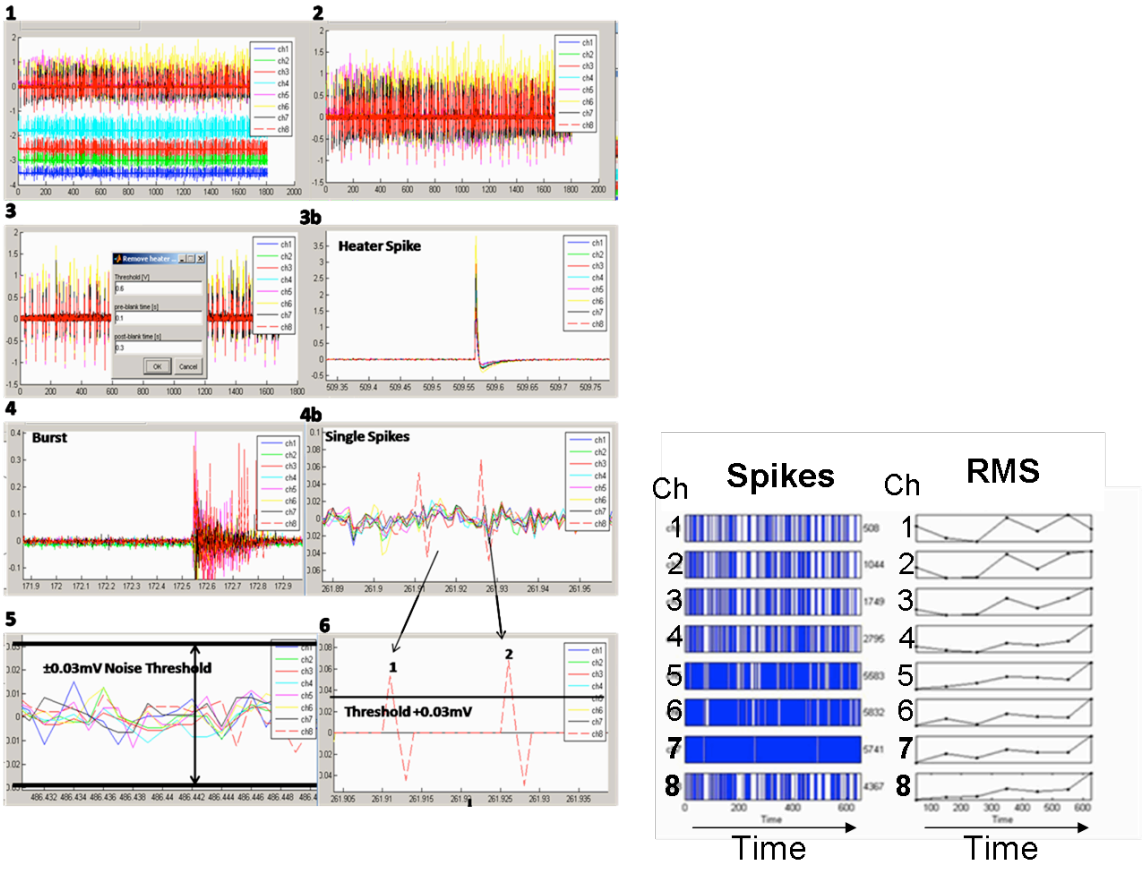

Figure 2.6: Flow chart of the spike and RMS program routine
The graph viewing window as a file is processed is shown. The file is loaded and the DC offset corrected to zero. Each channel is represented with a different colour. Once offset the heater spikes and noise can be removed. Heater spike artefacts are easily distinguished by their high amplitude and simultaneous appearance on all channels as shown in the expanded view in 3b. Electrophysiological unit activity is biphasic, showing clear spikes above the background electrical noise. Graph view 4 shows a burst recorded on 8 channels, different channels record different spikes and the spikes are of different amplitudes. The background noise level is typically < ±0.03mV shown in 5, a ±0.03mV threshold allows the removal of the non- biological noise without the removal of biological spikes as shown in 6. A spike is counted if it has a positive amplitude over the user defined threshold, usually set at 0.03mV.

After heater spike and noise removal, the number of spikes and root-mean-squared (RMS) value were calculated in 100 second time bins (Figure 2.6). Units of activity were defined as a positive spike crossing an operator set threshold. RMS allows the magnitude in change of the data to be plotted, this takes into account both spike number and the amplitude of the spikes (Figure 2.7).

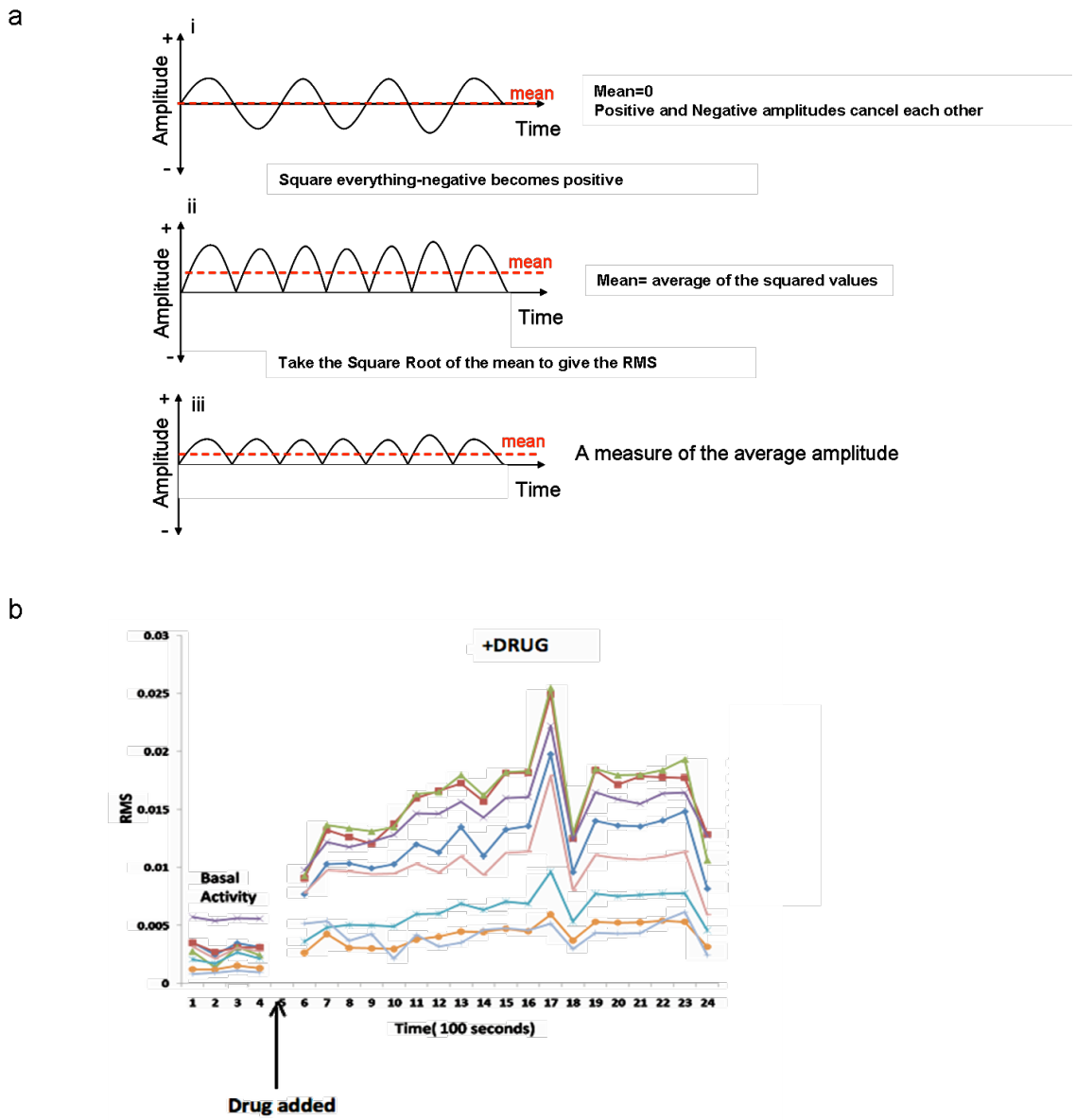

Figure 2.7: RMS calculation and example graph of increased RMS value on drug addition

a) Root Mean Squared (RMS) calculation: RMS is a statistical measure of the magnitude of a varying quantity. The figure gives a depiction of what RMS represents for a signal with both positive and negative amplitudes. The RMS gives a measure of activity because its value increases with increasing occurrence of large amplitude spikes.

b) Drug addition increases RMS value: Example of an increase in RMS value after drug addition. RMS is calculated in 100 Second time bins so that increase in activity over time can be observed. Graph shows activity recorded from 8 different channels on the MEA, each colour represents a different recording electrode.

Where comparisons were made the same spike detection parameters were used for all data. Idealized spike data was then calculated and exported to Excel (Microsoft, USA) and Prism (Graph Pad Software, Inc) for presentation.

2.9.2 Drugs

The drugs used in the pharmacological experiments were as follows Tetanus Toxin (gift from Lars Sundstrom), 6-Cyano-7-Nitroquinoxaline-2,3-Dione (CNQX; Tocris), D-amino-phosphovaleric acid (D-APV; Tocris) , bicuculline iodide (Tocris).

2.10 Tetanus Toxin

Tetanus toxin was added to the culture media at a final concentration of 100ng/ml from a stock of 2mg/ ml tetanus toxin in 2% BSA. P0 Hi-Spots at *DIV 21* were incubated with tetanus toxin for 48 hours by direct addition to the culture media and then analyzed by Western blot and MEA recordings. Prior to Western blot or MEA recordings the media was removed and three washes performed with BSA (2%w/v)/ PBS. All disposable pipette tips and syringes were incubated in acid to deactivate the toxin before autoclaving the waste.

2.11 Determination of cell death due to Glutamate toxicity

Cell death was determined using the fluorescent exclusion dye Propidium Iodine (PI) (Sigma). PI fluorescence was excited at 515-560nm using a rhodamine filter block. Images of whole Hi-Spots were captured using Leica imaging software and stored before analysis using 'ImageJ' analysis software. Microscope settings, gain, exposure and gamma were kept constant for each paired experiment.

12 hours before the glutamate exposure Hi-Spots were placed into serum free (SF) medium consisting of Neurobasal (24.35mmol/L glucose), B27 and PI (5µg/ml). This allowed screening for high levels of background cell death. Any Hi-Spots showing high levels of PI fluorescence were excluded from the analysis.

Glutamate (5mM, 1mM, 100µM, 5µM) and Sodium Azide (4.5mM; (Varming et al 1996)) were then added to the 6 well culture plates straight into media at the desired concentration. Controls consisted of Hi-Spots treated with SF media containing PI but not

glutamate or sodium azide. After two hours treatment the Hi-Spots were removed from the glutamate and azide containing medias and placed it into a pre-prepared 6 well culture dish well containing fresh SF media with PI. Hi-Spots were incubated in the SF/ PI media before analyses of the PI florescence the following day. All Hi-Spot incubation steps were conducted in the incubator, 37°C, 5% CO_2.

Cell death was quantified as the increase in PI fluorescence in Hi-Spots treated with glutamate above the PI fluorescence observed in the control (untreated) Hi-Spots, ΔPI. PI fluorescence was measured as a mean grey value with no threshold or background correction.

2.12 Animal Husbandry

C57B6 Charles River mice were housed according to Home Office regulations with a 12 hour light/ dark cycle. Postnatal day 0 and day 28 old mice were killed by cervical dislocation. Mice were identified by ear punches.

2.12.1 Establishment of pathogen free heterozygous (CSPα+/-) mice using rederivation

Cysteine String Protein alpha (CSPα) knockout heterozygous male and female mice were a generous gift from Fernández Chacon (University of Sevilla, Spain) and allowed the establishment of a breeding colony in Southampton BRF unit.

CSPα+/- mice were bred onto a C57B6 background using the Charles River mouse strain. To obtain clean pathogen free mice for breeding in normal holding rooms, male heterozygous (CSPα+/-) mice were mated with a super ovulating female wild-type C57B6 Charles River mouse. Embryos from the super ovulating mouse were then washed and transferred into an adventitious-pathogen-free pseudo-pregnant wild-type C57B6 female mouse to be born. The resulting pups were free from pathogenic organisms at birth based on the evidence that embryos in the uterus are in a pathogen free environment. The pups from a heterozygous (CSPα+/-) and wild-type (CSPα+/+) mating consisted of 50% wild-type and 50% heterozygous mice, providing clean heterozygous mice for mating to produce CSPα-/- mice.

Mice produced as above were transferred to normal holding rooms for breeding and on-going experiments. At least 5 heterozygous females and 5 heterozygous males for backup mating were kept in the clean room in a pathogen-free environment.

Heterozygous male/ female pairings should produce 50% heterozygous pups (CSPα+/-), 25% Wild type pups (CSPα+/+) and 25% CSP homozygous negative, (CSPα-/-) pups (Mendelian inheritance). However, initially this was rarely the case, CSPα-/- being under represented.

CSPα-/- mice were generated from heterozygous mice pairings. Trio pairings of two females with one male were used to obtain mouse litters. After P14 the CSPα-/- mice stop gaining weight, by P16-18 CSPα-/- mice can be distinguished on weight from their wildtype and heterozygous litter mates. However, CSPα-/-, CSPα+/- and CSPα+/+ mice have no discernable phenotypic differences at birth. Therefore, genotyping by DNA extraction and Polymerase Chain Reaction (PCR) had to be used to differentiate the mice.

In accordance with the licence agreement CSPα-/- mice were humanely sacrificed before their body weight was 20% below control CSPα+/+ and CSPα+/- mouse littermates. If given wet food containing higher protein the CSPα-/- mice maintained their weight for longer, allowing mice to be maintained for up to 28 days.

2.12.2 Genotyping of animals

2.12.2.1 DNA Extraction

DNA was extracted from ear punch or tail snip tissue samples. Mice could only be ear punched after 2 weeks due to their ear size. Mice requiring genotyping before this period were identified by marking tails twice a day with indelible marker. When tail snips were taken lidocane cream was placed onto the tip of the tail 10-15minutes prior to removing <5mm of the tail.

Tail or ear tissue was incubated in digestion buffer containing, Proteinase K (0.4mg/ml; promega), NaCl (100mM), SDS 0.5% in Tris buffer (10mM pH 8). Each sample was covered with digestion buffer and incubated at 54°C for about 2 hours or until tissue fragmented into tiny pieces upon shaking the sample.

Samples were then spun at 12,000rpm for 10mins to pellet undigested debris. The DNA solution was carefully removed and an equal volume of Isopropanol (2-propane) added to the solution to precipitate the DNA. This incubation was spun at 10,000rpm for 5 minutes and solution containing digestion mix and isopropanol removed to leave the DNA pellet. The DNA pellet was washed twice with 70% ethanol by adding 500µl 70% ethanol to the DNA pellet and spinning the solution at 10,000 rpm for 5minutes. Tubes containing pelleted DNA were upturned and pellet allowed to air dry for 10 minutes at room temperature. The DNA pellet was then re-suspended in 50µl distilled RNAase free water. The subsequent DNA in solution was stored at 4°C.

2.12.2.2 Polymerase Chain Reaction (PCR) for CSPα Genotyping

PCR was preformed on extracted DNA (Section 2.12.2.1). Primers used were the same as those documented in Fernández Chacon, (Neuron, 2004, Vol.42, 237-251) and designed to bind and distinguish between wild-type homozygous positive (CSPα+/+), heterozygous (CSPα+/-) and homozygous negative (CSPα-/-) genotypes (Figure 2.8).

Primer A ; TTGTAGACTAACCTAACATGGCCG;
Primer B ; TTGGCCCACCAGCTGGAGAGTAC;
Primer C ; GAGCGCGCGCGGCGGAGTTGTTGAC;

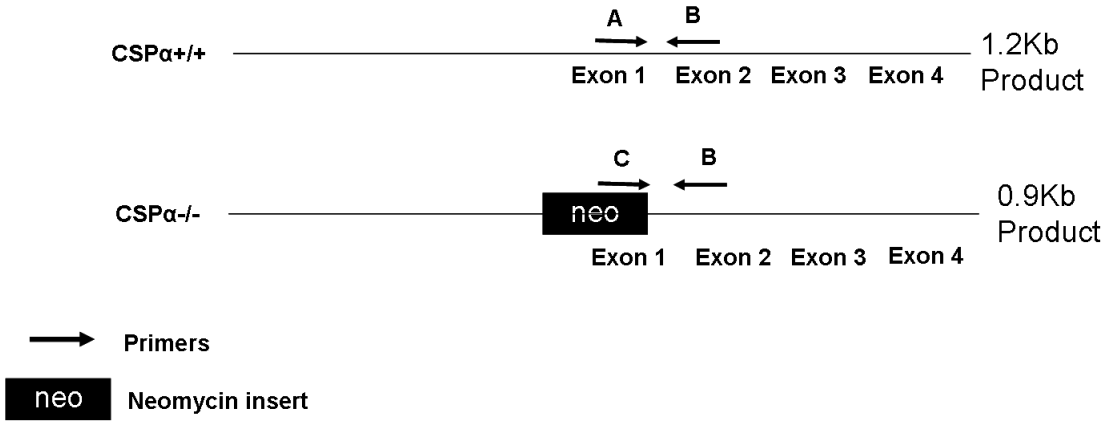

Figure 2.8: Primer binding sites for genotyping for CSPα-/- , CSPα+/+ and CSPα+/- mice

Schematic diagram of the wild-type CSPα+/+ gene, and the CSPα-/- gene. In the CSPα-/- gene exon 1 encoding residues 1–36 of CSPα is replaced by a neomycin resistance gene (neo). Primer C is designed to bind to the neomycin insert for selection of CSPα-/- and CSPα+/- mice. The positions of PCR primers A, B and C are show on the diagram. Adapted from (Fernandez-Chacon, Wolfel et al. 2004).

Red Taq ready mix (Sigma) containing Taq polymerase and dNTPs was used and primer combinations AB, BC added to individual reactions (0.4μM final primer concentration). Comparison of products from individual reactions was diagnostic of genotype (Figure 2.9).

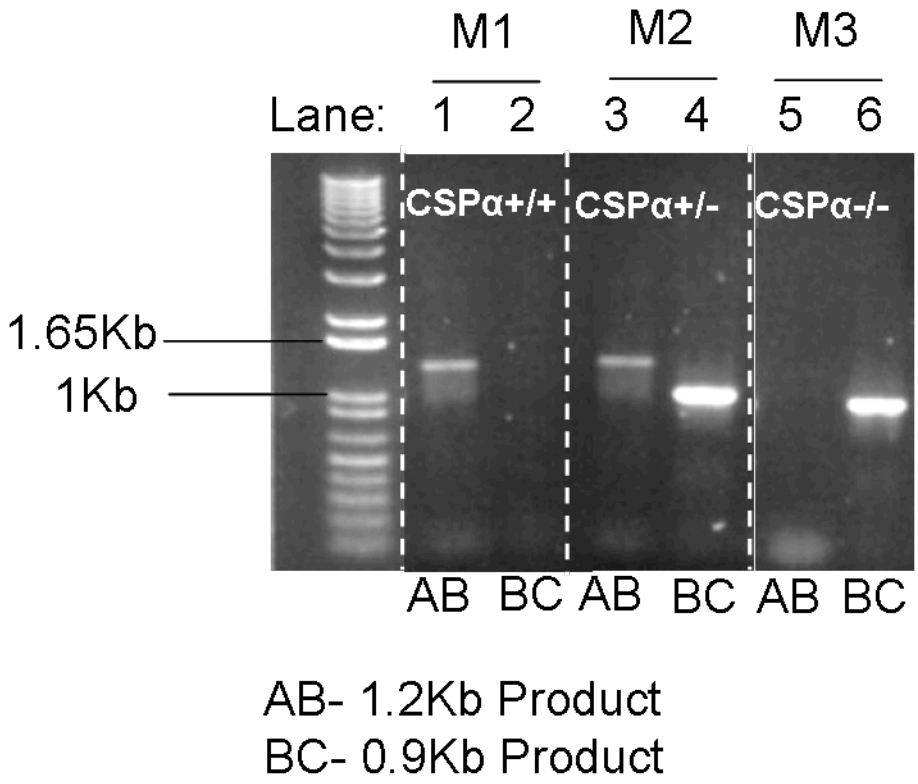

Figure 2.9: Genotyping mice for CSPα
Genomic DNA was used as a template in PCR with indicated primers. Primer paired used in the PCR reaction for each lane are shown at the bottom. M=Mouse, M1 lane 1 contains the 1.2Kb product and lane 2 is blank identifying the mouse as a CSPα+/+ genotype. M2 lanes 3 and 4 contain 1.2Kb and 0.9Kb products identifying the mouse as a heterozygous CSPα+/- genotype. M3 lane 5 is blank and lane 6 contains 0.9Kb product identifying the mouse as a CSPα-/- genotype.

The PCR conditions were as follows:

Initial denaturation	2 minutes	95°C	
Denaturation	30seconds	94°C	35 cycles
Annealing	30 seconds	60°C	
Extension	2 minutes	72°C	
Final Extension	10 minutes	72°C	

PCR products were then kept at 4°C until run on 1% Agarose gels containing Ethidium Bromide (0.5 ug/ml). 12µl of each PCR product was loaded into individual wells as was 5µl of DNA ladder (GeneRuler, 1kb DNA ladder, Fermentas) (Figure 2.9) .12µl of blank samples containing everything but the DNA were also loaded. Products were then visualised under UV light (Gene Amp PCR System 9700, Applied Biosystems).

2.13 Processing Hi-Spot Cultures for Electron Microscopy

2.13.1 Fixation

Fresh fixative was made up at room temperature containing PFA (2%w/v) / Glutaraldehyde (1.5% w/v) (from 25% EM grade stock) in neurobasal medium (Invitrogen) containing Hepes (20mM) pH 7.4. Fixative solution was made up immediately prior to fixation and the Hi-Spot serum containing media was removed before Hi-Spots were fixed for 20 minutes at room temperature. After fixation the samples were washed twice in Sodium Cacodylate (0.1M) at pH 7.2-7.4.

2.13.2 Osmication

After Sodium Cacodylate washing Hi-Spots were post fixed with Osmium (1% w/v) and potassium ferricyanide (1.5% w/v). Osmium solution was added to cells in the fume hood and incubated on ice for 1 hour. Samples were then washed three times with Sodium cacodylate (0.1M) (pH 7.2-7.4) and stored for no more that 1week in Sodium cacodylate (0.1M) at 4 °C. All osmium containing solutions and washes in sodium cacodylate buffer were collected in a dedicated osmium waste container in the fume hood.

2.13.3 Dehydration and Embedding

Osmicated samples were treated with tannic acid (1% w/v) in sodium cacodylate (0.1M) for 45 minutes at room temperature. After tannic acid the samples were rinsed in sodium sulphate (1%) in sodium cacodylate (0.05M) (pH7.2-7.4). The samples were then rinsed in distilled water before being dehydrated in ethanol. Dehydration started with two five minute incubations in 70% ethanol, followed by two five minute incubations in 90% ethanol, finishing with two five minute washes in 100% absolute ethanol. Hi-Spots on PTFE membranes were then transferred to a 50:50 solution of Epon (TAAB): Propylene oxide (PO) and incubated for an hour after which the initial resin mix was replaced with 100% Epon and left for 2 hours. The 100% Epon was replaced with fresh 100% Epon and incubated for further 2 hours.

Hi-Spots were then removed from the Epon solution and either mounted on previously polymerised studs or spun down and polymerised in fresh Epon in coffins (see below). This was followed by incubation at 65°C in an embedding oven, after which the samples can be sectioned and stained (summarised in Figure 2.10).

The EM processing affected the PTFE membranes causing them to curl up. However, one Hi-Spot was successfully processed flat and polymerised on resin for ‘en face’ preparation. To increase success rates multiple Hi-Spots of the same *DIV*/ genotype were removed from the PTFE membranes and spun down to form a pellet which could be embedded in Epon (Figure 2.11).

2.13.4 Tissue sectioning

Semi-thin sections (1-2µm) were cut on an microtome Ultra E, stained with (1% v/v Toluidine Blue in 1% w/v Borax), and used as a guide to ensure the specimen was contained in the sections.

Ultra-thin (grey <60nm) sections were cut with a Diamond knife using a Microtome Ultra E, and stained with Lead Citrate and Uranyl Acetate/ tannic acid.

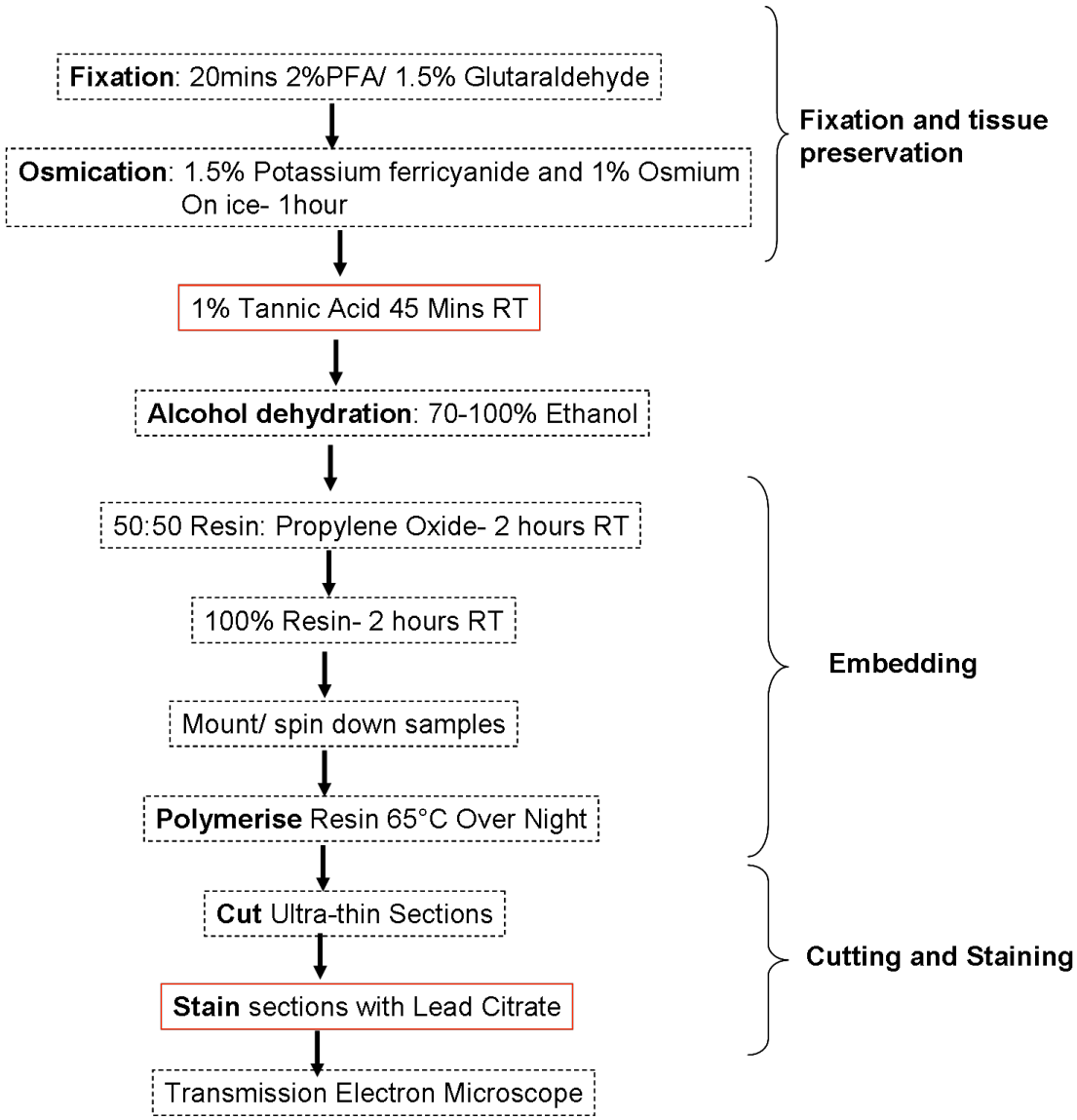

Figure 2.10: Flow Chart of Electron Microscopy Protocol:
Samples were fixed in serum-free media at room temperature to preserve the cell integrity. Once fixed the lipid membranes were fixed with Osmium. Staining with tannic acid in the red box is an optional part to the protocol. Tannic acid staining allows easy visualisation of the microtubules. After alcohol dehydration the Hi-Spots were embedded and polished with a glass knife and sections for EM cut with a diamond knife. Lead citrate staining allows contrast to be seen on the EM microscope.

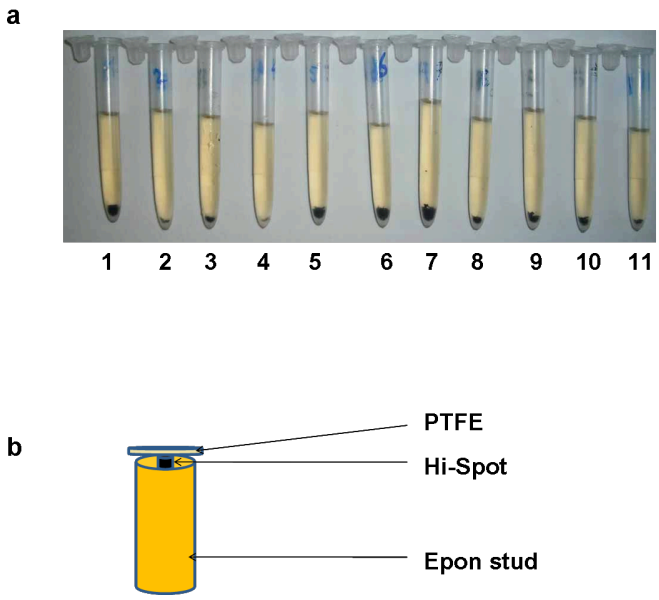

Figure 2.11: Sample preparation for Electron Microscopy

a) Hi-Spots were removed from PTFE and same genotype/ age Hi-Spots were spun through liquid resin which was polymerised at 65°C.
b) Epon stud was pre-polymerised; the Hi-Spot was mounted flat onto top of the stud into liquid un-polymerised epon. Un-polymerised epon was polymerised at 65°C embedding Hi-Spot flat on the surface of the stud. The Hi-Spot was cut 'en face'.

2.14 Processing Brain Sections for Electron Microscopy

For electron microscopy whole brains were fixed *in situ*.

2.14.1 Perfusion and dissection

Genotyped mice were terminally anaesthetised using 70 µl Sodium Pentobarbital, intraperitoneal injection. For CSPα-/- mice 20µl of Sodium Pentobarbital was sufficient due to their smaller size.

Once the animal was unresponsive the chest was opened and a butterfly needle (27-gauge, Venisystems, Eire) inserted into the left ventricle of the heart and the right atrium was cut. Animals were perfused with heparin saline (0.9% saline containing 5000U/L heparin) at 20-21°C. Perfusion continued for one more minute after the liver became clear.

The perfusate was transferred to allow fixation using formaldehyde (3.4%), glutaraldehyde (1.25%), picric acid (0.2%) in Sodium phosphate buffer (0.1 M) (pH 7.2) at room temperature. The animal was perfused with 200ml of primary fixative over 30 minutes. After the perfusion the intact animal was left to fix for a further hour at room temperature without perfusion.

Subsequently, the brain was removed and fixed by immersion in the same primary fixative overnight at 4°C, or for one hour at room temperature. The brain turned yellow and hard after this fixation. The brain was washed for 15 minutes in sodium phosphate buffer (0.1M) (pH 7.2). After washing the cerebellum was removed making a flat cut across the back of the brain. The flat surface was stuck to the vibratome stand using a small amount of super glue and immersed in a bath of Sodium phosphate (0.1M) buffer. Vibratome sections were cut through the brain and Hippocampal sections (150µm thick) were collected.

The Hippocampal sections were immersed into the same glutaladehyde/ picric acid fixative and incubated overnight at 4°C overnight. After overnight fixation the brain sections were washed with Sodium phosphate (0.1M) buffer and micro-dissected regions were cut from the pyramidal cells of the CA1 to the granule cells of the Dentate Gyrus containing the stratum Radiatum synapses (Figure 2.12). The sections were kept hydrated throughout the

micro-dissection by cutting the regions out in a small drop of 0.1M Phosphate buffer. Sections were always cut into a trapezoid shape with the cell body pyramidal cell layer at the top (thinnest part) of the trapezoid. Micro-dissected sections were manipulated into tubes using a fine tipped paint brush.

2.14.2 Osmification and further processing

After micro-dissection sections were washed (2x 10 minutes) in Sodium phosphate (0.1M) Buffer pH 7.4. The sections were then transferred to osmium tetroxide (1%) in Sodium phosphate (0.1 M) buffer at pH 7.2 for one hour at room temperature. The osmium was then washed off with Sodium phosphate (0.1M) Buffer pH 7.4, collecting all osmium washes and waste osmium in a dedicated waste osmium container.

After osmification the sections were dehydrated with ethanol. Dehydration consisted of successive incubations (10 minutes) with 30% and 50% ethanol. Staining consisted of incubation with 1% uranyl acetate in 70% ethanol (40 minutes). This was followed by incubation in 95% ethanol (10minutes) and 100% ethanol (2x15minutes).

The samples were then embedded into resin starting with a 10 minute incubation with acetonitrile followed by overnight incubation with 50:50 acetonitrile: resin. Overnight incubation was preformed at room temperature with continuous mixing. The samples were then incubated in resin for 6 hours and embedded in fresh resin and polymerised at 60°C for 20-24 hours.

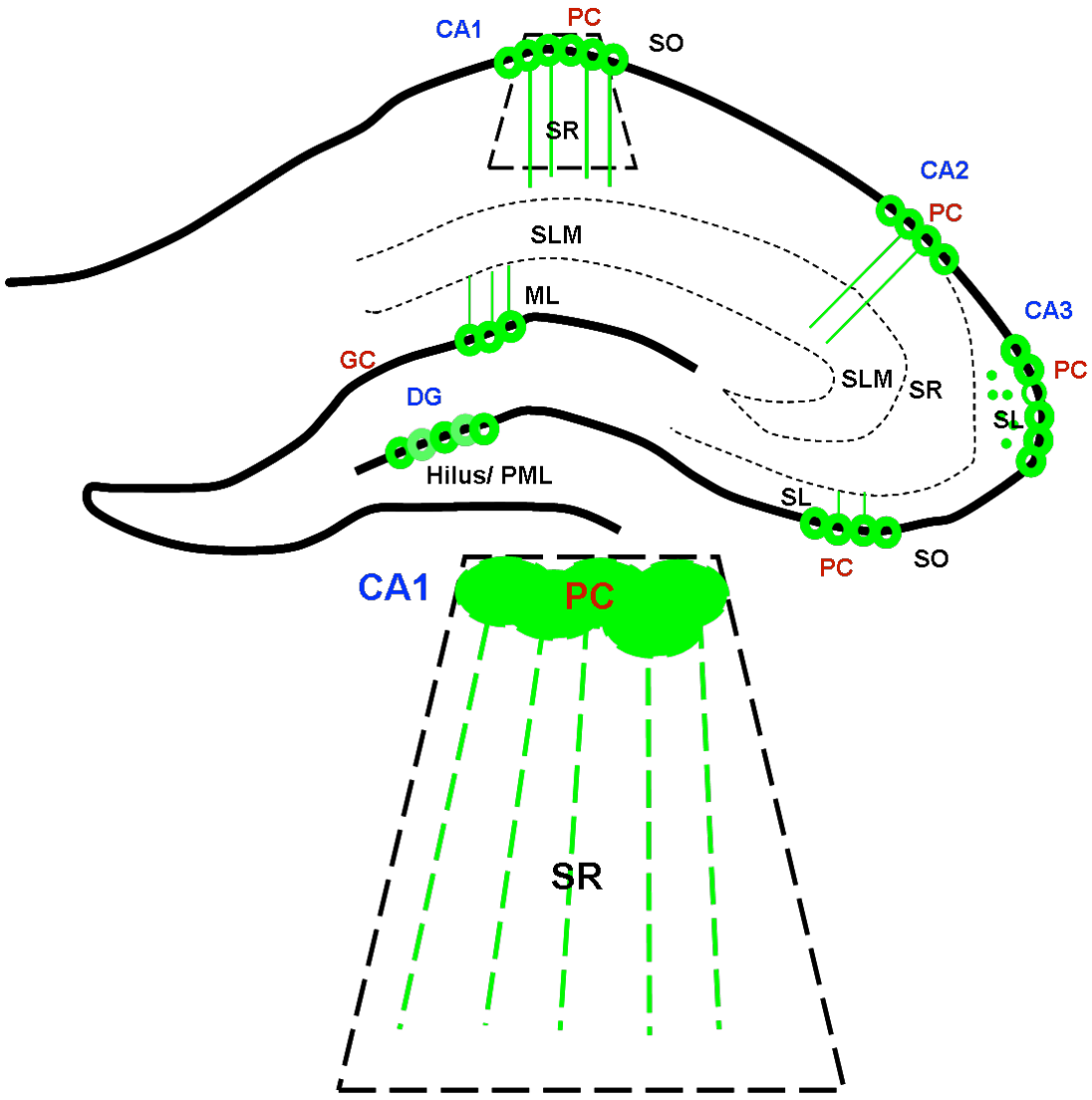

Figure 2.12: Micro-dissection of the CA1 for Electron Microscopy Analysis

A trapezoid shape containing the CA1 was micro-dissected from 150µm microtome cut sections from the Hippocampus. For orientation the trapezoid was always cut with the thinnest end at the top of the corresponding to the cell body layer of the pyramidal cells. PC, Pyramidal Cell, SR, Stratum Radiatum, DG, Dentate Gyrus, GC, Granule Cell, ML, Moleculare Layer, SO, Stratum Oriens, SL, Stratum Lacunosum, SLM, Stratum Lacunosum Moleculare.

2.14.3 Sectioning and Staining

Section staining followed the sample protocol stated in section 2.13.4. The trapezoid section was trimmed around and semi-thin sections taken and stained with 1% v/v Toluidine Blue in 1% w/v Borax to assess if the sample was being cut in the section. Ultra thin (grey <60nm) sections were then cut using a diamond knife and placed onto grids for staining and EM analysis. Sections were stained with Lead Citrate and viewed on TEM.

2.15 Quantitative Real Time Polymerase Chain Reaction- for Arc:Arg

Primers were designed for Arc:Arg 3.1 the forward primer reads 5'-AGAATGACACCAGGTCTCA, and the reverse primer reads 5'-CTCTGCCTTGAAAGTGTCTT.

The 140bp product was amplified using a Chromo 4 DNA Engine thermocycler (Biorad), running Opticon Monitor v3.1.32 software, with the following conditions:

Initial denaturation	2 minutes	94°C	
Denaturation	40 seconds	94°C	35 cycles
Annealing	30 seconds	55°C	
Extension	30 seconds	72°C	
Final Extension	10 minutes	72°C	

cDNA from a naive mouse was used to produce a standard curve to calculate the concentration of Arc: Arg 3.1 in the test samples.

iQ SYBR Green Supermix (Biorad) was used as supplied by the manufacturer, in 25µl reactions as follows: A master mix of iQ SYBR Green Supermix (12.5µl/ sample), forward primer (Final Concentration 0.4µM), reverse primer (Final Concentration 0.4µM), Nuclease-free water (9.5 µl/ sample) and Sample template DNA (1 µl) was used.

2.15.1 Data Preparation and GAPDH Normalisation

To allow direct comparison between different mice a plasmid GAPDH concentration curve was used to measure the amount of GAPDH in the samples. The amount of Arc:Arg 3.1 measured in the samples was normalised to the amount GAPDH reference gene in each sample.

After GAPDH normalisation, the data can be quantified by multiplying the normalised value by 1000 to obtain a more manageable number. The normalised values for each sample can be plotted on a graph to determine whether any changes can be seen between the samples being analysed. Samples assessed for Arc:Arg 3.1 levels were from synthesised cDNA from the hippocampus of 6 Cysteine String Protein (CSP)α -/- animals and 2 Wild Type (CSP α+/+) animals.

3 - Optimisation of Rat Hi-spots

3.1 Introduction

At its simplest, neurons removed from the brain and cultured *in vitro* allow direct access for the application of pharmacological agents, electrophysiological recordings, and morphological characteristics such as neurogenesis (Ghosh and Greenberg 1995), network formation (Van Pelt, Corner et al. 2004) and toxicity (Choi 1985; Choi, Maulucci-Gedde et al. 1987; van Vliet, Stoppini et al. 2007).

However, when neural cells are cultured *in vitro* they are classically dissociated to a single cell suspension, the connectivity of the tissue is destroyed and the cells are cultured with connectivity only in two dimensions. *In vivo* neuronal structures, however, are three dimensional and contain much higher connectivity between the neural cells. The context in which cells are grown is important and the environment can alter their behaviour, impacting on the rate of neurite out growth, differentiation and toxicity to glutamate (Choi, Maulucci-Gedde et al. 1987; Massieu, Morales-Villagran et al. 1995; Weaver, Petersen et al. 1997; Hayman, Smith et al. 2004).

Investigations of neuronal dysfunction in which the inhibitory to excitatory neuronal balance are altered demonstrate the importance of functional readouts to characterise the neuronal dysfunction (Gutierrez, Hung et al. 2009). The benefit of measuring neuronal network activity is that network wide changes which would not be detected in single cell analysis can be exposed (Varoqueaux, Aramuni et al. 2006; Gutierrez, Hung et al. 2009). Furthermore functional tests that can be investigated on a network level are likely more sensitive at detecting changes in the synaptic compartments of the neurons due to the subtle changes in signalling (Gutierrez, Hung et al. 2009). Such changes may precede more permanent changes such as synaptic and neuronal cell loss.

Therefore the ability to form an organised neural network *in vitro* capable of synaptic activity, controlled by balanced excitatory and inhibitory inputs and which provides a functional readout of neuronal viability with three dimensional cell-cell connectivity derived from a defined homogenous starting point, would be useful for the study of network function and dysfunction (van Vliet, Stoppini et al. 2007).

3.1.1 Dissociated Cell Cultures

Dissociated cultures are prepared from suspensions of individual cells obtained by dissociation of neural tissue. When plated the neurons begin to extend processes and form a neuronal network. The neuronal networks formed have been shown to become spontaneously active (Van Pelt, Corner et al. 2004) and contain both GABAergic and glutamatergic networks (Alho, Ferrarese et al. 1988; Benson, Watkins et al. 1994; Arnold, Hofmann et al. 2005). The networks formed have also been shown to undergo both short and long term plasticity (Lu, Man et al. 2001; Arnold, Hofmann et al. 2005; Hofmann and Bading 2006) and express neurotransmitter receptors and scaffolding proteins associated with mature neuronal cells (Naisbitt, Kim et al. 1999).

Dissociated cultures have been exploited for investigations of many neural cell functions including (but not limited to) studies of network formation (Chudotvorova, Ivanov et al. 2005; Voigt, Opitz et al. 2005), neuronal cell maturation and develop (Waites, Craig et al. 2005; Varoqueaux, Aramuni et al. 2006) and excitotoxicity studies (Choi, Maulucci-Gedde et al. 1987). *In vitro* dissociated cell cultures systems have also allowed the neuronal network changes due to the mutation or ablation of specific genes related to pathological diseases to be investigated (Almeida, Tampellini et al. 2005; Jugloff, Jung et al. 2005; Roselli, Tirard et al. 2005; Gutierrez, Hung et al. 2009). However, the single cell layer and unnatural environment in the cultures restricts the ability of these the cells and the networks thereof from expressing all the intricate cell-cell interactions attained from the complex networks formed *in vivo*.

The importance of cell-cell interactions has been demonstrated using glutamate toxicology studies. Investigations into glutamate excitotoxicity have shown that dissociated cultures have a lower tolerance to glutamate than observed *in situ* (Choi, Maulucci-Gedde et al. 1987; Massieu, Morales-Villagran et al. 1995; Morrison, Pringle et al. 2002). This is likely to be due to the lack of cell-cell interactions between astrocytes and neurons in dissociated culture systems. For this reason, investigations of neuronal toxicity and dysfunction may be more relevant in a culture system which allows neural cells to be cultured in a three dimensional environment. Organotypic and re-aggregated culture systems are such systems.

3.1.2 Organotypic Slice Cultures

Organotypic cultures represent the culture of intact fragments of tissue. Slice cultures from defined brain regions are useful for the study of physiological and pharmacological properties of neuronal circuits present *in vivo* because they retain the cytoarchitecture of the tissue of origin. Two methods for culturing brain slices exist; the roller tube technique developed in the 1940s and the culturing of organotypic slices on PTFE membrane at the liquid-air interface (Stoppini, Buchs et al. 1991). Both techniques start with the sectioning 100-400μm thick slices of the dissected brain. The techniques differ on how the culture is embedded and maintained. The roller tube technique involves embedding the slice in either a plasma clot or in a collagen matrix on a glass cover slip and rotating the tissue culture. The continuous rotation ensures the tissue is adequately oxygenated. The rotating of the culture also leads to considerable thinning of the culture allowing individual cells to be observed in the living tissue.

The tissue slices can also be cultured on porous, transparent membranes maintained at the liquid-air interface. Slices cultured in this way to do not thin to the same degree as those maintain in roller-tubes and thus are more useful for the study of neuronal cells in a three dimensional multi-cell layer environment (Stoppini, Buchs et al. 1991).

The tissues used for slice culture preparation are usually derived from early postnatal animals (P0-P7). At this stage the cytoarchitecture is already present in most brain areas and the brain is large and easier to dissect. The organotypic cultures maintain their local circuitry and their neuronal-glial cell close interactions. The close *in vivo* like cell-cell interactions are shown by the tissue like tolerance to glutamate observed for hippocampal slice cultures (Morrison, Pringle et al. 2002).

Hippocampal slice cultures have been the most extensively studied, but slice cultures from other brain regions such as the cerebellum, striatum, cortex and thalamus have been successfully cultured (Noraberg, Kristensen et al. 1999; Ghoumari, Ibanez et al. 2003; Uesaka, Hirai et al. 2005). In the hippocampal organotypic slices the vast majority of neuronal cells are found to innervate their normal targets. As *in vivo* the slice culture mossy fibre terminals projecting from the dentate gryrus are never seen to cross the CA3-CA1 border and the density of the dendritic spines from pyramidal cells very closely

matches the values found *in vivo* (Debanne, Guerineau et al. 1995; Gahwiler, Capogna et al. 1997). Pyramidal cells have also been shown to display normal synaptic transmission and also exhibit both short and long term plasticity (Debanne, Gahwiler et al. 1998). However, because of the loss of the afferent and efferent connections some of the intrinsic neuronal connections reorganise themselves and take over some additional synaptic sites (Gutierrez and Heinemann 1999).

Organotypic cultures have been shown to spontaneously form recurrent excitatory collaterals in the dentate gyrus and augmented recurrent synaptic collaterals between pyramidal cells in the CA1 (Gutierrez, Armand et al. 1999; Gutierrez and Heinemann 1999). Overexpression of recurrent collaterals in the CA3 has also been shown to develop in slice cultures, leading to the generation of seizure like events (Swann, Smith et al. 1993). Synaptic reorganisation that occurs is useful for investigations of temporal lobe epilepsy, because patients with the pathology also demonstrate augmented synaptic coupling between granule cells and increased seizure activity (Babb, Kupfer et al. 1991; Isokawa, Levesque et al. 1993). However, due to the development of recurrent collaterals and seizure like activity the long-term investigation of normal network activity is restricted.

Organotypic cultures allow access to living nerve cells which, because of the thinning of the cultures to a quasi monolayer thickness during the culture period, can be observed directly under the microscope, permitting cell developmental processes to be studied. Additionally slice cultures have been shown to parallel the morphological and physiological aspects of development seen *in vivo* (Annis, Robertson et al. 1993). At the stage of culture the neuronal cells may still be being generated and others may have only started to extend dendritric and axonal projections, and due to the natural microenvironment provided by the slice cultures the neuronal differentiation continues to occur *in vitro* (Annis, Robertson et al. 1993).

Neurite outgrowth and axonal connections can be investigated in slice cultures using co-cultures of different brain regions. Co-cultures can be made from brain regions which are anatomically remote from one another but interconnected *in vivo* (Distler and Robertson 1993). Neurite outgrowth can also be investigated using the neurites that grow out from the organotypic slices. These neurite outgrowths have been used to study the response of

growth cones to neurotrophic substances (Sato, Lopez-Mascaraque et al. 1994). In fact neurite outgrowths from organotypic slices were used to isolate and characterise the first molecularly identified chemotactic agent which guides growing axons (Kennedy and Tessier-Lavigne 1995).

3.1.3 Aggregated Cultures

Aggregated brain cell cultures are prepared from mechanically dissociated brain tissue. The dissociated cells re-aggregate under gentle agitation to form evenly sized spheroids. The re-aggregated cultures are maintained in suspension by continuous gentle agitation and have been shown to contain all of the different brain cell types, including major neuronal subpopulations, astrocytes, oligodendrocytes, and microglial cells, and form intricate cell-cell contacts.

A large number of studies investigating the toxicity of lead, insecticides and mercury have used aggregated cultures; this is because neurotoxic insults have been shown to involve inflammatory responses in both neuronal and glial cells. Aggregated cell cultures also permit cells to develop in three dimensions, offering a favourable environment for neuronal maturation, synapse formation and function (Zurich, Eskes et al. 2002; Monnet-Tschudi, Zurich et al. 2007; van Vliet, Stoppini et al. 2007).

By combining cell populations dissociated from different brain regions re-aggregated cultures allow the interaction between afferents and targets to be investigated (Vidal, Heller et al. 1995). The conditions within aggregated cultures also allow a favourable environment for division of neural precursors which do not proliferate well in dissociated cultures (Gage, Coates et al. 1995). Aggregated cell cultures have also been shown to have both spontaneous and evoked neuronal activity, demonstrating the presence of functional neural networks (van Vliet, Stoppini et al. 2007). However, because re-aggregated cultures are grown in a suspension and allowed to re-aggregate into small balls of cells, access for morphological microscopy investigation is harder, cells have to be fixed and physiological analysis is difficult.

3.1.4 Three dimensional cultures made in a matrix

Three dimensional (3D) scaffolds have been developed to try and recreate the environment in living tissues *in vitro*. Cells which can be cultured to resemble and act more like their *in vivo* counterparts, and combined with a 3D scaffold that is biodegradable could be useful to address the problem of organ shortages for tissue repair or transplants. The process involves culturing cells on biodegradable polymers such as poly (glycolic) acid, poly (lactic) acid and their co-polymer poly (lactic-co-glycolic) acid (Hayman, Smith et al. 2004; Hayman, Smith et al. 2005).

Using 3D scaffolds to culture cells *in vitro* has shown that cancer cells grown in this way undergo a pattern of changes in gene expression that more closely reflect the activities in living tissues (Wang, Weaver et al. 1998). Cell differentiation has also been shown to be enhanced when using 3D scaffolds, for example, fibroblasts demonstrated an increased proliferation rate and migration, and assumed a morphology more characteristic of fibroblasts *in vivo* (Cukierman, Pankov et al. 2001). Neuronal cells from human pluripotent stem cells were also shown to increase their neurite outgrowth when cultured in a 3D scaffold made of a polyHIPE (high internal phase emulsions) styrene scaffold when compared to a 2D environment (Hayman, Smith et al. 2004). However, composition and structure of the matrices may vary between preparations (Mazzoleni, Di Lorenzo et al. 2009).

3.1.5 Hi-Spots neural cell cultures

Hi-Spot cultures were developed at Capsant Neurotechnologies; a Pharma Biotech company founded by Dr Lars Sundstrom, Dr John Chad and Dr Ash Pringle (http://www.capsant.com/). Hi-Spots were designed to provide a method of cell culture allowing cells to be cultured at high density in a three dimensional environment that would be more physiological relevant to *in vivo* tissue, and reducing the need for animal testing by forming an *in vitro* physiological alternative, amenable to high-throughput investigations of toxicology and drug discovery.

Hi-Spots are re-aggregated brain tissue grow at the liquid air interface which randomly organises to produce a multi-cell layered organotypic like *in vitro* structure. Hi-Spot cultures have attributes of both organotypic, re-aggregated and dissociated cultures, presenting a multi-layered cellular neural culture, which forms an active neuronal network

from dissociated cells on a PTFE membrane (van Vliet, Stoppini et al. 2007). Hi-Spots allow the study of neuronal network formation, network activity and cellular composition.

Electrophysiological recording of neural activity is the functional output of the neural network and has the potential to provide sensitive measures of neuronal dysfunction. It has been previously reported that functional impairments can be detected by electrophysiological measurements before the appearance of morphological changes (Melani, Rebaudo et al. 2005). Furthermore extracellular non-invasive electrophysiological recordings using multielectrode arrays (MEAs) have been used to demonstrate the functional changes to pharmacological agents such as ethanol (Xia and Gross 2003).

.

The aim of the Hi-Spot system was to allow the *in vitro* development of *in vivo* like complexity whilst maintaining an optimal number of cell cultures from each animal reducing the number of animals required, and provide an *in vitro* alternative for high-through put analysis of pharmacological substances. This system has the advantage of allowing neuronal networks, to be assessed using electrophysiological techniques.

The following chapters will investigate the Hi-Spot culture system for use as an *in vivo*-analogue and show that Hi-Spots produced from embryonic and postnatal tissue develop a culture formed of neurons and glial cells. The chapters will discuss the necessary modifications to the original '*Capsant*' formulated Hi-Spot protocol to produce viable Hi-Spots from postnatal tissue, and demonstrate that the Hi-Spots cultures can be used to investigate network changes due to loss of the synaptic protein CSPα.

The Hi-Spot protocol was modified for the use of postnatal tissue because using postnatal tissue would remove the need to kill the dam, providing economic benefit by replacing the dam back into the breeding cycle and the arrangement of timed matings. The ability to culture cells from postnatal animals also means it is possible to sacrifice only one animal at a time, saving the rest of the litter for later use. Also, when embryonic animals are used their true developmental stage can only be determined after the pregnant dam has been killed. Cell culture from a postnatal starting point would also fulfil the three Rs of animal testing: (reduce, replace, refine) because using postnatal tissue reduces the number of animals sacrificed. It also reduces the severity of procedures required, and allows refinement of experiments to improve the information from each animal.

However, culture and dissociation of postnatal tissue to a single cell suspension is harder than for embryonic tissue. This is because during gestation through to birth and adulthood the neural network develops and the number of cell-cell interactions increases. The proteoglycan cell-cell adhesions and cell-extracellular matrix (ECM) adhesions have been shown to mature postnatally (Milev, Maurel et al. 1998; Song, Ichtchenko et al. 1999; Biederer, Sara et al. 2002), and could make mechanical disruption more difficult.

Cells can be sheared during mechanical dissociation of the postnatal tissue. The shearing processes can lead to release of intracellular glutamate from excitatory neurons and glia, and glutamate can rise to levels that lead to excitotoxicity of neurons (Choi, Maulucci-Gedde et al. 1987; Budd and Nicholls 1996; Sattler and Tymianski 2001; Schubert and Piasecki 2001). Cell shearing and glutamate release has further implications for postnatal tissue because of the developmental increase of functional glutamate receptors after birth (Marks, Friedman et al. 1996; Babb, Mikuni et al. 2005). The amino acid L-glutamate is the major mediator of excitatory signalling in the mammalian nervous system, but chronic exposure can lead to cell dysfunction and cell death (Hartley and Choi 1989).

3.2 Aim

To establish conditions required for culturing Hi-Spots from postnatal rat cortical tissue.

3.3 Methods

Hi-Spots from rat E17 tissue were produced using the method detailed in general methods section 2.1. Hi-Spots produced from both postnatal day 0 and 2 were also produced using this method. This protocol will be referred to as the '*Capsant'* Protocol. The modifications to this protocol for the production of viable postnatal cultures are detailed below, and are referred to as the '*Soton'* Protocol.

3.3.1 Modifications to the '*Capsant*' Hi-Spot protocol for postnatal Hi-Spot production

The '*Soton'* Protocol follows the same general procedure as the '*Capsant'* Protocol (Section 2.1), but contains 10μM MK801 in the dissociation solution. MK801 was added to medium and cells were dissociated in the presence of drug. MK801 was not added at any other point in the protocol or to the culture media.

Bright field imaging, Western blotting, immunohistochemistry and multielectrode recordings and were all conducted as detailed in chapter 2.

3.4 Results

3.4.1 Test of standard '*Capsant*' method for embryonic tissue

To form a baseline in this experimental series we used the standard protocol (*Capsant*) with embryonic tissue. Hi-Spots made from E17 tissue were cultured for 21 days. Hi-Spots were imaged in bright field to assess their gross morphology with increasing time in culture. During the culture period Hi-Spots analysed from E17 tissue remained intact, showed no holes in the re-aggregated spot and the Hi-Spot surface remained flat (Figure 3.1 a). The neuronal marker (syntaxin) and synaptic maturational marker (PSD-95) showed low levels of expression at the beginning of the culture period that increased by *DIV 14*.

The expression of NMDA receptors was investigated by measuring immunoreactivity against the obligatory subunit, NMDA receptor subunit 1 (NR1) of the NMDA receptor. NR1 immunoreactivity was not readily detected in the freshly dissociated sample; however its expression increased throughout the time in culture peaking at *~DIV 14* (Figure 3.1b). Glial cells were identified using the marker glial fibrillary acidic protein (GFAP), the marker revealed an initially low/ absent level in the freshly dissociated tissue followed by a steady increase during the culture maturation.

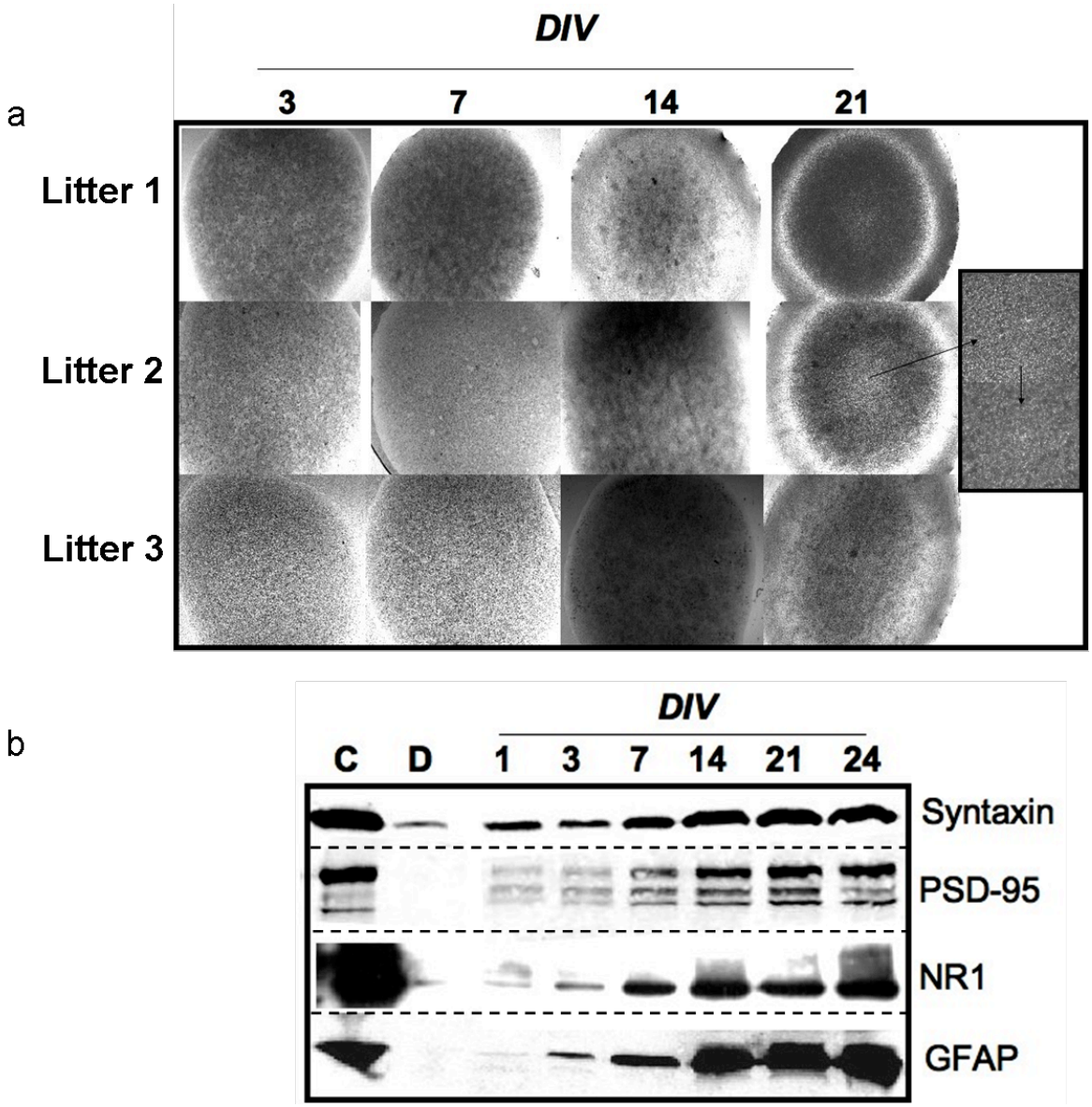

Figure 3.1: Hi-Spots made from embryonic day 17 tissue using the *Capsant* method

a) Bright field images of Hi-Spots after 3, 7, 14 and 21 *DIIV*. Hi-Spots remain flat on the surface and do not show cell clumping. Inset is a magnified image of the Hi-Spot surface. Each row shows Hi-Spots made from a different litter of E17 pups marked as litter 1, 2, 3.

b) Representative Western blot from 3 E17 litters. Syntaxin is a neuronal marker, PSD-95 is a marker associated with mature cultures, NR1 is an NMDA receptor marker, and GFAP (Glial Fibrillary Acidic Protein) is an astrocyte marker. Proteins were separated by PAGE on a 10% acrylamide gel. C represents the immunoreactivity in adult rat cortex, (12µg loaded), D represents the freshly dissociated sample (12µg loaded). Samples are from protein extracted from Hi-Spots at *DIV 1-24*. (Samples are from equal loading of Hi-Spots normalised by volume). Western blot figure was assembled from multiple nitrocellulose membrane western blots.

3.4.2 Standard '*Capsant*' method with postnatal tissue

Hi-Spots were also produced from P2 tissue using the *Capsant* method. These Hi-Spots were allowed to age to *DIV* 21 and their gross morphological appearance observed by bright field microscopy. Hi-Spots generated using the *Capsant* method from P2 tissue (Figure 3.2a) developed with a more amorphous surface. In P2 cultures large clumps of cells were observed, (Figure 3.2a inset), cell clumping was never observed in E17 cultures. Clumps correlate with areas of dead cells shown by Propidium Iodide staining (data not shown).

Western blot analysis of Hi-Spots generated from P2 tissue demonstrates that Hi-Spots made using the *Capsant* method show relatively weak levels of syntaxin and PSD-95 expression. The levels of the neuronal marker syntaxin were high in the freshly dissociated tissue (lane D) and at *DIV* 1 and 3 but declined markedly after this point. Levels of the neuronal maturational marker PSD-95 were only detected in the control (adult brain) and NMDA receptors marked with NR1 demonstrated a pattern of expression that was highest at the point of dissociation and decreased after this period becoming absent after *DIV* 3. GFAP the marker for astrocyte glial cells showed the same pattern as observed for E17 cultures. GFAP levels were lowest in the freshly dissociated tissue and showed a steady increase throughout the culture period (3.2b).

Hi-Spots produced from P0 tissue using the *Capsant* method showed smaller darkened cell clumps and sometimes holes devoid of cells that were not present on initial plating. Aggregated clumps of cells were not as frequent as those seen in Hi-Spots generated using the *Capsant* method from P2 tissue (3.3a).

Western blot against neuronal marker Syntaxin showed high levels in the freshly dissociated tissue and at *DIV*1-3 after which expression markedly declined and remained low for the duration of the culturing period. PSD-95 showed high expression in the freshly dissociated tissue but only very low levels in the culture period samples. GFAP showed the same expression profile observed for E17 and P2 Hi-Spots in which it increases throughout the culture period (Figure 3.3b). As with the P2 tissue the dissociate sample showed high levels of NR1, which is in contrast to the E17 dissociate sample (Figure 3.1, 3.2, 3.3, 3.4).

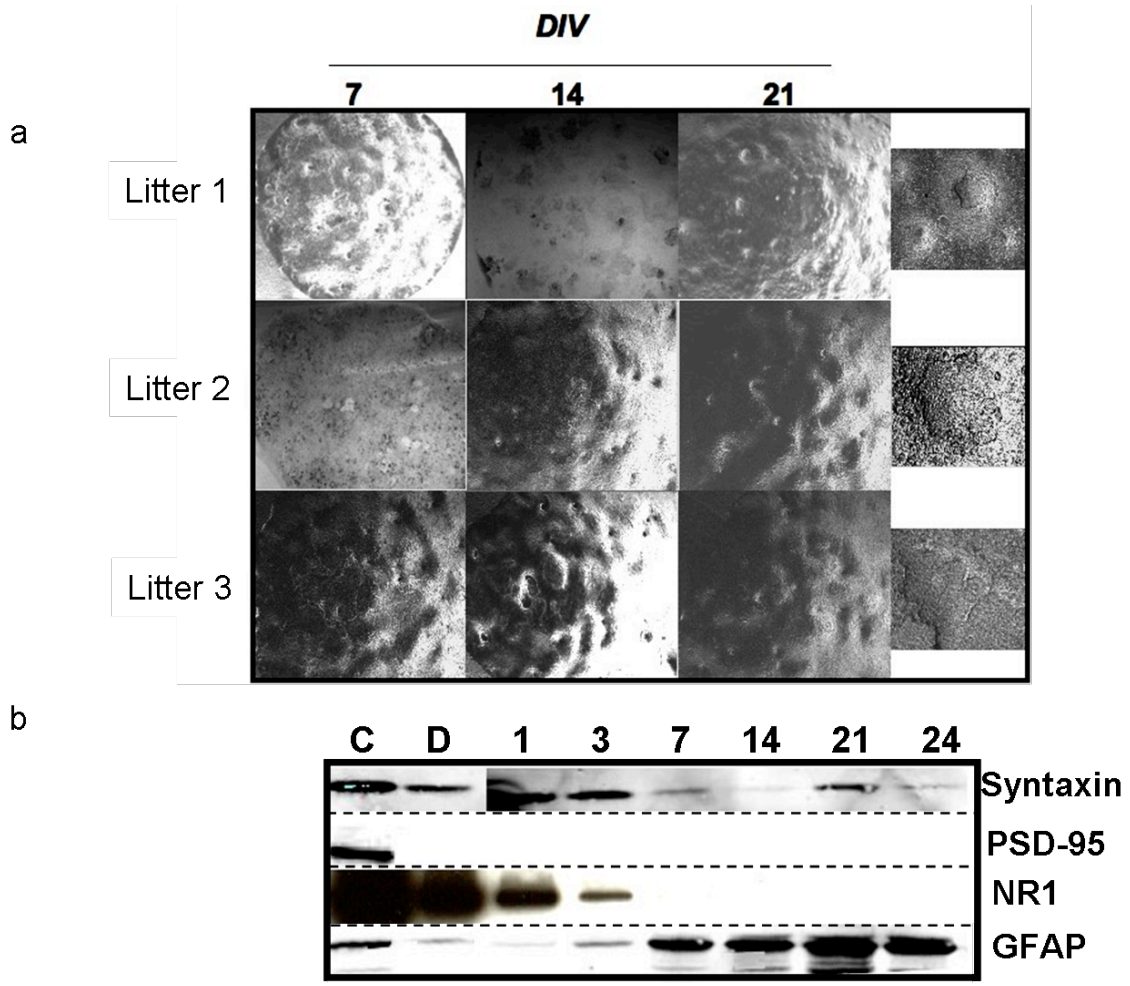

Figure 3.2: Hi-Spots made from P2 tissue using the *Capsant* method

a) Bright field images of Hi-Spots after 7, 14 and 21 *DIV*. Hi-Spot surface shows clumps of cells. Cell clumps correspond to areas of cell death. Inset images are of magnified cell clumps from *DIV* 21 Hi-Spots. Each row shows Hi-Spots made from a new litter of P2 pups marked as litter 1, 2, 3.

b) Representative Western blot from 3 independent P2 litters. Proteins were separated by PAGE on a 10% acrylamide gel, C represents the positive control, adult rat cortex (12µg loaded), D dissociated sample (12µg loaded). (Samples are from equal loading of Hi-Spots at *DIV 1-24* normalised by volume).

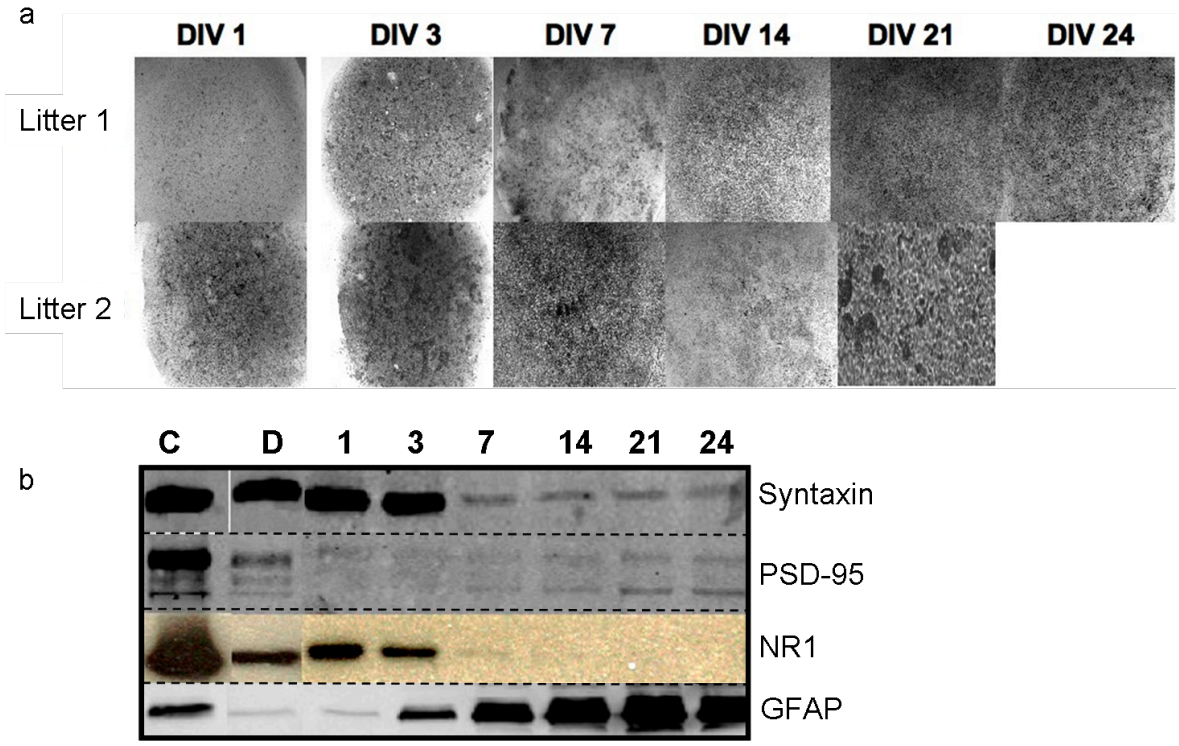

Figure 3.3: Hi-Spots made from postnatal day 0 tissue using the *Capsant* method

a) Bright field images from P0 Hi-Spots after 1, 3, 7, 14, 21 and 24 *DIV*. Each row shows a different litter.

b) Representative Western blot from Hi-Spots made from 3 litters. GFAP is an astrocyte marker, Syntaxin is a neuronal marker, PSD-95 is a neuronal maturational marker, and NR1 is an NMDA receptor marker. Proteins were separated by PAGE on a 10% acrylamide gel, C- adult rat cortex (12µg loaded), D is freshly dissociated sample (12µg loaded). (Samples are from equal volume loading of Hi-Spots at *DIV 1-24*).

Overall these results demonstrate that Hi-Spots produced using the *Capsant* method from E17 tissue form an intact culture which creates an environment capable of maintaining a neuronal population. The neuronal population shows evidence for maturation which occurs alongside a glial astrocyte population. However, Hi-Spots produced from postnatal P0 and P2 tissue using the same *Capsant* method had more amorphous surfaces than those seen for the E17 cultures. P0 and P2 cultures did not show a sustained neuronal population and in contrast to E17 cultures also did not show evidence for a maturing population of neuronal cells alongside a glial astrocyte population.

The evidence from the Western blots suggests that at E17 there is little NR1 expressed at the point of dissociation, however at the postnatal ages NR1 showed strong immunoreactivity in the freshly dissociated sample (Figure 3.4). Because NMDA receptor activation is strongly implicated in excitotoxicity we examined whether the presence of functional NMDA receptors in the postnatal tissue was a key issue in the successful use of postnatal tissue. To this end we tried to block routes of excitotoxicity using the NMDA receptor activation dependent antagonist MK801. We compared Hi-Spots produced from postnatal P0 and P2 tissue using the *Capsant* method and cultures produced using the NMDA receptor antagonist MK801 (*Soton* method) to block chronic activation of NMDA receptors by glutamate released during the dissociation.

3.4.3 Hi-Spots produced from P2 tissue using the '*Soton*' method

To compare if the MK801 *Soton* method better suited cell culture from postnatal tissue, rat litters were split, half of each litter was used to produce Hi-Spots using the *Capsant* method and half was used to produce Hi-Spots using the *Soton* method.

The bright field appearance of the *Soton* P2 cultures resembled more closely that observed for E17 Hi-Spots (Figure 3.5). *Soton* cultures did not show large clumps of cells and/ or holes devoid of cells. This suggests that the modification using MK801 was having an effect on the culture morphology and potentially viability.

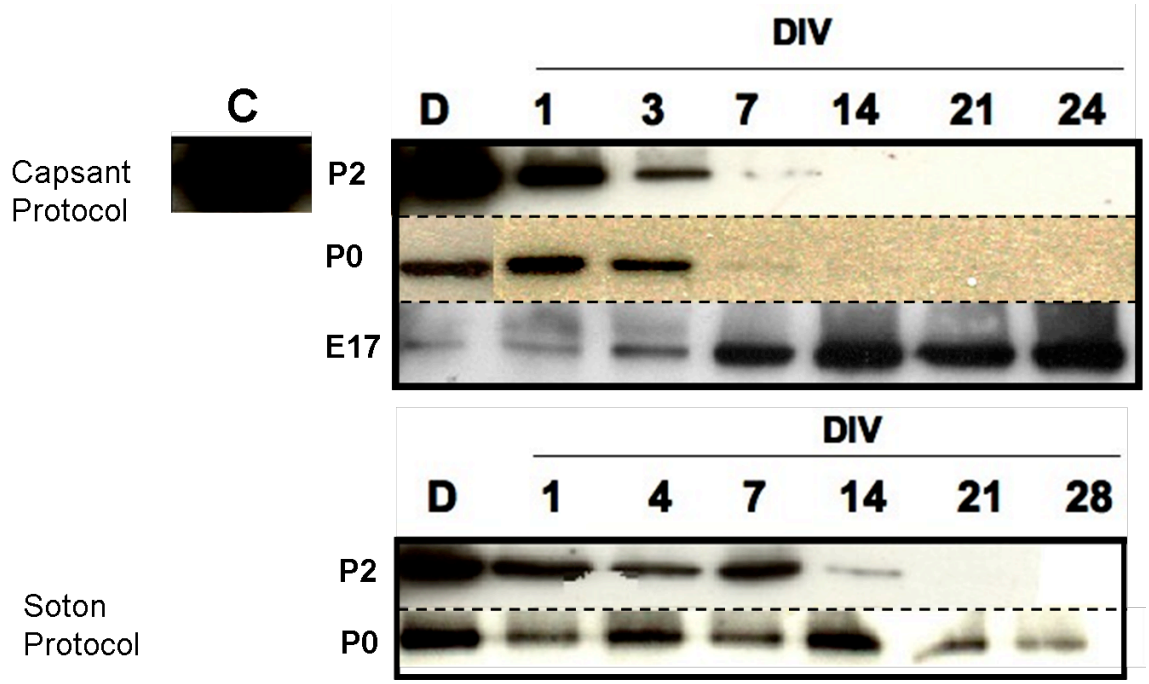

Figure 3.4: NMDA Receptor Subunit 1 (NR1) in P2, P0 and E17 Hi-Spot cultures
Western blot results from P2, P0 and E17 cultures. In P2 and P0 cultures made using the *Soton* or *Capsant* method the freshly dissociated sample D (t=0) shows strong detection of NR1. Strongest expression is seen in dissociated sample (D) from P2 cultures followed by P0> E17. P2 culture sample D shows equivalent loading to sample C, mature rat cortex showing similar high levels of NR1 detection. The dissociated sample of E17 tissue has a lower expression of NR1.
Equal volumes loaded, proteins separated by SDS PAGE, ran on a 10% acrylamide gel. C= adult rat cortex (12µg loaded), D= freshly dissociated sample from which the Hi-Spots are made (12µg loaded). E17 culture n=3 litters, P0 n=4 litters, P2 n=4 litters.

Western blot analysis of cultures produced using the *Soton* method revealed an increased expression of syntaxin and PSD-95 at later culture stages (*DIV* 21-28), compared to Hi-Spots produced from P2 tissue using the *Capsant* method which showed decreases in syntaxin expression after *DIV* 3 (Figure 3.5). In *Soton* cultures PSD-95 was detected throughout the culture period 1- 35*DIV* at higher levels than those observed for cultures produced with the *Capsant* method. NR1 demonstrated highest expression in the freshly dissociated samples for both *Capsant* and *Soton* Hi-Spots. Hi-Spots produced using the *Capsant* protocol showed immunoreactivity for NR1 till ~*DIV* 3, whereas *Soton* cultures retained expression till ~*DIV* 7. The expression of the astrocyte marker GFAP was unaffected by the method used (Figure 3.5). These observations suggest that MK801 addition is providing an optimisation to the culture protocol for the production of postnatal Hi-Spots.

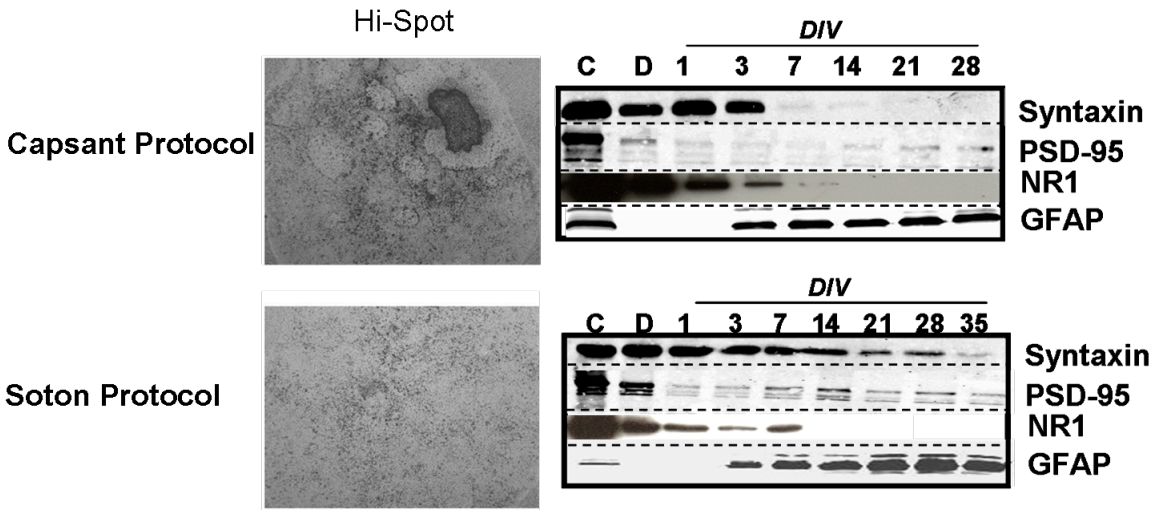

Figure 3.5: Hi-Spots made from P2 tissue using the *Capsant* and *Soton* method
Bright field images of Hi-Spots made using the *Capsant* method show cell clumping and holes devoid of cells. Bright field images of Hi-Spots made using the *Soton* method have a more even appearance showing morphology more like E17 Hi-Spots.

Western blots from Hi-Spots made using the *Capsant* method showed the decline of neuronal markers after *DIV* 3. In *Soton* cultures Western blots show increased immunoreactivity of neuronal markers and neuronal maturational markers across time in culture. n=2 for age and litter matched *Capsant* and *Soton* Hi-Spots.
C= Adult rat cortex (12µg), D= dissociated sample (12µg) from which Hi-Spot cultures are made. Equal volumes loaded, proteins separated by SDS PAGE, ran on a 10% acrylamide gel. n=2 *Capsant* cultures n=5 *Soton* cultures.

3.4.4 Hi-Spots produced from P0 tissue using the '*Soton*' method

To compare the *Capsant* and *Soton* method, litters of P0 rats were spilt; half were used for production of Hi-Spots using the *Capsant* method and half using the *Soton* method. Bright field analysis of *Soton* cultures revealed that unlike *Capsant* cultures, *Soton* Hi-Spots do not form large clumps of cells or show holes. The morphology seen in *Soton* cultures is closer to that observed in E17 cultures (Figure 3.6).

In *Capsant* and *Soton* cultures syntaxin immunoreactivity is high in the freshly dissociated P0 sample. *Capsant* cultures show a marked decline in syntaxin levels after *~DIV 3*; however, *Soton* cultures sustained syntaxin throughout the culture period. *Capsant* and *Soton* cultures both showed strong PSD-95 immunoreactivity in the freshly dissociated sample (D). Initially both cultures showed low levels of PSD-95 in the culture samples, but in the *Soton* cultures immunoreactivity increased to a maximal level at *~DIV 21,* this increase is not seen in the *Capsant* cultures. The astrocyte marker GFAP demonstrated the same expression profile regardless of the protocol, showing the same increase after *DIV 3* and peaking at *DIV 14-21* (Figure 3.6).

To extend the analysis expression of β III Tubulin a marker of neuronal processes and the synaptic vesicle marker synaptobrevin was investigated. In *Capsant* cultures β III Tubulin expression was only detected in the dissociated sample and at *DIV 1*. *Soton* cultures demonstrated expression of β III Tubulin until *~DIV 21-28*. In *Soton* Cultures synaptobrevin immunoreactivity initially declined markedly before increasing again to maximum values at *~DIV 21*, which was not seen for *Capsant* postnatal Hi-Spots. The pattern of NR1 immunoreactivity was highest in the freshly dissociated samples for both *Capsant* and *Soton* Hi-Spots. In *Capsant* cultures NR1 immunoreactivity is lost after *DIV* 14, but in *Soton* cultures NR1 expression is detected until *DIV 28* (Figure 3.6).

Soton cultures have an increased expression of markers for neurons (syntaxin) synapses (synaptobrevin), neuronal maturation (PSD-95) and neuronal process (β III Tubulin) relative to cultures made with the *Capsant* method. We next assessed the cellular morphology of the cultures and the patterns of expression of these markers. This was done using immunohistochemistry (IHC) using fluorescent secondary antibodies and confocal microscopy.

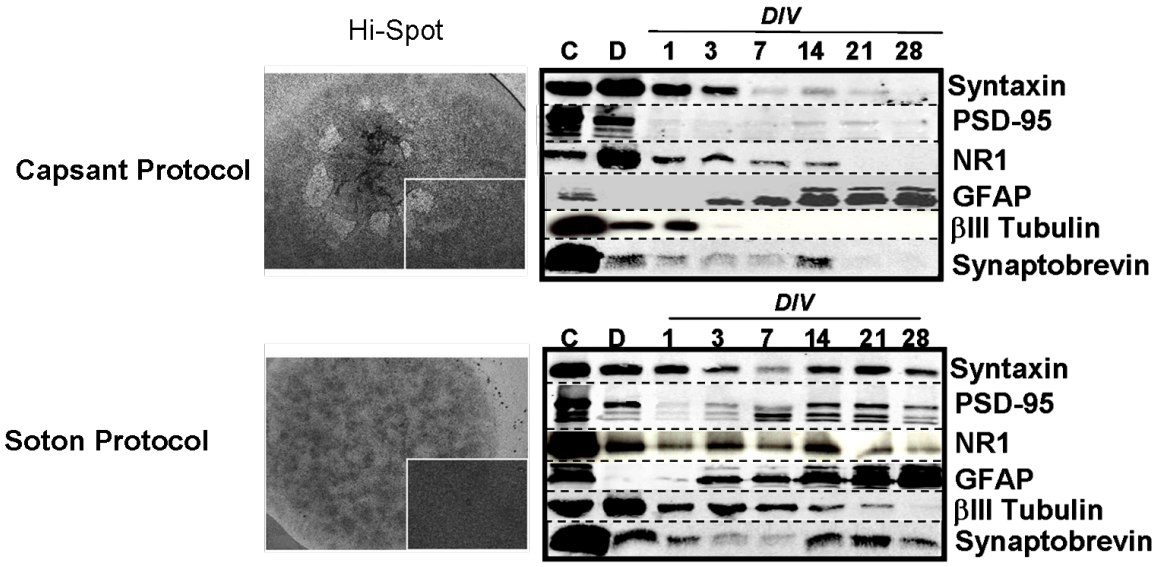

Figure 3.6: Hi-Spots made from P0 tissue using the *Capsant* and *Soton* methods
Bright field images of Hi-Spots made using the *Capsant* method show cell clumping and holes devoid of cells. Bright field images of Hi-Spots made using the *Soton* method have a more even appearance showing morphology more alike E17 Hi-Spots. Inset pictures show magnified images of Hi-Spot surface, culture made using the *Soton* method have a smooth surface like that observed for E17 cultures.

Western blots from Hi-Spots made using the *Capsant* method show lack of neuronal markers after *DIV* 3. In *Soton* cultures Western blots show increased detection longevity of neuronal markers and neuronal maturational markers. Syntaxin is a neuronal marker, PSD-95 is a neuronal maturational marker, NR1 is a NMDA receptor marker and GFAP is an astrocyte marker. n=2 for age and litter matched *Capsant* and *Soton* Hi-Spots. C= Adult rat cortex (12µg loaded), D= dissociated sample (12µg loaded) for Hi-Spot cultures. Equal volumes loaded, proteins separated by SDS PAGE, ran on a 10% PAGE gel for all markers except synaptobrevin- 12% PAGE gel. n=2 litters for *Soton* cultures, n=5 litters for *Capsant* cultures.

3.4.5 Comparison of neural network formation in Hi-Spots created from P0 tissue using the '*Capsant*' and '*Soton'* methods

Western blot results show that P0 cultures made using the *Capsant* and *Soton* method have β III Tubulin expression after dissociation. *Soton* cultures retain β III Tubulin detection until *DIV 21-28* with low levels detected at *DIV* 28, but Hi-Spot cultures produced using the *Capsant* method lack β III Tubulin detection after *DIV* 3 (Figure 3.6). Immunohistochemical (IHC) staining was used to visualise whether the β III Tubulin detected via Western Blot came from a neuronal network of processes and how the β III Tubulin staining was organised relative to other cells in the culture.

IHC analysis showed that after *1 DIV* Hi-Spots produced using the *Soton* method developed a neuronal network. Figure 3.7 shows representative images of Hi-Spots produced using the *Soton* method compared to those produced using the *Capsant* method. In *Soton* cultures β III Tubulin staining shows long dense neuronal processes which are mixed with low levels of GFAP stained astrocytes. As the culture matured the β III Tubulin staining becomes less dense and the astrocyte stained processes stained with GFAP became more pronounced. This supports the Western blot results which also show decreasing levels of β III Tubulin and increasing levels of GFAP detection (Figure 3.6).

IHC analysis in cultures produced using the *Capsant* method does not show a dense network of neuronal processes. At *DIV* 1 the neuronal network formed shows fragmented β III Tubulin staining and long neuronal processes are not observed. As the cultures aged the β III Tubulin staining decreased further and by *DIV* 21 β III Tubulin staining is mainly situated around cell bodies. At *DIV* 28 β III Tubulin staining is hardly detectable, these results support the Western blot data showing very low levels of β III Tubulin after *DIV* 3 (Figures 3.7 and 3.6).

From the Western blot and IHC data combined, Hi-Spots produced using the *Soton* method show expression of key neuronal and synapse markers and the neuronal cells form a network surrounded by glial cells. However, neither of these results can show if the neuronal network is functional and if the synapses present are localised in such a manner as to allow synaptic transmission between different neurons. Multi electrode array (MEA)

recording allows electrophysiological activity to be measured; the system uses extracellular non-invasive planar electrodes.

The Hi-Spot protocol includes the plating of Hi-Spot cultures on to a 6mm in diameter PTFE round disc, the Hi-Spots themselves are only a few millimetres in diameter allowing the edge of the PTFE disc to be picked up and placed on top of the planar electrodes on the MEA (culture side down). Functional analyses can demonstrate whether the neuronal network observed via IHC is active and if functionally connected synapses are present between neurons.

a

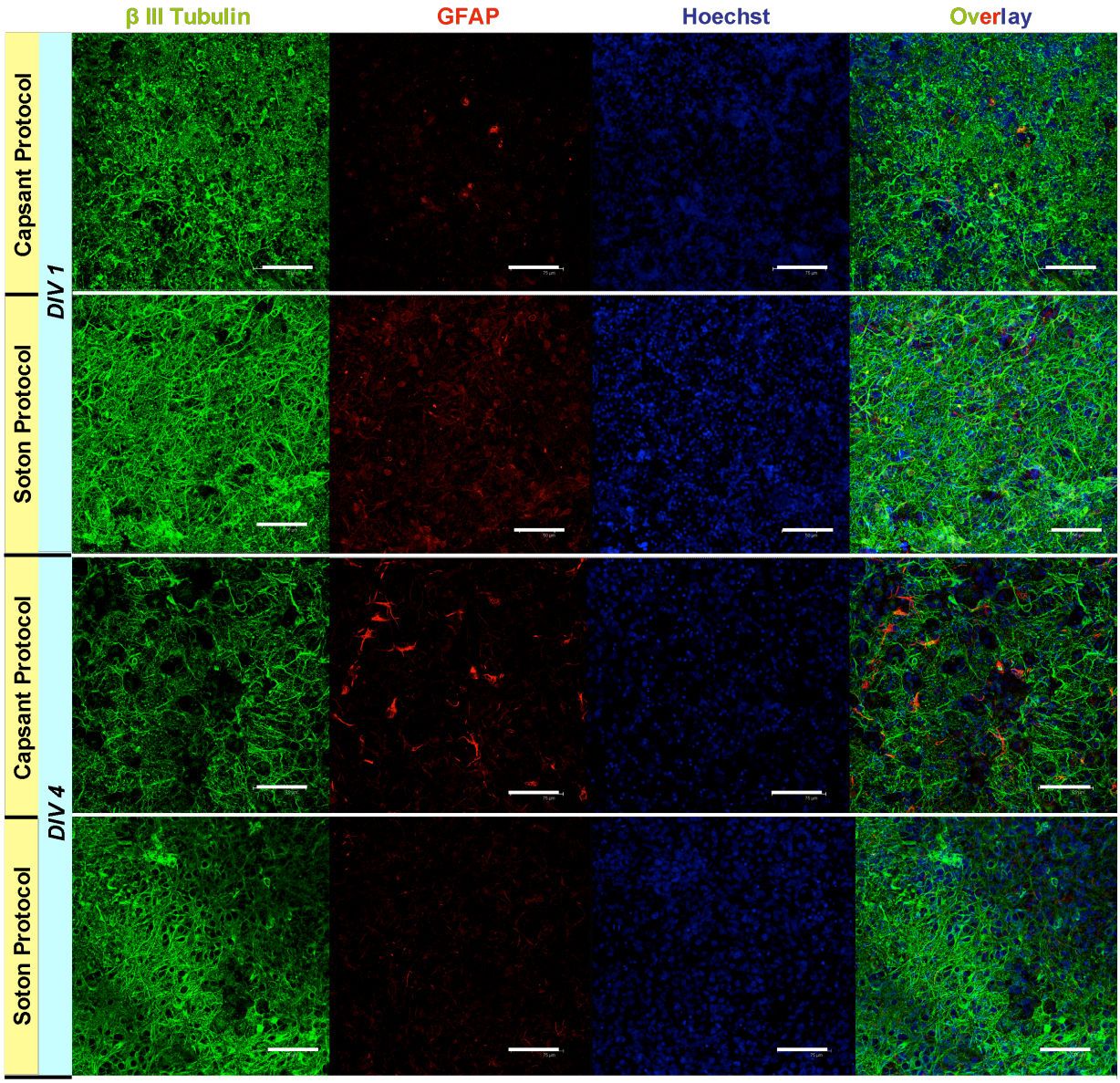
β III Tubulin
GFAP
Hoechst
Overlay
Capsant Protocol
Soton Protocol
DIV 1
Capsant Protocol
Soton Protocol
DIV 4

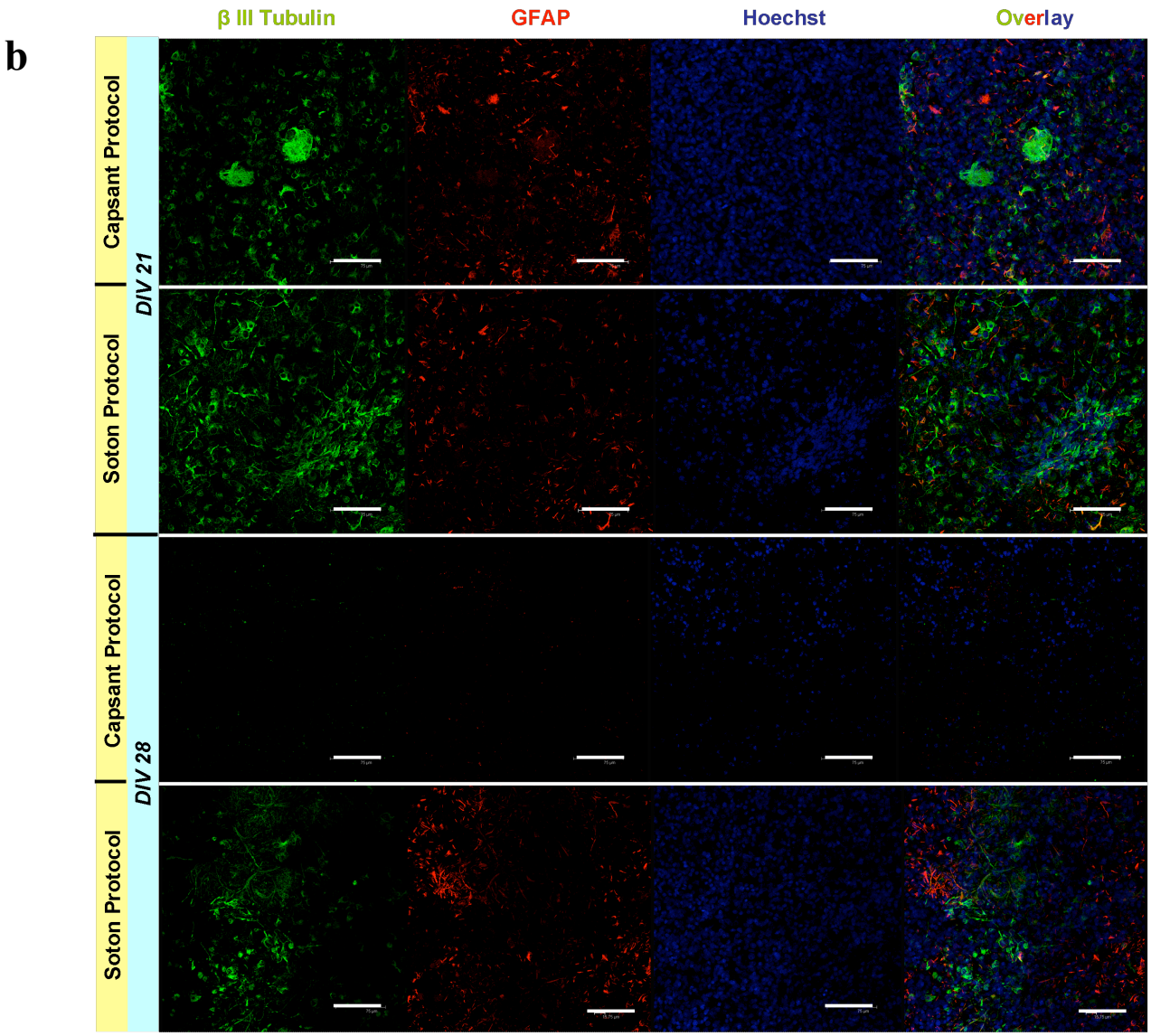

Figure 3.7: Neuronal network formation in *Capsant* and *Soton* P0 cultures
Confocal pictures of maximum projection images from a 12 z stack scan.

a) *Capsant* and *Soton* cultures after *DIV 1* and *DIV 4*. In *Capsant* cultures the β III Tubulin appears fragmented, whereas *Soton* cultures possess a β III Tubulin network of neuronal processes after *DIV* 1.

b) *Capsant* and *Soton* cultures after *DIV 21* and *DIV 28*. At *DIV* 28 *Capsant* cultures show very low amounts of β III Tubulin staining. *Soton* cultures show reduced amounts of β III Tubulin as culture ages. Green β III Tubulin, Red GFAP, Blue Hoechst 33342. Scale bar 75µm

3.4.6 Direct comparison of electrophysiological activity in '*Capsant*' and '*Soton*' cultures

Soton cultures developed spontaneous electrical activity. The recorded activity was qualitatively assessed to consist of single spiking and bursting events. Figure 3.8a shows the bursting and single spiking activity profiles. Single spikes of activity are normally uncorrelated across the channels and consisted of individual units of activity which could be easily distinguished. Bursts of activity consisted of a series of spikes in quick temporal

succession. During bursts the activity between the channels was highly correlated and single spikes that formed the burst were of higher frequency than those observed for isolated consecutive single spikes on a single channel (Figure 3.8).

Single spiking activity was associated with immature cultures (*DIV 1-7*) and bursting was observed in more mature cultures (*DIV 7-35*). Hi-Spots produced from E17 tissue have also been shown to develop spontaneous activity consisting of single spiking and bursting events (van Vliet, Stoppini et al. 2007).

Soton cultures have higher activity in terms of RMS (Root Mean Squared) and spike number compared to *Capsant* cultures. Figure 3.9 shows the spike number and RMS values from *Capsant* and *Soton* cultures.

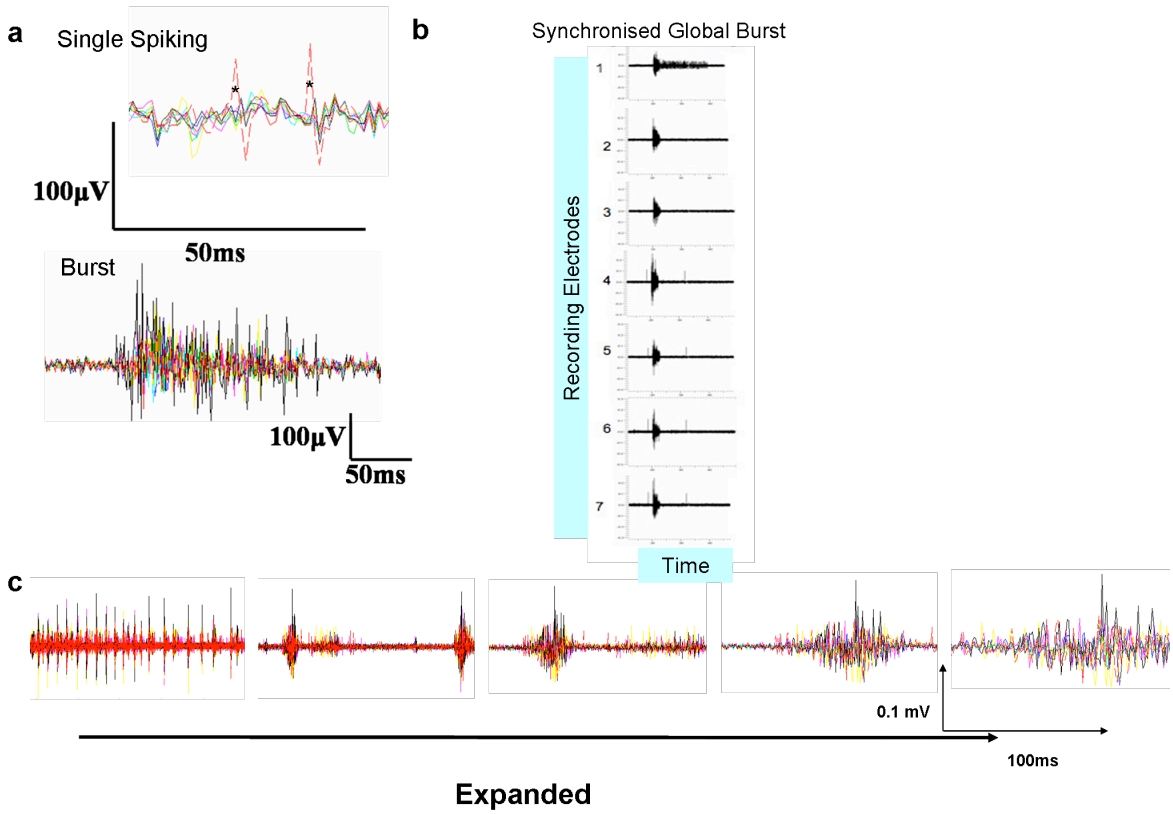

Figure 3.8: P0 Hi-Spots Multi-electrode array recordings showing single spiking and bursting activity.

a) Single spiking and bursting activity were recorded on the MEA from a *Soton* P0 Hi-Spot. Single spikes are denoted by *. Bursting activity was generally higher in amplitude and frequency and correlated across the 8 different channels. Each channel is denoted by a different colour

b) The synchronised activity recorded from 7 recording electrodes during a burst of activity in the Hi-Spot. Each spatially distinct electrode records activity but the activity recorded from each electrode differs. This suggests that the electrodes are not all recording from the same set of neuronal cells.

c) The first trace shows a series of consecutive bursts after heater spike removal, following windows show traces which have a progressively expanded time scale. The expanded time scale traces highlight the structure of a single burst. Each colour shows the spiking activity of a different recording channel recording from a spatially distinct site in the Hi-Spot. Bursts occurred as high frequency spikes of activity from spatially different sites with high temporal precision.

In *Soton* cultures spike number and RMS value increase as the cultures ages, increasing significantly between *DIV 14* and *21* (Spikes P=0.0403, RMS P=0.0470). From *DIV 21* to *DIV 28* the activity level is maintained at a high level, becoming more variable between Hi-Spots at *DIV 35* (denoted by error bar size Figure 3.9).

Figure 3.10 demonstrates increased activity levels in *Soton* cultures and shows that the activity recorded from *DIV 35* Hi-Spots is skewed due to one highly active Hi-Spot. This shows that the activity level for the majority of Hi-Spots has decreased at *DIV 35*.

Capsant cultures show low levels of activity throughout. There was some increase in spike number between *DIV 1-4* and *DIV 14-21* (P= 0.0305 and P= 0.0343 respectively), but neither the spike number nor RMS value reach the level of activity observed for the *Soton* cultures. *Soton* cultures showed significantly increased spike number compared to Hi-Spots produced with the *Capsant* method at *DIV 21* and *28*, and RMS value at *DIV 7, 14, 21,* and *28* (Spikes *DIV 21* P=0.0381, *DIV 28* P=0.0127, RMS *DIV 7* P=0.0287, *DIV 14* P=0.0139, *DIV* 21 P=0.0293 and *DIV* 28 P= 0.0165). The *Soton* cultures show the highest level of activity at *DIV* 21.

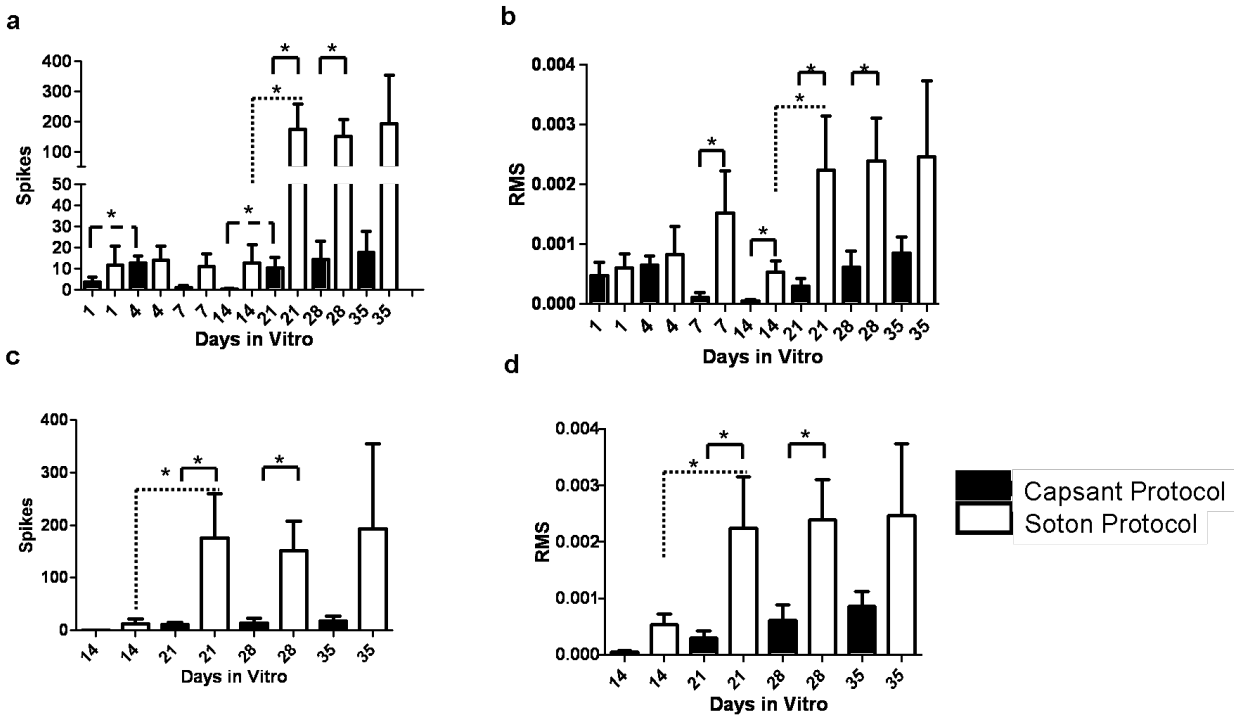

Figure 3.9: MEA recording of P0 *Capsant* cultures (black) compared to cultures made with the *Soton* method (White)

Soton cultures have a higher spike frequency and RMS value

a) Number of spikes counted in a 300 second recording sample from age matched *Capsant* and *Soton* cultures.

b) RMS value in a 300 second recording of age matched culture made using the *Capsant* and *Soton* cultures.
Spike number and RMS values for *DIV* 14, 21, 28 and 35 to highlight differences in older cultures.

c) Number of spikes counted in a 300 second recording for *Capsant* and *Soton* cultures at *DIV* 14-35.

d) RMS value for 300 seconds of recording from *Capsant* and *Soton* cultures *DIV* 14-35, showing the difference between *Soton* and *Capsant* cultures at the later time points in culture.

*P=<0.05, Statistics- unpaired one tailed t-test 95% confidence value
Broken line shows significance between different aged *Capsant* Hi-Spots
Dotted line shows significance between different aged *Soton* Hi-Spots
Solid line shows significance between *Soton* and *Capsant* cultures.
n= 2 rat litters *Soton* cultures, 16 Hi-Spots, n=2 rat litter *Capsant* cultures, 16 Hi-Spots.

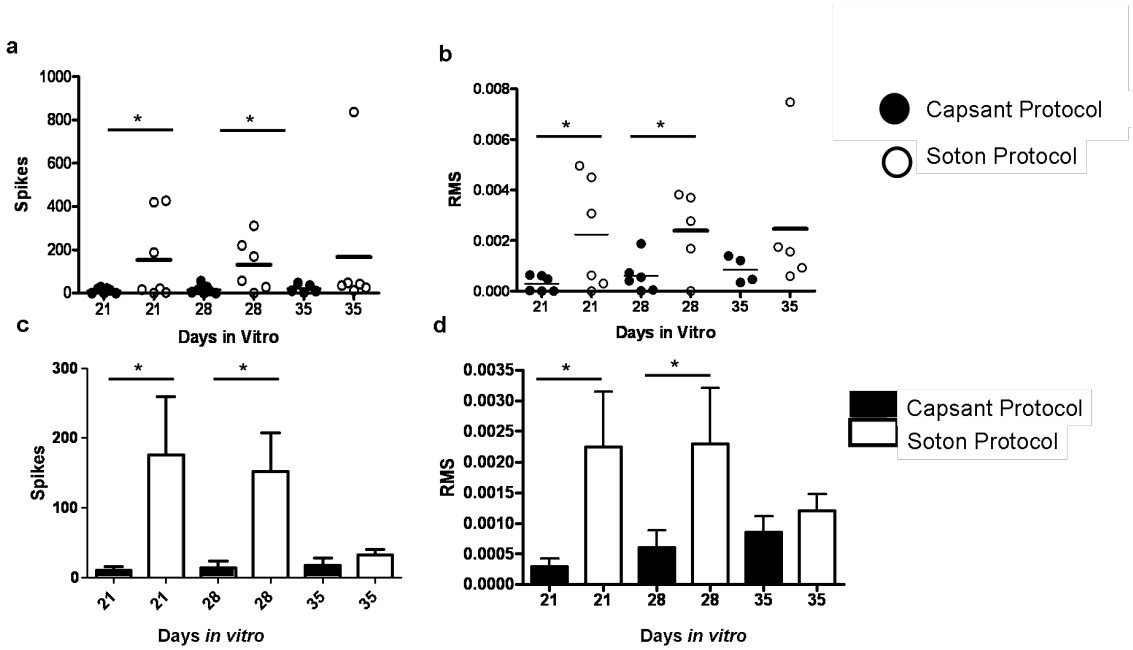

Figure 3.10: Older cultures demonstrate a more variable level of spontaneous activity

a) A scatter plot of the spike number recorded from 300 seconds of activity in *Capsant* and *Soton* cultures at *DIV* 21, 28 and 35. Five of the *Soton DIV* 35 Hi-Spots show similar spike numbers, one Hi-Spot show uncharacteristically high spike numbers. This shows that at this age Hi-Spots cultures can be highly active showing activity levels as high as *DIV* 21-28 but the majority of Hi-Spots have low activity could be associated with neuronal loss as this age.

b) A scatter plot of the RMS value recorded from 300 seconds of activity in *Capsant* and *Soton* cultures at *DIV* 21, 28 and *DIV* 35.

c) Bar chart of the spike frequency at *DIV* 21, 28 and 35 cultures. *DIV* 35 samples shows activity difference between *Capsant* and *Soton* Hi-Spots with highly active *Soton* Hi-Spot spike frequency removed. P= 0.0381 *DIV*21, P=0.0127 *DIV* 28

d) Bar chart of the RMS value at *DIV* 21, 28, and 35 cultures, *DIV* 35 sample shows activity differences between *Capsant* and *Soton* Hi-Spots with highly active *Soton* Hi-Spot RMS value removed. P=0.0293 *DIV* 21, P=0.0165 *DIV* 28
Statistics calculated using an unpaired one tailed 95% confidence t-test.
n= 2 rat litters *Soton* cultures, 16 Hi-Spots, n=2 rat litters *Capsant* cultures, 16 Hi-Spots.

3.4.7 Direct comparison of electrophysiological activity in Hi-Spots produced from P2 tissue using '*Capsant*' and '*Soton*' method

Soton method culture show enhanced activity in terms of RMS value and spike number compared to *Capsant* cultures. Figure 3.11 shows that at *DIV* 14 the level of RMS activity

is significantly higher in P2 cultures produced using the *Soton* method compared to those made with the *Capsant* method (P= 0.0458). The difference in spike number falls just below the level of significance (P=0.0560). At *DIV* 21 the *Soton* Hi-Spots demonstrated a higher spike number and RMS value than the cultures produced using the *Capsant* method but the difference is not statistically significant (Figure 3.11).

Even though the P2 *Soton* cultures show increased activity compared to P2 cultures made using the *Capsant* method, P2 *Soton* cultures do not demonstrate the same level of activity as that recorded from P0 *Soton* cultures (Figure 3.12). P0 *Soton* cultures demonstrate a much higher spike number and RMS value that P2 *Soton* cultures.

In summary, these results have shown that Hi-Spot cultures made from E17 tissue form a culture that under bright field microscopy inspection does not form holes or cell clumps, and expression of the neuronal marker syntaxin and maturational marker PSD-95 increase with culture age (Figure 3.1) The E17 cultures also contain astrocytes and express the excitatory NMDA receptor marker NR1. Postnatal cultures produced using the same method as E17 cultures form blebs of clumping cells and in some case disaggregate (Figures 3.2, 3.3, 3.4 and 3.5). The postnatal cultures do not express detectable levels of the neuronal marker syntaxin and PSD-95 at later culture ages (Figure 3.5, 3.6). The main difference observed between E17 and postnatal tissue is the expression levels of NR1 in the freshly dissociated tissue (Figure 3.4). Using the *Soton* method (containing the NMDA receptor antagonist) for postnatal Hi-Spot production resulted in the formation of a neuronal network surrounded by glial that had spontaneous functional activity (Figure 3.9, 3.11). The recorded activity from the *Soton* cultures is higher than those formed using the *Capsant* method and Hi-Spots produced using P0 tissue had higher activity that those produced from P2 tissue (Figures 3.12).

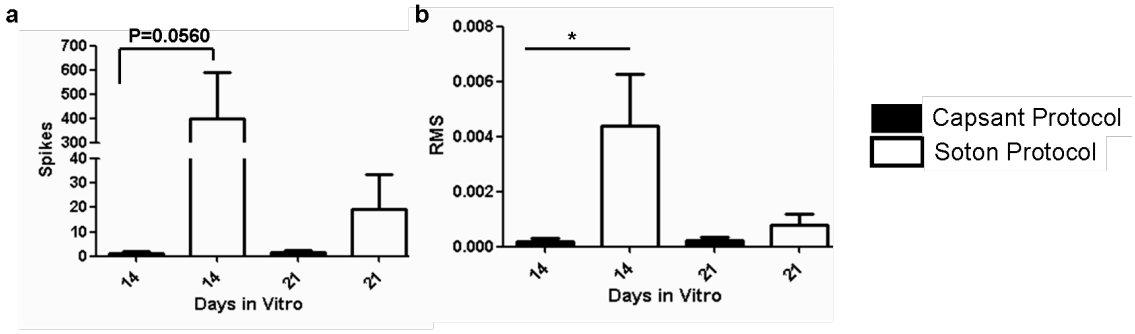

Figure 3.11: MEA activity of P2 *Capsant* cultures (black) compared to cultures made using the *Soton* method (white). P2 *Soton* cultures show higher spike frequency and RMS value.

a) Spike number calculated from 300 second recording from *Soton* cultures and cultures made using the *Capsant* method at *DIV* 14 and *DIV* 21. At both time points, cultures produced using the *Soton* method had a higher spike number compared to cultures made using the *Capsant* method

b) RMS value calculated from 300 second recording of *Soton* and *Capsant* cultures at *DIV* 14 and *DIV* 21. Cultures produced using the *Soton* method showed a significantly higher RMS value compared to cultures produced using the *Capsant* method- P=0.0458

Statistics calculated using an unpaired one tailed 95% confidence t-test. *P=<0.05 *Capsant*: *DIV* 14 n=4, *DIV* 21 n=2, *Soton*: *DIV 14* n=5, *DIV 21* n=4 Hi-Spots, from two sets of P0 and two sets of P2 litters.

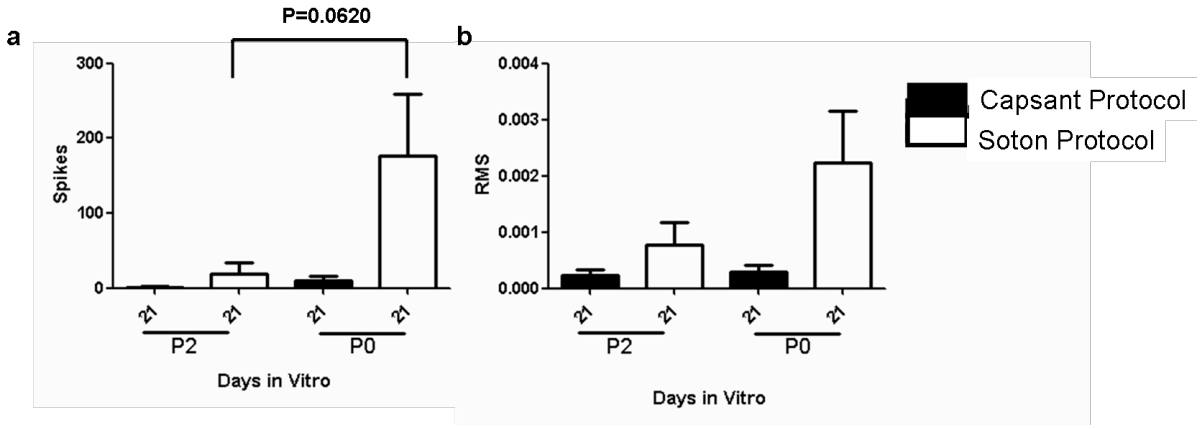

Figure: 3.12: *Soton* P2 cultures have a higher spike frequency and RMS value compared to *Soton* P0 cultures.

a) Difference in spike number between P2 and P0 cultures at *DIV* 21. *DIV* 21 is characteristically the culture age which showed the highest level of activity. At this stage *Soton* P0 culture had nearly three times higher activity levels in terms of both spike number and RMS compared to *Soton* P2 cultures.

b) Difference in RMS value between P2 and P0 cultures at *DIV* 21.

3.5 Discussion

The aim of this chapter is to expand on the initial experiments that had allowed development of dissociated re-aggregated cultures based on E17 tissue. Re-aggregated cultures produced from E17 tissue have been shown to form a neuronal network and develop spontaneous activity (van Vliet, Stoppini et al. 2007) but there had been no characterisation of the neuronal markers expressed in the E17 cultures and unsuccessful attempts to produce re-aggregated Hi-Spot cultures from postnatal tissue.

We investigated if neuronal cells, cultured as re-aggregated Hi-Spot cultures from postnatal tissue would survive, mature and form an active neuronal network surrounded by glia. Western blotting demonstrated the presence of specific markers for neurons, neuronal maturation, synapses and neuronal processes. Using the *Capsant* method of Hi-Spot production for postnatal tissue did not produce a culture containing maturing neuronal cells; neuronal markers were lost early in the culture period leaving a sustained glial cell population.

Our analysis used classical markers that revealed that embryonic and postnatal tissue contained different levels of NR1 at the point of dissociation (Figure 3.4). There was little NR1 expressed in E17 dissociates, whereas large amounts of NR1 were detected in P2 and P0 dissociates. We postulated that differential levels of excitotoxicity could explain this difference in success of cultures. This led us to develop a *Soton* protocol based on blockade of any functional NMDA receptors in the P2 and P0 dissociates with the use of the NMDA receptor dependent antagonist MK801. This modification allowed neuronal networks to form from the dissociated postnatal tissue in Hi-Spots.

Taken together, these results show that in the absence of MK801 there is an excitotoxicity occurring in the postnatal cultures. The toxicity may be relatively selective for postnatal cultures because of lower expression of functional NMDA receptors at embryonic stages (Figure 3.4)(Babb, Mikuni et al. 2005). The inhibition of NMDA receptors during production permitted the use of postnatal tissue for Hi-Spots with similar properties to those seen in embryonic tissue. These include a flat morphological appearance with no cell clumping or disaggregation, a maturing neuronal network surrounded by glial cells and spontaneous network activity, which has previously been reported to in re-aggregated embryonic cells (van Vliet, Stoppini et al. 2007).

3.5.1 Properties of Hi-Spots produced using E17 tissue

Hi-Spots produced from E17 tissue contained neuronal and astrocyte cells. Astrocytes are the main type of glial in the CNS (Ullian, Sapperstein et al. 2001), GFAP is an 8-9nm intermediate filament protein expressed in mature astrocytes. GFAP is thought to be important for modulating astrocyte motility and shape by providing the astrocyte processes with structural stability (Eng, Ghirnikar et al. 2000). Following injury, trauma, disease or chemical insult astrocytes can become reactive (Chow, Yu et al. 2009), and this is termed 'astrogliosis'. Astrogliosis is characterised by rapid synthesis of GFAP leading to increased GFAP protein.

The increasing GFAP expression in the E17 cultures suggests that the astrocyte population is either proliferating or hyper-functioning. This indicates that the neuronal population matures simultaneously with an increase in astrocyte GFAP expression, as indicated by the increasing syntaxin and PSD-95 expression. Therefore, the astrocyte either proliferation of hyper-functioning occurring in the E17 Hi-Spot cultures is unlikely to be detrimental to the health of the neuronal population.

At the point of dissociation, Hi-Spot cultures made from E17 tissue express lower levels of NR1 compared to P2 and P0 tissue (Figure 3.4). This is consistent with a developmental up-regulation of NR1 expression since NR1 is first detected at E16 and NR2B/2A at E14, however functional association of the two subunits to form a functional NMDA receptor does not occur until P0 (Babb, Mikuni et al. 2005). Due to the lack of NR1 expression observed at the point of dissociation in E17 tissue, any glutamate released during the dissociation step may not stimulate an excitotoxic reaction. Conversely the P2 and P0 tissue showed selective high NR1 expression at the point of dissociation, and functional heteromeric NMDA receptors are likely to exist and become activated by extracellular glutamate released during the dissociation from sheared cells.

NMDA receptor activation is vital for cell survival but pathological chronic activation can lead to cell death by apoptosis or necrosis. Increase in extracellular glutamate levels activating NMDA receptors is the primary cause of neuronal death following acute trauma such as stroke or seizure (Lipton and Rosenberg 1994)(Dirnagl, Iadecola et al. 1999) and is also thought to contribute to the aetiology of many chronic neurodegenerative disorders such as ALS (Rothstein, Van Kammen et al. 1995), Huntington's, and Alzheimer's disease

(Lancelot and Beal 1998). Thus it seems likely that MK801 improves the quality of Hi-Spots made from postnatal tissue due to the blockade of NMDA receptors at the point of dissociation and hence reduction of associated excitotoxicity (Figure 3.13).

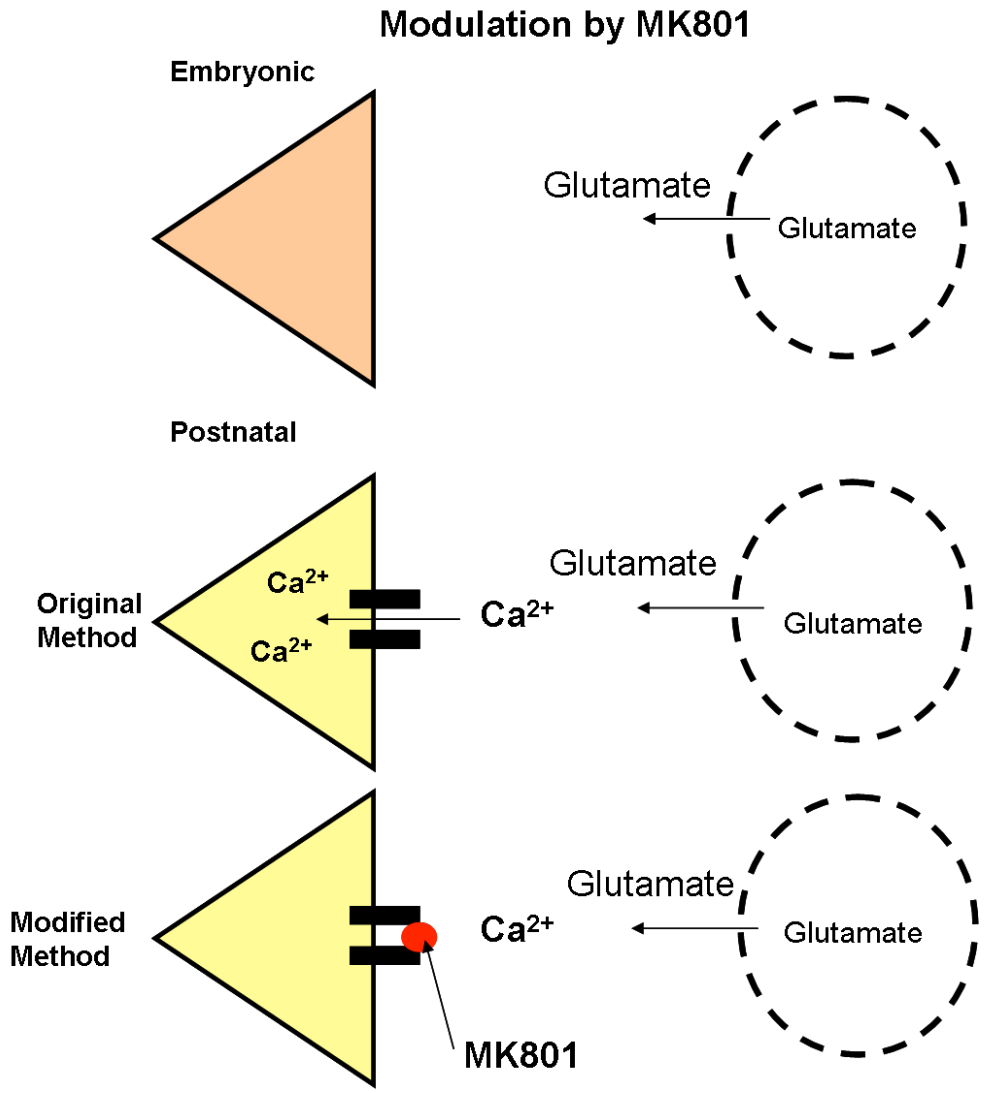

Figure 3.13 Model MK801 action
Hi-Spots made from postnatal tissue undergo degeneration due to NMDA receptor over activation. Glutamate released during the mechanical dissociation of the cortical tissue leads to excitotoxicity and cell death of postnatal cultures. Hi-Spot made from E17 tissue to not undergo this degeneration because they do not possess functional NMDA receptors at the point of dissociation. MK801 acts to protect the postnatal cells formed from postnatal tissue by antagonising the extracellular glutamate released inhibiting NMDA receptors.

Astrocytes are important for the uptake of extracellular glutamate; a low number of astrocytes at the point of dissociation may affect the ability of the culture preparation to buffer against increased glutamate released during mechanical dissociation (Rothstein, Van Kammen et al. 1995; Rothstein, Dykes-Hoberg et al. 1996). This coupled to the higher

expression of NR1 (Figure 3.4) and the evidence that functional heteromeric NMDA receptors are expressed in rats from P0 (Babb, Mikuni et al. 2005) may explain the lack of neuronal markers in the postnatal cultures that are not treated with MK801 during the dissociation.

3.5.2 Protective effects of MK801 on postnatal tissue

MK801 is an open channel NMDA receptor uncompetive antagonist (Foster and Wong 1987). During the mechanical trituration of the cells from the cortex into a single cell suspension any cells that are tightly bound to one another via cell adhesion molecules may be pulled apart and potentially sheared. The mechanical shearing could result in increased glutamate in the dissociation solution from intracellular stores such as vesicles in both neurons and astrocytes (Araque, Li et al. 2000). The released glutamate could then bind to glutamate receptors such as NMDA receptors leading to chronic NMDA receptor activation, excitotoxicity and cell death. The cell death caused by excitotoxicity is thought to occur due to calcium overload in the cell. Calcium ions are ubiquitous intracellular messengers governing a large number of cellular functions from exocytosis to cell growth (Kater and Mills 1991; Brose, Petrenko et al. 1992). Neurons have a very low resting intracellular calcium concentration (~100nm) allowing a high signal to noise ratio during calcium signalling.

Experiments have shown that the source of the calcium influx can determine whether the signal is toxic: the calcium signals being tightly constrained to domains in space and time (Chad and Eckert 1984). Free calcium loads produced by influx through L-type voltage-gated calcium channels are not harmful but intracellular calcium increase through NMDA receptors are toxic (Tymianski, Charlton et al. 1993). NMDA receptors are linked intracellularly to many scaffolding and signalling proteins. PSD-95 binds to NMDA receptors through a PDZ-PDZ domain interaction with the NR2 subunit on NMDA receptors. Through PSD-95 NMDA receptors are linked to neuronal Nitric Oxide Synthase (nNOS), thus NMDA receptor activation can lead to the generation of Reactive Oxygen Species (ROS) (Sattler, Xiong et al. 1999). Calcium overload can also lead to mitochondrial dysfunction. Mitochondria take up calcium during glutamate receptor over activation, and excessive mitochondrial calcium has been shown to de-energize mitochondria triggering mitochondrial production of ROS. Mitochondrial calcium loading

has also been shown to cause release of cytochrome C, a pro- apoptotic factor able to activate caspases by binding to the cytosolic protein apoptotic protease activating factor-1 (Buki, Okonkwo et al. 2000). Calcium influx through NMDA receptors can also activate the neutral cysteine protease calpain-1, which cleaves cytoskeletal proteins, enzymes and transcription factors (del Cerro, Arai et al. 1994).

3.5.3 Neural networks formed from P0 tissue

Western blotting demonstrated neuronal and glial cells are cultured together in the Hi-Spots when the *Soton* protocol was used to antagonise the NMDA receptors during the dissociation of P0 tissue. IHC identified that the two cell types co-exist together in close association.

The dissociation step in the protocol removes any pre-existing cell-cell contacts and organisation, IHC reveals that after one day in culture *Soton* Hi-Spots have formed a β III Tubulin positive neuronal network extending over the entire Hi-Spot. As the culture ages the neuronal cells appear to reside in groups of cells linked by β III Tubulin positive processes. The neural cells self-organise into a network that exhibits spontaneous electrophysiological activity. The astrocytes present may aid the formation of the network (Ullian, Sapperstein et al. 2001; Ullian, Christopherson et al. 2004).

Functional Spontaneous activity in *Soton* cultures show higher levels of spontaneous activity at later culture ages compared to *Capsant* cultures. The lower level of spontaneous activity in cultures generated using the *Capsant* method is consistent with the lower levels of synaptic markers and the lack of detectable β III Tubulin neuronal processes labelling at later cultures ages.

Soton cultures demonstrated spontaneous activity in the form of single spikes of unit activity and bursts of consecutive spikes in close temporal precision (Figure 3.8). This supports research conducted by Van Vilet et al on E17 re-aggregated cultures recorded on a MEA (van Vliet, Stoppini et al. 2007). The developmental time frame of the activity and the nature of activity observed are consistent with other observations of dissociated cortical cultures recorded on MEAs (Kamioka, Maeda et al. 1996; Chiappalone, Bove et al. 2006; van Vliet, Stoppini et al. 2007).

In *Soton* P0 Hi-Spots the early phase of isolated unit activity (*DIV*4) precedes the development of the synaptic components (Figure 3.6 Western blot), but is coincident with the increase in GFAP, which is a marker of astrocyte maturation. Astrocytes have been shown to be capable of generating calcium waves and regenerative release of glutamate (Innocenti, Parpura et al. 2000) that can signal to neurons via extra-synaptic NMDA receptors (Araque, Sanzgiri et al. 1998). We have shown that NR1 is present in *Soton* P0 Hi-Spots at this stage (Figure 3.4, 3.6 Western blot), and therefore glutamate release from astrocytes could be contributing an excitatory drive at this stage of development (Angulo, Kozlov et al. 2004). The importance of neuronal-astrocytic interactions, both physiologically and pathologically, are increasingly being recognised (Halassa and Haydon 2010) thus reinforcing the value of the mixed cell-type and high density nature of the Hi-Spot culture system.

The mature culture bursting activity has been show to correlate to synchronized calcium transients and depend on the existence of both glutamatergic and GABAergic neurons (Robinson, Kawahara et al. 1993). Spontaneous activity has been shown to depend on the activation of NMDA and AMPA receptors (Martinoia, Bonzano et al. 2005), and the failure of neurons to participate in spontaneously generated activity has been shown to result in their elimination (Voigt, Baier et al. 1997). The spontaneous bursts recorded are highly correlated across the different electrodes. Electrodes are 100μm in diameter and positioned 250μm apart, therefore, although one electrode can recorded from more than one cell the activity record from different electrodes is unlikely to be from the same cell or group of cells. This is demonstrated when single spikes of activity are recorded on individual electrodes and not detected by other nearby electrodes.

Correlated activity is also seen, (*in vivo*), in immature embryonic tissue, and in the adult brain spontaneous activity is observed as network oscillations (Section 1.8). Many mechanisms have been postulated to explain how the temporal synchronicity occurs between spatially distinct sites; interneurons have been heavily implicated the in generation of spontaneous activity (Wulff, Ponomarenko et al. 2009)(Voigt, Opitz et al. 2001). Further mechanisms include cellular control by pacemaker cells and regulation of cellular excitability by the activation of Hyperpolarisation-activated cyclic nucleotide dependent channels (Mao, Hamzei-Sichani et al. 2001).

3.5.4 *Soton* P2 cultures are not as active as *Soton* P0 Hi-Spot cultures

Hi-Spots made from P2 tissue using the *Soton* method exhibited increased levels of spontaneous activity (both spike number and RMS value) compared to cultures produced using the *Capsant* method. Due to noise level variability and incidences of 50Hz electrical noise pollution some of the P2 Hi-Spot recordings had to be excluded from the spike and RMS analysis, leaving only recordings from *DIV 14* and *DIV 21*.

Comparison of activity levels shows a clear difference between P0 and P2 cultures. P2 Hi-Spots made using the *Soton* protocol have an earlier decline in neuronal and maturation markers (syntaxin and PSD-95, respectively) compared to *Soton* P0 Hi-Spots (Figure 3.5 and 3.6). Neuronal markers and spontaneous activity levels are not as high as those detected in *Soton* P0 cultures. This could be due to the increased maturity of the cells in the P2 dissociated tissue, these cells could be more strongly linked by cell-cell adhesions thereby increasing the number of cells sheared. Further improvements to Hi-Spots made using P2 tissue could be the use of proteolytic enzyme to remove the extracellular proteins to make the dissociation less damaging.

3.6 Conclusion

We have demonstrated that viable Hi-Spots can be successfully produced from postnatal rat brain tissue if the NMDA receptor is blocked during the cell dissociation. Our current view of the processes of MK801 protection is outlined in Figure 3.13. Furthermore, we have shown (based on biochemical, immunohistochemical and electrophysiological evidence) that P0 cultures prepared with the *Soton* protocol have similar properties to E17 cultures and superior properties to P2 cultures. These cultures self-organise into functional neural networks that develop through time in culture. Therefore the *Soton* method of Hi-Spot production from P0 tissue treated with MK801 was used for subsequent investigations.

.

4 -Characterisation of P0 Rat Hi-Spots

4.1 Introduction

The previous chapter discussed modification of the protocol to allow generation of Hi-Spots from postnatal rat tissue. This chapter characterises Hi-Spots in order to determine the feasibility and utility of their use in investigations of CNS function. In particular the network spontaneous activity is tested for GABAergic and glutamatergic networks and the cell-cell interactions formed in the Hi-Spot are tested to establish whether the culture formed has *in vivo*-like cell connectivity.

An example of the importance of cell-cell interactions is demonstrated by the tolerance to glutamate toxicity observed in *in vivo* and organotypic cultures. Measured elevations in extracellular glutamate for >30mins that peaked to calculated values >200μM *in vivo* were found to be non-toxic unless coupled with another energetic insult (Masliah, Alford et al. 1996). Organotypic cultures contain neural networks and cell-cell interactions established *in vivo*, and show *in vivo*-like tolerance to prolonged exposure to millimolar concentrations of glutamate (Morrison, Pringle et al. 2002). However, *in vitro* dissociated cultures, which do not contain the cell-cell connectivity of *in vivo* or organotypic cultures, show high sensitivity to relatively low levels of glutamate. Choi et al demonstrated an ED_{50} for 5min exposure from 50-100μM glutamate (Choi, Maulucci-Gedde et al. 1987). This demonstrates that *in vitro* dissociated cultures fail to mimic the glutamate homoeostasis found *in vivo,* and this discrepancy is likely to result from the cellular interactions between neuronal and glial cells in tissues which are not mimicked in dissociated cultures.

Here we describe the properties of a system that allows the production of large numbers of small, self-organising neuronal networks from postnatal rat cortices. These aggregates may spontaneously form an experimentally tractable analogue of the molecular, cellular and network functions of *in vivo* tissue. Having modified the production of these cultures for postnatal tissue use we demonstrate that the Hi-Spots have the properties of complex neuronal networks and highlight the tissue-like insensitivity of these cultures to glutamate toxicity. We show that Hi-Spots provide a biological analogue of functional CNS tissue at a level of complexity that allows for detailed functional analyses and that may potentially reduce the need for *in vivo* experiments.

In this study Hi-Spots were generated from P0 rat cortical tissue using the *Soton* method. The Hi-Spots were tested for their expression of markers for neurons, neuronal maturation,

neuronal processes, glial cells (both astrocytes and microglia), glutamate receptors and synapses. Spontaneous activity recorded from P0 Hi-Spots was tested for glutamatergic and GABAergic inputs, and that the activity recorded is synaptically driven. Tests were done between *1-35 DIV*.

4.2 Aims

To further characterise Hi-Spots made from Postnatal day 0 (P0) tissue made using the *Soton* protocol and assess:

- Whether the functional spontaneous activity is synaptically driven
- Whether the functional activity can be modified by pharmacological agents that antagonise GABAergic and glutamatergic receptors
- Whether Hi-Spots mimic the neural- neuronal interactions of *in vivo* cells
- The presence of both astrocytes and microglia

4.3 Methods

Hi-Spots were prepared as stated in section 3.3.1 using the *Soton* method. Samples were collected for Western blotting and immunohistochemistry (IHC) as detailed in sections 2.2 and 2.6. All antibody concentrations and Confocal microscope settings are as indicated in tables 2.2, 2.3 and 2.4. MEA recording conditions are as detailed in section 2.9 where paired observations are made the same heater spike, noise and spike threshold were set. Glutamate toxicity was tested as stated in General Methods section 2.11 and tetanus toxin sensitivity was tested as described in General Methods section 2.10.

4.4 Results

4.4.1 Hi-Spots are formed of high density re-aggregated cells

Figure 4.1 shows a confocal image of a region of a Hi-Spot made using the *Soton* modified method after 21 days *in vitro (DIV21)*, which has been stained with Hoechst 33342 nuclear stain. The image shows a single mid-section XY confocal image of the nuclei of cells within the Hi-Spot. Also shown are transverse sections taken centrally on the orthogonal axes (views along x and y axes) showing the distribution of the high-density of cells throughout the Hi-Spot which has a thickness of approximately 60μm after compression under a glass cover slip. The cell density (ca. 80,000cell/mm^2) can be appreciated from the maximum projection image

of all x100 z-sections (Figure 4.1aii) from this region of the Hi-Spot. Figure 4.1b shows transverse sections taken on the orthogonal axes showing the distribution of neuronal stained β III Tubulin processes and astrocytes processes stained with GFAP throughout the Hi-Spot. Neuronal and astrocyte cells can be seen throughout the Hi-Spot culture.

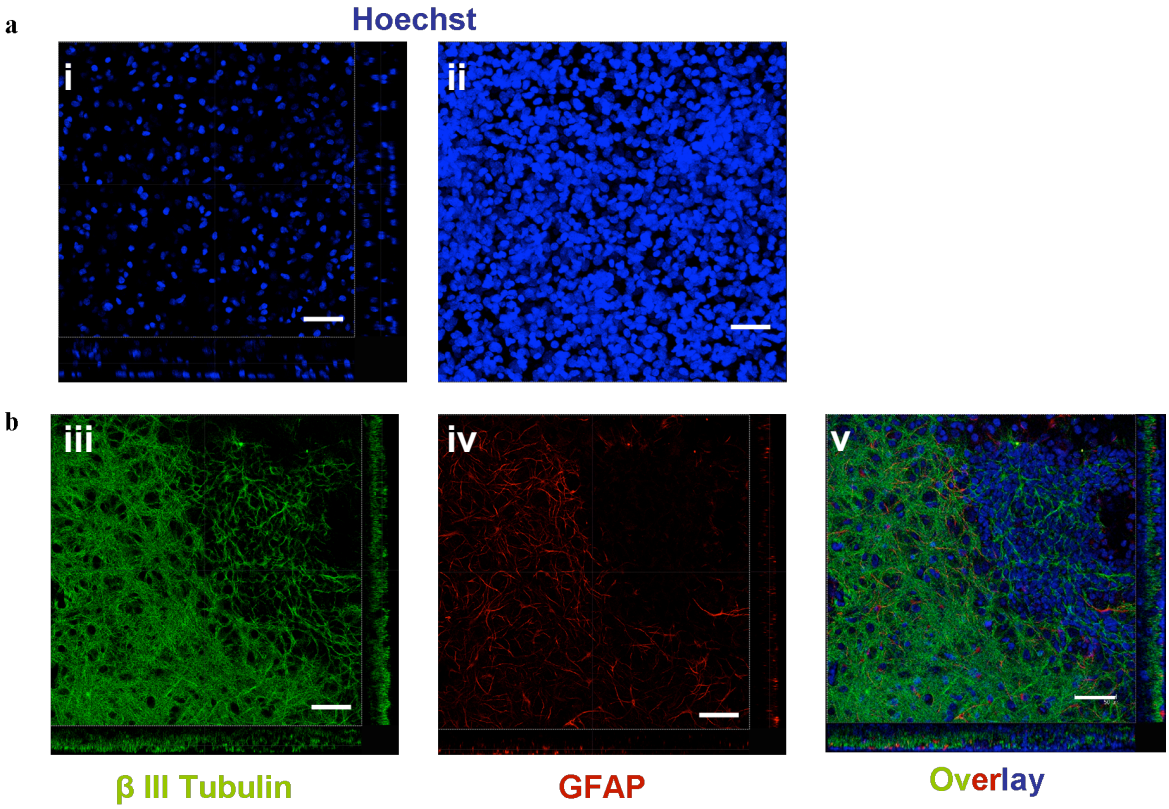

Figure 4.1: Hi-Spots form high density re-aggregated cultures with multiple neuronal and glial cell layers

a) i. Hi-Spots are 3D cultures composed of multiple cell layers. The image show is a trans-section image of a Hoechst stained Hi-Spot. The image was obtained using a confocal microscope and illustrates that Hi-Spots are multi-cellular layers and are at least 60μm thick. ii. A confocal image of a maximum projection confocal image of 100 z-sections of a 60μm thick Hi-Spot stained with Hoechst. The image illustrates the vast number of highly aggregated cells in the Hi-Spot. Scale bar 50μm

b) The multiple cell layers in the Hi-Spot contain both neuronal and glial cells. The image shows a *DIV 7* Hi-Spot trans- section of a iii. B III Tubulin (green) stained neuronal processes, iv. GFAP (red) stained astrocyte processes and v. an overlay of the β III tubulin, GFAP and Hoechst staining. Scale bar 50 μm

4.4.2 Hi-Spots consist of a mixed population of neural cells:

The Hi-Spot cells self-aggregate to produce dense non-homogeneous aggregations of cells by *DIV7* and these aggregations are maintained through *DIV21* (Figure 4.2). We have identified key cell types within Hi-Spots using fluorescence immunohistochemistry with a series of specific antibodies against distinct cellular and synaptic markers.

NeuN is a transcription factor selectively expressed in post-mitotic neurons. At *DIV7* NeuN staining showed a dense distribution of neurons labelled green (Figure 4.2 c), at *DIV21* (Figure 4.2 f) NeuN staining is still present but appears reduced. β III tubulin is a neuron-specific marker which is expressed in cell bodies and axons. Labelling with antibodies to β III tubulin (Figure 4.2a/d) allowed the visualisation of neuronal cell bodies and axons throughout the Hi-Spots labelled green. The maximum projection confocal image of β III tubulin staining shows a dense network of neuronal processes at *DIV7* (Figure 4.2a) these persist at *DIV21* (Figure 4.2d) but become more sparse, relative to early time points.

Staining for Glial Fibrillary Acidic Protein revealed GFAP-positive cells intermingled with the NeuN and β III tubulin-positive cells (Figure 4.2 a, b, e, f) with increased levels of immunoreactivity through time *in vitro*.

Additionally we looked for the presence of microglial cells. We found a population of ED1-positive cells labelled green (Figure 4.2 b, e), in which ED1 staining was punctate and perinuclear within the cell body, as expected for microglial cells (4.2 e inset). The level of ED1 staining appears to increase between *DIV7* and *DIV21* which could reflect an increase in the number or activation of microglial cells (Damoiseaux, Dopp et al. 1994).

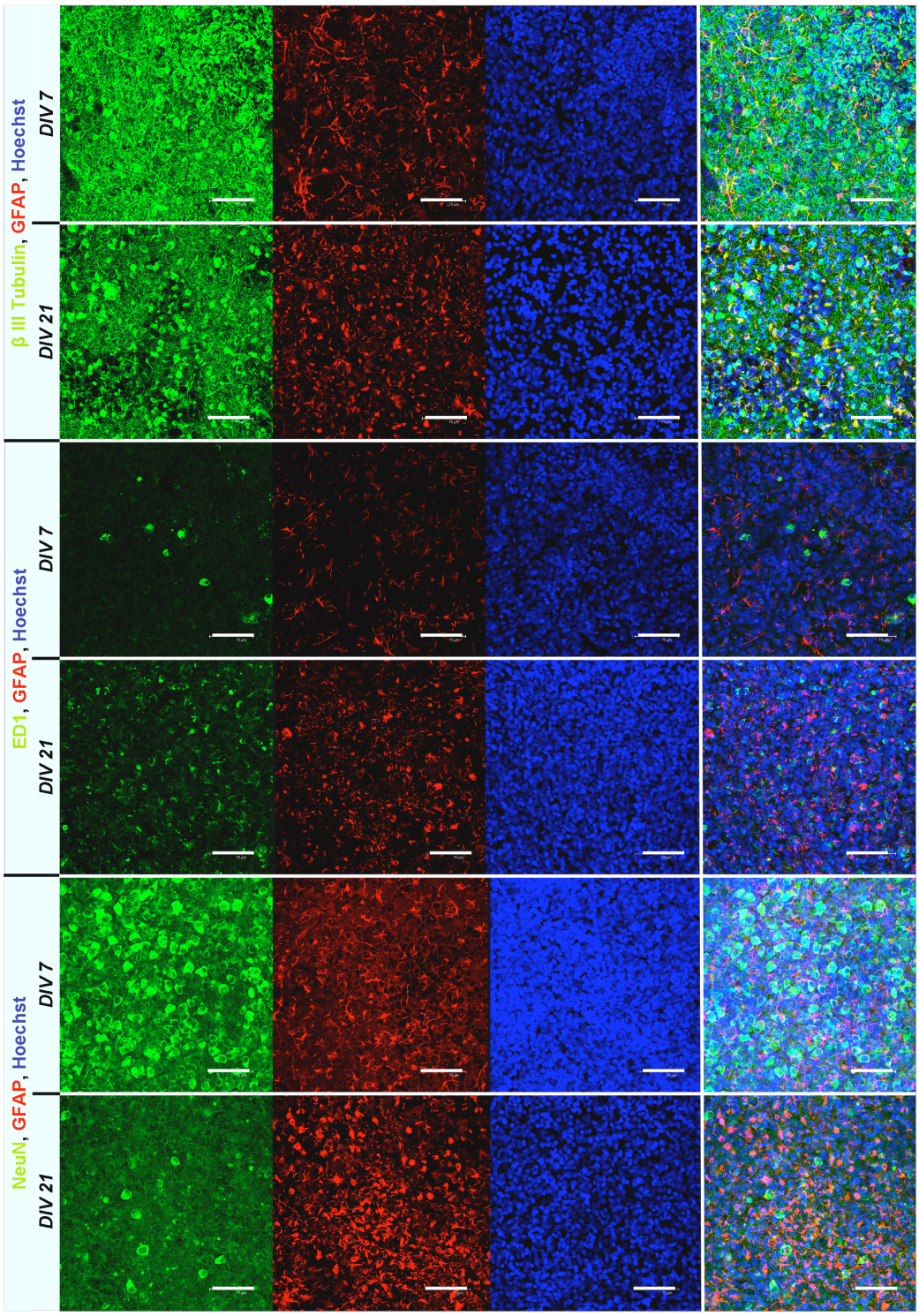

Figure 4.2: **Hi-Spots are formed of neurons, astrocytes and microglia**
Maximum projection confocal images of representative areas of whole P0 Hi-Spots. In all pictures cell bodies are stained with Hoechst (blue). Representative *DIV 7*and *DIV 21* P0 Hi-Spots. At *DIV 7* there is a dense β III Tubulin processes with GFAP stained astrocytes in close association, ED1 stained microglial cells with GFAP stained astrocytes and NeuN stained neuronal cells with GFAP stained astrocytes. At *DIV 21* β III Tubulin staining is less dense and shows some areas of poor coverage not seen in younger Hi-Spots. The expression of ED1 has increased compared to *DIV 7* along with the GFAP staining. At *DIV 21* there is notably less NeuN (compared to that stained at *DIV 7*) stained cells and a clear increase in GFAP staining. Scale bar 75µm.

4.4.3 Hi-Spots contain synaptic proteins both somatically and in discrete puncta:

Having demonstrated the presence of neuronal and glial cells by both Western blots (Figure 3.6 Chapter 3) and immunohistochemistry (Figure 4.2), we then used immunohistochemistry and confocal imaging to determine the presence of synapses by visualising the distribution of both pre- (synaptophysin, synaptobrevin) and post-synaptic proteins (PSD-95) during the maturation of cultures.

The pre-synaptic vesicle proteins synaptobrevin and synaptophysin were apparent by *DIV10* and had a partially punctate distribution. The early expression of these synaptic vesicle proteins included a clear somatic distribution likely associated with the biosynthetic compartment of the secretory pathway. Later in culture the staining was dominated by punctate staining which remained obvious at the later time points when general neuronal markers were decreasing (Figure 4.3). At *DIV21*, confocal images of synaptophysin and synaptobrevin labelling show a dense distribution of pre-synaptic puncta, illustrating the complex, closely packed, neuronal network within the 3D environment of the Hi-Spot.

Post-synaptic compartments in these cultures were labelled with antibodies against PSD-95. Confocal images of the PSD-95 labelling show dense puncta at both *DIV10* and *DIV21* (Figure 4.3). Again like that of synaptophysin and synaptobrevin staining, some puncta are observed surrounding the cell bodies or in the perinuclear space in the Golgi complex, with some puncta appearing to be distributed along the length of axonal processes. All three synaptic markers show punctate staining consistent with the development of synapses (Figure 4.3). The amount of punctate staining appears to increase from *DIV10* to *DIV21* consistent with the maturation of synaptic connectivity in the Hi-Spot cultures.

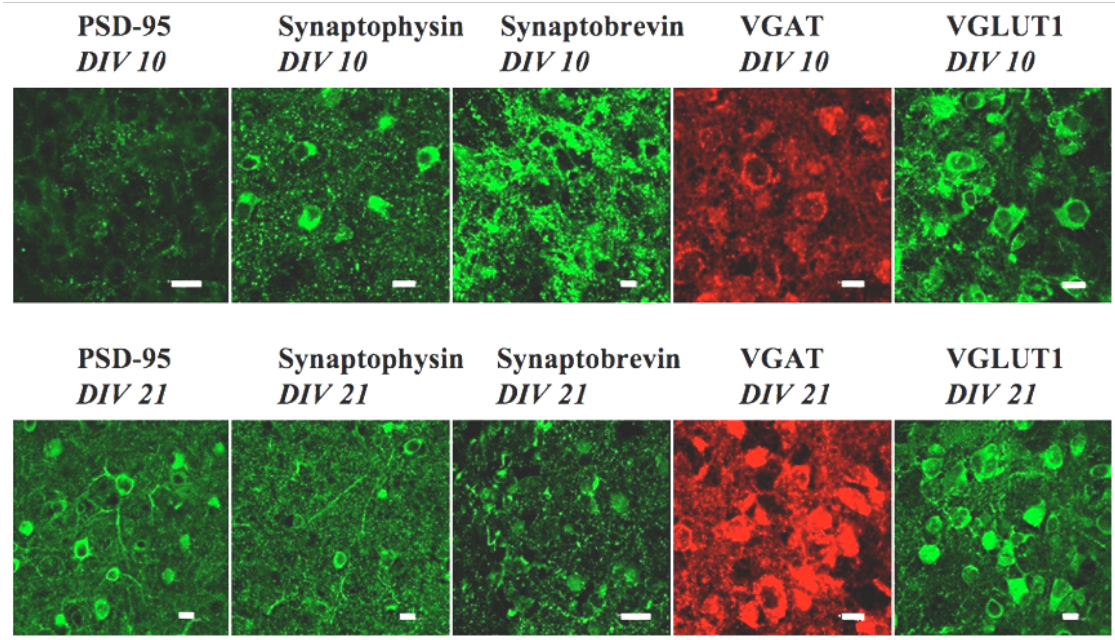

Figure 4.3: Expression of synaptic proteins and markers for GABAergic and Glutamatergic neurons
4% PFA fixed IHC staining and confocal imaging of P0 Hi-Spots at *DIV 10* and *DIV 21*. Synaptophysin and PSD-95 show punctate staining representing pre and post-synaptic terminals, respectively. Synaptophysin and PSD-95 staining increases surrounding the cell nucleus in *DIV 21* Hi-Spots. Synaptobrevin staining is also observed at both *DIV 10* and *DIV 21*. VGAT and VGLUT1 staining shows punctate staining reminiscent of expression in neuronal cells and provides evidence for glutamatergic ad GABAergic neuronal populations.

Further evidence for the existence of synaptic specialisations comes from investigation of the GABAergic and glutamatergic vesicle uptake proteins VGAT and VGLUT1. Confocal imaging of antibody labelling shows VGAT and VGLUT1 distributed within the cell body and also as puncta along the network of neurites present in the Hi-Spot (Figure 4.3).

There are approximately 16 identified subtypes of GABAergic interneuron in the hippocampus; the different subtypes are differentiated in terms of their protein expression, distribution and electrophysiological properties. The calcium binding protein parvalbumin is expressed in two different subtypes of GABAergic interneurons, the fast spiking basket cells and the chandelier interneurons (Kawaguchi and Kondo 2002). The chandelier cells target the axon initial sub-region and the basket cells target the perisomatic region of the excitatory cells, and these interneurons are classed as fast spiking cells (Ribak, Nitsch et al. 1990) (for a review see:(Markram, Toledo-Rodriguez et al. 2004). Parvalbumin positive

cells are very important for the generation of gamma oscillations in the brain and entrain large numbers of principal cells (Fuchs, Doheny et al. 2001; Fuchs, Zivkovic et al. 2007). To test if this subtype of GABAergic neurons was present in the Hi-Spot cultures we investigated the expression of parvalbumin using IHC.

Figure 4.4 shows parvalbumin immunoreactivity in *DIV 21* Hi-Spots. The Hi-Spots were assessed for their parvalbumin content at *DIV 21* because *in vivo* parvalbumin is not fully upregulated until the second postnatal week (de Lecea, del Rio et al. 1995). Figure 4.4 shows that parvalbumin positive interneurons are present in the Hi-Spot culture and that the parvalbumin staining allows visualisation of the interneuron cell bodies and some neuronal processes.

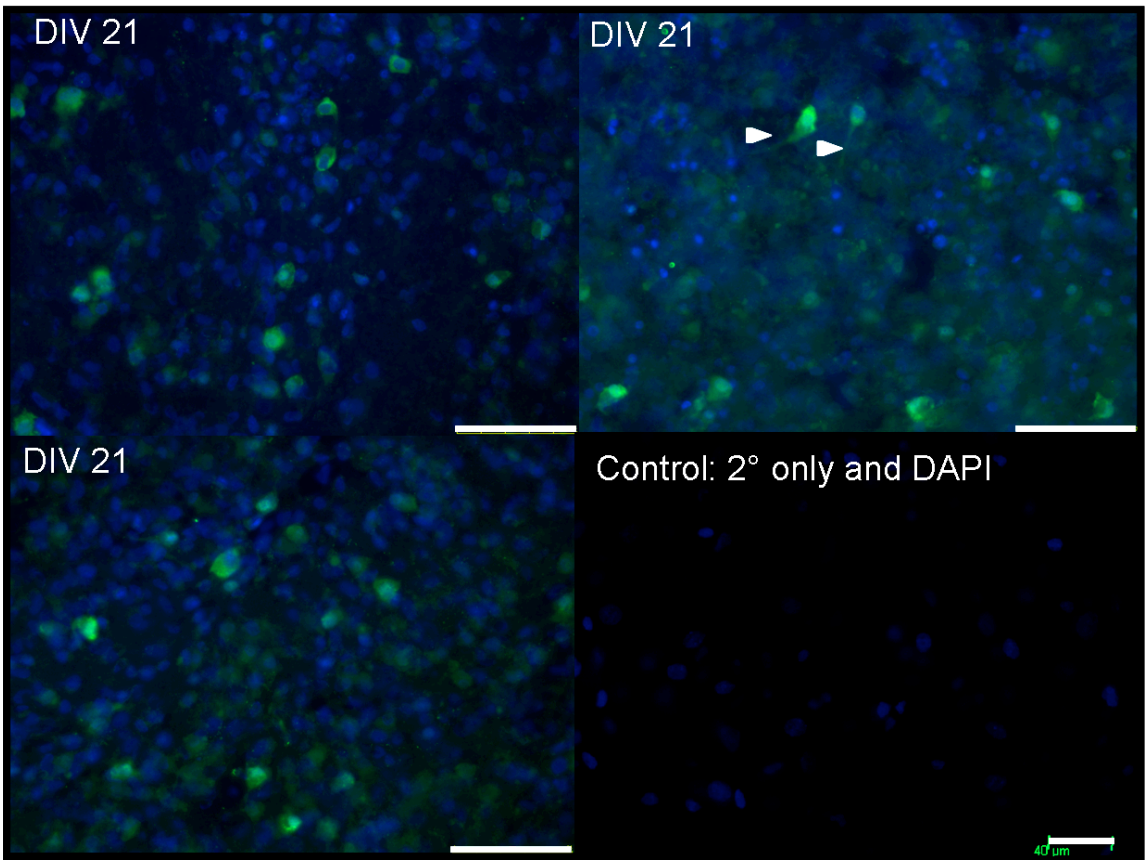

Figure 4.4:Parvalbumin positive interneurons in *DIV 21* Hi-Spots
Hi-Spots 4% PFA fixed and IHC stained against parvalbumin. Staining was visualised on an upright fluorescent microscope. Hoechst stained cell bodies are blue and parvalbumin positive cells are green. Parvalbumin visualised the cell bodies of the interneurons as well as some of the neuronal processes (arrow heads). (n=4 Hi-Spots) Scale bar 75µm. Control staining shows secondary antibody staining with DAPI (Scale bar 40µm).

4.4.4 Maturation of electrophysiological function in culture:

MEA analysis of cultures was used to assess the physiological activity associated with development of the Hi-Spots. The experimental data (Figure 4.5a) is representative of 3 independent batches of cultures monitored over five consecutive weeks. Each Hi-spot was recorded on the MEA rig for 5-15 minutes and from each batch of Hi-Spots. Three to six Hi-Spots were recorded per time point. The results show representative raster plots at *DIV7* and *DIV21* (Figure 4.5a). Each row shows the activity through time (300 seconds) recorded from single electrodes and each vertical line represents biological unit activity of greater than the set threshold (~ ±0.03).

Spontaneous activity increases over time in culture (Figure 4.5a). By *DIV7* most Hi-Spots have developed an irregular pattern of low frequency activity that can be synchronous across multiple electrodes. This activity develops and at *DIV21* cultures show the highest average frequency of activity with most having periods of bursting activity interspersed with quiescent periods. These bursts appear synchronously across multiple, spatially separated electrodes (Figure 4.5b).

In general the bursting behaviour is predominantly seen in older more mature Hi-Spots (peaking at *DIV21*) and is normally observed to occur synchronously across all of the recorded channels.

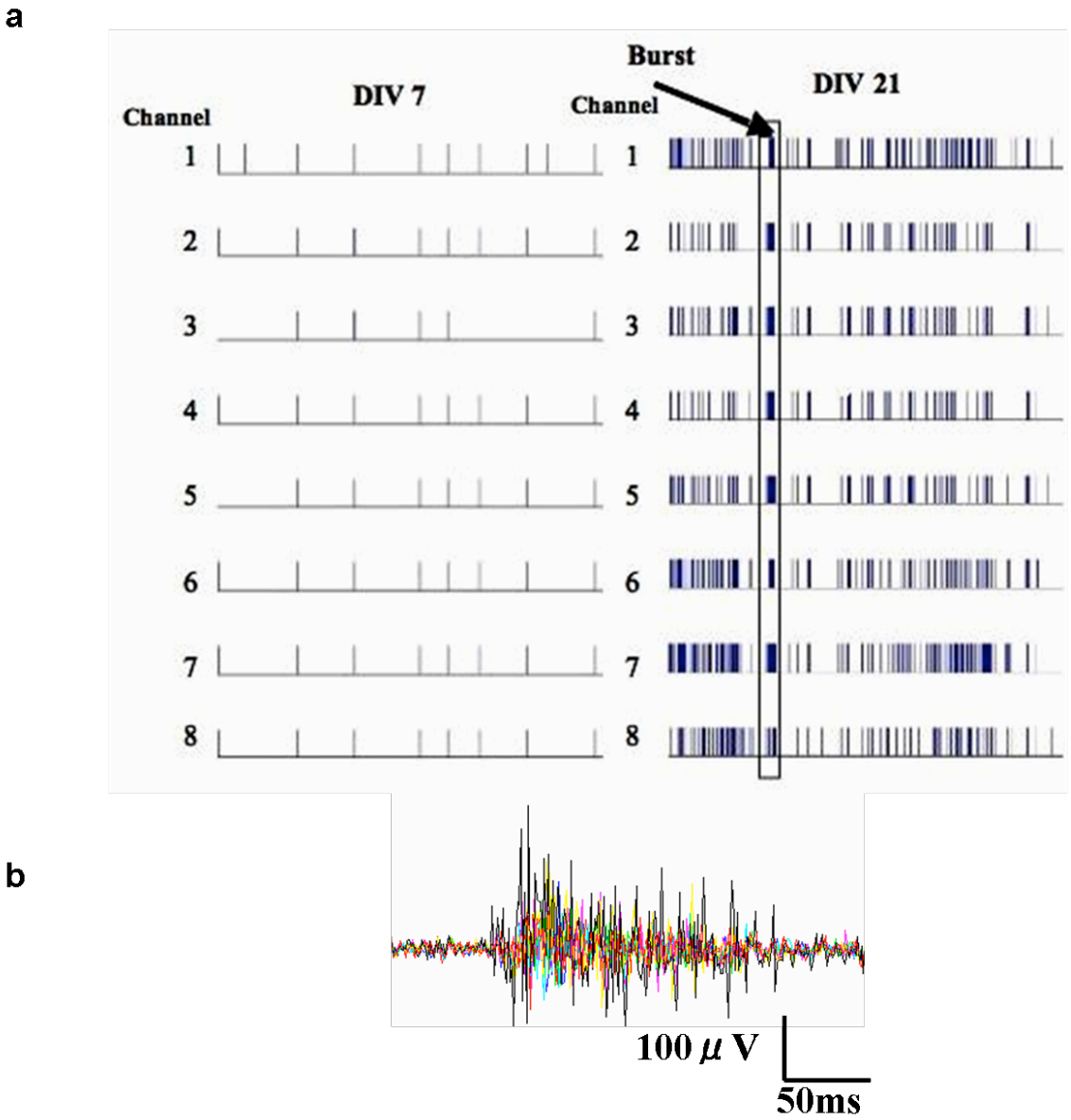

Figure 4.5: Spontaneous activity increases during the culture period and higher frequency bursts of activity are seen more frequently as the culture ages.

a) MEA raster plot data of 300 seconds of recordings from 8 different channels on the 40 electrodes MEA chip. Each vertical line represents a spike event and each horizontal line a different channel (electrode) recording from a spatially different area in the Hi-Spot. At *DIV 7* the activity observed is mainly composed of single spiking events, which by *DIV 21* are joined by bursting activity. Bursts are clusters of action potentials that occur in very short succession. The bursts occur in high temporal synchronicity from recording sites in spatially distinct areas. On the raster plot the bursts are shown as blocks of activity, one burst is boxed in the *DIV 21* Hi-Spot. Raster plot generated in MatLab

b) Raw MEA data showing a burst of spontaneous activity, each colour represents a different electrode recording from a spatially distinct site in the Hi-Spot.

4.4.5 Does synaptic activity drive the spontaneous network activity?

In order to determine whether the bursting activity seen at *DIV21* is the product of a synaptic drive in the neuronal network, we pre-exposed cultures to Tetanus toxin (48hrs) and examined the electrophysiological activity using MEAs, comparing their activity to untreated sister cultures as controls (Figure 4.6a). Tetanus toxin inhibits the release of neurotransmitters by selectively cleaving the v-SNARE synaptobrevin. The efficacy of the tetanus toxin treatment was demonstrated by Western blotting for synaptobrevin which showed the selective and complete cleavage of synaptobrevin relative to the unaffected expression of the t-SNARE syntaxin (Figure 4.6b)

The unexposed, control cultures (n=6 Hi-Spots, one batch) showed the characteristic patterns of synchronised bursting activity that characterized *DIV21* cultures as described above (Section 4.4.4). However the tetanus toxin treated sister cultures (n=6) showed much lower levels of unit activity with greatly reduced bursting (Figure 4.6a).

Morphologically the toxin treated Hi-Spots appeared no different from the untreated sister cultures, showing no visible signs of apoptosis or necrosis. This together with the fact that the toxin treated Hi-Spots showed some single spiking spontaneous activity is consistent with the Hi-Spots being functionally silenced by the toxin. Overall this shows that network activity is driven by synaptic interactions mediated by the release of neurotransmitter.

a

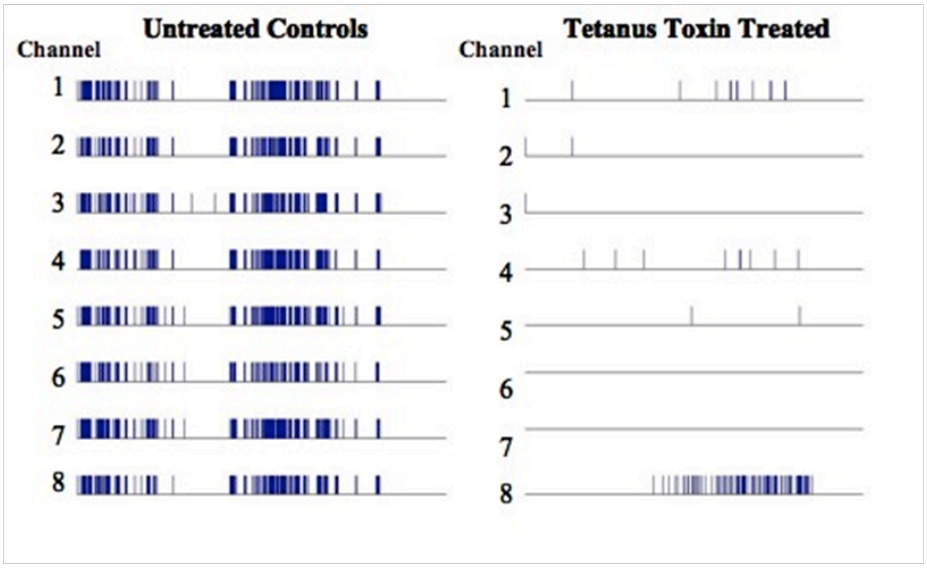

b

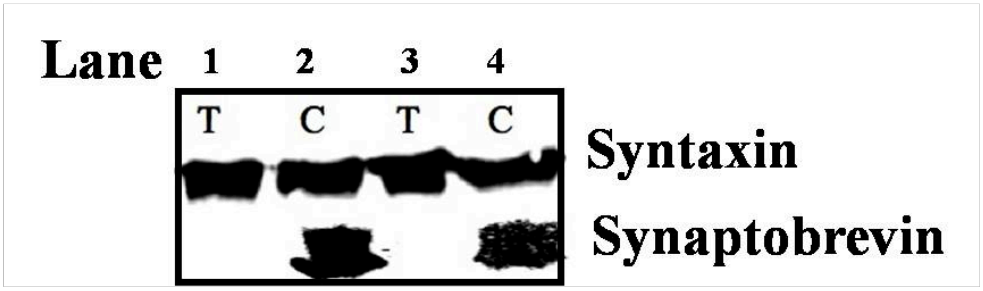

Figure 4.6: The spontaneous recorded on the MEA activity is synaptically generated

a) Raster plots of 300 seconds of representative MEA (n=6) recordings of tetanus untreated and toxin treated and Hi-Spots *DIV 21*, whilst tetanus treated Hi-Spots displayed only modest single spiking activity compared to untreated control Hi-Spots. Untreated Hi-Spots showed characteristic bursting and single spiking activity.

b) Western Blot of tetanus treated (T) and untreated control (C) for syntaxin and synaptobrevin. Each lane represents 20% of the homogenate from 6 Hi-Spots. Lane 1 corresponds to Hi-Spots used for the MEA recordings displayed in fig 4.6a tetanus toxin treated.

4.4.6 Does pharmacological antagonism of spontaneous synaptic transmission affect network activity?

Given the reduced bursting activity observed after tetanus toxin treatment, we investigated how selective pharmacological blockade of glutamatergic or GABAergic signalling would modify the network activity. In these experiments the drugs were perfused onto the same culture from which the control recordings were made. Data from one representative Hi-Spot is shown, before (control) and after 15mins of equilibration with the indicated drug. The control *DIV18-21* Hi-Spots showed characteristic synchronous bursting activity.

Exposure to the AMPA receptor antagonist, CNQX (50µM) greatly reduced the general level of activity but occasional synchronous bursts were still observed. Similar results were obtained in 3 separate Hi-Spots from 2 batches (Figure 4.7a). The functional role of the NMDA-receptor in network behaviour at *DIV21* was investigated by perfusion with the antagonist D-APV (50µM). Under control conditions the Hi-Spots showed typical bursting activity. Following exposure to D-APV (Figure 4.7b) there was a general reduction in network activity and an apparent reduction in duration of bursting activity. Similar results were obtained in 3 separate Hi-spots from two different batches. In order to quantify these changes we determined the RMS of the spike activity for 100s bins, averaging the values over 3 bins at stable times under both conditions. This showed that the inhibition by perfusion of D-APV and CNQX were statistically significant in all Hi-Spots tested ($p<0.005$), unpaired one tailed t-test (Figure 4.7c).

Immunohistochemically we have shown the presence of the vesicular GABA transporter (VGAT) as puncta which are potential inhibitory presynapses. If a GABAergic inhibitory drive is present in the network activity then it would be expected that antagonism would increase overall activity. We therefore made control MEA recordings from 6 Hi-spots from 3 different batches (Figure 4.7a) and then exposed them to the $GABA_A$ antagonist bicuculline (10-50µM). Fifteen minutes following bicuculline perfusion there was a large and sustained increase in unit activity with more synchronised bursting apparent, this was maintained for the duration of the recording. The relative amplitudes of the unit activity recorded from each electrode are shown in the graphs (Figure 4.8b). The left-hand graph shows the control activity, whilst the right-hand graph shows the pattern of increasing activity following addition of bicuculline (Figure 4.8b), showing increases in both frequency and amplitude. These changes were quantified by analysis of the RMS in 100sec

bins showing the increases on all channels (Figure 4.8c). This effect was statistically significant for the set of cultures monitored as shown by the histogram (Figure 4.8c; n=3 for 10μM and n=3 for 50μM bicuculline, taken from 2 batches).

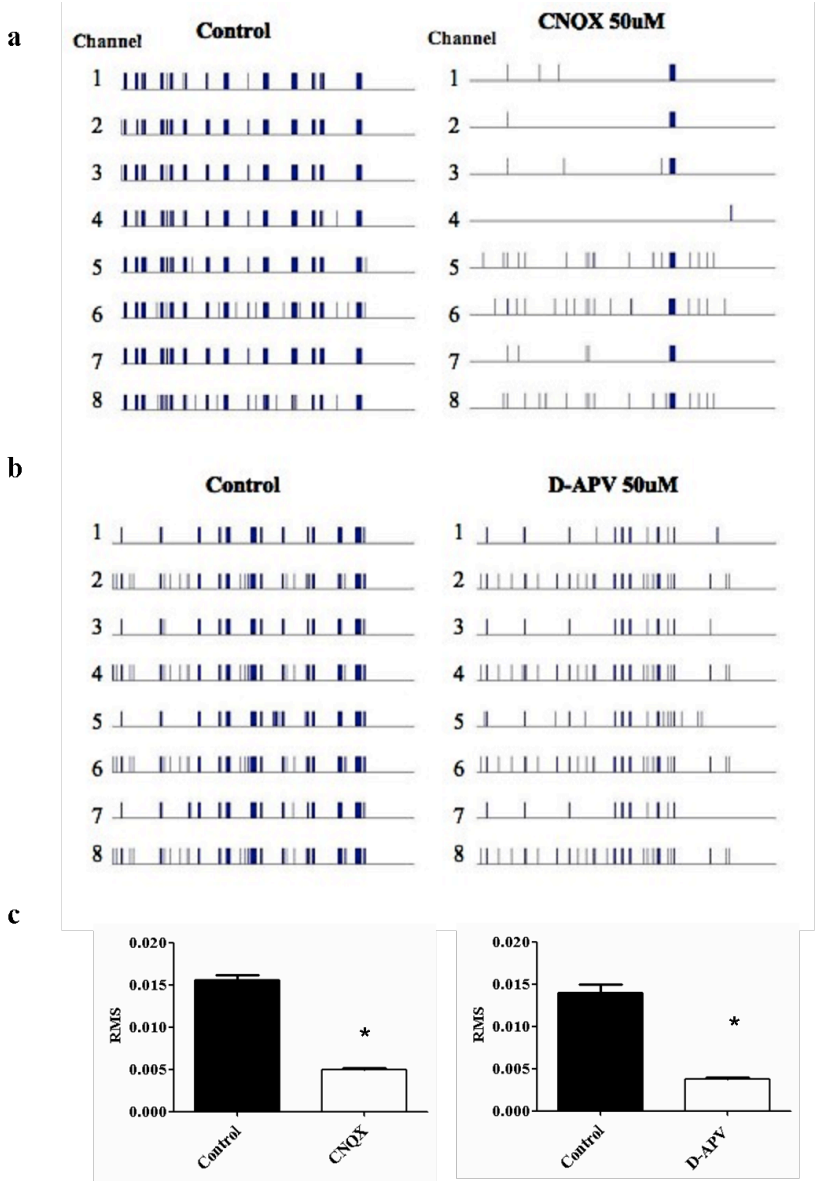

Figure 4.7: Hi-Spots have a glutamatergic network with functional NMDA and AMPA receptors

a) Representative raster plots of spike events recorded in control *DIV21* culture before (left) and following CNQX (50µM) addition, the total duration of the recordings shown is 300s (x3 cultures from x2 batches). CNQX treatment results in decreased spontaneous activity over all channels.

b) Representative raster plots of spike events recorded in control *DIV21* culture before (left) and following D-APV (50µM) addition, the total duration of the recordings shown is 300s (x3 cultures from x2 batches). D-APV treatment appears to reduce spontaneous activity with a decrease in bursts.

c) Quantification of activity before and during drug applications, the RMS of the spike activity was measured for 100s bins and the average of x3 bins under both conditions is shown with the SD in the histograms. The effects of both D-APV (left) and CNQX addition were statistically significant in all Hi-Spots. (Students unpaired one tailed t-test $p<0.005$)

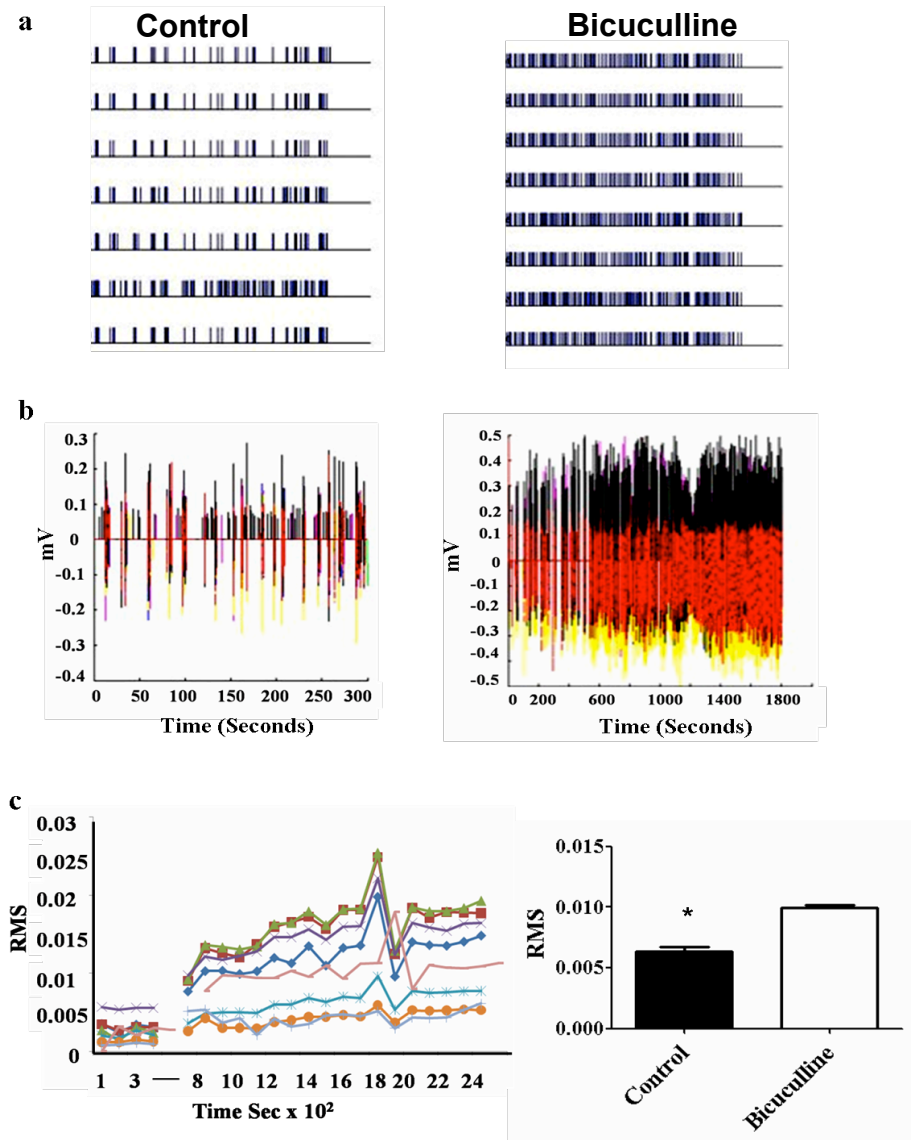

Figure 4.8: Hi-Spots show an active GABAergic network

a) Raster plot of 300 seconds of representative MEA (n=6 from 2 batches) recording of basal activity in *DIV 21* Hi-Spot and activity induction after bicuculline addition. The cultures exhibit both single spiking and bursting behaviour which is increased on bicuculline addition.

b) Graph of 300 seconds of basal activity and 1800 seconds of spontaneous activity from when bicuculline was added. Recording started from immediately after bicuculline addition. Ramping up of activity can be observed after 500 seconds. Raster plot above shows 300 seconds of activity 15 minutes after bicuculline addition. The level of both single spiking and bursting are increased. All 8 channels recording on the MEA show an increase in activity. The amplitude of the activity is also increased on bicuculline addition.

c) The graphed RMS values of the above recording. RMS values are calculated in 100 second bins and show the increase in the level of activity increasing in each channel. The bar graph shows the quantification of the increase in the RMS value after bicuculline incubation. (Statistics- students paired one tailed t- test *<0.05)

4.4.7 Hi-Spots have *in vivo* levels of glutamate tolerance

Dissociated cultures have been shown to have a very low tolerance to glutamate, demonstrating an ED_{50} for 5min exposure at 50-100μM (Choi, Maulucci-Gedde et al. 1987). *In vivo,* glutamate is much better tolerated, *in vitro* organotypic cultures (Stoppini, Buchs et al. 1991) are intact slices of the brain and have been shown to demonstrate *in vivo* like tolerances to glutamate (Morrison, Pringle et al. 2002). Dissociated cultures may be more susceptible to glutamate because they lack the tissue like integrated cell-cell interactions present in the *in vivo* tissue and organotypic slice cultures. Hi-Spots are plated as re-aggregated cultures which form a network composed of neuronal and glial cells (Figure 4.2), to assess if Hi-Spot self-organise into a tissue analogue that can tolerate elevated glutamate without neuronal damage we opted to test the effects of long exposure periods, in the absence of other stressors.

The results show that no glutamate sensitivity was detected in the presence of serum in the media (Figure 4.9). In order to produce measurable effects we had to sensitise the cultures by removing serum (Figure 4.10). Under these conditions Hi-Spots were assayed for their glutamate susceptibly at *DIV14*. At this stage Hi-Spots show high levels of immunoreactivity for GFAP, syntaxin, PSD-95 and NR1 (Figure 3.6 Chapter 3), and extensive βIII tubulin staining of dense neuronal processes (Figure 4.2), and spontaneous electrical unit activity was also detected at this culture point (Figure 3.9) Glutamate, at doses between 50μM and 5mM, was added to the Hi-Spots in culture and incubated for 120mins. This was conducted on four batches of Hi-Spots, with 10 Hi-Spots per treatment. The medium was then replaced and Hi-Spots incubated for a further 12 hours with propidium iodide before analysis to allow development of delayed neurodegeneration. As a positive control, exposure to sodium azide (4.5mM) (Varming, Drejer et al. 1996) with the same timings was also tested (1 batch 10 Hi-Spots) (Figure 4.10).

Hi-Spots were imaged live for cell damage (Figure 4.10). Representative images of propidium iodide fluorescence are shown in the left hand panel (Figure 4.10). There was a greater number of PI-positive cells associated with the higher concentrations of glutamate. This data was quantified as the difference in average fluorescence measured between control (zero added glutamate) and the cultures treated with the respective concentrations indicated (Figure 4.10). This analysis showed that millimolar glutamate concentrations

were needed to produce statistically significant increases in propidium labelling despite the long exposure times and absence of serum.

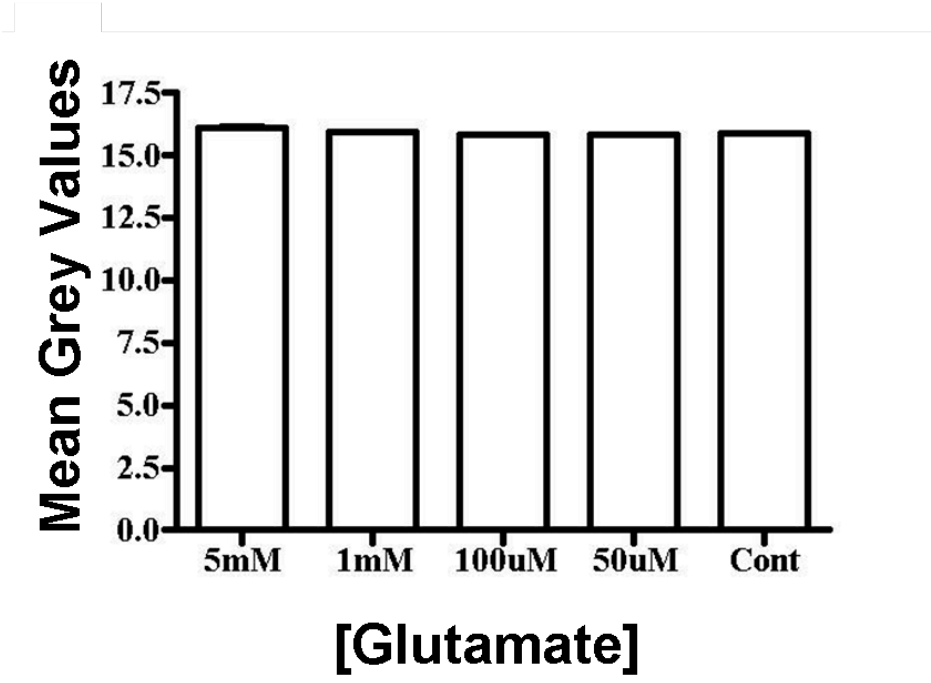

Figure 4.9: Long-term exposure to millimolar levels of glutamate produce no damage in media containing serum.
Quantitative measurement of the levels of propidium iodide fluorescence in Hi-Spots subjected to 120min exposure to the levels of glutamate indicated whilst maintained in serum-containing media. No evidence of cell damage was observed under these conditions, error bars (SEM) are within histogram line width (n>18 for each dose).

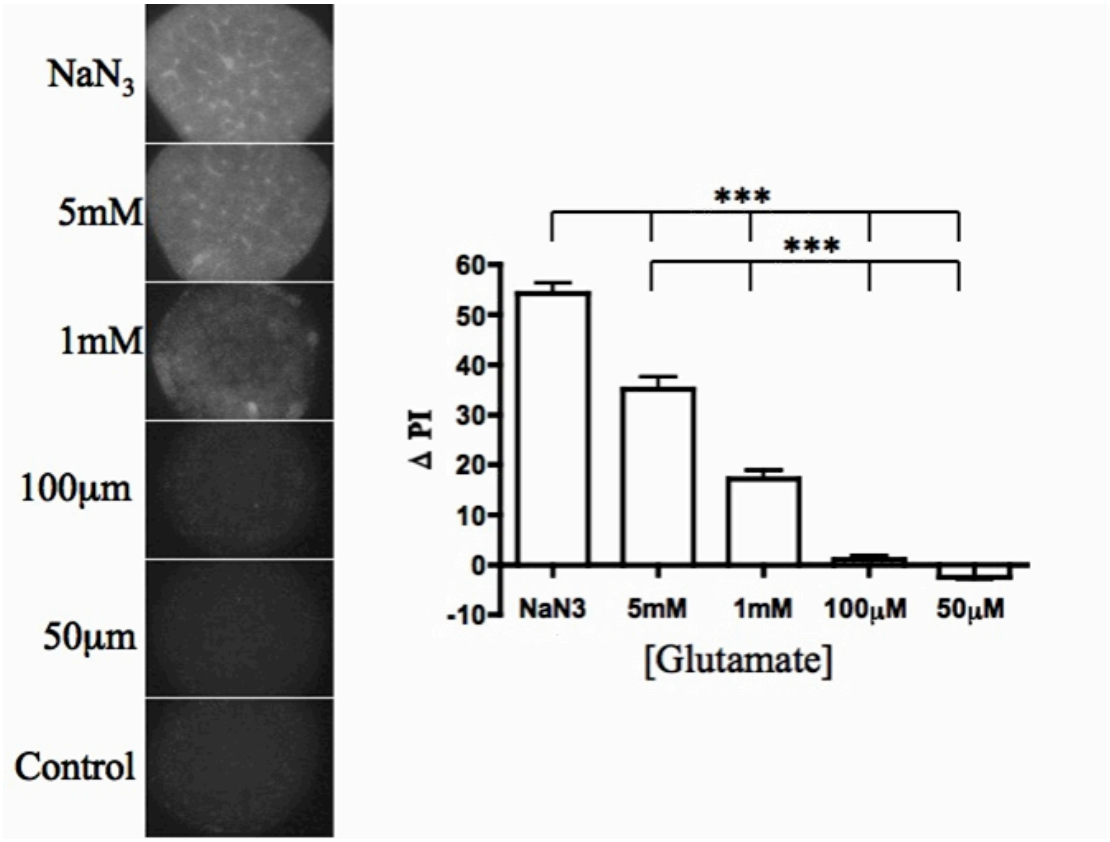

Figure 4.10: Hi-Spots have an *in vivo* like intolerance to glutamate
Representative pictures of PI fluorescence in Hi-Spots after NaN_3 or 5mM, 1mM, 100µm, 50µm glutamate or incubation for 120 minutes. Only 5mM glutamate was sufficient to cause increased PI fluorescence above that observed in control untreated Hi-Spots. NaN_3 (4.5mm) statistically increased PI Florescence above that observed for all glutamate concentrations.
Statistics: Student paired t-test, one tailed.

4.5 Discussion

Neural networks that are formed upon high density re-aggregation to form Hi-Spots are a potentially powerful model for the investigation of functions and dysfunctions that operate at the cell-cell level. Our results show that Hi-Spots demonstrate many properties of intact CNS tissue such as synaptic connectivity, spontaneous activity, and glutamate resistance. This is, to our knowledge, the first characterisation of such cultures produced from postnatal tissue. Dissociation of postnatal brain tissue to homogeneity permits the pipetting of equivalent populations of cells onto the permeable culture membranes where the cells re-aggregate to form a high-density organotypic-like tissue. A key requirement for the utility of the system is that the cell types present in cortical tissue are present in the analogues. Our immunohistochemical analysis shows that the tissue contains β III tubulin and NeuN-positive neurons, GFAP-positive glia and ED1-positive microglia, with each cell type having the expected morphology. Their distributions do not appear to be homogeneous, rather neurons group together into discrete regions. The β III tubulin staining at *DIV7* shows dense neuronal processes extending over the entire network suggestive of the formation of extensive cell-cell interactions. The evidence presented suggests that the Hi-Spots form an environment containing cell populations' representative of the CNS, allowing analysis of cell-cell interactions, biochemical analysis of protein expression, electrophysiological analysis of function and immunohistochemistry analysis of morphology on neural cells.

4.5.1 Self-Organising Synaptic Network

The presence of the full complement of potential cell types will contribute to the development and sculpting of the networks that develop in culture. The presence of astrocytes and microglia may be particularly important as they have been implicated in both the initial development and physiological and pathological re-modelling of networks (Ullian, Sapperstein et al. 2001; Stevens, Allen et al. 2007). The dissociation that initiates culturing destroys the pre-existing organisation and removes neurites from the neurons; however the presence of the non-neuronal cell types may facilitate the formation of the self-organised network, providing structural and chemotactic cues as in normal neurodevelopment (Huettner and Baughman 1986; Ullian, Sapperstein et al. 2001; Ullian, Christopherson et al. 2004; Platel, Dave et al. 2010; Platel, Dave et al. 2010). Evidence for

the development of synaptic specialisations was obtained from both Western blot analysis and imaging of antibody labelling (Figure 3.6 Chapter 3 and Figure 4.3 Chapter 4). Both of these techniques showed patterns of changes in the expression of synaptic proteins through time in culture and support data from other culture systems which show the development and stabilization of synaptically driven neuronal networks (Maeda, Robinson et al. 1995; Segev, Shapira et al. 2001; Opitz, De Lima et al. 2002).

The presence of oligodendrocytes was not probed for in these cultures. Oligodendrocytes are an important cell type in the brain, performing many important functions (Dupree, Mason et al. 2004; Kassmann and Nave 2008; Nave and Trapp 2008), and an *in vitro* model of the brain should contain all the important cell types found *in vivo*. Unpublished work by scientists at Capsant Neurotechnologies and Stoppini et al (unpublished) has shown that myelin basic protein is expressed in Hi-Spots from embryonic and postnatal tissue. Therefore, although oligodendrocytes were not assayed for in these cultures, Hi-Spot cultures made using the same *Soton* protocol have been shown to express myelin basic protein, suggesting the existence of oligodendrocytes. Future work at the ultrastructural level would need to assess if the oligodendrocytes in the Hi-Spots functionally ensheath axonal processes with myelin.

4.5.2 Functional, Spontaneously Active, Neuronal Network

The acid test of a CNS analogue is that it should be capable of sustained electrophysiological activity reflecting the electrical excitability of neurons and their co-ordinated activity (Egert, Schlosshauer et al. 1998; Jimbo and Robinson 2000). In order to directly measure electrophysiological function we have used multi-electrode array recordings at different stages in culture. These extracellular electrodes allow measurement of electrical unit activity that is produced by action potentials occurring in neurons close to individual electrodes, and the regularly spaced array allows determination of spatial synchrony (Figure 4.5). Hi-Spots begin to show some single unit activity at around *DIV4*, which progressively increases and develops into patterns of bursting and single spiking activity by *DIV14*. The greatest level of activity is seen at *DIV21* after which activity appears to decrease in most, but not all Hi-Spots (Figure 3.10). Thus it is clear that the networks are capable of sustained electrophysiological activity. The later decline in activity correlates with degeneration of neurons as indicated by loss of NeuN and β III tubulin immunoreactivity.

Our data indicates that there is a progressive development of synapses over time in the Hi-Spots (Figure 4.3), reaching a high expression at *DIV21,* co-incident with the maximum electrophysiological network activity observed. Spontaneous activity has been reported to occur in dissociated neuronal and slice culture models (Kamioka, Maeda et al. 1996). Over time in culture, not only does the general level of activity increase, the pattern changes from temporally and spatially isolated unit activity into bursts of consecutive unit activity which are observed across multiple electrodes (Figure 4.5). This may reflect stronger and more developed synaptic and cell-cell connections (Muramoto, Ichikawa et al. 1993; Maeda, Robinson et al. 1995; Mukai, Shiina et al. 2003; Yoshitaka Mukai 2003) that are particularly suited to developing in the complex cellular microenvironment provided by the Hi-Spots.

Developing cortical neurons *in vitro* also show single stochastic spiking activity as well as synchronized bursting behaviour (Opitz, De Lima et al. 2002) and highly correlated activity patterns in neurons have been linked to maturity and functional connectivity of a network (Chiappalone, Bove et al. 2006). The burst duration observed in dissociated cultures can vary from hundreds of milliseconds to over a second and are normally separated by quiescent inter-burst intervals (van Pelt, Wolters et al. 2004; van Pelt, Vajda et al. 2005) similar to the activity observed in Hi-Spots.

4.5.3 Neuronal Network Activity is Synaptically Driven

Synchronicity is readily observed in our cultures and provides a functional measure of the increasing maturity of the network. In the brain such synchrony is tightly controlled by the interplay between inhibitory and excitatory neurons (Salinas and Sejnowski 2001). GABAergic interneurons are thought to play a critical role in synchronous network activity. GABAergic interneurons can phase the output of excitatory pyramidal cells, leading to oscillatory activity in different frequency bands (Cobb, Buhl et al. 1995) (Section 1.8). Synchronized gamma oscillations (20-100Hz) in the brain are thought to provide a temporal structure for information processing in the brain. They contribute to cognitive functions, such as memory formation and sensory processing, and are disturbed in some psychiatric disorders (Gonzalez-Burgos and Lewis 2008; Gonzalez-Burgos, Hashimoto et al. 2010; Jones 2010) (Section 1.9). Networks of GABAergic interneurons

play a key role in the generation of gamma oscillations. In particular parvalbumin positive basket cells (Section 1.1.1 and 1.6.1), which we have shown are present in the Hi-Spot cultures (Figure 4.4), are important due to their fast spiking kinetics and extensive neuronal connections to other parvalbumin positive basket cells and to pyramidal cells, are principally important in gamma oscillation production (Fuchs, Zivkovic et al. 2007; Sohal, Zhang et al. 2009).

In Hi-Spots, we have observed evidence for glutamatergic and GABAergic synaptic transmission underpinning network activity. The global reduction of synaptic release produced by exposure to tetanus toxin (Link, Edelmann et al. 1992; Ahnert-Hilger, Kutay et al. 1996) greatly reduces network activity. Antagonism of glutamatergic transmission in mature Hi-Spots *(DIV21)* also reduces activity. CNQX blockade of AMPA-receptors (Blake, Brown et al. 1988) greatly reduced the overall level of activity and the spatial synchrony, suggesting a role for fast excitatory transmission which would produce a positive feedback in a network of excitatory neurons. Whereas, antagonism of NMDA-receptors with D-APV (Choi, Koh et al. 1988) in mature Hi-Spots partially reduced overall activity and appeared to reduce bursting, which would be consistent with a role for slow excitatory transmission in driving excitability and bursts (Xiang, Pan et al. 2007). Our data shows expression of NR1 prior to maximal network activity implying a role for NMDA-receptors in development of the synaptic network before full recruitment of AMPA-receptors, as seen in both development and synaptic plasticity (Ben-Ari, Khazipov et al. 1997; Liao, Scannevin et al. 2001) . However further work is required to substantiate the subtleties of changes in network behaviour.

GABAergic inhibition has a profound effect on CNS network activity both *in vivo* and in acute tissue slices, bicuculline inhibition of $GABA_A$ receptors leading to epileptiform behaviour (Borck and Jefferys 1999; Ma, Wu et al. 2004). In mature Hi-Spots bicuculline (50μM) produced a substantial and long-lasting increase in spontaneous unit activity (Figure 4.8). Interestingly, in the few cultures that were largely electrically quiescent under control conditions but showed no other signs of degradation, bicuculline exposure led to the generation of sustained spontaneous activity suggesting previous inhibitory dominance. Thus we infer that Hi-Spots contain a functional, self-organised GABAergic inhibitory network in addition to an excitatory glutamatergic network.

The fact that we observe some variation in overall network activity of the Hi-Spots, despite the controlled tissue-engineering used in making them, implies that subtle variations in their composition, such as the ratio of glutamatergic to GABAergic neurons, or in their self-organisation, can lead to the emergence of greater apparent differences in activity. This in itself may prove to be an important property of Hi-Spots for investigations of the types of subtle disturbances that produce overt neurological disorders.

4.5.4 Glutamate Tolerance

We have provided evidence that the Hi-Spots contain viable and spontaneously active neurons interconnected in a network by functional synapses. However, to be useful CNS analogues it is necessary to show that the Hi-Spot has properties more akin to *in vivo* than conventional dissociated neuron cultures. Dissociated isolated neurons are highly sensitive to glutamate toxicity (Choi, Maulucci-Gedde et al. 1987), where as, neurons *in vivo* appear to be highly resistant to glutamate (Massieu, Morales-Villagran et al. 1995), therefore we have investigated the effect of exogenous glutamate on neurons in Hi-Spots.

In vivo the clearance of glutamate from the synaptic cleft is a highly regulated process contributing to the glutamate insensitivity. The clearance is shared between the pre- and post-neurons and the peri-synaptic astroglia (Attwell, Barbour et al. 1993). This tripartite interaction is proving to be important in terms of modulating signalling and potentially dysfunction (Araque, Sanzgiri et al. 1998; Araque, Parpura et al. 1999; Volterra and Meldolesi 2005) and if functionally present in Hi-Spots should render them insensitive to exogenous glutamate.

We have found no toxicity from hour-long exposures to millimolar glutamate when serum is present in the media. Only by removing serum could we measure a dose-dependent toxicity which showed statistical significance to 2hr/5mM glutamate exposures. The protective effects of serum have been related to its trophic properties because protection is preserved when serum is replaced by fibroblast growth factor (FGF) or transforming growth factor- beta (TGF-β1), but not when serum proteins are heat inactivated (Uto, Dux et al. 1994). Evidence suggests that serum proteins are able to protect neurons from glutamate toxicity by preventing mitochondrial calcium accumulation and improving calcium homeostasis in the cell (Dux, Oschlies et al. 1996).

The implications of this *in vivo*-like glutamate tolerance are that either there are processes protecting the neurons from high local levels of glutamate (eg. astrocytic uptake and metabolism) or the neurons are energetically resilient and hence resistant to high glutamate levels, or both conditions are true. The former interpretation is likely to be true on the grounds that failure of astrocytic glutamate uptake leads to greater glutamate toxicity both in culture (Rosenberg and Aizenman 1989; Rosenberg, Amin et al. 1992) and in transgenic animals lacking the major transporters responsible for glutamate clearance (GLAST & GLT-1) (Rothstein, Dykes-Hoberg et al. 1996).

4.6 Conclusion

We have demonstrated that re-aggregated, postnatal, mammalian brain tissue can self-organise into a synaptically-driven, spontaneously active, neuronal network that has *in-vivo* levels of glutamate tolerance. We conclude that these Hi-Spot cultures are biological analogues of CNS tissue at a level of complexity that allows for detailed functional analyses. We believe that their use could reduce the need for *in vivo* experiments by extending the utility of *in vitro* studies, permitting the detailed analysis of synaptic, neuronal and network properties in relation to the developing properties of brain tissue.

5 -Optimisation of Mouse Hi-Spots

5.1 Introduction

The previous chapter demonstrated that Hi-Spots made from P0 rat tissue using the *Soton* modified method with MK801 produced functional tissue-like neural networks in a re-aggregated culture system. This chapter investigates if mouse P0 tissue can also be used to produce re-aggregated Hi-Spot cultures containing neuronal and glial cell populations and functional neuronal networks.

Both rats and mice are commonly used as a source of tissue for neuronal cultures (Galea, Feinstein et al. 1992; Kudo, Aono et al. 2001; Garcia-Junco-Clemente, Cantero et al. 2010). Although rat cells survive the conditions of tissue disruption and culture at much higher rates than mouse cells (Hatten, Gao et al. 1998) mice offer additional benefits to rats because a large variety of neurological mutant mice have been generated (Hayashi, Raimondi et al. 2008; Burre, Sharma et al. 2010).

Neural cell culture from these mouse mutants provides an opportunity for analysing the effects of specific genes on neuronal development and function (Kofuji, Hofer et al. 1996; Varoqueaux, Aramuni et al. 2006). This approach has been combined with cell culture to study the susceptibility of neurons to neurotoxic damage (Dawson, Kizushi et al. 1996) and functions of specific synaptic proteins (Gutierrez, Hung et al. 2009; Garcia-Junco-Clemente, Cantero et al. 2010). Cell culture also allows analysis of neuronal function in mice with late embryonic or very early postnatal lethality. Another advantage of this approach is that it allows us to make cultures from single animals, which can be genotyped thus the genotype of the individual culture is fully defined.

Combining the tissue-like Hi-Spot culture system (optimised using rat tissue) with transgenic mutant mice would be beneficial for the study of neuronal function and dysfunction in the context of transgenic models. To adequately study neural dysfunction in mutant mice, mouse Hi-Spots should be amenable to functional analysis of the molecular, cellular and system bases of neuronal network activity. The Hi-Spot culture should contain excitatory and inhibitory neuronal cells which communicate with one another to form an intricate microcircuit, with similarities to that *in vivo*.

To investigate mouse transgenic models of neurological dysfunction, Hi-Spots generated from mice need to be characterised. The results in this chapter show that mouse Hi-Spots

prepared using the *Soton* protocol modified for rat tissue did not form Hi-Spot cultures with a sustained maturing population of neuronal cells. The protocol to make Hi-Spots from P0 mouse tissue required further modification at the dissociation stage.

5.2 Aim

- To generate functional Hi-Spots from single mouse brains containing a neuronal network surround by glial cells.

5.3 Methods

5.3.1 Production of Hi-Spots from cortical mouse tissue

Mouse P0 Hi-Spots were made using the same protocol as previously described in chapter 2 section 2.1, with the modification of MK801 addition as described in chapter 3 Section 3.3.1. This method is described as the '*Soton*' method.

Rat P0 cortical tissue weighs approximately twice as much as P0 mouse cortical tissue, weight of the example brains was ~0.26g, rat and ~0.13g, mouse. The dissociation volume was halved for mouse brains, making the 'dissociation volume/ brain weight' equivalent. Mouse brains were dissociated in 1500µl/ brain (approximately 1:10 by volume).

5.3.2 Modifications to the Hi-Spot protocol for postnatal mouse Hi-Spot production

This protocol will be referred to as the '*Soton-P*' protocol. The *Soton-P* protocol follows the same procedure as that documented for the production of Hi-Spots from P0 rat tissue, but uses the papain Worthington Life kit (Lorne Laboratories) to dissociate the P0 mouse cortical tissue. The papain Worthington Life kit protocol is described in figure 5.1.

Western blotting, immunohistochemisty and multielectrode recordings and were all conducted as detailed in chapter 2. Where indicated confocal images were taken on an Olympus 1x70 microscope with an ATTO biosciences CARV unit and CCD imaging sensicam attached (BD IP lab software), or a Leica TCS SP2 TCS MP (Leica software).

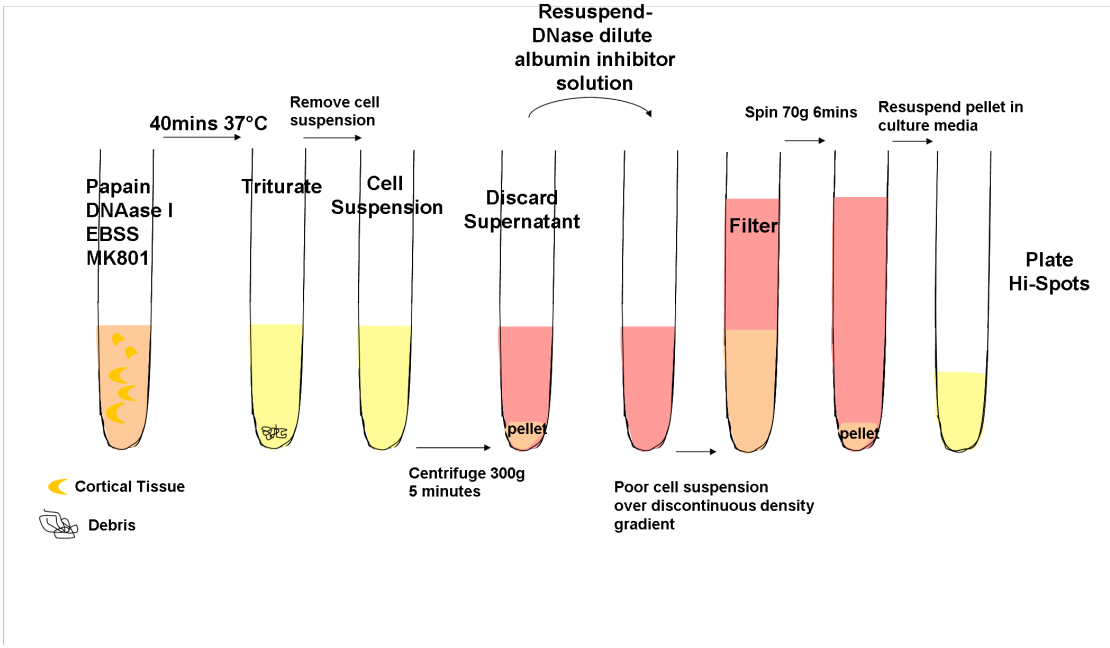

Figure 5.1: Worthington Life Papain Kit Protocol (*Soton-P* protocol)
Cortices are dissected and chopped into small cubes; cortices are incubated in a papain DNAase I solution for 40minutes at 37°C. The cortices are dissociated in the papain solution to a single cell suspension. The single cell suspension is removed and the solution is spun for 5 minutes at 300g to pellet the cells. The cells are re-suspended in the albumin inhibitor solution which is laid over the top of the discontinuous density gradient which acts as a cell filter. The cells are spun through the filter at 70g for 6 minutes. The discontinuous density gradient is removed and the cell pellet is re-suspended in culture media at the desired cells/µl.

5.4 Results

5.4.1 Mouse Hi-Spots produced using the *Soton* protocol

Mouse cortical tissue from P0 mice was dissociated and cultured using the same *Soton* method modified for P0 rat Hi-Spot culture. Bright field microscopy was used to assess culture morphology and to watch for signs of cell clumping and disaggregation. Cell clumping and culture disaggregation were shown in chapter 3 to correlate with unhealthy cultures which did not contain a sustained neuronal population (Figures 3.2, 3.3).

Hi-Spots made from mouse tissue using the *Soton* rat modified method showed formation of cell clumping and culture disaggregation (data not shown). This morphology was observed in all mouse cultures made using this protocol (n= 2 time courses). To assess if this morphology was related to unhealthy cultures that did not maintain a neuronal population Hi-Spots were collected for Western blotting against neuronal and glial cell markers. At *DIV 7, 14, 21, 28* Hi-Spots were removed from culture and tested for the expression of syntaxin, PSD-95 and GFAP.

Mouse Hi-Spots made using the *Soton* rat modified method demonstrated little immunoreactivity for the neuronal marker syntaxin at all culture time points tested. Syntaxin immunoreactivity was abundantly expressed in the freshly dissociated sample (D) from which the re-aggregation was made but decreased to almost undetected able levels by *DIV 7*. PSD-95 was not detected in the freshly dissociated sample (D) or at any of the time points tested. GFAP immunoreactivity was absent from the freshly dissociated sample but was detected after *DIV 7* and subsequently increased throughout the culture period (Figure 5.2).

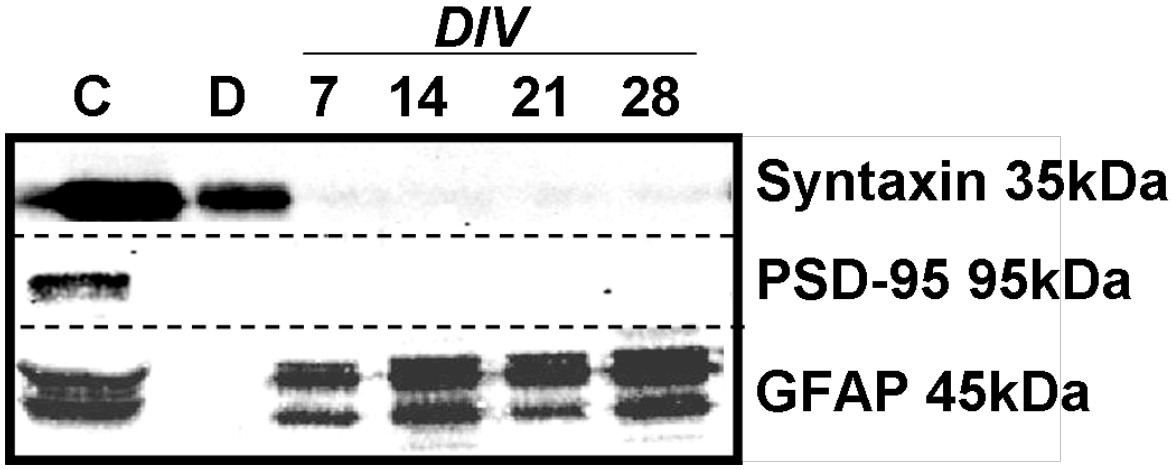

Figure 5.2: Western blots from mouse Hi-Spots produced using the *Soton* method modified for rat tissue
Hi-Spots made from P0 mouse cortical tissue made using the *Soton* protocol modified for rat P0 tissue were extracted and resolved using SDS-PAGE. Western blot analysis against syntaxin and PSD-95 demonstrate that the mouse Hi-Spots did not produce a culture containing a maturing population of neuronal cells. Astrocytes marker GFAP showed increased immunoreactivity during the culture period. C- mature mouse cortex (12µg loaded), D- freshly dissociated sample from which Hi spots were re-aggregated (12µg loaded). Western blot results are representative of one time course of Hi-Spot cultures collected for analysis.

Rat cells survive the conditions of tissue disruption and culture at much higher rates than mouse cells (Hatten, Gao et al. 1998), therefore the lack of neuronal cell propagation in the mouse Hi-Spot culture could be due to greater sensitivity of the mouse cells to mechanical dissociation.

Protease enzymes such as papain and trypsin have been extensively used to aid cell dissociation. The protease enzyme papain provided the best cell viability (Huettner and Baughman 1986; Brewer 1997) when used to dissociate cells. Such observations are the basis for Lorne laboratories kit for neural cell dissociation (Worthington Life papain dissociation kit LK003150), Figure 5.1 summarises the steps used when dissociating cells with this kit. The following results will describe the morphological features and immunoreactivity of neuronal and glial cell markers from Hi-Spots made using the Worthington Life papain dissociation kit. These Hi-Spots will be referred to as produced using the *Soton-P* protocol.

5.4.2 Mouse Hi-Spots produced using the *Soton-P* protocol

Hi-Spots produced using the *Soton-P* protocol were examined under bright field microscopy for signs of cell clumping and culture disaggregation. Using the *Soton-P* protocol mouse Hi-Spots cultures did show signs of cell clumping or disaggregation (n=4 time courses of Hi-Spots) (data not shown).

One set of Hi-Spot cultures was assessed by Western blot for immunoreactivity to neuronal and glial cell markers after *DIV 7, 14, 21* and *28*. The results show that the *Soton-P* Hi-Spots demonstrated increasing immunoreactivity for syntaxin throughout the culture period. The neuronal maturation marker PSD-95 was detected in the freshly dissociated sample and at each stage in the culture period. Immunoreactivity for the astrocyte marker GFAP was absent from the freshly dissociated sample but detected at *DIV 7* and increased throughout the culture period (Figure 5.3).

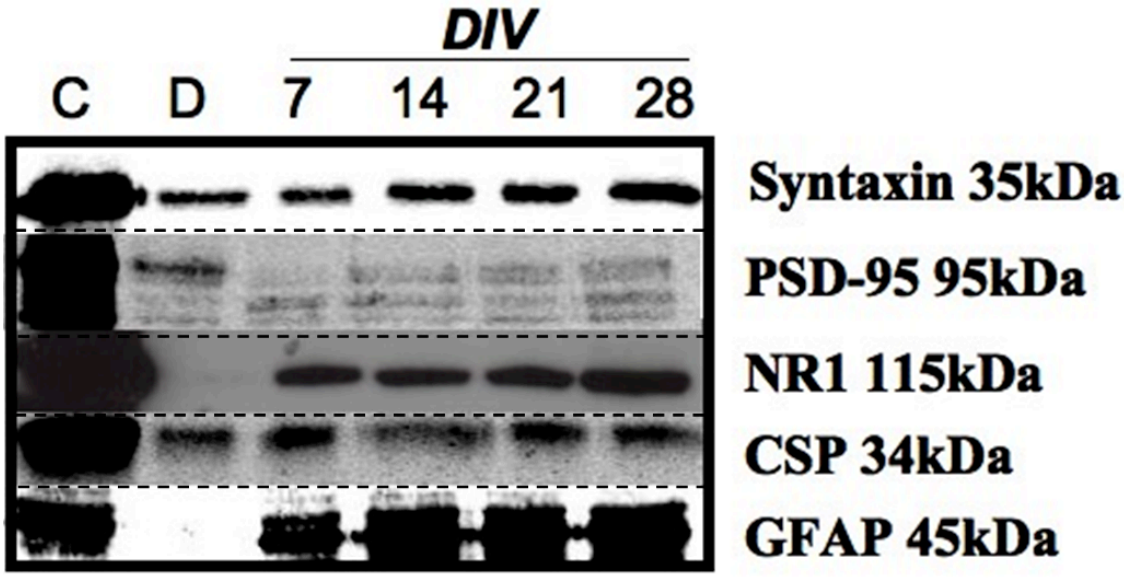

Figure 5.3: Western blots from mouse Hi-Spots produced using the *Soton-P* protocol
Soton-P Hi-Spots were extracted and resolved using SDS-PAGE. The neuronal markers syntaxin and PSD-95 showed increasing immunoreactivity throughout the culture period. The neuronal markers CSP and NR1 were also detected throughout the culture period. The astrocyte marker GFAP showed no immunoreactivity in the freshly dissociated samples but increasing immunoreactivity during the culture period.
C- adult mouse cortex(12µg loaded), D- freshly dissociated sample from which Hi-Spots were plated (12µg loaded). Western blot results are representative of one time course of Hi-Spot cultures collected for analysis

The *Soton-P* Hi-Spots were further characterised for the expression of NR1 and the synaptic vesicle protein Cysteine String Protein (CSP). NR1 immunoreactivity was not detected in the freshly dissociated sample but was detected at *DIV 7* in culture. The immunoreactivity of NR1 increased throughout the culture period. CSP was detected in the freshly dissociated sample and at all culture ages tested (Figure 5.3).

5.4.3 *Soton-P* protocol dissociation results in less dead cells

When the mouse cortices were dissociated and processed using *Soton-P* protocol the number of dead cells assessed by the trypan blue exclusion were significantly (P=0.0190) reduced compare to those counted from mouse tissue processed using the *Soton* rat modified method (Figure 5.4). The *Soton-P* protocol did not significantly increase the live cell yield/ brain as would be expected after observing the significantly decreased number of dead cells/ brain. This could be due to *Soton-P* dissociation protocol not generating as many live cells as judged by the trypan blue negative cell counts. However, the cells dissociated using the *Soton-P* protocol are more viable than those dissociated using *Soton* protocol judged by the expression of neuronal markers (Figures 5.2 and 5.3). Therefore, the decreased number of live cells after the *Soton-P* protocol probably reflects a higher undissociated fraction due to gentler dissociation with papain.

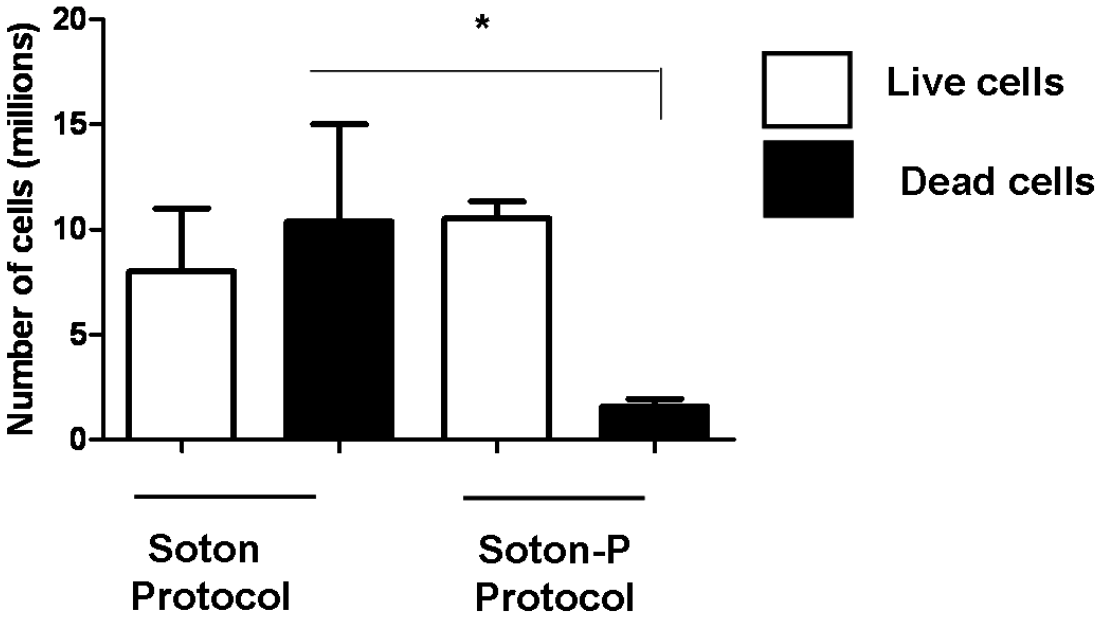

Figure 5.4: Quantification of the number of dead and live mouse cells using trypan blue exclusion dye
After dissociation the numbers of dead and live cells were counted in dissociates from the *Soton-P* protocol and the *Soton* protocol. Cells that were trypan blue negative were counted as live and cells that were trypan blue positive were counted as dead. Mouse P0 tissue dissociated with the *Soton-P* protocol results in significantly (P=0.0190) less dead cells than mouse tissue dissociated using the *Soton* protocol modified for rat tissue. The results are displayed as number of dead and live cells/ brain. Statistics: One tailed unpaired students t-test 95% confidence. n= 2 dissociations using the *Soton* rat modified protocol, n=4 using the *Soton-P* protocol.

5.4.4 Mouse Hi-Spots produced using the *Soton-P* protocol develop a neural network

Mouse *Soton-P* cultures were immunostained with antibodies against β III Tubulin, PSD-95, GFAP and Hoechst. The Hi-Spots were imaged on a CAVA confocal which does not have the resolution of the Leica TCS SP2 TCS. The high cell density of the cultures can be appreciated by the close association of the Hoechst stained cell bodies (Figure 5.5). Images taken at *DIV 14* and *DIV 21* show that cultures produced using the *Soton-P* protocol form a β III Tubulin neuronal network (green) surrounded by GFAP (red) positive astrocyte processes. PSD-95 expression is also shown for a *DIV 21* Hi-Spot, PSD-95 staining shows a dense distribution of puncta which appear to form in lines possibly along neuronal processes (Figure 5.5).

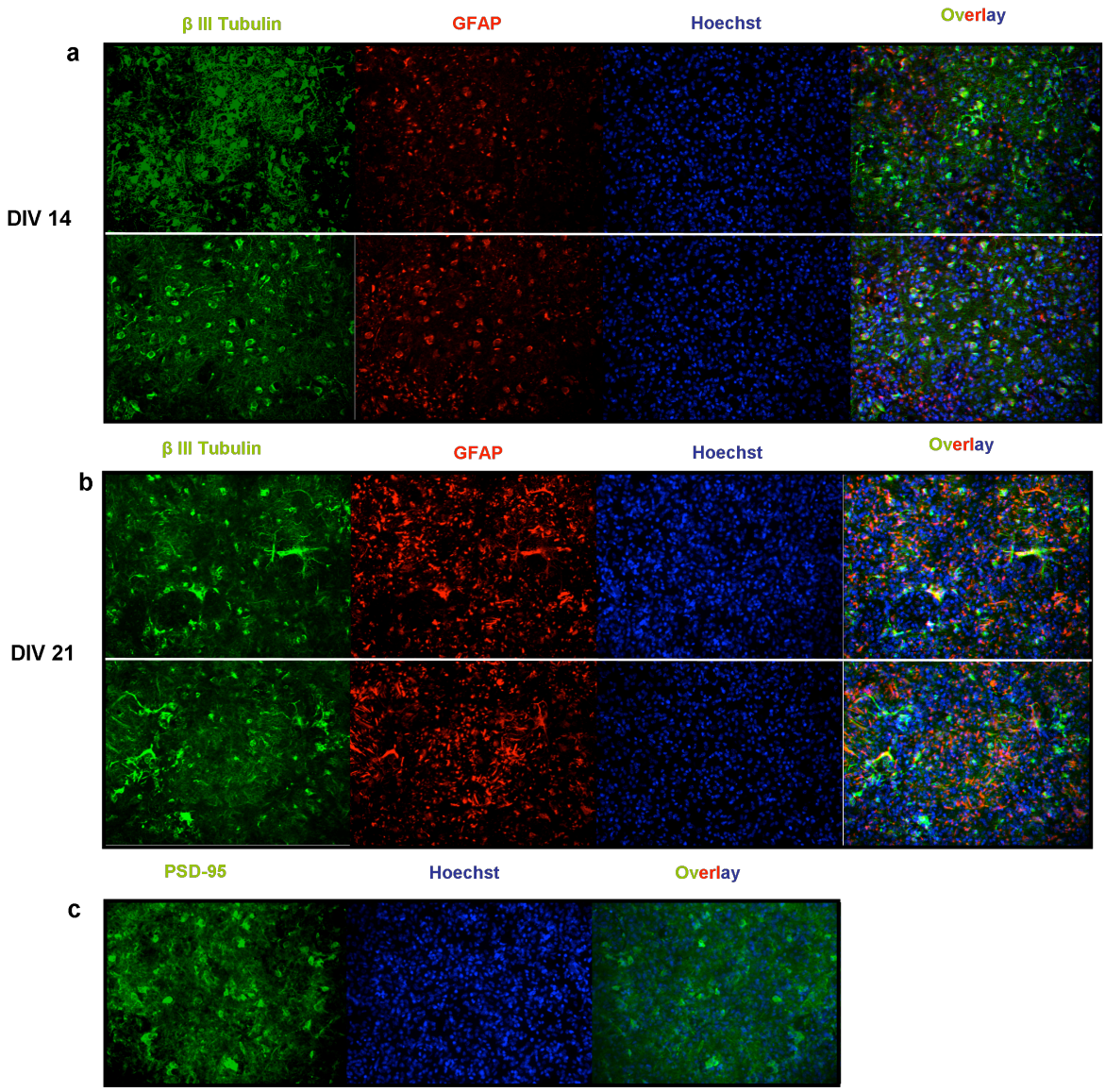

Figure 5.5: Neuronal network formation in mouse cultures produced using the *Soton-P* protocol

Maximum projection confocal images from a scan through each Hi-Spot using 0.5µm steps.

a) *DIV 14 Soton-P* Hi-Spots show a β III Tubulin network of neuronal processes surrounded by GFAP stained processes.

b) *DIV 21 Soton-P* Hi-Spots show a β III Tubulin network of neuronal processes surrounded by GFAP stained processes.

c) *DIV 21* PSD-95 labelling shows a punctate staining consistent with expression in neuronal cells and evidence for presence of synaptic specialisations.

Together the Western blot and IHC results show that P0 *Soton-P* Hi-Spots contain a maturating population of neurons. Therefore we next tested if *Soton-P* Hi-Spots generated from mouse tissue developed spontaneous activity.

5.4.5 Mouse Hi-Spots produced using the *Soton-P* protocol form an active neural network

Hi-Spots were removed from culture and were tested for spontaneous activity. Figure 5.6 shows that the mouse Hi-Spots produced using the *Soton-P* protocol developed spontaneous activity by *DIV 14* which persisted to *DIV 35*. The results show the spike numbers and RMS values from two sets of mouse cultures, an average of 4 Hi-Spots was recorded from per time point.

The spontaneous activity recorded develops first as single spiking activity with higher frequency bursting events which were correlated across the spatially distinct electrodes associated with later culture ages (data not shown). Figure 5.6 shows that there is a significant (P=0.0356) increase in the number of spikes and the RMS value (P=0.0140) between *DIV 7* and *DIV 14*. After *DIV 14* there is no significant difference in spike or RMS value at *DIV 21, 28* or *DIV 35*.

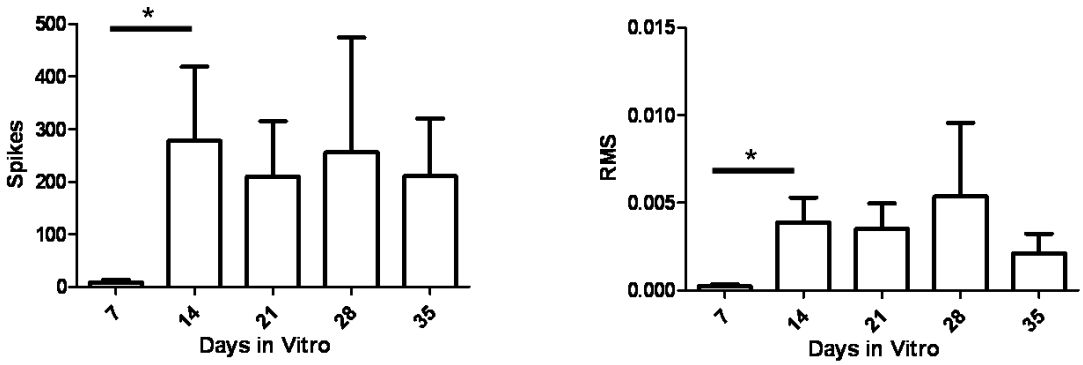

Figure 5.6: Mouse Hi-Spots develop spontaneous activity
Soton-P Mouse Hi-Spots develop spontaneous activity. Activity shows a significant increase between *DIV 7* and *DIV 14* in terms of both spike number and RMS (Spikes P=0.0356, RMS P=0.0140). The results show average activity taken from 300 seconds of activity from two sets of cultures with an average of 4 Hi-Spots recorded/ stated *DIV*. Stats, unpaired one tailed t-test, error bars are SEM.

Together these results support the use of *Soton-P* to produce Hi-Spots from re-aggregated P0 mouse tissue. The MEA recordings show that the *Soton-P* cultures develop spontaneous network activity and the activity recorded shows the same single spiking and bursting activity development previously described for Hi-Spots produced from *Soton* protocol modified for rat Hi-Spots (Chapter 4 Figure 4.5).

5.4.6 Single brain dissociations for genotyped mice

In order to generate genotypically defined Hi-Spots, cultures need to be made from genotypically defined animals. For transgenic lines that have to be bred from heterozygous matings this implies the need to produce Hi-Spots from individual mice that can be genotyped. Accordingly, as a next step we investigated whether single P0 cortices could be dissociated and re-aggregated to form Hi-Spots. This was done by using a reduced dissociation volume and dissociating the tissue using the *Soton-P* protocol (Section 5.3.2).

The dissociation volume was equivalently adjusted for the weight of a single mouse brain such that each brain was independently dissociated in 1500µl papain solution.

The morphological appearance of the single brain dissociate Hi-Spots was assessed by bright field microscopy. The Hi-Spots did not show signs of cell clumping, but areas of the Hi-Spots disaggregated. Figure 5.7 shows that Hi-Spots plated at 50,000 cells/ µl disaggregated to from islands of cell connected by thin processes. 50,000 cells/ µl is the same plating density used to produce rat and the mouse Hi-Spots produced from multiple brain dissociations, which do not show this morphology.

The morphology demonstrated by the single brain dissociate Hi-Spots is similar to that produced when micro-islands or microcultures are formed for *in vitro* culture experiments. Microcultures are formed by plating cells at low density, around 20,000 cells/ ml (Mennerick, Que et al. 1995) and are useful when single cell electrophysiology analysis needs to be performed. We therefore decided to investigate if the morphology observed in the single brain dissociation cultures was due to a decreasing cell density in the single brain dissociate Hi-Spots.

To investigate if the microculture-like morphology was cell density dependent we increased the cell density from 50,000 cell/ µl to 60,000, 80,000 and 90,000 cells/ µl. The morphology was assessed in the increased cell density Hi-Spots using bright field microscopy. At all days *in vitro* the cultures plated at 90,000 cells/ µl (450,000 live cells/ Hi-Spot) remained intact and did not disaggregate to show microculture-like morphology (n=12) (Figure 5.7). This increased the number of live cells per Hi-Spot from 250,000 in Hi-Spots made using the rat *Soton* and *Soton-P* protocol to 450,000 live cells, decreasing

the number of Hi-Spots / brain to approximately 30 Hi-Spots/ mouse brain, but resulted in a culture that remained intact and did not show formation of microculture-like morphology (Figure 5.7).

Analysis of the live and dead cell numbers between the single and multiple mouse brain dissociations using the *Soton-P* protocol demonstrated that there was no significant difference in the number of dead or live cells counted using a haemocytometer and trypan blue (Figure 5.8). Therefore, the microculture-like morphology can not be due to an increased number of dead cells plated in the single brain Hi-Spot dissociations.

To assess if the Hi-Spots produced using the *Soton-P* protocol and plated at the increased cell density of 90,000 cell/ µl formed a culture that developed a neuronal network surrounded by astrocytes we conducted IHC and confocal microscopy.

5.4.7 Single brain dissociation Hi-Spots plated at 90,000 cells/ µl form a neural network

Hi-Spots generated from single brain dissociations plated at 90,000 cells/ µl were immunostained for β III Tubulin, GFAP and cell body marker Hoechst. The Hi-Spots were imaged on a Leica TCS SP2 TCS MP confocal microscope (Leica software). Figure 5.9 shows images of Hi-Spots after *DIV 14* and *DIV 21*, the upper panels show lower magnification views of the Hi-Spots demonstrating that the Hi-Spots are formed from a neuronal network inter mixed with astrocytes. The lower panels show higher magnification images and allow the neuronal processes and the close association between the neural cells to be appreciated. The high cell density of the Hi-Spots is shown at both *DIV 14* and *DIV 21* and can be appreciated from the close association of the Hoechst stained cell bodies (Figure 5.9).

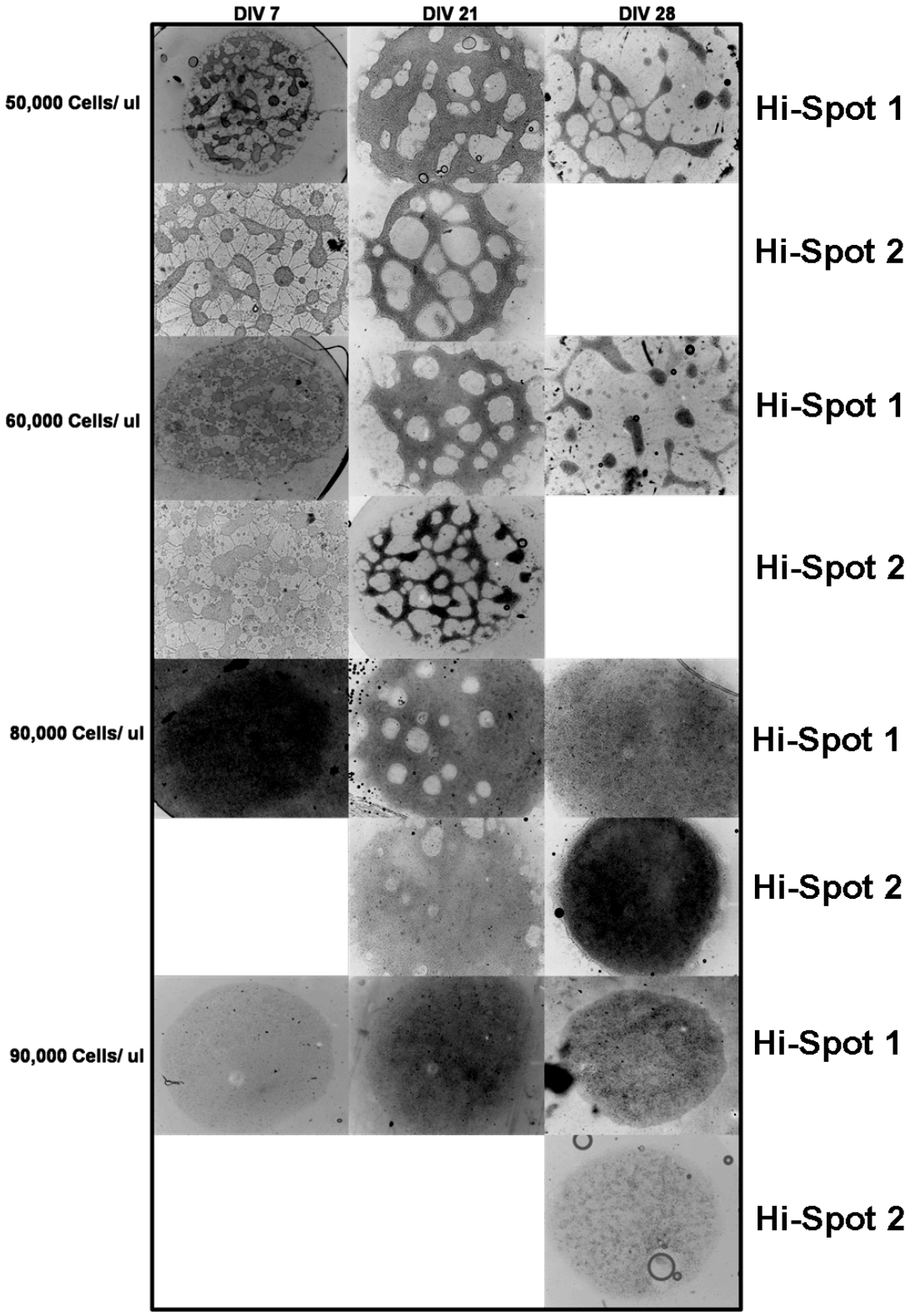

Figure 5.7: Single brain dissociated Hi-Spots can be made be plating at 90,000 cells/ µl
Bright field images of Hi-Spots containing increasing numbers of cells from 50,000 to 90,000 cells/ µl. Single cell dissociated cultures break apart to form micro islands of cells if not seeded at the increased cell number of 90,000 cell/ µl.
The results are representative of 2 sets of Hi-Spots plated at 50, 60 and 80,000 cells/ µl, and 12 sets of Hi-Spots plated at 90,000 cells/ µl.

The Hi-Spots produced from the mouse tissue formed cultures that were only one cell thick, each Hi-Spot ~10μm thick. Hi-Spots formed from rat tissue were characteristically 6 cells thick (~60 μm thick after compression under a glass cover slip) (Figure 4.1). The neural cells in the mouse Hi-Spot are still densely packed together but the multi-cellular layers observed in the rat Hi-Spots were not readily observed.

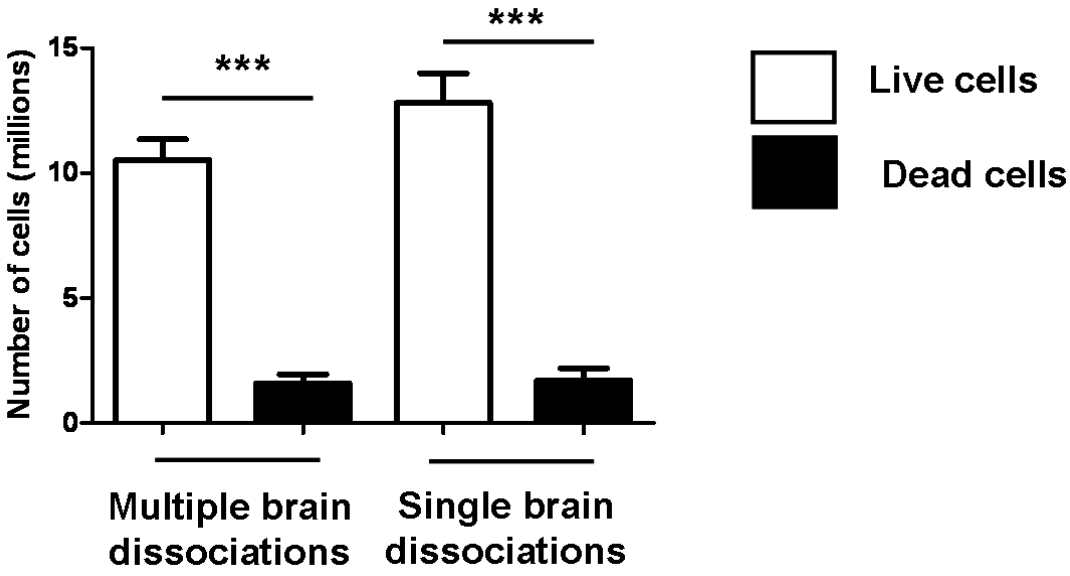

Figure 5.8: Dead and live cell number from single and multiple brain dissociations
Live and dead cells were quantified on a haemocytometer using trypan blue to discriminate between dead and live cells. There are significantly more live cells than dead cells in each of the dissociations (P=<0.0001***). There is no significant difference in the number of live or dead cells between the multiple and single brain dissociations. The results are displayed as number of dead and live cells/ brain.
n=4 multiple brain dissociations, n=12 single brain dissociations.
Statistics: unpaired one tailed t-test 95% confidence value.

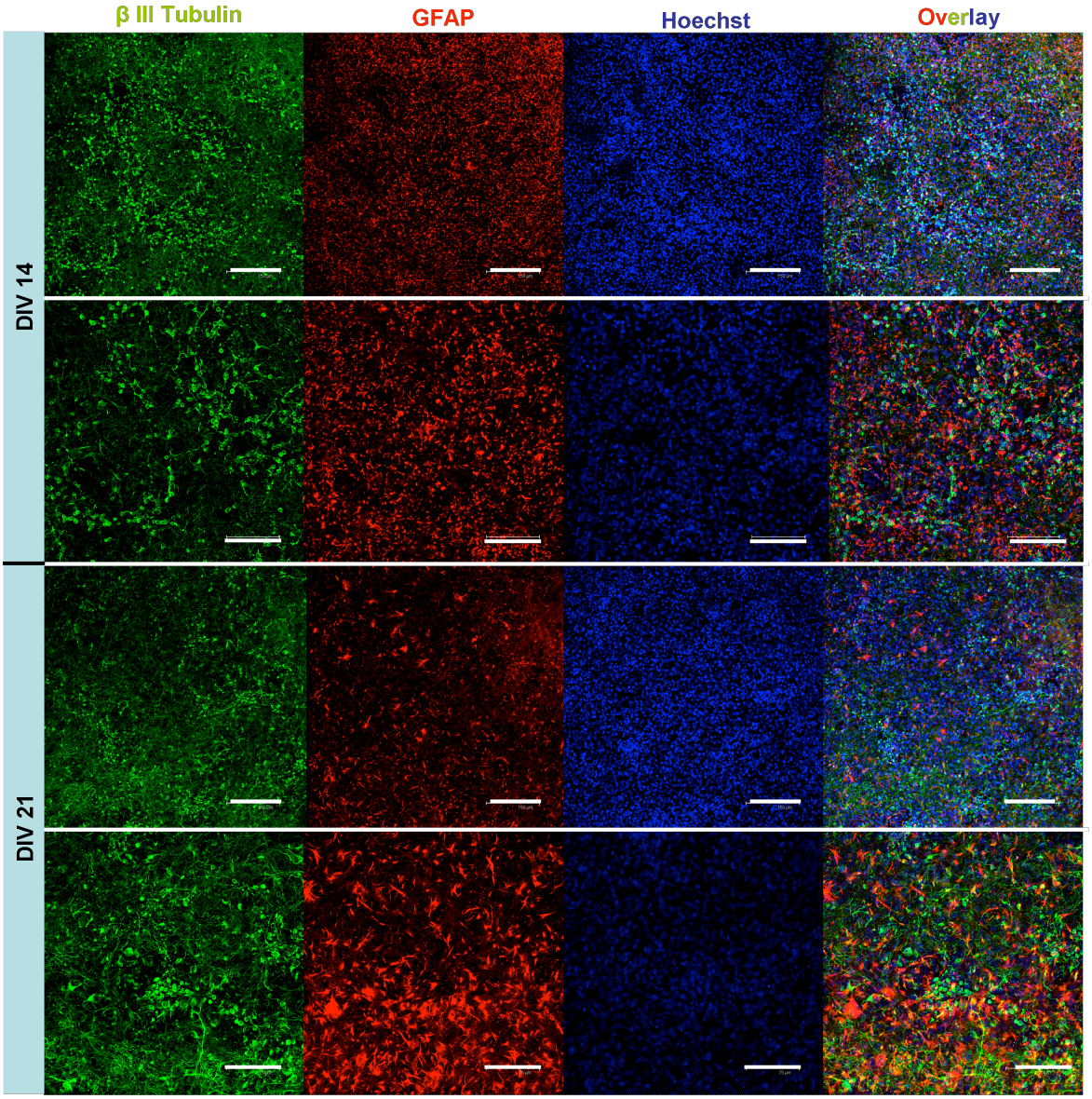

Figure 5.9: Single brain dissociated cultures plated at 90,000 cells/ µl form a neuronal network surrounded by glial

Soton-P Hi-Spot cultures of single cortices were fixed and subject to IHC and confocal analysis. Images shown are maximum projection images from a 12 z stack scan. The top *DIV 14* panels show lower magnification views of the Hi-Spot neuronal network and glial cells (Scale Bar 150µm). The second panel images show higher magnification images of a *DIV 14* Hi-Spot showing the close interaction between the neuronal network and the glial cells (75µm). The top *DIV* 21 panels show lower magnification views of the Hi-Spot neuronal network and glial cell network (150µm). The lower *DIV 21* panels show the close interaction of the neuronal and glial cells (75µm). In all images the cell bodies are stained with Hoechst 33342 (Blue), β II Tubulin marks neuronal processes (Green), GFAP marks astrocyte (red).

5.5 Discussion

We have developed an *in vitro* re-aggregated culture model using rat tissue. In chapter 4 we demonstrated that this culture model developed an active neuronal network containing both GABAergic and glutamatergic neuronal networks and that the activity recorded was synaptically driven. We also demonstrated that the Hi-Spot cultures contained both neuronal and glial cell populations which developed together and formed tissue-like neural interactions. In this chapter we have refined the protocol used to produce re-aggregated Hi-Spot cultures from mouse tissue. To culture mouse tissue as re-aggregated Hi-Spots two further modifications were introduced to the protocol, firstly the mouse tissue was dissociated using the papain Worthington Life papain kit, and secondly to produce Hi-Spots from single brain dissociations the cell density was increased from 50,000 cells/ µl (the cell density used for rat Hi-Spots) to 90,000 cells/ µl.

In this chapter we have demonstrated that Hi-Spots can be formed from mouse tissue using the *Soton-P* modified method. The Hi-Spots formed develop a neuronal network surrounded by glial and demonstrate functional spontaneous activity. The spontaneous activity which develops matches previous observations of mouse dissociated cultures grown on MEAs (Van Pelt, Corner et al. 2004; Wagenaar, Pine et al. 2006) and that documented for rat Hi-Spots (Chapter 4 Figure 4.5). Single spiking activity was associated with early culture ages (*DIV 1-7*) developing to bursting behaviour in more mature cultures (*DIV 14-35*).

Mouse tissue dissociated using the MK801 (*Soton*) protocol did not form Hi-Spot cultures with a maturing neuronal network. Mouse neural cells have been reported to not survive the mechanical dissociation and cell culture conditions as well as rat cells (Hatten, Gao et al. 1998). In support of this the neuronal cells dissociated from mouse tissue without papain (i.e. MK801, *Soton* method) did not survive in the Hi-Spot cultures leaving a culture composed of mainly glial cells (Figure 5.2). Therefore in order to decrease the severity of the mechanical trituration, a proteolytic enzyme was used. Papain is a cysteine protease enzyme. Because the enzyme is large it cannot enter the cells and therefore protease treatment removes externally exposed cell surface proteins and proteins involved in cell adhesion without damage to the cells.

Papain has been shown to be an effective proteolytic enzyme for improving subsequent cell viability. Huettner and Baughman (Huettner and Baughman 1986) found papain the best enzyme to use for cell viability after tissue dissociation, and more recently Brewer found papain the best of 6 enzymes tested for optimisation of cell survival (Brewer 1997). The papain Worthington Life papain kit was based on the original findings of Huettner and Baughmann (1986) and uses the enzyme papain to aid cell dissociation.

Implementing the *Soton-P* protocol for mouse tissue dissociation produced a culture that maintained a neuronal population. The neuronal cells demonstrated evidence of maturation and expression of the obligatory NMDA receptor subunit NR1. The glial cell marker GFAP showed that the neuronal cells were maintained and matured in the presence of a proliferating or hyperfunctioning astrocyte population much the same as that previously documented for rat Hi-Spots produced using the *Soton* method (Chapter 3 Figures 3.6 and 3.7).

The papain dissociation did not increase the number of live cells measured using trypan exclusion, however, the cells are evidently different in that they are more capable of producing viable Hi-Spots. The number of trypan positive cells significantly decreased, hence the overall cell number was lower, and this implies that some cells are missing from the trypan cell count following papain treatment. This could be due to the different processing of the tissue between the *Soton* and the *Soton-P* protocols. The latter involves several centrifugation steps which lead to improvement of the live: dead ratio, but will inevitably lead to some loss of cell numbers. No cells were found trapped in the filtration gradient implying cell loss before this stage.

5.5.1 Hi-Spots from genotypically defined single brains

We have shown that to culture Hi-Spots from single brain dissociations the cultures had to be plated at a higher cell density. Initial experiments where brains were individually dissociated using the *Soton-P* protocol and plated at 50,000 cells/ µl produced Hi-Spots that disaggregated and demonstrated microculture-like morphology (Figure 5.7). It has been reported that microcultures can be produced by culturing cells at a lower cell density than that used for mass cultures (Mennerick, Que et al. 1995). Therefore the Hi-Spot single

brain dissociates could be forming this morphology because the cell density in the Hi-Spots is decreasing as the culture ages.

We have shown that increasing the cell plating density to 90,000 cells/ µl prevented disaggregation and retention of intact re-aggregated Hi-Spot cultures. The difference between the single and multiple brain dissociations resulting in formation of microculture-like morphology in the single brain dissociations was not due to an increased dead cell population after dissociation in the single brain dissociations (Figure 5.8). The only difference between the two dissociations is the volume of papain solution the cells were dissociated in. Single mouse brains were dissociated at an equal weight/volume ratio to multiple brain dissociations. The decreased volume used to dissociate the single brain dissociates could result in a more vigorous tritutration. However, the more vigorous trituration did not lead to an increased number of dead cells counted after the dissociation, but the cells could have been damaged and died after culture plating leading to a decreased live cell density in the single brain dissociate Hi-Spots and microculture-like morphology development.

A further modification to the single brain Hi-Spot dissociation protocol would be to dissociate the brains in an increased dissociation volume. However, by modifying the cell density single brain dissociate Hi-Spots formed a neuronal network surrounded by glial cells (Figure 5.9). The neuronal network is present across the Hi-Spot at both *DIV 14* and *DIV 21* and the densely packed neuronal cell bodies are shown using the indiscriminate marker Hoechst.

5.6 Conclusion

We have shown that it is possible to generate genotypically defined Hi-Spots from genotypically defined individual animals. This is a significant advantage for work on transgenic lines that have to be bred from heterozygous matings.

To allow this mouse P0 tissue was dissociated with the *Soton-P* protocol and plated at an increased cell density (90,000 cells/ µl). Re-aggregated Hi-Spot cultures were formed that contained a maturing neuronal population, which form a neuronal network alongside glial cells. Even though the mice Hi-Spots are generally a monolayer, they still formed a high

density culture in which the neural cells are in close association (Figure 5.9). Like the rat Hi-Spot cultures the mouse Hi-Spots are re-aggregated cultures of postnatal tissue that develop functional neural networks. Because of these advantages mouse Hi-Spots present a useful model for the functional genetic study of network development, function and dysfunction.

The next chapter will focus on using mouse Hi-Spots from single brain dissociations to investigate the network dysfunction occurring in the CSP α knockout mice.

6 -Neuronal dysfunction in CSPα-/- Hi-Spots revealed by MEA analysis

6.1 Introduction

We have characterised the re-aggregated Hi-Spot culture system for both rat and mouse postnatal cortical tissue. This chapter will describe experiments in which we use the optimised Hi-Spot system for transgenic mice to investigate the neuronal dysfunction(s) that may arise out of synaptic degeneration. To this end we investigated the characteristics of Hi-Spot cultures from dissociated re-aggregated cultures of CSPα-/- mice cortical tissue as an example of synaptopathy (Fernandez-Chacon, Wolfel et al. 2004; Garcia-Junco-Clemente, Cantero et al. 2010).

6.1.1 CSPα-/- mice as a neuronal degeneration model and network changes

CSPα is a synaptic vesicle associated protein, it has been shown to associate and act as a co-chaperone for the chaperone protein Hsc70, and has been implicated as functioning in the neuronal regulation of calcium homeostasis, evoked neurotransmitter release and prevention of nerve terminal degeneration as reviewed section 1.10.

CSPα-/- mice show marked and progressive degeneration of the calyx of Held synapse (Fernandez-Chacon, Wolfel et al. 2004), the parvalbumin positive interneurons (Garcia-Junco-Clemente, Cantero et al. 2010), the neuromuscular junction (nmj) and the ribbon synapses of the photoreceptors (Fernandez-Chacon, Wolfel et al. 2004; Schmitz, Tabares et al. 2006). Interestingly these degenerations appear relatively discrete and although correlated with organism death it appears that only sub-types of synapses die as the brains of animals at death are relatively intact and major anatomies and synapses are not affected. In cortical regions Garcia et al (2010) showed that glutamatergic hippocampal synapses are refractory to the degeneration, however, the parvalbumin positive basket cells show degenerating synapses (Garcia-Junco-Clemente, Cantero et al. 2010). A shared feature of the types of synapses that degenerate appear to be that they are involved in fast frequency transmission; either fast frequency firing synapses, calyx (>100Hz), parvalbumin positive interneurons (~100Hz), or synapses that are tonically active, the nmj and photoreceptors (Section 1.10)

Loss of the fast firing inhibitory neuronal cells, in a neuronal network in which the output of excitatory cells is finely controlled has been shown to have implications for the network

activity (Fuchs, Zivkovic et al. 2007) and the health of the animal (Powell, Campbell et al. 2003; Cobos, Calcagnotto et al. 2005). This may provide insight into the network changes that occur when the neuronal excitatory and inhibitory balance is compromised, such as that thought to occur in autism spectrum disorders (Gutierrez, Hung et al. 2009)

Network dysfunction in the CSPα-/- mice could be studied *in vitro* in a culture system which allowed network activity to be measured and manipulated to demonstrate the contribution of network activity from inhibitory and excitatory cell populations. Network activity *in vitro* has been manipulated with bicuculline to demonstrate the function of the inhibitory interneuronal networks (Jimbo, Kawana et al. 2000; Hofmann and Bading 2006), and the parvalbumin positive basket cells have been shown to represent 50% of the interneuronal population *in vitro* and have *in vivo*-like fast firing kinetics (Kinney, Davis et al. 2006).

Many different *in vitro* cultures systems have been developed and the one chosen for a particular investigation should be the culture system that best mimics or has the optimal niche for the question that is being investigated. For the study of network dysfunction in the CSPα-/- mice, a culture system which allows neural network development in an *in vivo*-like environment and development of network activity, which can be recorded and probed, using pharmacological manipulations, would be necessary.

6.1.2 Hi-Spots to investigate network dysfunction

We have previously shown that network activity can be recorded in Hi-Spot cultures, which permit neuronal networks to develop in an *in vivo*-like environment, and that rat Hi-Spots contain the subtype of interneurons (parvalbumin positive), which have been shown to degenerate in the CSPα-/- mice (Figure 4.4) (Garcia-Junco-Clemente, Cantero et al. 2010).

In the Hi-Spot cultures spontaneous activity develops and becomes established between *DIV 7-28*. This time period also correlates with expression of neuronal and glial cell proteins and with expression of NR1 (Figure 5.3 and 5.6). In CSPα-/- mice degenerative changes in calyx of Held, photoreceptors and parvalbumin positive interneurons were detected between 2 and 3 weeks after birth (Fernandez-Chacon, Wolfel et al. 2004;

Chandra, Gallardo et al. 2005; Schmitz, Tabares et al. 2006; Garcia-Junco-Clemente, Cantero et al. 2010). Therefore the Hi-Spot culture period fits well with this period for network analysis.

6.2 Aims:

- To investigate if the Hi-Spot cultures produced from CSPα-/- murine cortical tissue shows specific degeneration
- To investigate if network wide activity changes can be seen in the CSPα-/- Hi-Spots compared to CSPα+/+ Hi-Spots.

6.3 Methods

6.3.1 Hi-Spot Protocol

Pups from heterozygous crosses were genotyped from tail tips (Section 2.12.2). DNA was extracted using the protocol described in section 2.12.2 and PCR used to identify CSPα-/- and CSPα+/+ pups. Hi-Spots from individual CSPα genotypes were made by taking mice pups after birth, which were kept warm under a red light while DNA extraction and PCR took place. Genotyping was complete within 4 hours of taking the pups from the dam and pups were sacrificed for tissue culture immediately after the genotype had been identified.

Individual CSPα+/+ and CSPα-/- cortices were dissociated using the *Soton-P* protocol (Section 5.3.2). The Hi-Spots were re-aggregated at a concentration of 90,000 cells/ µl and plated at 450,000 cells/ Hi-Spot (5µl).

6.3.2 Propidium Iodide staining

At *DIV 28* Hi-Spots produced from CSPα-/- and +/+ mice had their culture media (serum containing normal media) replaced with media containing 3µg/ml of PI. The Hi-Spots were incubated with the PI containing media overnight and subsequently imaged using Leica Software for their PI florescence. Images were analysed using Image J software and data presented as mean grey values (Section 2.11).

6.3.3 Electron Microscopy

Sample fixation and processing were conducted as stated in section 2.13.

Hi-Spots from CSPα-/- and +/+ mice were fixed and processed at *DIV 23*. The CSPα-/- sample is from several Hi-Spots embedded together by removing the Hi-Spots from the PTFE membrane insert, and spinning the aggregated layers into a pellet which was embedded in resin. The CSP α+/+ Hi-Spots samples corresponds to one Hi-Spot embedded flat on the PTFE membrane so that the sample could be cut 'enface'.

Electron microscopy was also performed on a CA1 brain section from a CSPα-/- mouse at P28 as described in section 2.14.

6.3.4 Multielectrode Array (MEA) recordings

MEA recordings were performed on *DIV 14-16* and *DIV 21-23* on both CSPα -/- and CSPα +/+ cultures. CSPα+/+ litter matched mice were used to make control cultures. MEA recordings were performed as previously documented in section 2.9. Recordings were made pair-wise from different litters of mice and in total 4 sets of CSPα-/-, and 4 sets of CSPα +/+ mouse Hi-Spots were recorded from. A 5th set of CSPα-/- and CSPα+/+ cultures were prepared but neither genotypes demonstrated any basal spontaneous activity at either 2 or 3 weeks in culture. These Hi-Spots did not differ in their bright field gross morphology to the active sets of cultures, but because both genotypes failed to develop spontaneous activity they were discarded from the analysis.

The Hi-Spots were placed into the recording cassette for 25-30 minutes before recording basal activity for 5-10 minutes. The ACSF was then replaced with ACSF containing 50μm bicuculline. Hi-Spot activity was recorded for 25-30mins in the presence of bicuculline. The results shown are from 300 seconds of basal MEA activity and 300 seconds of bicuculline induced activity. The bicuculline induced activity is taken from a 300 second window from 900-1200 seconds after bicuculline exposure. The 0-900 seconds allows an incubation time for the bicuculline to perfuse to the Hi-Spot through the MEA pores and take effect (Figure 6.1).

Figure 6.1 summarises the incubation times and drug additions. Results are displayed as number of spikes and RMS values for the 300 seconds recorded. Statistics are unpaired one tailed t-tests and error bars are SEM.

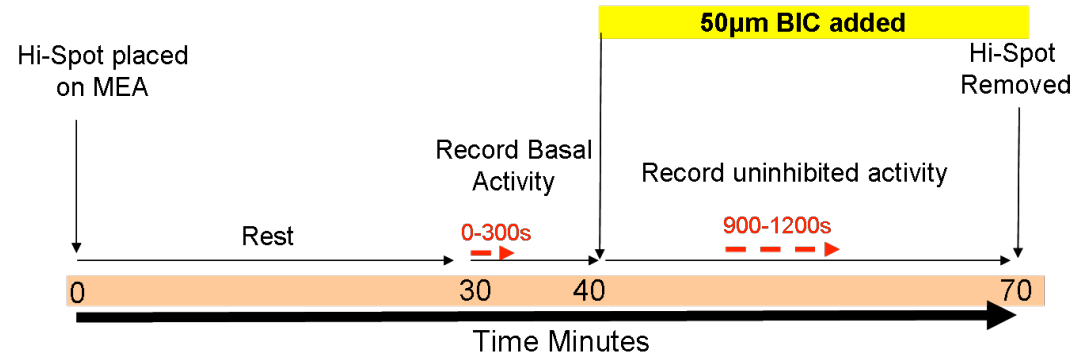

Figure 6.1: Multielectrode array experiment time line for recording from CSPα+/+ and -/- Hi-Spots
Hi-Spots are place on the MEA cassette in contact with the electrodes. The Hi-Spots were allowed to recover inside the recording cassette maintained at 37°C. Basal activity was then recorded for 300 seconds. The ASCF in the bottom chamber was removed and replaced with ASCF containing 50µm bicuculline. Once the MEA cassette had been placed back into the recording cassette the recording was started. Inducible activity was recorded for up to 30 minutes. The timing in red indicate the times used to for analysis of the activity of CSPα-/- and CSPα++ Hi-Spots.

6.3.5 Immunohistochemisty and Confocal Imaging of Hi-Spot cultures

Two CSPα+/+ and two CSPα-/- Hi-Spots were fixed and processed for IHC staining as previously described in section 2.6. CSPα-/- and CSPα+/+ Hi-Spots are from the same litter of mice and were fixed at *DIV 22*.

6.3.6 Immunohistochemisty and microscopy of brain sections

IHC on wax embedded brain sections was preformed as described in section 2.7 in the General Methods.

6.3.7 Quantitative Real Time PCR

RT-PCR was preformed as described in section 2.15 in the General Methods.
rt-PCR was preformed on 6 samples of cDNA from the hippocampi of 6 individual CSPα-/- mice and for comparison from 2 different CSPα +/+ mice. Primers were designed and used to amplify a 140 base product of Arc:Arg 3.1 from synthesised cDNA.

6.4 Results

6.4.1 Bright field images of Hi-Spot gross morphology

Hi-Spots were imaged under bright field microscopy and signs of darkened clumps of cells and disaggregation were noted. Darkened areas and cell clumping were shown in chapter 2

to correlate with loss of neuronal markers and low levels of spontaneous activity (Figures 3.3, 3.6, 3.9).

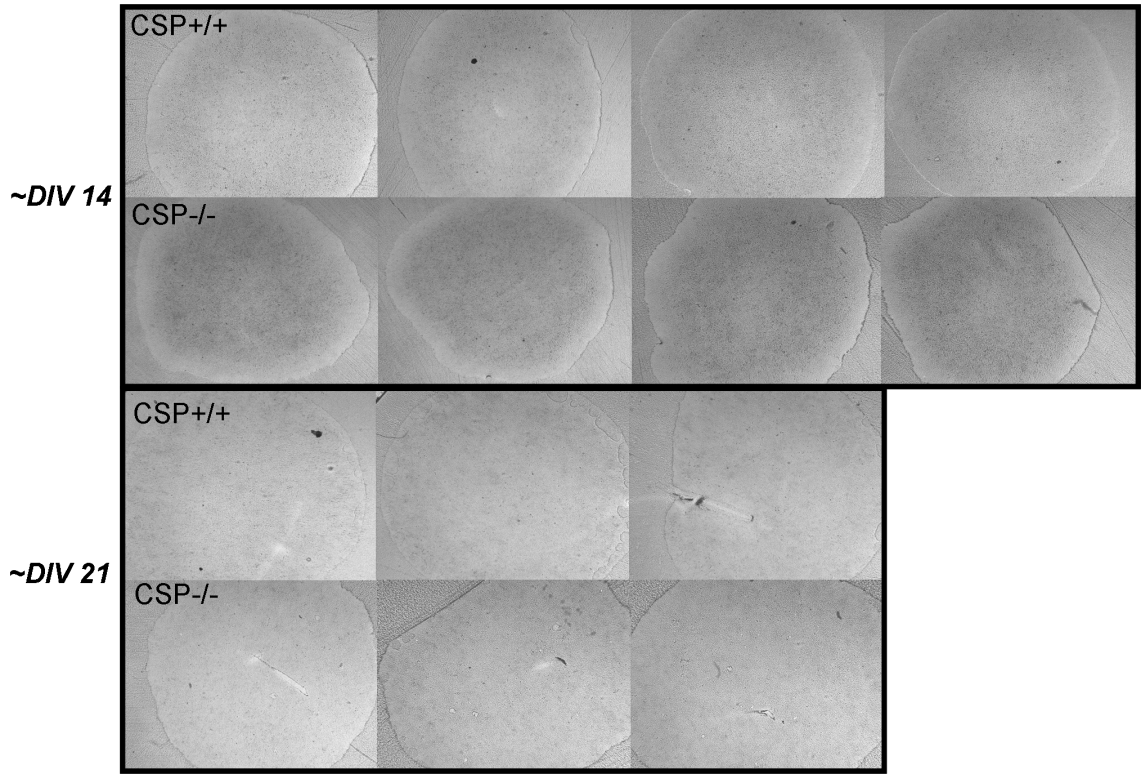

Figure 6.2: Representative bright field images of CSPα-/- and CSPα+/+ Hi-Spots
Bright field images of 2 and 3 week old Hi-Spot cultures. Hi-Spots made from CSPα-/- and CSPα+/+ tissue were viewed under bright field microscopy for signs of cell clumping and disaggregation, which was not observed. No difference between the CSPα-/- and CSPα+/+ Hi-Spots was observed. These images are representative of 5 sets of CSPα+/+ Hi-Spots and 5 sets of CSPα-/- Hi-Spots, in total ~100 Hi-Spots from each genotype.

To assess if the Hi-Spots made from CSPα-/- tissue could be distinguished from Hi-Spots made from CSPα+/+ tissue based on their gross morphology, CSPα-/- and CSPα+/+ Hi-Spots were viewed under a light microscope after *~DIV 14* and *~DIV 21*. Figure 6.2 shows representative images of *~DIV 14* and *~DIV 21* cultured Hi-Spots from CSPα-/- and CSPα+/+ tissue. The images are representative of ~100 Hi-Spots from each genotype from 5 different sets of dissociations.

Figure 6.2 shows that there were no gross morphological differences between the CSPα-/- and CSPα+/+ Hi-Spots, and that neither set of Hi-Spots showed evidence of cell clumping or disaggregation.

To determine if there was any gross differences in cell death between CSPα-/- and CSPα+/+ Hi-Spots, the Hi-Spots were tested for their PI fluorescence at a late stage in culture (*DIV 28*).

6.4.2 Are the CSPα-/- Hi-Spots dying?

PI fluorescence was shown in chapter 4 (Figure 4.10) to allow the differential cell death caused by increasing concentrations of glutamate to be distinguished in a dose dependent manner. Therefore we tested the Hi-Spots for their basal levels of cell death at *DIV 28* using incubation with PI and measuring PI fluorescence. *DIV 28* represents a late time point in the culture period where maximum differences in cell death would be expected to be observed in a progressively degenerating network based on the assumption that the CSPα-/- model represents a progressively degenerating phenotype (Fernandez-Chacon, Wolfel et al. 2004).

At *DIV 28* Hi-Spots from CSPα+/+ and CSP-/- mice did not show any difference in basal levels of cell death. Figure 6.3 shows images of CSPα+/+ and CSPα-/- Hi-Spots treated with PI. Figure 6.3 also shows a rat Hi-Spot from a separate experiment treated with sodium azide (4.5mM). Sodium azide treatment demonstrates the level of cell death observed due to a toxic insult and allows this to be compared to the cell death occurring in the CSPα+/+ and -/- Hi-Spots.

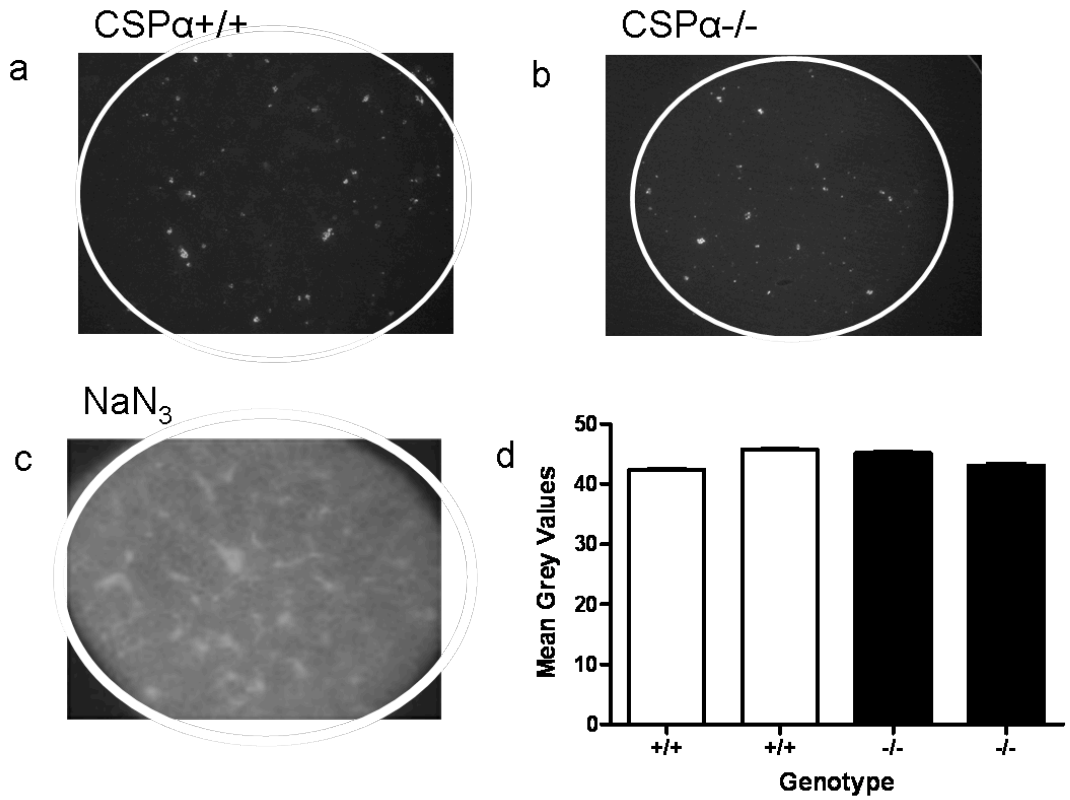

Figure 6.3: CSPα-/- and +/+ Hi-Spots have similarly low levels of cell death at *DIV 28*.

a) Representative pictures of PI fluorescence in a. CSPα+/+ Hi-Spot after over night incubation with of PI(3µl/ ml)..
b) Representative pictures of PI fluorescence in CSPα-/- Hi-Spot after overnight incubation with of PI.
c) Positive control showing high levels of cell death associated with sodium azide toxicity. Representative picture of a rat Hi-Spot from a separate experiment incubated with sodium azide for 2 hours. The Hi-Spot shows intense PI fluorescence associated with a high degree of cell death in the culture.
d) PI fluorescence quantified as mean grey values on Image J showing no difference in PI fluorescence between CSPα-/- and +/+ Hi-Spots

The PI experiment only addresses the level of cell death in the cultures and not the type of cells present or the type of cells dying. To test if the Hi-Spots produced from CSPα-/- cortical tissue contained neuronal cells that developed to form a neuronal network IHC labelling and confocal imaging were conducted. The Hi-Spots were assessed for the formation of a neuronal network using antibodies against β III Tubulin and for the formation of discrete presynaptic puncta using antibodies against synaptophysin.

6.4.3 CSPα-/- Hi-Spot develop a neuronal network

IHC analysis and confocal imaging revealed that both CSP α+/+ and CSP α -/- cultures formed a neuronal network containing immunohistochemical correlates of synaptic specialisations. IHC analysis shows dense distribution of the synaptophysin puncta consistent with a relatively dense arrangement of presynaptic specialisations. β III Tubulin labelling reveals that at *DIV 22* both CSP α-/- and CSP α+/+ Hi-Spots develop a neuronal network (Figure 6.4). Labelling the neuronal cells with an antibody to β III Tubulin allows visualisation of both the neuronal cell bodies and the processes. In both the *DIV 22* CSP α -/- and +/+ cultures β III Tubulin positive neuronal cell bodies are observed in groups surrounded by neuronal processes (Figure 6.4). Synaptophysin staining appears as discrete puncta and no obvious differences in the amount of presynaptic synaptophysin can be seen between the CSP α+/+ and -/- cultures. Figure 6.4e shows a higher magnification image of β III Tubulin and synaptophysin staining in a CSP α+/+ Hi-Spot.

Further IHC analysis on CSP α+/+ and CSP α-/- cultures revealed that the β III Tubulin staining appeared fragmented or very fine in some of the CSP α-/- Hi-Spots tested, however this staining profile was also observed in CSP α+/+ Hi-Spots at the same age (n=2 Hi-Spots tested CSP α +/+ and n=2 CSP α -/-, Figure 6.5).

Together these results show that Hi-Spots produced from CSP α-/- cortical tissue do not show gross morphological degeneration based on bright field images. This is reinforced in the PI exclusion experiment. Further IHC analysis at the cellular level provides evidence that the CSP α-/- Hi-Spots form a neuronal network comparable to the CSP α+/+ Hi-Spots. Previous work investigating the synaptic changes occurring in the CSPα-/- mice identified ultrastructural synaptic changes in the ribbon synapses of the photoreceptors (Schmitz, Tabares et al. 2006), the calyx of Held and the nmj (Fernandez-Chacon, Wolfel et al. 2004) by electron microscopy. To preliminarily assess if synaptic changes were occurring in the cortical synapses in the CSPα-/-, Hi-Spot cultures were processed from CSPα+/+ and CSPα-/- Hi-Spots for electron microscopy.

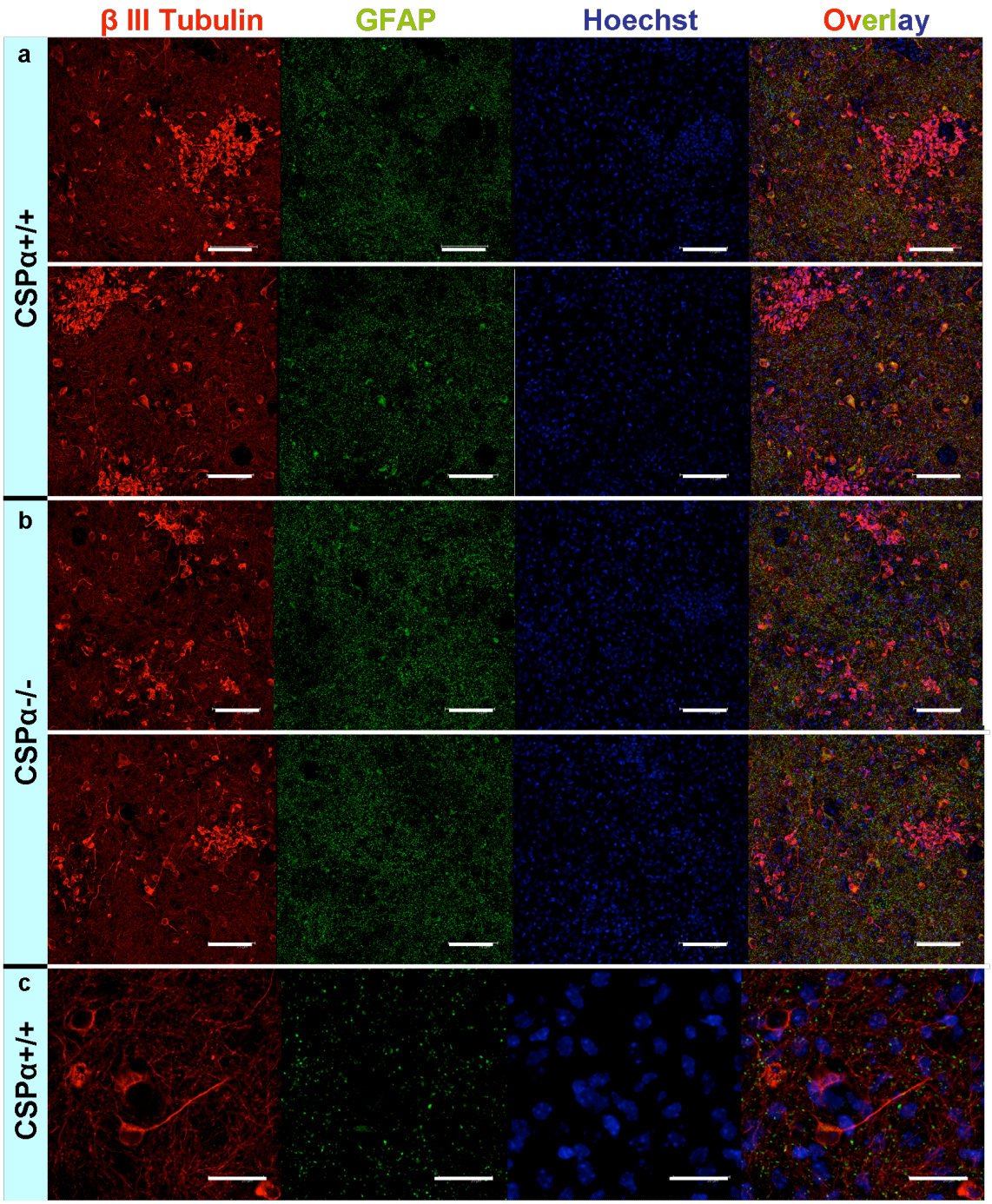

Figure 6.4: Overt signs of degeneration can not be seen in the CSPα-/- cultures using immunohistochemistry staining and confocal imaging

Confocal maximum projection images of a 12 z stack scan of CSPα+/+ and -/- cultures after 22 days in culture.

a) Hi-Spots produced from CSPα+/+ cortical tissue, presynaptic vesicle protein synaptophysin is shown in green and β III Tubulin staining in red and Hoechst stained cell bodies in blue. Scale Bars 75µm
b) Hi-Spots produced from CSPα-/- cortical tissue synaptophysin and β III Tubulin staining show a neuronal network surrounded by punctate synaptophysin staining. Evidence of blebbing and fragmenting neuronal processes are not observed. Scale Bars 75µm.
c) Higher magnification image of the β III Tubulin network in a CSPα+/+ Hi-Spot, Scale

Bar 20µm.

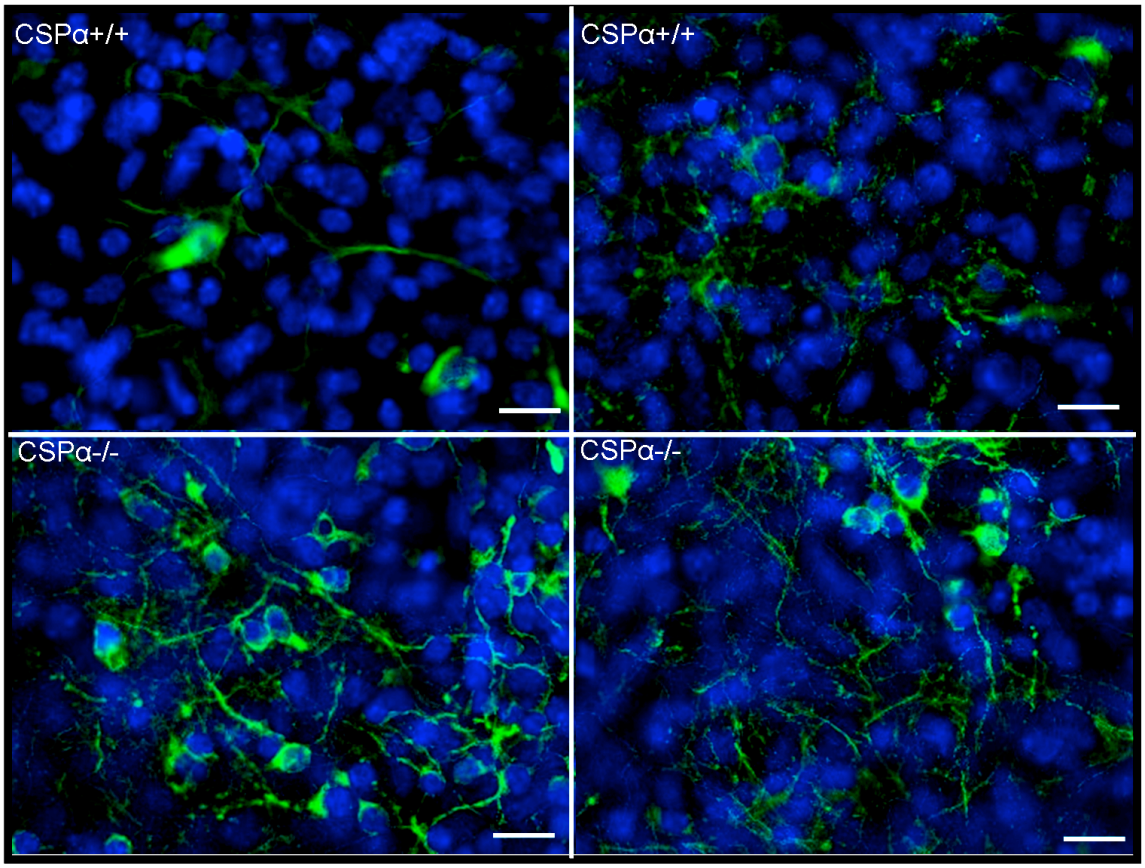

Figure 6.5: β Tubulin staining of CSPα+/+ and CSPα-/- Cultures.
Immunofluorescence of β III Tubulin in CSPα+/+ and CSPα-/- Hi-Spots at *DIV* 24. Hi-Spots from both genotypes demonstrated dense staining of Hoechst and β III Tubulin. Some cultures exhibited fragmented β III Tubulin staining but this was observed in both culture genotypes and not selective for CSPα-/- cultures. Scale bar 20µm.

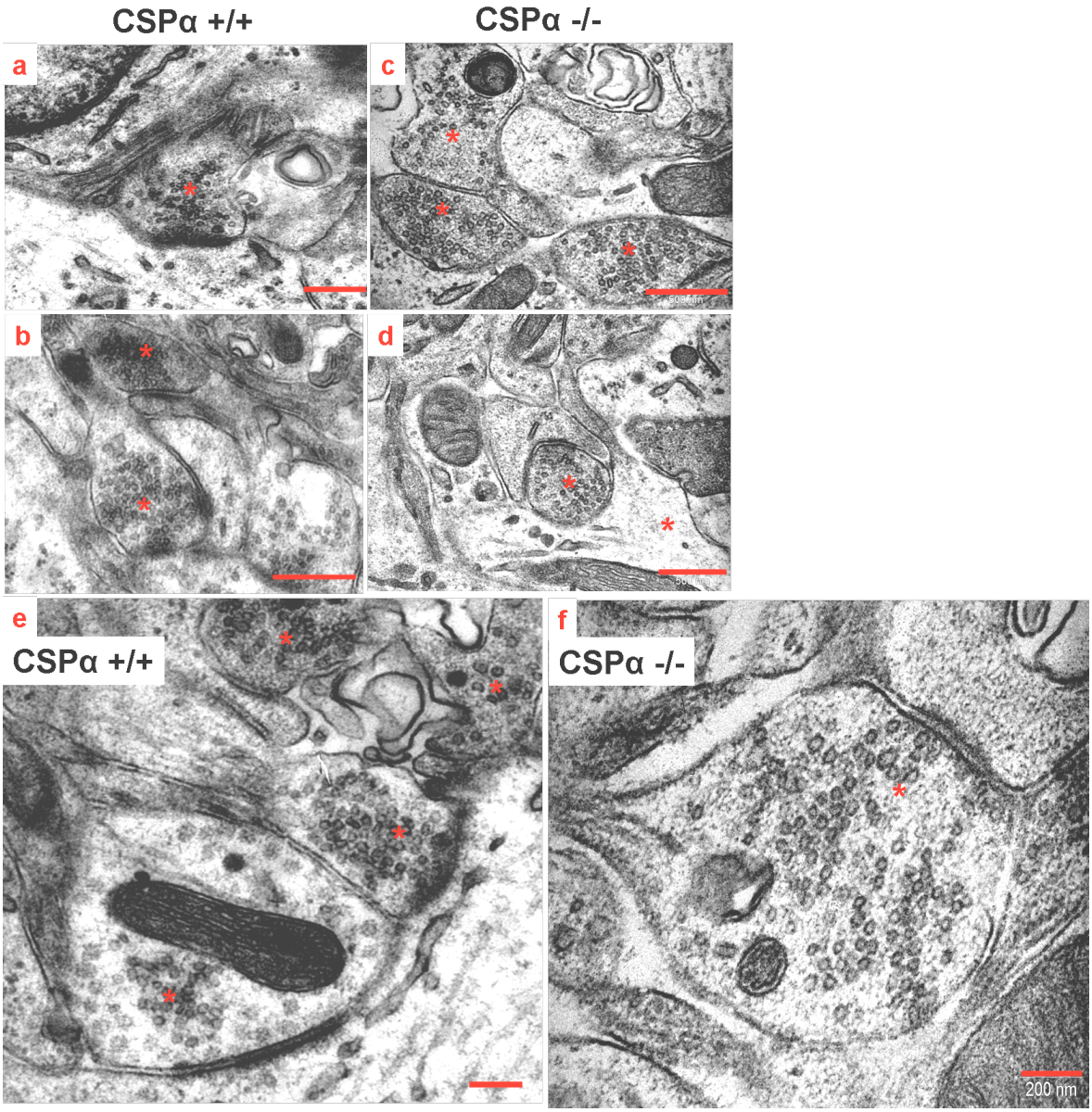

Figure 6.6: Electron microscopy of synapses from CSPα+/+ and CSPα-/- Hi-Spots
a,b- CSPα+/+ electron microscopy images of synapses, presynaptic specialisations containing vesicles are marked with a * and can be see opposing postsynaptic densities. c,d- CSPα-/- electron microscopy images of synapses, presynaptic specialisations (*) are opposed postsynaptic densities. The postsynaptic densities are darker in the CSPα+/+ sample because these sections were additionally stained with uranyl acetate (scale bars-500nm). e,f-higher magnification images of synapses from (e) CSPα+/+ (asymmetric synapses) (f) and CSPα-/- (symmetric synapse) Hi-Spots, CSPα+/+ Hi-Spot images appears with more contrast because of additional section staining with uranyl acetate. (Scale bar 200nm).

EM images of the synaptic ultrastructure of the CSPα-/- Hi-Spots reveals no overt signs of degeneration. Preliminary work was conducted on one section cut from CSPα-/- Hi-Spots and one CSPα+/+ section. The CSPα+/+ Hi-Spot images appear with more contrast because they underwent additional staining with uranyl acetate see section 2.13.

Figure 6.6 shows representative images of synapses from the CSPα+/+ and CSPα-/- sections. The calyx of Held synapse has been reported to undergo ultra-structural changes consistent with degeneration of the synapse, these include electron dense mitochondria, electron lucent spaces and widened synaptic clefts (Fernandez-Chacon, Wolfel et al. 2004). The ribbon synapse of the photoreceptors were described as containing fewer synaptic vesicles, electron dense aggregates in some terminals and as containing a higher number of coated synaptic vesicles (Schmitz, Tabares et al. 2006). None of these changes were apparent when 20 CSPα+/+ and 14 CSPα-/- synapses were viewed in our preliminary investigation of Hi-Spot cultures using electron microscopy.

6.4.4 MEA recordings reveal a bicuculline insensitivity in the CSP α-/- Hi-Spots

At the 2009 Biochemical society meeting Fernández Chacon presented data that suggested inhibitory synaptotagmin 2 positive cells were lost in hippocampal dissociated cultures from CSPα-/- mice, and that a specific subset of GABAergic neuronal cells degenerated. These were the fast spiking parvalbumin positive Basket cells. This work has since been published (Garcia-Junco-Clemente, Cantero et al. 2010). To investigate if changes in neuronal network could be identified between the CSPα-/- and CSPα+/+ Hi-Spots we conducted MEA recordings after 2 and 3 weeks of culture.

We decided to test the CSPα-/- Hi-Spots for differences in their bicuculline sensitivity. Bicuculline acts to relieve inhibition onto excitatory and inhibitory neuronal cells by blocking $GABA_A$ receptors (Nyiri, Freund et al. 2001; Klausberger, Roberts et al. 2002). Bicuculline has been shown to lead to measurable activity increases recorded on MEAs when tested in the rat Hi-Spot cultures (Figure 4.8) and in other *in vitro* dissociated cultures (Jimbo, Kawana et al. 2000).

A degeneration of GABAergic neurons would be expected to be followed by increased excitatory activity resulting in a higher level of basal spontaneous activity, with potential effects on network wide synchrony and oscillatory activity (Fuchs, Zivkovic et al. 2007). Additionally, if fast spiking GABAergic neurons degenerate leading to a change in the excitatory: inhibitory balance in the CSP α-/- Hi-Spots, the response to bicuculline would be expected to be decreased (Dahlhaus, Hines et al. 2010).

6.4.5 Analysis periods

To investigate the network changes occurring in the CSP α+/+ and CSP α -/- Hi-Spots were analysed for their spontaneous activity after two and three weeks of culture at approximately *~DIV 14* and *~DIV 21*. Hi-Spot basal activity was recorded for 300 seconds before 50µM of bicuculline was added and 300 seconds of activity was recorded after 900 seconds of incubation with the drug.

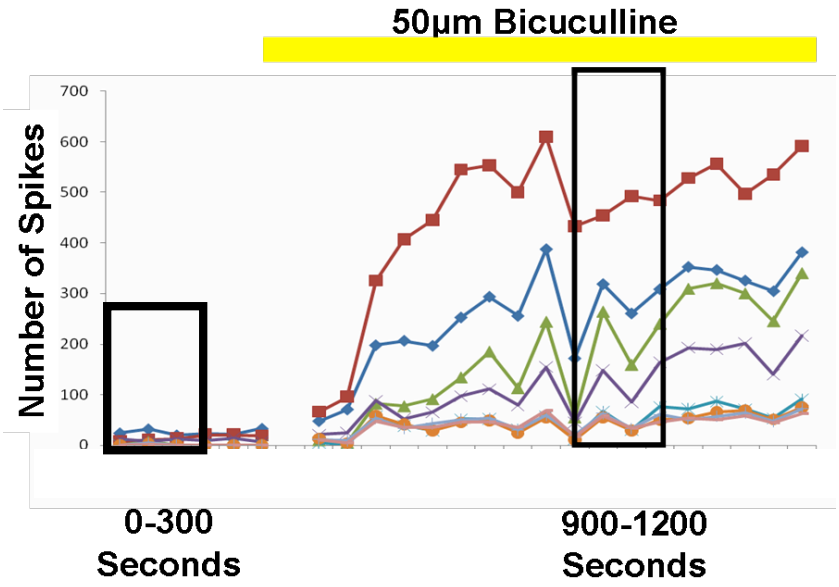

Figure 6.7:Multielectrode array sampling zones
The graph shows the increase in spike number from each of the 8 channels recorded, each colour represents a different recording electrode. For comparison of spontaneous activity between basal and bicuculline induced activity, 300 seconds of basal activity was compared against 300 seconds of bicuculline induced activity. The Hi-Spots were incubated with bicuculline for 900 seconds before the comparison analysis took place. A 900 second incubation period allowed the bicuculline to perfuse through the MEA pores and take effect across the Hi-Spot. After 900 seconds of incubation with bicuculline most Hi-Spots had reach a steady state of activity.

The time period between 900 and 1200 seconds was chosen because post analysis revealed that after a 900 second incubation with bicuculline the maximum increase in activity was observed and remained at a steady increased activity level in most cultures recorded. Figure 6.7 shows a graph of 300 seconds before bicuculline addition and the activity increase upon bicuculline addition. The data points on the graph are plotted as number of spikes/ 100 seconds (i.e 100 second bins). The period of 900-1200 seconds during the bicuculline addition is boxed showing the steady increased level of activity observed after a 900 second incubation with bicuculline.

6.4.6 Different activity profiles

Table 6.1 shows the different types of activity recorded from the CSPα+/+ and CSPα-/- Hi-Spots upon incubation with bicuculline. At ~*DIV 14* most of the CSPα+/+ Hi-Spots (60%) demonstrated an induction in action potential frequency, in which activity increased on each channel. Each recorded electrode did not show the same level of basal spontaneous activity or the same level of bicuculline induced activity, but a general theme was that electrodes recording from areas of higher basal activity consequently recorded high levels of bicuculline induced activity and vice versa. From the CSPα-/- Hi-Spots recorded, only 33% demonstrated an induction of activity upon bicuculline addition, and the majority of CSPα-/- Hi-Spots were qualitatively assessed to have no change in activity.

At the later time point of *DIV 21,* 67% of the CSPα+/+ Hi-Spots showed an induction in activity compared to 29% of the CSPα-/- Hi-Spots. Most of the CSPα-/- Hi-Spots were qualitatively assessed to not demonstrate an induction of activity upon bicuculline addition. This data shows that different electrodes recording from different areas in the Hi-Spots record different levels of activity, and that different Hi-Spots show different levels of basal activity, and different activity changes in response to bicuculline. To analyses the different basal and bicuculline induced activity levels the 300 seconds of basal activity and the 300 seconds of bicuculline induced activity (spike number and RMS value) were summed and plotted as a bar chart to allow average differences in activity levels to be assessed (Figure 6.8 spike number and Figure 6.9 RMS value).

	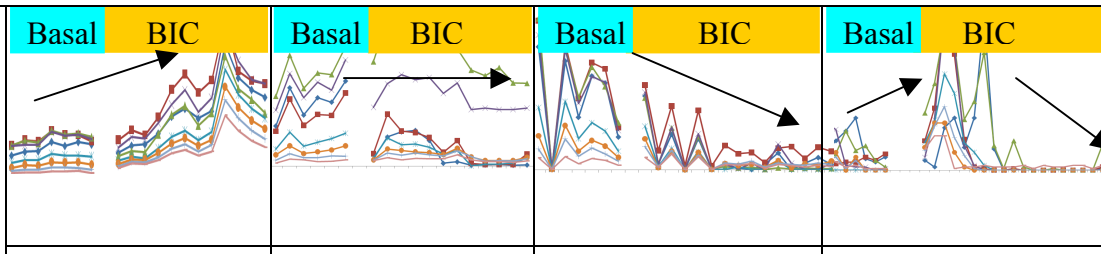			
	Induction of activity	**No induction**	**Decrease from basal**	**Induction followed by decrease**
DIV ~14 **CSPα+/+**	**58.8%**	**23.5%**	**5.8%**	**11.7%**
DIV ~14 **CSPα-/-**	**33.3%**	**40%**	**6.6%**	**20%**
DIV ~21 **CSPα+/+**	**66.6%**	**33.3%**	**-**	**-**
DIV ~21 **CSPα-/-**	**28.57%**	**66.6%**	**4.7%**	**-**

Table 6.1: Quantified qualitative changes in Hi-Spot action potential frequency upon bicuculline exposure
Hi-Spot activity from CSPα+/+ and CSPα-/- murine Hi-Spots could be classified under the broad titles of those that demonstrated induction in activity upon bicuculline addition, those that showed no change from basal activity, those that showed a decrease in activity, and those that demonstrated an early induction in activity which subsequently decreased. Representative graphs to illustrate different activities are in the top row of the table. Basal activity is shown on the left of the graph, marked by a blue bar, and the yellow bar marks bicuculline incubation. Each recording channel on the MEA is shown in a different colour for each trace.
Quantified below the graphs are the number of Hi-Spots which demonstrated these behaviours, red corresponds to **CSPα+/+ Hi-Spots** and green to **CSPα-/- Hi-Spots**. **Basal**, **Bicuculline induced**. *DIV 14* CSPα +/+ n=14, *DIV 14* CSPα-/- n=15, *DIV 21* CSPα+/+ n=15, *DIV 21* CSPα-/- n=21.

6.4.7 Spike number changes CSPα+/+ and CSP-/- Hi-Spots after bicuculline addition

Figure 6.8 shows the spike frequency activity changes in CSPα-/- and CSPα+/+ Hi-Spots after bicuculline addition. The graph shows the number of spikes counted during 300 seconds of basal activity and 300 seconds (900-1200 seconds) of activity after bicuculline addition. Hi-Spots that demonstrated a 2 fold or more increase in spike number after bicuculline addition are red, those that decreased by 2 fold or more are blue and those that showed less than a 2 fold change either positively or negatively are green.

Hi-Spots produced from CSPα+/+ mice at *DIV 14* displayed an average basal activity of 160 spikes/300 seconds (thus approx 0.5Hz) which on average increased to 485 spikes/ 300

seconds (1.6Hz) upon bicuculline addition. The degree of increased activity from basal to bicuculline induced was not uniform for each culture, but the majority of cultures demonstrated a 2 fold or more increase in spike number (Figure 6.8 red lines). In general Hi-Spots that demonstrated higher basal activity levels also demonstrated higher spike numbers after bicuculline addition.

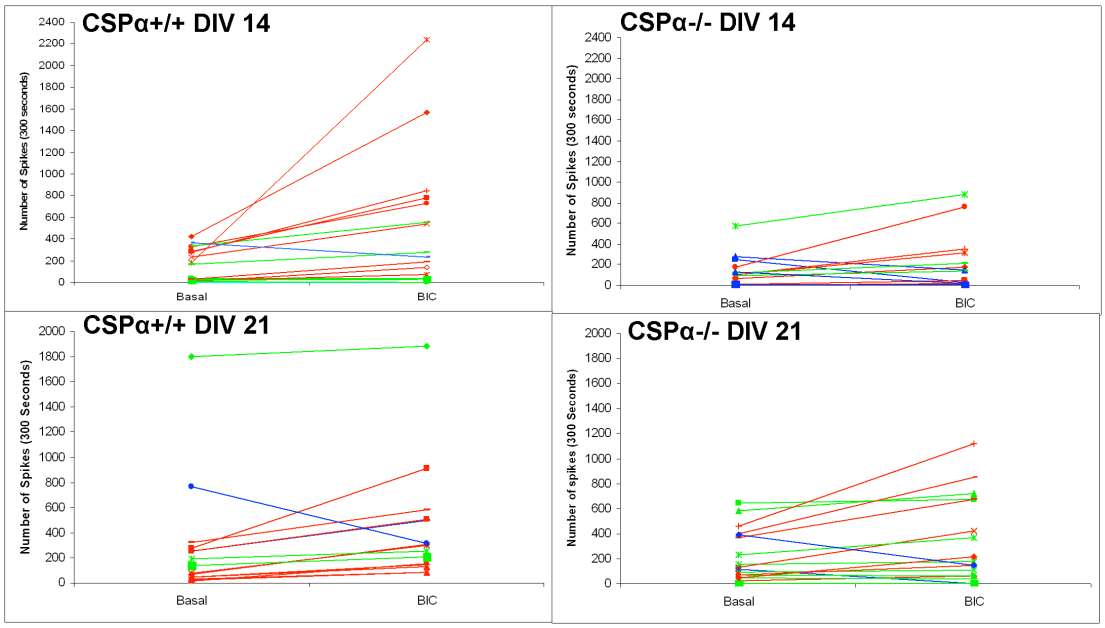

Figure 6.8: Spike number changes after bicuculline addition in CSPα-/- and CSP+/+ Hi-Spots
The graphs show the activity level changes after bicuculline addition in CSPα+/+ and CSPα-/- Hi-Spots after *DIV 14* and *DIV 21*. Each of the lines on the graphs represents one Hi-Spot. Lines that are marked in red show activity increases that are more than or equal to two fold increases in activity. Blue lines show Hi-Spots that demonstrated a two fold or more decrease in spike number after bicuculline addition. Green lines show Hi-Spots that demonstrated a less than two fold increase or decrease in spike number.

Hi-Spots produced from CSPα-/- mice at *DIV 14* demonstrated an average basal activity level of 127 spike/ 300 seconds (0.4Hz), which on average increased to 206 spikes/ 300 seconds (0.69Hz) after bicuculline addition. The range of basal activity between the Hi-Spots is comparable to that of CSPα+/+ Hi-Spots and both Hi-Spot genotypes displayed similar levels of average basal activity (~0.5Hz) (Figure 6.8). However, CSPα-/- Hi-Spots did not show comparable increase in activity on stimulation with bicuculline and less than half of the Hi-Spots recorded displayed a 2 fold or more increases in spike number. Furthermore, more of the CSPα-/- Hi-Spots displayed a decrease in spike number recorded after 900 seconds of bicuculline addition (Figure 6.8) (blue lines).

At *DIV 21* the CSPα+/+ Hi-Spots displayed an average basal activity of 288 spikes/ 300 seconds (0.96Hz) which increased to an average of 423 spikes/ 300 seconds (1.4Hz) upon bicuculline addition. The CSPα-/- cultures displayed an average basal activity of 200 spikes/ 300 seconds (0.7Hz), which increased to 304 spikes/ 300 seconds (1Hz) upon bicuculline addition. Figure 6.8 shows that more CSPα+/+ Hi-Spots (11/15, 73%) displayed 2 fold or more increase in activity upon bicuculline addition at *DIV 21* than CSPα-/- Hi-Spots (6/19, 32%). The majority of CSPα-/- Hi-Spots demonstrated less than a 2 fold increase or decrease in activity (Figure 6.8) (green lines).

6.4.8 RMS value changes in CSPα+/+ and CSP-/- Hi-Spots upon bicuculline addition

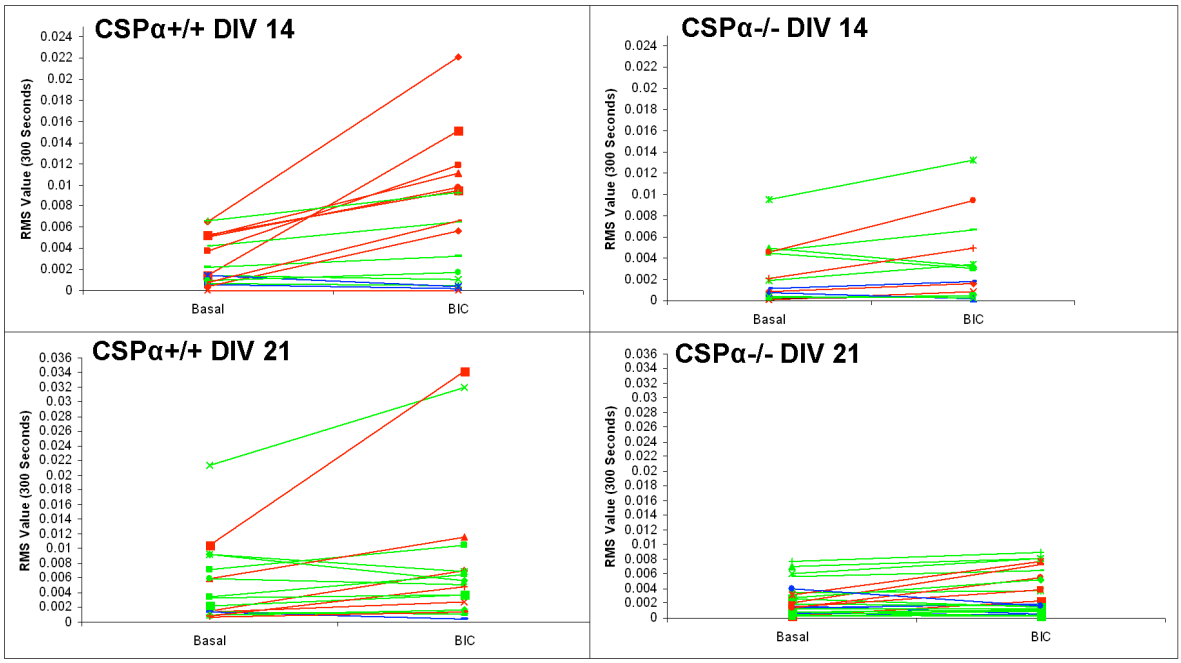

Figure 6.9: RMS value changes after bicuculline addition in CSPα-/- and CSP+/+ Hi-Spots
The graphs show the activity level changes after bicuculline addition in CSPα+/+ and CSPα-/- Hi-Spots after *DIV* 14 and *DIV* 21. Each of the lines on the graphs represents one

Hi-Spot. Lines that are marked in red show activity increases that are more than or equal to two fold increases in activity. Blue lines show Hi-Spots that demonstrated a two fold or more decrease in RMS value after bicuculline addition. Green lines show Hi-Spots that demonstrated a less than two fold increase or decrease in RMS value.

Similar results to those described for the spike number changes were obtained when the data was analysed for RMS, with Hi-Spots displaying higher basal RMS value demonstrating higher values after bicuculline addition (Figure 6.9). Most of the *DIV 14* CSPα+/+ Hi-Spots demonstrated a 2 fold or more increased RMS value after bicuculline addition, where as only 1/3 of the CSPα-/- Hi-Spots demonstrated a 2 fold or more increased RMS value upon bicuculline addition, and the majority showed a less than 2 fold increase or decrease in activity (Figure 6.9 green lines).

At *DIV 21* the average RMS value for 300 seconds of recorded basal activity was higher in CSPα+/+ (0.0047) compared to CSPα-/- (0.0024) Hi-Spots. Figure 6.9 shows that 2/19 of the CSPα+/+ Hi-Spots recorded displayed a much higher basal RMS value. With the basal activity from these two Hi-Spots removed CSPα+/+ Hi-Spots still displayed a higher average RMS value (0.0334) than CSPα-/- cultures. Upon addition of bicuculline the RMS value in CSPα+/+ Hi-Spots increased to 0.0076 (0.0047- with the two highly active Hi-Spots removed), demonstrating a higher RMS value than that recorded from CSPα-/- Hi-Spot (0.0033) (Figure 6.9).

To assess the activity difference between the CSPα+/+ and CSPα-/- Hi-Spots, the data from the basal and bicuculline induced analysis periods from each CSPα+/+ Hi-Spot from each channel were pooled, and plotted against the pooled data from the CSPα-/- Hi-Spots.

6.4.9 Pooled MEA data from CSPα+/+ and CSPα-/- Hi-Spots

The summed data from different genotypes shows that at *DIV 14* there was no clear difference between basal activity levels in terms of both spike number and RMS value between CSPα+/+ and CSPα-/- Hi-Spots (Figure 6.10). However, at ~*DIV 14* CSPα +/+ cultures demonstrated a significant increase in spike number (P=0.0218) and RMS (P=0.0087) value after bicuculline addition (Figure 6.10). This indicates an induction in activity when inhibition is relieved. CSPα -/- Hi-Spots conversely, did not show a significant increase in spike number or RMS value following application of bicuculline.

Furthermore, bicuculline induced RMS activity was shown to be significantly higher in CSPα +/+ Hi-Spots compared to CSPα-/- Hi-Spots at *DIV 14* (P=0.0377) (Figure 6.10).

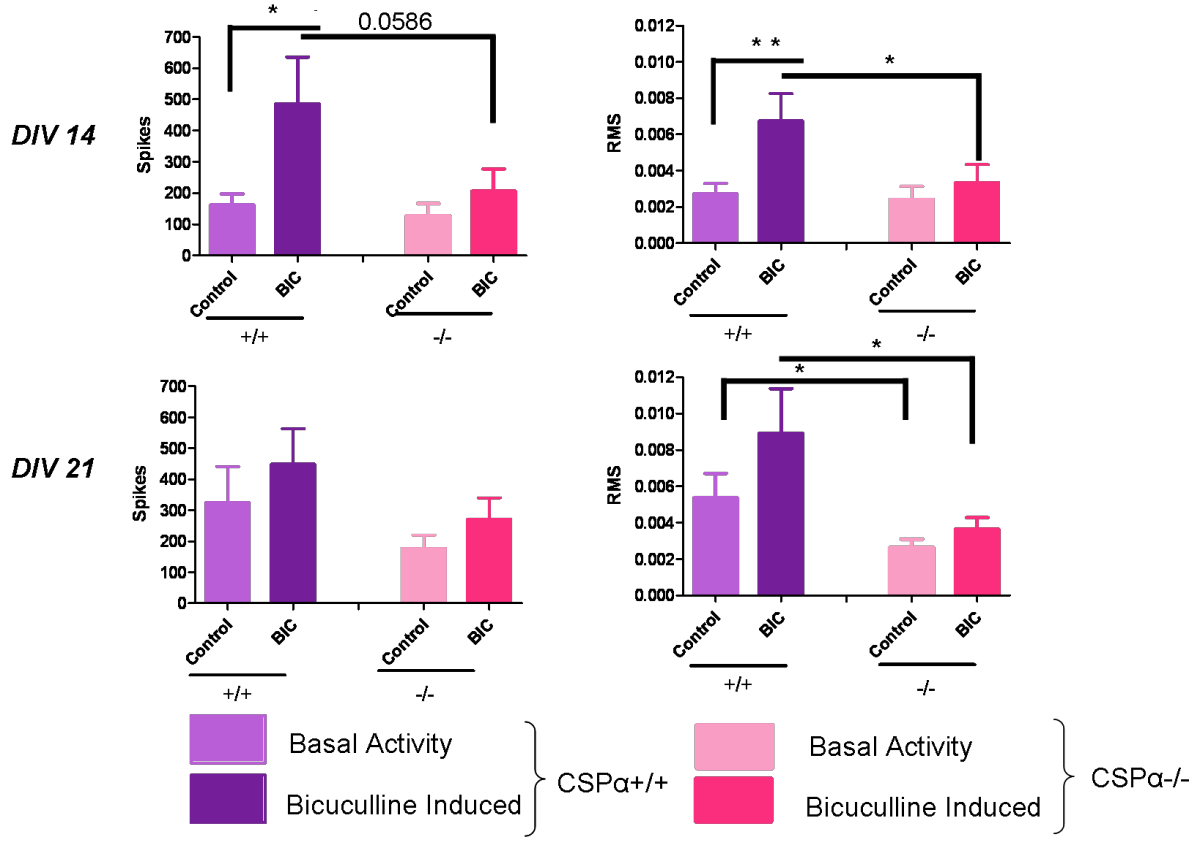

Figure 6.10: Multielectrode array analysis reveals a functional deficit in the CSPα-/- Hi-Spots.
Multielectrode array recordings from CSPα+/+ and CSPα-/- cultures of basal spontaneous activity and activity induced on bicuculline addition. Left column shows spike numbers, right column shows RMS values. CSPα+/+ Hi-Spots show increased activity levels on addition of bicuculline which is not matched by the CSPα-/- Hi-Spots.
DIV 14 spikes CSPα+/+ control v's bicuculline P=0.0218, RMS CSPα+/+ control v's bicuculline P=0.0087, CSPα+/+ bicuculline v's CSPα-/- bicuculline P= 0.0377
DIV 21 RMS CSPα+/+ Control v's CSPα-/- Control P= 0.0192, CSPα+/+ bicuculline v's CSPα-/- bicuculline P= 0.0117. Stats: unpaired one tailed t test 95% confidence, error bars SEM, *=P=<0.05

At ~*DIV 21* there are three notable differences. Firstly, the CSPα+/+ Hi-Spots demonstrated a significantly higher level of basal RMS activity compared to the CSPα-/- Hi-Spots (P=0.0192) (Figure 6.10). Secondly, the CSPα+/+ Hi-Spots did not demonstrate a significant increase in activity upon bicuculline addition. Thirdly, the bicuculline induced activity although not significantly increased from the level of basal RMS activity in

CSPα+/+ Hi-Spots was significantly higher than that recorded in CSPα-/- Hi-Spots (P=0.0117) (Figure 6.10).

Figure 6.11 shows the pooled data displayed to demonstrate the developmental increase in basal spontaneous activity from *DIV 14* to *DIV 21* in the CSPα+/+ Hi-Spots (light purple bars). Figure 6.11 shows that between *DIV 14* and *DIV 21* the CSPα+/+ Hi-Spots demonstrated no developmental difference in the bicuculline induced activity (dark purple bars). The CSPα-/- Hi-Spots did not demonstrate a developmental increase in their basal activity (light pink bars), and the activity level recorded after bicuculline addition does not show an induction from basal activity, instead the activity remains at approximately the same level (dark pink bars).

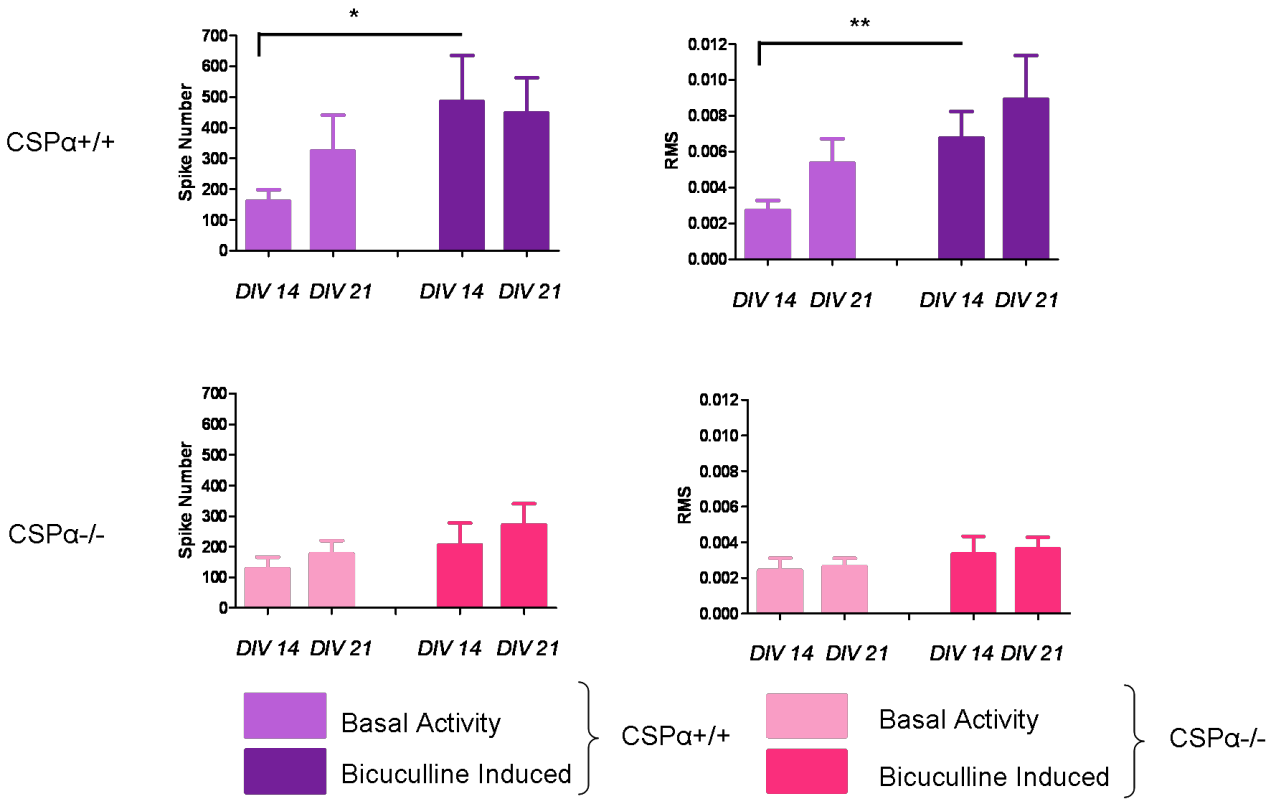

Figure 6.11: CSPα+/+ Hi-Spots show a developmental increase in basal spontaneous activity Multielectrode array recordings from CSPα+/+ and CSPα-/- Hi-Spots after 2 and 3 weeks in culture. Left column shows spike numbers, right column shows RMS values. CSPα+/+ Hi-Spots show a developmental increase in basal spontaneous activity demonstrated by an increase in spike and RMS value. CSPα+/+ Hi-Spots also show an induction in activity upon bicuculline addition. CSPα-/- Hi-Spots show the same level of basal spontaneous network activity after 2 and 3 weeks of culture and after incubation with bicuculline. This result is consistent with the CSPα-/- Hi-Spot activity being held at a set level. CSPα+/+ *DIV 14* Spike basal v's bicuculline added P=0.0218, CSPα+/+ *DIV 14* RMS basal v's bicuculline added P= 0.0192.

6.5 Discussion

6.5.1 No overt degeneration in the CSPα-/- Hi-Spots

The main findings from this investigation were firstly that no overt degeneration could be observed in the CSPα-/- cultures compared to the CSPα+/+ Hi-Spots. This was based on gross morphology assessed using bright field microscopy (Figure 6.2), and gross cell death assessed by PI exclusion from the culture cells (Figure 6.3). More detailed investigation of the neuronal network in the CSPα+/+ and CSPα-/- Hi-Spots demonstrated that both genotypes showed comparative levels of β III Tubulin and synaptophysin staining, the latter organised into discrete puncta. In both cases neuronal cell bodies appeared in groups surrounded by β III Tubulin positive neuronal processes and presynaptic synaptophysin staining (Figure 6.4).

Preliminary investigations of the ultrastructure of synapses in the CSPα+/+ and CSPα-/- Hi-Spots also revealed no overt synaptic differences or signs of degeneration in the CSPα-/- Hi-Spots, based on visual inspection of the synapses (Figure 6.6). However, a more systematic study would be required to compare the two genotypes properly. A comparison of differences in the synaptic vesicle type (coated/ uncoated), number, and distribution would be useful (Schmitz, Tabares et al. 2006). Furthermore, because of the recently published work showing that fast spiking parvalbumin positive interneurons are selectively affected in the CSPα-/- hippocampal cultures and brains (Garcia-Junco-Clemente, Cantero et al. 2010) a detailed analysis of the symmetric and asymmetric synapses (Carlin, Grab et al. 1980) in the Hi-Spots cultures would be informative to assess if the ratio between inhibitory and excitatory synapses.

A preliminary investigation of the degenerative changes in the CSPα-/- synapses *in vivo* was conducted by electron microscopy examination of synapses in the CA1 Stratum Radiatum from P28 CSPα-/- mice (Figure 6.12). Figure 6.12 shows presynaptic specialisations containing synaptic vesicles opposing electron dense postsynaptic densities in Stratum Radiatum synapses from a CSPα-/- mouse. The types of degenerative changes associated with the calyx of Held and photoreceptor were not observed (Fernandez-Chacon, Wolfel et al. 2004; Schmitz, Tabares et al. 2006). However, the emergence of selective degeneration in CSPα deficient mice suggests that regions replete in inhibitory innervations should be investigated.

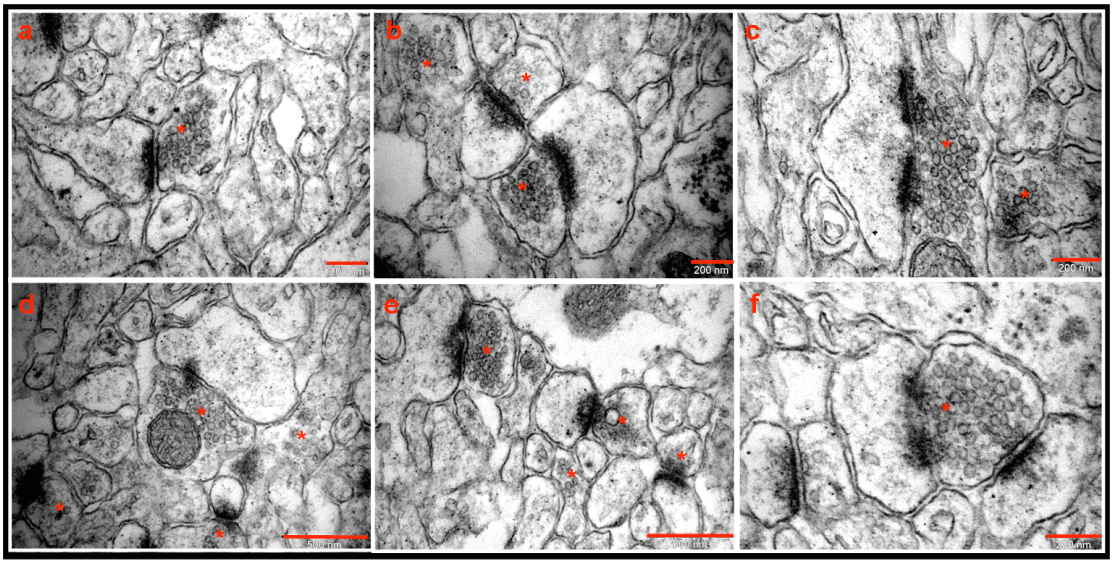

Figure 6.12: Electron Microscopy of CA1 stratum Radiatum synapses from a P28 CSPα-/- mouse

The images show the ultrastructure of Stratum Radium synapses. Synapses observed have presynaptic specialisations containing synaptic vesicles (~50nm) opposing the postsynaptic specialisation containing an electron dense postsynaptic density. The presynaptic sites are marked with a *. Overt signs of degeneration are not observed. Images a, b, c, f scale bar- 200nm, and d, e, scale bar-500nm.

Parvalbumin positive basket cell interneurons send their axonal projections to the pyramidal cell soma and to proximal dendrites to form perisomatic synapses (Figure 1.2). The parvalbumin positive neurons do not innervate the pyramidal cells in the Stratum Radiatum. The lack of degenerative changes in these asymmetric synapses further supports the absence of degeneration in glutamatergic pyramidal synapses (Garcia-Junco-Clemente, Cantero et al. 2010). Future work will assess if degenerating symmetric perisomatic synapses can be observed.

6.5.2 CSPα+/+ Hi-Spots show a developmental increase in spontaneous activity

CSPα+/+ Hi-Spots show a developmental increase in spontaneous activity between *DIV 14* to *DIV 21* (Figure 6.11), from ~150 Spikes/ 300 seconds to ~350 spikes/ 300 seconds. This developmental increase in activity is not observed in the CSPα-/- Hi-Spots. The increase in basal spontaneous activity in *DIV 21* CSPα+/+ cultures could be due to; a developmental increase in the number of synapses in the culture. Synapse number has been shown to correlate with the level of spontaneous activity (Kamioka, Maeda et al. 1996). Alternatively, because activity has been shown to increase upon inhibition of the GABAergic neuronal network (Figure 4.8) the activity could increase due to an age dependent loss of GABAergic neurons in the culture. Selective loss of GABAergic neurons during culture development has been reported, but was not shown to occur until week 11 *in vitro* (Li, Zhou et al. 2007). Additionally, the increased basal activity could be due to a developmental increase in the ratio of glutamatergic to GABAergic neurons.

Upon bicuculline addition the *DIV 21* CSPα+/+ Hi-Spots demonstrated induced activity levels but it was not significant (Figure 6.10). The spike number recorded upon bicuculline induction is approximately the same at both *DIV 14* and *DIV 21* (Figure 6.11), suggesting that the activity level induced by bicuculline did not change during development. Therefore, the data suggests that at *DIV 21* there has been a developmental increase in the ratio of glutamatergic to GABAergic synapses leading to a higher level of basal activity. Lack of induction upon bicuculline addition in cultures with high levels of basal activity has also been observed in hippocampal neurons over-expressing neuroligin 1, and was correlated with an increase in the number of excitatory synapses and increased basal excitatory activity. Therefore because there was a greater excitatory input removing the

inhibition had less of an effect (Dahlhaus, Hines et al. 2010). This further supports the idea that the increased basal activity level between *DIV 14* and *DIV 21* is due to an increase in the ratio of glutamatergic to GABAergic synapses in the Hi-Spots.

At *DIV 21* CSPα-/- Hi-Spots demonstrated a significantly reduced basal RMS level compared to that observed in the CSPα+/+ Hi-Spots (Figure 6.10). This could be due to a loss of neuronal cells in the CSPα-/- Hi-Spots; however, this is not supported by the electron microscopy, immunohistochemisty or PI data which show no overt degeneration in the CSPα-/- Hi-Spots. Furthermore, figure 6.11 shows that between *DIV 14* and *DIV 21* the level of basal activity remains constant; this is consistent with the data that shows no overt degeneration in the cultures, because activity has not decreased, and that the cultures network activity maybe being maintained at a set level. This could be by a homeostatic plasticity mechanism, as suggested by Garcia et al (2010) (Garcia-Junco-Clemente, Cantero et al. 2010). This would prevent excitotoxic cell death in response to degenerating inhibitory cells and be consistent with the lack of neuronal death in the CSPα-/- Hi-Spots and stratum radiatum synapses (Figure 6.3, 6.4, 6.6, 6.12).

6.5.3 Why doesn't each electrode record the same amount of activity?

Figure 6.7 shows a graph of the activity recorded during basal activity and during bicuculline incubation, each channel is shown as a different colour. Figure 6.7 shows that each electrode is recording different levels of basal activity, this is likely to be due to the non-uniform distribution of neuronal cells in the Hi-Spots. Figure 6.4 shows that the neuronal cells tend to group together to form small clusters, and because the electrodes are 250μm apart it is likely that different electrodes are recording from different clusters of neurons, which could be more or less active, or contain more or less neurons.

Upon addition of bicuculline, electrodes which recorded higher levels of basal activity recorded the highest levels of induced activity. This relationship between the basal activity and the bicuculline induced was routinely seen, and fits with the idea that areas recording higher activity may contain more neuronal cells or more active cells.

6.5.4 Why don't Hi-Spots at the same age from the same genotype show exactly the same activity profile?

Table 6.1 shows the different activity profiles recorded upon bicuculline incubation with the cultures. Most CSPα+/+ cultures demonstrated the expected increase in activity which reached a plateau at a higher sustained level. A small population demonstrated no increase in activity or a decreased level of activity upon bicuculline incubation, or an initial increase in activity followed by a decrease.

There are not obvious criteria that can predict from the level of basal activity whether a Hi-Spot will show an induction of activity upon bicuculline addition. Some Hi-Spots that did not show an induction had relatively high levels of basal activity and subsequently showed no induction, others demonstrated relatively low levels of basal activity which remained low. The criteria that relate to whether a network will be more or less active, or be more or less inducible with bicuculline are likely to be related to network formation, and how the excitatory and inhibitory cells interact, and the ratios of excitatory and inhibitory cells in the network. Previous work has shown that the level of activity recorded on MEAs is related to synapse number, the cell densities and the maturation of the network (Muramoto, Ichikawa et al. 1993; Wagenaar, Pine et al. 2006), and that even when these things are carefully controlled, different MEA activity is recorded from different cultures (Wagenaar, Pine et al. 2006).

6.5.5 Selective degeneration evidenced in Hi-Spots

Investigations into the neuronal degeneration occurring in the CSPα-/- mice have so far shown that four different types of neuron are degenerating. These are the calyx of Held synapses, the nmj, the ribbon synapses of the photoreceptors, and the parvalbumin positive interneurons (Fernandez-Chacon, Wolfel et al. 2004; Schmitz, Tabares et al. 2006; Garcia-Junco-Clemente, Cantero et al. 2010). The calyx of Held synapses and the parvalbumin positive interneurons represent fast firing neuronal cells (firing at >~100Hz), the nmj and ribbon synapses in the rod and cone photoreceptors represent tonically active synapses. All of these neuronal types are highly active compared to principal glutamatergic neurons (Csicsvari, Hirase et al. 1999), and thus have a higher rate of activity dependent vesicle exocytosis, vesicle and plasma membrane fusion, and vesicle endocytosis and replenishment.

Vesicle endocytosis is critical for the synapses to maintain multiple bouts of activity dependent exocytosis. For example, the ribbon synapses of the cone photoreceptors tonically release neurotransmitter in the dark at an unusually high rate allowing small changes in light intensity to generate significant changes in neurotransmitter release. For this to be achievable the synapse must maintain a continuous cycle of both exocytosis and endocytosis (Rieke and Schwartz 1996).

Our data fits well with the selective degeneration of highly active neuronal cells; firstly, because of the lack of overt degeneration in the Hi-Spot cultures, demonstrating that neuronal cells are not degenerating en masse, and secondly, because MEA recordings reveal a deficient induction in network activity in the CSPα-/- Hi-Spots upon application of the $GABA_A$ receptor antagonist bicuculline.

6.5.6 MEA recordings reveal a network activity difference between CSPα+/+ and CSPα-/- Hi-spots

Using the MEA recordings we have shown that at *DIV 14* CSPα-/- Hi-Spots have a similar level of basal spontaneous activity compared to the CSPα+/+ Hi-Spots. This suggests that at *DIV 14* both the CSPα+/+ and CSPα-/- Hi-Spots have the same level of network activity, and that both networks are being regulated by comparable excitatory and inhibitory activity.

Considering the implicated GABAergic neuronal dysfunction in the CSPα-/- mice (Garcia-Junco-Clemente, Cantero et al. 2010) we tested the CSPα-/- Hi-Spots for bicuculline induced activity. $GABA_A$ receptors are expressed on both excitatory and inhibitory neuronal cells (Nyiri, Freund et al. 2001; Klausberger, Roberts et al. 2002), therefore inhibition of $GABA_A$ receptors will block inhibition onto both excitatory and inhibitory neurons. $GABA_A$ receptor antagonism in the *DIV 14* CSPα+/+ Hi-Spots led to a significant induction in activity in terms of both spike number ($P= 0.0218$) and RMS ($P= 0.0087$). This induction was not matched by the CSPα-/- Hi-Spots which demonstrated no increase in activity in terms of spike number or RMS. Furthermore, the CSPα+/+ Hi-Spots demonstrated a significantly higher RMS value ($P=0.00377$) after bicuculline addition compared to bicuculline induced CSPα-/- Hi-Spots (Figure 6.11).

Release from inhibition would liberate not only excitatory neuronal cells but also inhibitory neuronal cells including any fast spiking parvalbumin positive neurons in the culture. Therefore, the increase in spike number in the CSPα+/+ Hi-Spots could be due to an increase in activity of the faster spiking cells as well as a general increase in activity of all cells in the network. The lack of bicuculline induced activity in the CSPα-/- Hi-Spots may reflect a deficit in the neuronal cells capable of high frequency firing in the CSPα-/- Hi-Spots. This could be because these cells are absent due to disappearance through degeneration, alternatively the CSPα deficit may mean that these cells although existing in the CSPα-/- culture are not capable of higher frequency firing because of the increased stress associated with sustained high activity in the absence of CSPα.

To assess if loss of the parvalbumin positive interneurons in the CSPα-/- Hi-Spots is the cause of the network deficient bicuculline effect, murine Hi-Spots would need to be assessed for their expression of parvalbumin to evaluate the contribution of parvalbumin positive interneurons to the network, and to assess if their number is decreased or absent as observed for hippocampal cultures (Garcia-Junco-Clemente, Cantero et al. 2010) compared to that in CSPα+/+ cultures.

Preliminary analysis of the hippocampus in P28 mice revealed a deficiency in parvalbumin positive interneurons in the CSPα-/- mice compared to CSPα+/+ mice (Figure 6.13). This supports the findings of Garcia-Junco-Clemente et al (2010) who also detected a loss of parvalbumin positive neurons in the dentate gyrus and CA1 of CSPα-/- mice (Garcia-Junco-Clemente, Cantero et al. 2010). Figure 6.13 shows that in all hippocampal regions; dentate gyrus, CA3, CA2, and CA1, there were less parvalbumin stained neuronal cell bodies and neuronal processes in the CSPα-/- mice. Furthermore, because the majority of parvalbumin positive cells are fast spiking cells (basket and axo-axonic (chandelier) cells) (Galarreta and Hestrin 2002) we interpret these preliminary results to suggest a degeneration of the fast spiking parvalbumin positive neuronal cells in CSPα-/- mice.

Furthermore, the reduction in parvalbumin positive neurons is not accompanied by a loss of cells in the pyramidal cell layer. The DAPI staining in figure 6.13 shows that the pyramidal cell layers in the dentate gyrus, CA3, CA2 and CA1 are comparable in the CSPα+/+ and CSPα-/- mice. Overt degeneration of the hippocampus in Prion disease is

associated with thinning of the pyramidal cell layer after loss of their asymmetric synapses (Cunningham, Deacon et al. 2003), this is not seen in the CSPα-/- mice at P28 supporting a selective loss of a subtype of neuronal cells and not global degeneration (Garcia-Junco-Clemente, Cantero et al. 2010).

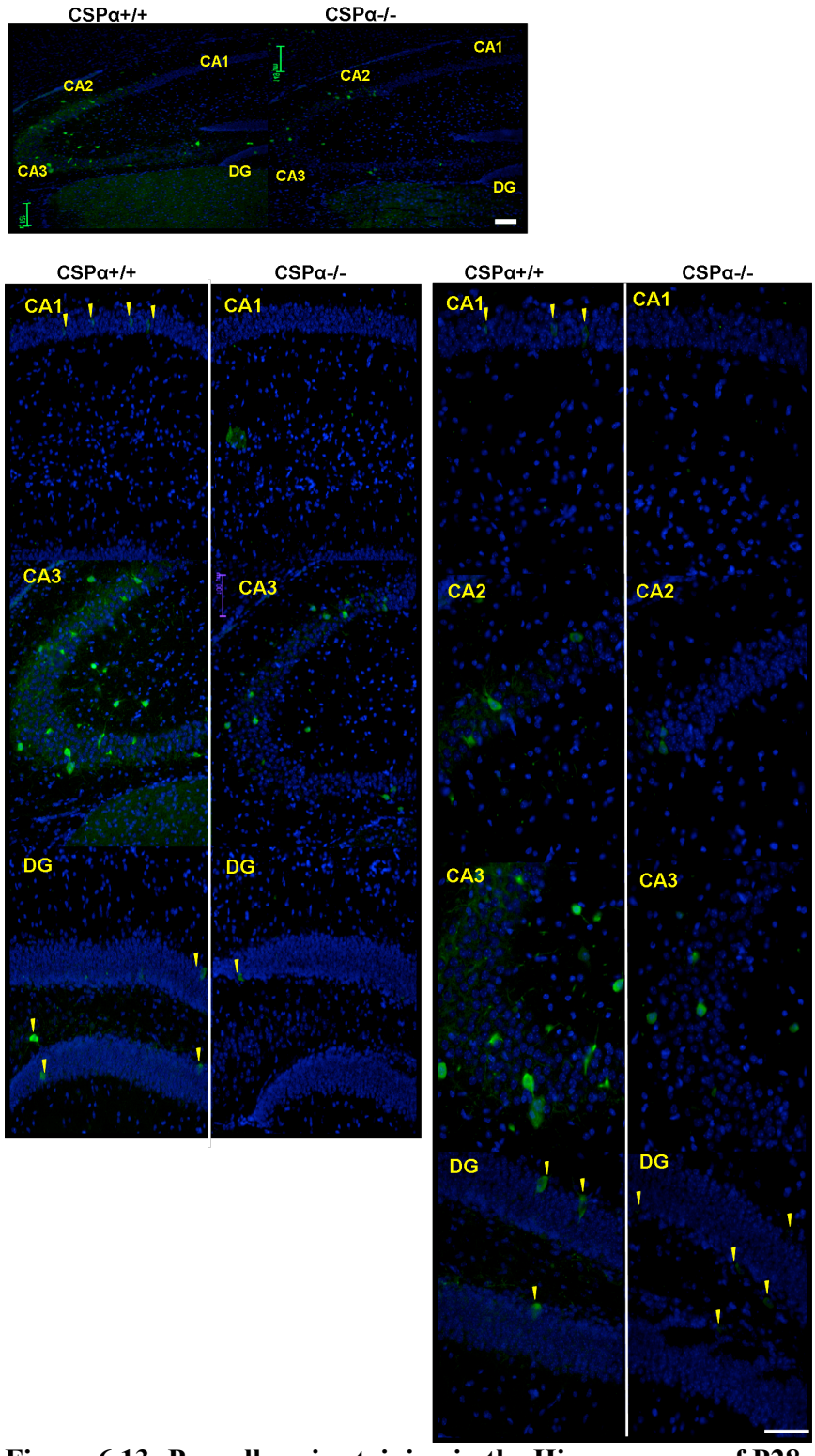

Figure 6.13: Parvalbumin staining in the Hippocampus of P28 mice
Parvalbumin staining was decreased in each area of the hippocampus assessed. The dentate gyrus, CA3, CA2 and CA1 all showed decreased parvalbumin staining in the cell body layer and in neuronal processes in the CSPα-/- mice compared to the CSPα+/+ mice. The yellow arrow heads mark cell body staining where it is particularly faint. Low magnification images scale bar 150μm, higher magnification images scale bar 100μm

6.5.7 Why don't the CSPα-/- cultures undergo excitotoxic cell death due to loss of inhibitory neurons?

If the loss of parvalbumin positive and/ or other fast spiking interneurons is the reason for the lack of significant induction of activity in CSPα-/- Hi-Spots, then why do the CSPα-/- Hi-Spots have the same rather than an increased basal spontaneous activity compared to the CSPα+/+ Hi-Spots? Loss of inhibitory neurons would be expected to lead to dis-inhibition of the network and increased spontaneous activity. Lack of excitotoxicity despite a decrease in mIPSC (miniature inhibitory postsynaptic potential) frequency in hippocampal CSPα-/- cultures was shown to coincide with a reduction in the amplitude of AMPA receptor mediated mEPSCs (miniature excitatory postsynaptic potential) (Garcia-Junco-Clemente, Cantero et al. 2010). Activation of a homeostatic plasticity mechanism was suggested to occur due to inhibitory neuron degeneration, leading to increased network activity, triggering down-regulation of synaptic strength by AMPA receptor internalisation, which returns the culture to normal basal ('set point') activity levels (Garcia-Junco-Clemente, Cantero et al. 2010). This relationship is shown in figure 6.15.

6.5.8 Homeostatic plasticity

Homeostatic plasticity is a form of plasticity that acts to stabilise the activity of a neuron or a neuronal circuit in the face of changes such as increase in synapse number or strength which lead to altered excitability. Maintaining stability in neuronal circuits is fundamentally important to maintain regulated network activity and counteract network over-excitability. Neuronal circuits employ multiple mechanisms to regulate neuronal activity, including presynaptic (Wilson, Kang et al. 2005) and postsynaptic forms of excitatory synaptic plasticity, including synaptic scaling (Shepherd, Rumbaugh et al. 2006), which adjusts the strength of all excitatory synapses in a neuron up or down to stabilise firing, balancing excitation and inhibition within complex connected neuronal networks (Zha, Green et al. 2005; Wierenga, Walsh et al. 2006). Investigation into these mechanisms of homeostatic plasticity have shown that these compensatory changes in synaptic and neuronal properties restore the neuronal firing rate to normal basal levels, the neurons set-point activity level, after the network activity has been perturbed (Shepherd, Rumbaugh et al. 2006).

Little is known about the underlying signalling mechanisms that lead to homeostatic plasticity. Homeostatic synaptic compensation has been shown to occur through both presynaptic and postsynaptic mechanisms, which can act either synergistically or in isolation. Presynaptic changes can act to increase or decrease quantal size by up or down-regulation of VGLUT1 (Wilson, Kang et al. 2005). Postsynaptic homeostatic plasticity mechanisms involve synaptic scaling, whereby changes in activity level lead to bidirectional changes in the accumulation of AMPA receptors (Shepherd, Rumbaugh et al. 2006). Activity deprivation has also been shown to lead to boosting effects of postsynaptic synaptic potentials due to accumulation of dendritic sodium channels (Aptowicz, Kunkler et al. 2004).

GABAergic synapses are also important for modulating network set-point activity, and for maintaining a network inhibitory: excitatory balance. Induction of seizure activity *in vitro* by application of $GABA_A$ receptor antagonists has been shown to selectively favour the loss of synapses on spines but not on dendritic shafts resulting in increased dendritic inhibition, whereas inhibition of activity using TTX has the opposite effect (Zha, Green et al. 2005), changing the balance of excitation: inhibition depending on the neuronal activity level.

Activity regulated cytoskeleton associated protein (Arc) also known as activity-regulated gene 3.1 (Arg 3.1) is an immediate-early gene (IEG), which is regulated by activity, and upon activity induction undergoes rapid transport to dendrites where it is locally translated (Steward, Wallace et al. 1998). Tight association between Arc:Arg 3.1 expression and the strength of excitatory synapses suggests it plays a role in homeostatic plasticity, and has been used as a marker for intense synaptic activity *in vivo* (Chowdhury, Shepherd et al. 2006; Rial Verde, Lee-Osbourne et al. 2006; Shepherd, Rumbaugh et al. 2006; Kawashima, Okuno et al. 2009).

In cultured neurons, levels of Arc:Arg 3.1 have been shown to be increased or decreased in response to chronic changes in neuronal activity (Shepherd, Rumbaugh et al. 2006), and the effects of Arc:Arg 3.1 have been shown to be mediated through the internalisation of AMPA receptors (Chowdhury, Shepherd et al. 2006; Rial Verde, Lee-Osbourne et al. 2006). In view of this and the AMPA receptor mEPSP changes observed by Garcia et al (2010) we conducted a preliminary investigation to test the Arc:Arg 3.1 expression in P28

CSPα+/+ and CSPα-/- mice to assess if Arc:Arg 3.1 was induced in the CSPα-/- mice and could be leading to down-scaling of synaptic AMPA receptors.

Although Arc:Arg 3.1 was detected in the CSPα-/- hippocampi there was no induction compared to that of control CSPα +/+ hippocampus (Figure 6.14). Therefore at this stage (P28) an upregulation of Arc:Arg 3.1 was not detected. Lack of induction in the P28 animals may be because Arc:Arg 3.1 up-regulation had already occurred before P28 due to the earlier dysfunction in parvalbumin positive interneurons (Figure 6.13) (Garcia-Junco-Clemente, Cantero et al. 2010).

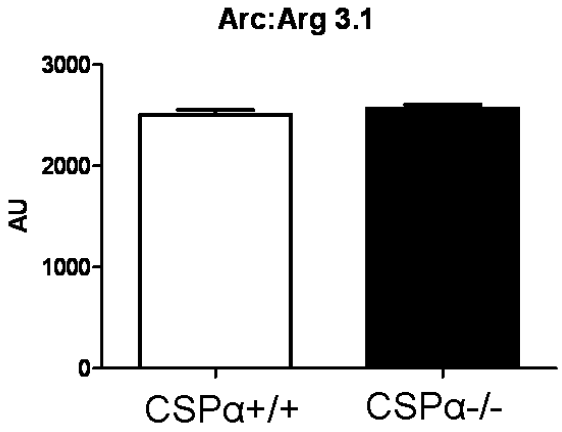

Figure 6.14:Quantitative rt-PCR shows that at P28 there is no up-regulation in the plasticity marker Arc:Arg 3.1 in CSPα-/- mice
Quantitative rt-PCR from 6 CSPα-/- Hippocampus samples and 2 CSPα+/+ Hippocampus samples. Levels have been normalised to GAPDH.

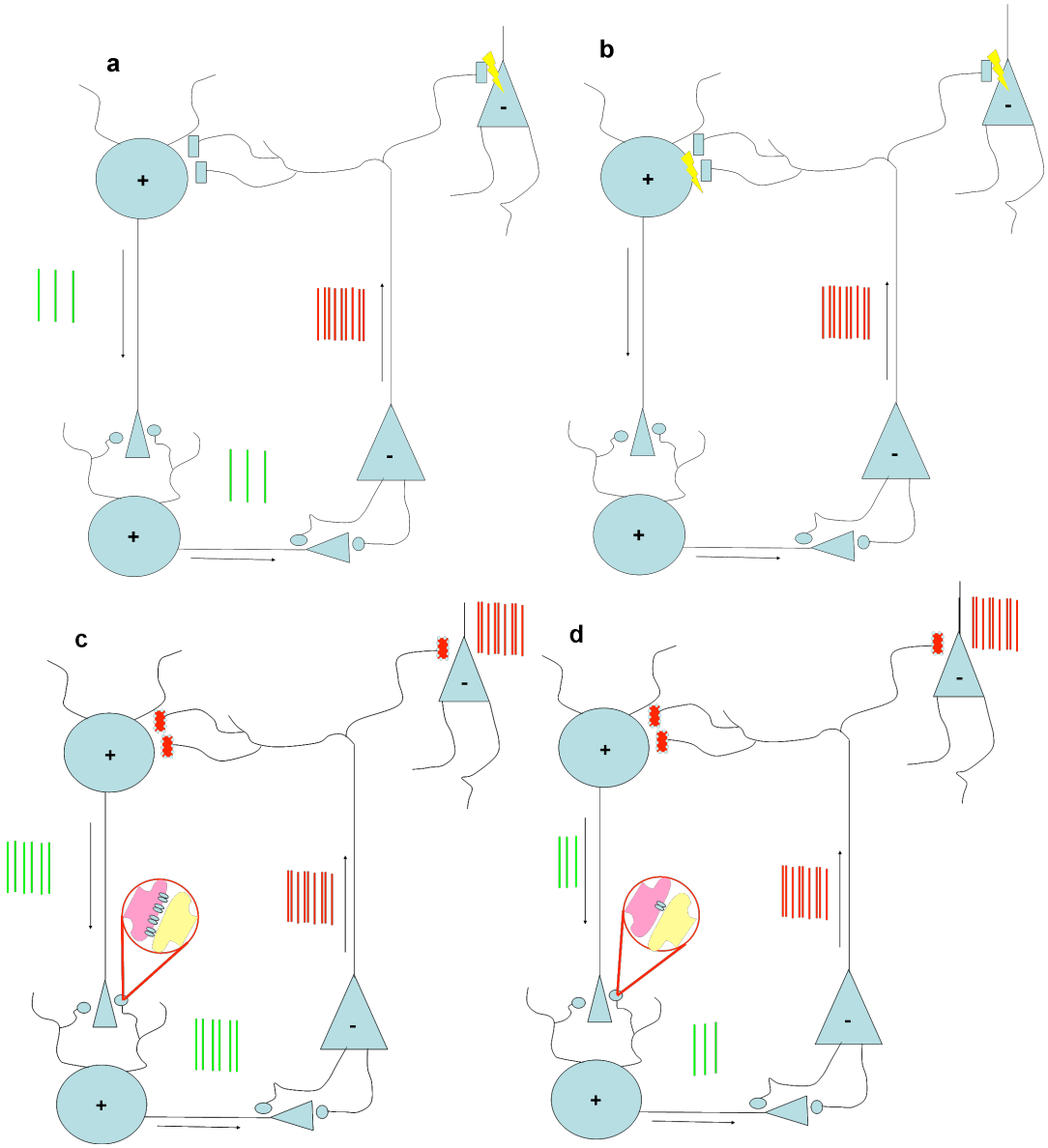

Figure 6.15: Model of the possible network changes occurring in the CSPα-/- Hi-Spots

a) Normal network activity regulated by excitatory and inhibitory neuronal cells. Green line- action potentials from excitatory cells (+, circles), red lines are action potentials from fast spiking inhibitory cells (-, triangles).
b) Upon inhibitory (-) neuronal cell activation excitatory (+) neurons are inhibited
c) Lack of CSPα leads to presynaptic dysfunction in the highly active fast spiking inhibitory neuron leading to network dis-regulation and increased excitatory network activity
d) The increase in network activity is returned to its set point by activation of a homeostatic plasticity mechanism leading to down regulation of synaptic strength through AMPA receptor internalisation. (Adapted from Garcia-Junco- Clemente et al 2010).

6.5.9 How does the loss of CSPα modulate the neuronal network activity?

Neuronal degeneration that occurs due to the absence of CSPα has been shown to be selective for neuronal cells that operate at high activity levels to perform their physiological functions (Fernandez-Chacon, Wolfel et al. 2004; Chandra, Gallardo et al. 2005; Schmitz, Tabares et al. 2006; Ruiz, Casanas et al. 2008; Garcia-Junco-Clemente, Cantero et al. 2010), whereas neuronal cells with lower activity demands have been shown to be refractory to the degeneration, and instead undergo activity dependent modulation to maintain their activity (Garcia-Junco-Clemente, Cantero et al. 2010).

At the synapse CSPα has been proposed to function as a co-chaperone, to regulate calcium channel activity, and exocytosis, see table 1.8 and section 1.10 of the general introduction. Although CSP deficiency has been suggested to not affect vesicle endocytosis (Ranjan, Bronk et al. 1998) the demands of highly active neurons such as the calyx and parvalbumin positive neurons may put greater strain on the recycling of the release machinery, including SNARE refolding, clathrin polymerisation, endocytosis, and clathrin coat disassembly. In the absence of CSPα the chaperone complex formed by Hsc70 and SGT may still be targeted to the synaptic membrane through interaction with the Dna J domain co-chaperone auxilin and its interaction with clathrin and the adaptor protein AP-2, however, without CSPα the ATPase activity of Hsc70 may not be optimally stimulated. Additionally, absence of CSPα has been shown to lead to reduced targeting of SGT to the vesicle membrane, again suggesting lack of CSPα may lead to dysfunction Hsc70 activity (Tobaben, Thakur et al. 2001; Tobaben, Varoqueaux et al. 2003).

The ability to maintain high frequency or tonic quantal release may require efficient temporal SNARE refolding, calcium coupling to vesicle release, and efficient replenishment of the presynaptic vesicles. Without CSPα, the chaperoning activity of Hsc70 may be not efficient enough to cope with high activity demands in synapses driven by high frequency spike trains and becomes rate limiting for presynaptic function. Lack of CSPα may then lead to presynaptic dysfunction through accumulation of folded SNARE complexes, and/ or clathrin coated vesicles; in severely degenerated ribbon synapses of the photoreceptors few uncoated synaptic vesicles were observed but many coated vesicles could still be identified (Schmitz, Tabares et al. 2006), this suggests that at this highly

active synapse clathrin uncoating together with loss of vesicle replenishment could be failing.

The substrates for the CSPα chaperone complex have not yet been defined, but the synaptic vesicle localisation of CSPα and the selective dependence of highly active neurons to CSPα expression suggest that it is involved in synaptic activity dependent events. CSPα has been shown to bind to the SNARE proteins (Leveque, Pupier et al. 1998; Nie, Ranjan et al. 1999; Wu, Fergestad et al. 1999; Evans, Wilkinson et al. 2001; Evans and Morgan 2002; Boal, Laguerre et al. 2010) and the absence of CSPα has been shown to lead to formation of an unstable SNARE complexes and reduced expression of SNAP-25 (Chandra, Gallardo et al. 2005), CSPα has also been suggested to regulate synaptic calcium channels and have a role in calcium-vesicle exocytosis coupling at the synapses (Ruiz, Casanas et al. 2008).

CSPα loss may lead to dysfunction of transmitter release (Dawson-Scully, Bronk et al. 2000; Dawson-Scully, Lin et al. 2007; Ruiz, Casanas et al. 2008) due to SNARE protein folding dysfunctions (Chandra, Gallardo et al. 2005) or dysfunction in calcium homeostasis. The selective dysfunction of highly active neurons is likely to have a network wide effect, especially if the network activity is regulated by the degenerating neuronal type, for example the degeneration of parvalbumin positive interneurons is likely to affect the generation and coherence of gamma oscillation and cognitive behavioural tasks (Fuchs, Zivkovic et al. 2007).

Selective loss of parvalbumin positive interneurons *in vivo* has been shown not to lead to death, and only 6% of the affected rodents demonstrated epileptic seizures (Powell, Campbell et al. 2003). Loss of several subtypes of interneurons, the calretinin and somatostatin positive interneurons due to mutation of the transcription factor *Dlx1* also did not lead to rodent death, but these rodents displayed epileptic seizures (Cobos, Calcagnotto et al. 2005). However, loss of 75% of neocortical and 95% of hippocampal interneurons was shown to lead to rodent death at P0 (Anderson, Eisenstat et al. 1997). This suggests that although the loss of CSPα-/- function in the mice leads to their premature death (Fernandez-Chacon, Wolfel et al. 2004) the mice are not likely to die due to the degeneration of the fast spiking parvalbumin positive neurons. Additionally, no seizure

activity was observed in the CSPα-/- mice due to handling stress, and previous studies have not reported seizure like activity in these mice (Fernandez-Chacon, Wolfel et al. 2004).

The death of the CSPα-/- mice was previously reported to be due to a sensorimotor disorder (Fernandez-Chacon, Wolfel et al. 2004). Progressive muscle weakness due to nmj degeneration may lead to degeneration of phrenic nerve leading to respiratory dysfunction and early death (Llado, Haenggeli et al. 2006).

6.5.10 Summary

In summary the results of this chapter have shown that Hi-Spot cultures made from CSPα-/- cortical tissues have a deficiency in bicuculline-induced network response (Figure 6.10 and 6.11). Network deficiency is not detected in basal activity levels or due to overt degenerative changes in the CSPα-/- cultures (figures 6.3, 6.4, 6.5 and 6.6), and only became apparent when the network was tested for its induced bicuculline-sensitive response (Figure 6.10 and 6.11).

The results show that the CSPα-/- Hi-Spots are not undergoing overt degenerative changes, but suggest that subtle degeneration of discrete highly active inhibitory neurons is occurring. This would reduce inhibitory drive and hence bicuculline blockage of GABAergic receptors would be ineffective. However, background activity levels are not elevated suggesting compensatory excitatory network down-regulation, and maintenance of a set-point level of network activity (Figure 6.10). The down-regulation of network activity appears to occur before *DIV 14* (Figure 6.10) and would be predicted to occur after a period of heightened basal network activity. Our results support those published by Garcia et al 2010, and show that the Hi-Spot cultures can be used to investigate network changes occurring due to the loss of the presynaptic protein CSPα.

7 -General Discussion

Prior to this study the scientists at Capsant Neurotechnologies generated Hi-Spots from embryonic tissue and had begun to characterise the cell types and development of spontaneous electrophysiological network activity in the cultures. The focus of the work was to generate an *in vitro* model that could be used for neurotoxicity studies for high-throughput analysis of pharmacological compounds.

Embryonic Hi-Spot cultures were shown to contain both neuronal and glial cells and develop spontaneous network activity regulated by excitatory and inhibitory neurons (van Vliet, Stoppini et al. 2007). Work on Hi-Spot cultures produced from postnatal animals had begun but the postnatal cultures were observed to develop a cell clumping morphology not seen in the embryonic cultures.

My work began with producing Hi-Spots from embryonic tissue and investigating the expression of neuronal and glial cell markers; Chapter 2 demonstrated that the neuronal cells matured and glial cells, astrocytes, underwent an astrocytosis during the culture period (*DIV 1-28*). However, progression to using postnatal tissue for Hi-Spot cultures using the same protocol as that used for the embryonic tissue (*Capsant*-protocol) did not produce Hi-Spot cultures with a maturing population of neuronal cells. The reason for the disparity was hypothesised to be due to the differential expression of NR1, the obligatory subunit for the NMDA receptor.

Dissociated tissue from embryonic rats displayed reduced expression of NR1 compared to dissociated tissue from postnatal (P0 and P2) rats. This supports the reported findings that levels of NR1 are low at birth in rats and progressively increase during the first two weeks after birth (Babb, Mikuni et al. 2005). Additionally, although functional homomeric, NR1 and NR2B NMDA receptors may exist embryonically, functional heteromeric NMDA receptors formed of both NR1 and NR2 subunits are not formed and functional until after birth, from which the expression levels increase (Babb, Mikuni et al. 2005). Therefore, we inferred that the Hi-Spot cultures produced from the postnatal tissue may be selectively susceptible to excitotoxicity resulting from released glutamate during the mechanical tritutration period in the protocol.

NMDA receptor antagonists such as MK801, Ifenprodil and memantine have been shown to protect against excitotoxic damage in neurons (Ma, Endres et al. 1998; Gorgulu, Kins et

al. 2000; Hardingham and Bading 2002; Chen, Lu et al. 2008). Incubation of the postnatal tissue with the NMDA receptor antagonist MK801 improved the Hi-Spots produced from postnatal tissue. Hi-Spots produced with MK801 in the dissociation solution (*Soton*-protocol) developed with a morphological appearance comparable to the Hi-Spot culture produced from embryonic tissue. Furthermore, cultures produced from postnatal tissue using the *Soton* method were shown to contain a population of neuronal cells which matured alongside an astrocyte population.

Further characterisation of the *Soton* and *Capsant* cultures using IHC demonstrated the development of a neuronal network in the *Soton* Hi-Spots which was fragmented and diminished in the *Capsant* postnatal Hi-Spots. NMDA receptors have been shown to lead to the activation of the enzyme calpain, which when activated can cleave β III Tubulin, and cleave and activate the cysteine enzyme caspase-3 promoting cell death (Blomgren, Zhu et al. 2001). The fragmentation observed in the *Capsant* cultures could represent a downstream effect of NMDA receptor over-activation and calpain activation.

Van Vilet (2007) demonstrated that re-aggregated cultures produced from embryonic tissue and grown on PTFE membranes developed spontaneous network activity (van Vliet, Stoppini et al. 2007). We tested the postnatal Hi-Spots for their network activity and demonstrated that the *Soton* cultures from both P0 and P2 tissue developed higher levels of network activity in terms of both spike number and RMS than the *Capsant* cultures. We also found that the *Soton* P0 Hi-Spot cultures developed higher levels of spontaneous activity compared to the *Soton* P2 cultures. The level of network activity has been shown to correlate with cell density (Wagenaar, Pine et al. 2006) and synapse number (Muramoto, Ichikawa et al. 1993). This supports our Western blot data showing reduced neuronal markers in *Capsant* treated cultures, and in *Soton* cultures made from P2 tissue compared to *Soton* cultures made from P0 tissue.

The spontaneous network activity which developed in the *Soton* cultures began with single spiking activity recorded from individual electrodes, and matured into single spiking and bursting activity. Bursting activity consisted of series of consecutive spikes in quick succession, and was seen on multiple electrodes recording from different sites in the culture. These phenomena; single spiking and bursting, and the temporal development of

bursting activity in more mature cultures, has been previously described in dissociated cell cultured on MEAs (Van Pelt, Corner et al. 2004; Wagenaar, Pine et al. 2006).

7.1.1 P0 *Soton* cultures develop a synaptically connected active network

Based on the MEA network activity recordings and expression of neuronal markers in the P0 *Soton* cultures, we decided to further characterise these cultures, and investigate the origin and regulation of the spontaneous network activity. Chapter 4 describes further characterisation the P0 *Soton* cultures and demonstrated that the cultures contained neuronal cells, astrocytes and microglial cell. The neuronal and glial cells were shown to be in close association and not distributed in different regions in the Hi-Spot. Astrocytes have been shown to regulate neuronal synapses and network formation (Ullian, Christopherson et al. 2004; Christopherson, Ullian et al. 2005) and support neuronal cells by maintenance of the extracellular environment and nutrient supplementation (Volterra and Meldolesi 2005). The existence of a glial cell population is not only important for an *in vitro* culture analogue of the brain but also for neuronal health and network activity (Boehler, Wheeler et al. 2007).

Immunohistochemical analysis also revealed punctate staining of presynaptic and postsynaptic marker proteins, and showed evidence for glutamatergic and GABAergic neuronal networks. More explicit analysis revealed that a subtype of interneuronal cell, the parvalbumin positive interneurons, were also cultured in the rat Hi-Spots. Excitatory and inhibitory networks have been shown to be important for the generation of spontaneous network activity *in vitro,* and for mature network oscillations *in vivo* (Bartos, Vida et al. 2007). In particular the fast spiking parvalbumin positive interneurons have been shown to be important for synchronising the output of pyramidal cells in the generation of gamma oscillations and loss of these cells leads to behavioural abnormities and increased susceptibility to seizures (Powell, Campbell et al. 2003; Fuchs, Zivkovic et al. 2007).

To further characterise the spontaneous network activity in *Soton* P0 cultures, we used tetanus toxin to investigate whether the recorded activity was synaptically driven. Astrocytes have been shown to communicate though Ca^{2+} signalling with each other in an astrocytic syncitium, and with neuronal cells using gliotransmitters in a tripartite synapse (Araque, Parpura et al. 1998; Kang, Jiang et al. 1998; Araque, Parpura et al. 1999; Pasti,

Zonta et al. 2001). Astrocyte Ca^{2+} signalling has been correlated with neuronal activity and some studies have found evidence suggesting astrocytes maybe the mediators of correlated neuronal network activity (Parri and Crunelli 2001; Parri, Gould et al. 2001; Fellin, Pascual et al. 2004). Tetanus toxin incubation, which inhibits neurotransmission by cleaving the v-SNARE synaptobrevin, demonstrated that the network activity recorded on the MEA was due to synaptic activity and not Ca^{2+} fluxes through the astrocyte network or random depolarisations of sodium channels.

Pharmacological manipulation using AMPA and NMDA receptor antagonists provided further support for a glutamatergic network. Also the effects of bicuculline the $GABA_A$ receptor antagonist, provided additional functional evidence supporting the IHC analysis showing a GABAergic network. Spontaneous network activity in dissociated cultures has also been shown to be sensitive these pharmacological antagonists (Xiang, Pan et al. 2007).

7.1.2 P0 *Soton* cultures develop *in vivo* like cell-cell interactions

Both astrocytes and neuronal cells contain glutamate transporters, but astrocytes are thought to be the main regulators of extracellular glutamate concentration. *In vivo* astrocytes interact intimately with the synapse and can take up glutamate (Vermeiren, Najimi et al. 2005; Halassa, Fellin et al. 2007). Loss of the intimate synaptic and astrocytic interactions in dissociated cultures due to the unnatural culturing conditions and the reduced cell density compared to the *in vivo* brain could be the reason dissociated cultures have a low tolerance to glutamate toxicity (Choi, Maulucci-Gedde et al. 1987). Organotypic hippocampal cultures which retain the architecture and cell-cell interactions of the *in vivo* brain have a glutamate tolerance which approximates that *in vivo* (Morrison, Pringle et al. 2002). Re-aggregated Hi-Spot cultures also demonstrated a high tolerance to glutamate toxicity, demonstrating tolerance to mM concentrations for several hours. We concluded from this data that like organotypic cultures Hi-Spots contain intricate cell-cell interactions between neuronal and glial cells similar to *in vivo*.

Interestingly Hi-Spot cultures demonstrated complete tolerance to glutamate with no cell death above basal levels judged by propidium iodide when maintained in serum containing media. Previous related studies have also shown this result, and examination of the serum constituents revealed the trophic effects were due to FGF or TGFβ1, and that this effect

was due to prevention of mitochondrial Ca^{2+} accumulation (Uto, Dux et al. 1994; Dux, Oschlies et al. 1996).

Characterisation of the *Soton* Hi-Spot cultures made from P0 rats, has shown that these cultures develop neuronal and glial cell populations, the neuronal cells form a network and mature in the presence of astrocyte and microglial cell populations. The neuronal network develops *in vivo* like cell-cell interactions and spontaneous activity, and mature activity results in high frequency bursting activity correlated across multiple regions in the culture. Due to its economic and animal research advantages the characterised Hi-Spots formed using the *Soton* protocol from postnatal day 0 tissue are now routinely used by Capsant Neurotechnologies. Hi-Spots made from P0 tissue using the *Soton* protocol I have developed are currently being used to investigate the effect of Glioblastoma on the brain. This work by Capsant scientists has led to the development of a brain-glioblastoma model which is currently in the process of being patented for commercial use.

For investigations of neuronal network changes due to the loss or dysfunction of synaptic proteins an *in vitro* model which forms an active neuronal network which can be manipulated with pharmacological drugs and probed with biochemical and immunohistochemical techniques, would be useful. Neuronal network dysfunctions are thought to occur in psychiatric disorders such as autism and schizophrenia and lead to the cognitive dysfunctions (Zhang, Sun et al. 2002; Rubenstein and Merzenich 2003). Dysfunction associated with these diseases has been shown to be due to loss of a particular subtype of neuron or to a developmental imbalance in the ratio of excitatory and inhibitory neuronal synapses (Hussman 2001; Zhang, Sun et al. 2002; Rubenstein and Merzenich 2003; Gutierrez, Hung et al. 2009).

Dysfunction of some presynaptic and trans-synaptic proteins has been shown to selectively affect neuronal cells with higher activity stresses, and the associated synaptic dysfunction has been shown to be relieved by inhibition of the network activity (Hayashi, Raimondi et al. 2008; Gibson, Huber et al. 2009; Burre, Sharma et al. 2010). For example, investigations into the mechanism of endocytosis using dynamin-1 null mice have shown that nerve terminals of neurons lacking this presynaptic protein demonstrate functional and structural deficits consistent with dysfunction of vesicle recycling (Hayashi, Raimondi et al. 2008). Nerve terminals displayed delayed internalisation of synaptic vesicles and

increased accumulation of endocytotic clathrin-coated pits, and closer inspection revealed a subset of more active neurons that were uniquely sensitive to the endocytotic deficit. These neurons were identified as inhibitory interneurons and demonstrate a more critical dependence of inhibitory synapses on the clathrin-coated vesicle recycling machinery over excitatory synapses. This appears essential for maintenance of inhibitory neuron synaptic pools (Hayashi, Raimondi et al. 2008). This highlights a functional difference in the mechanism of vesicle endocytosis, in which more active neuronal cells may rely on different endocytosis mechanisms (Section 1.6.1), which make different neuronal subtypes more susceptible to dysfunction in the absence of a protein involved in the core mechanism of vesicle endocytosis.

7.1.3 Different Hi-Spots show variability in their electrophysiological activity

The activity recorded on MEAs has been shown to depend on the density of the cultures recorded and the culturing conditions (Voigt, Opitz et al. 2001; Wagenaar, Pine et al. 2006). Hi-Spots from postnatal rat and mouse tissue were made using three different protocols. Rat Hi-Spots were made by dissociating pooled brains in the presence of MK801 using the *Soton* protocol, mouse Hi-Spots were also made by dissociated pooled brain in the presence of MK801 but also used papain to aid the dissociation, *Soton-P* protocol. Lastly, mouse Hi-Spots from single brain were dissociated in the presence of MK801 and papain but seeded at the increased cell density of 90,000 cell/ µl, compared to 50,000 cells/ µl in the above two protocols.

Previous results have shown that an increased cell density leads to higher MEA spiking activity (Wagenaar, Pine et al. 2006), this can be observed when comparing rat *Soton* cultures seeded at 50,000 cells/ µl (Figure 3.9) and Mouse *Soton-P* cultures seeded at 90,000 cells/ µl (Figure 6.10). The mouse cultures have a higher spiking activity at both *DIV 14* and *DIV 21* compared to the rat cultures. However, because the different cultures were produced using three very different protocols and demonstrated inherent differences in culture thickness, plating density, and enzyme dissociation comparing the activity difference between the protocols may not be viable. Previous research has shown that repeated controlled culturing conditions are needed to produce cultures with similar activity profiles and that variability still occurs between sister cultures and between cultures generated between different animal litters when the same protocol is maintained.

Therefore it is not surprising that the different protocols used to produce rat and mouse Hi-Spots displayed different basal activity levels.

The difference in RMS activity between the rat and mouse cultures (Figures 3.9, 5.9 and 6.10) could be due to the recording electrodes selected and the different culture protocols. The RMS takes into account the amplitude of the recorded activity and therefore maybe affected by the number of active neurons near the recording site as well as number of spikes generated. RMS was used because it was noticed that upon addition of bicuculline two things happened, the spike number increased and the amplitude of the spikes increased. This could suggest that more neuronal cell surrounding the recording electrodes become active. Therefore, the RMS measure was used to quantify the data because it takes spike and amplitude changes into account.

7.1.4 CSPα+/+ and CSPα-/- Hi-Spots

Cysteine string protein α (CSPα) is a presynaptic protein associated with synaptic vesicles, and loss of this protein has been show to lead to use-dependent stress of highly active neuronal cells (Fernandez-Chacon, Wolfel et al. 2004; Chandra, Gallardo et al. 2005; Schmitz, Tabares et al. 2006; Garcia-Junco-Clemente, Cantero et al. 2010). To use the Hi-Spot system to investigate the neuronal network changes due to loss of CSPα, Hi-Spots generated from P0 mouse cultures were characterised. The cell culture *Soton* protocol, which was used successfully for culturing rat Hi-Spots, did not produce a neuronal population in Hi-Spots produced from mouse tissue. Instead neuronal markers were lost early in the culture period, and cultures displayed an unhealthy morphology, consisting of cell clumping and disaggregation. Mouse neural cells have been previously described to be more susceptible to death in cell culture than rat cells (Hatten, Gao et al. 1998), and modification of the mouse tissue dissociation, and processing using the Worthington life papain cell dissociation kit to aid more gentle dissociation led to cultures with an active maturing neuronal network (Chapter 5). A further optimisation of increasing the cell plating density was necessary to produce Hi-Spots from single mouse brain dissociations; this protocol was called the *Soton-P* protocol.

7.1.5 No Overt degeneration in the CSPα-/- Hi-Spots

Hi-Spot cultures from single mouse brain dissociates were used in chapter 6 to investigate network activity in Hi-Spots made from CSPα-/- mice. The cultures were first analysed for overt degeneration using bright-field microscopy. Chapter 3 highlighted the different morphological appearances of healthy embryonic and postnatal *Soton* cultures compared to those containing a degenerating neuronal population in postnatal *Capsant* cultures. However, the bright-field appearance of the CSPα-/- cultures was no different to that of CSPα+/+ cultures, and neither the CSPα+/+ or the CSPα-/- cultures display cell clumping or disaggregation, features shown to correlate with unhealthy cultures. Further analysis using propidium iodide, confirmed that the CSPα-/- cultures displayed similarly low levels of basal cell death compared to CSPα+/+ cultures.

Both CSPα-/- and CSPα+/+ cultures developed a neuronal network, and the neuronal network formed by CSPα-/- Hi-Spots could not be distinguished morphologically from that formed by CSPα+/+ Hi-Spots. The synaptic ultrastructure in the CSPα+/+ and CSPα-/- Hi-Spots was assessed by electron microscopy. Previous electron microscopy analysis on the calyx of Held, the ribbon synapse of the photoreceptors, and the synapses of interneuronal cells in the CSPα-/- mice has shown a degenerating phenotype (Fernandez-Chacon, Wolfel et al. 2004; Schmitz, Tabares et al. 2006; Garcia-Junco-Clemente, Cantero et al. 2010). Electron microscopy analysis of synapses in CSPα+/+ and CSPα-/- cultures showed no overt differences in the synaptic structure, and there were no overt signs of degeneration.

This data could be consistent with a selective synaptic degeneration of a subtype(s) of neurons, but not global degeneration of the entire neuronal population, and supports the findings of Garcia et al (Garcia-Junco-Clemente, Cantero et al. 2010). Chapter 4 demonstrated the presence of the parvalbumin positive interneurons in the rat Hi-Spot cultures. Parvalbumin positive interneurons are classified as a subtype of fast firing inhibitory neurons, and have been shown to selectively degenerate in the absence of CSPα (Garcia-Junco-Clemente, Cantero et al. 2010). Specific loss of interneurons in the CSPα-/- mice was presented by Fernandez Chacon in the Biochemical Sciences meeting in Cornwall 2009, and on reviewing this information we decided to test the network activity in Hi-Spots made from CSPα+/+ and CSPα-/- cultures for their bicuculline sensitivity.

7.1.6 Bicuculline revealed network dysfunction in the CSPα-/- Hi-Spots

Bicuculline is a $GABA_A$ receptor blocker. Activation of $GABA_A$ receptors by GABA released from the presynaptic neuron leads to postsynaptic $GABA_A$ receptor activation and Cl^- influx which hyperpolarises and reduces excitability of the postsynaptic cell. By blocking the activation of $GABA_A$ receptors, $GABA_A$ receptor mediated inhibition onto excitatory and inhibitory neurons is blocked (Prenosil, Schneider Gasser et al. 2006; Mohler 2007), therefore both excitatory and inhibitory neurons will be relieved from $GABA_A$ mediated inhibition.

Equal levels of basal activity were observed in the CSPα+/+ and CSPα-/- at ~*DIV 14*, but not at *DIV 21*. Compared to *DIV 14* the *DIV 21* CSPα+/+ Hi-Spots undergo a developmental increase in basal spontaneous activity not paralleled by the CSPα-/- Hi-Spots. Instead the CSPα-/- Hi-Spots retained a steady level of basal activity. The level of spontaneous network activity recorded in dissociated cultures has been correlated with cell density and synapse number and the balance between excitatory and inhibitory synaptic connections (Ichikawa, Muramoto et al. 1993; Muramoto, Ichikawa et al. 1993; Kamioka, Maeda et al. 1996; Chiappalone, Bove et al. 2006; Xiang, Pan et al. 2007) and the presence of astrocytes (Boehler, Wheeler et al. 2007). This suggests that at *DIV 14* there is no difference in the synapse number and neuronal cell density between the CSPα+/+ and CSPα-/- Hi-Spots. An astrocytosis in the CSPα mice has been reported (Chandra, Gallardo et al. 2005; Schmitz, Tabares et al. 2006), but we have no data to predict whether this is occurring the Hi-Spot cultures.

On the addition of bicuculline the network activity in the CSPα+/+ Hi-Spots increased. At ~*DIV 14* the level of network activity in the presence of bicuculline was significantly above the level of basal activity. The developmental increase in basal activity in the CSPα+/+ Hi-Spots by *DIV 21* will have reduce the potential of the network to increase its relative activity level although the absolute level in the presence of bicuculline is high. However, the increase in network activity upon bicuculline addition at ~*DIV21* was not statistically significant overall. The increased basal level of activity at *DIV 21* in CSPα+/+ cultures could be due to an increase in the ratio of excitatory to inhibitory synapses in the culture leading to a higher level of excitatory network activity (Dahlhaus, Hines et al. 2010). Network activity in the CSPα-/- Hi-Spot was not significantly increased from the

basal level at *~DIV 14* or *~DIV 21* instead the network activity remained at a steady-level during development and upon blockade of GABAergic inhibition.

Maintenance of the network activity at a steady-basal and bicuculline-induced level suggested that the excitatory capacity of the network has been modified. This supports the finding of Garcia et al (2010) who provided evidence that the selective loss of the GABAergic parvalbumin positive inhibitory neurons without the associated increase in glutamatergic activity was due to homeostatic down-scaling of AMPA receptors in the hippocampal glutamatergic pyramidal cells. Analysis of the level of parvalbumin positive neurons in the hippocampus of P28 mice and electron microscopy of glutamatergic Stratum Radiatum synapses in chapter 6 also supports the observed reduction in parvalbumin positive interneurons and the absence of degeneration in the CSPα-/- glutamatergic neurons (Figure 6.13) (Garcia-Junco-Clemente, Cantero et al. 2010).

7.1.7 Synaptic scaling

AMPA receptor downscaling is proposed to occur through internalisation of AMPA receptors regulated by synaptic activity (Chung, Xia et al. 2000; Hanley and Henley 2005; Chowdhury, Shepherd et al. 2006; Shepherd, Rumbaugh et al. 2006). Arc:Arg 3.1 is an immediate-early gene (IEG) regulated by activity and tight association between Arc:Arg 3.1 expression and the strength of excitatory synapses suggests it plays a role in the synaptic scaling of neuronal activity. Arc:Arg 3.1 has also been used as a marker for intense synaptic activity *in vivo* (Chowdhury, Shepherd et al. 2006; Rial Verde, Lee-Osbourne et al. 2006; Shepherd, Rumbaugh et al. 2006; Kawashima, Okuno et al. 2009). No difference in the levels of Arc:Arg 3.1 were seen between P28 CSPα+/+ and CSPα-/- mice. Suggesting that at P28 Arc:Arg 3.1 levels were not activated above control (CSPα+/+) levels.

Lack of an observed increase in Arc:Arg 3.1 expression in the CSPα-/- mice could be due to it being transient, the increases occurring before P28. Arc:Arg 3.1 mRNA levels have been suggested to be regulated by mRNA degradation by translation dependent mRNA decay (Giorgi, Yeo et al. 2007). This mechanism regulates the level of Arc:Arg 3.1 protein and action at the synapse, therefore changes in Arc:Arg 3.1 expression would be expected to be only transient. A time course of CSPα-/- mice could be used to track changes across

different ages and assess if the Arc:Arg 3.1 induction was occurring earlier in the hippocampal network.

The lack of increased neuronal network activity upon bicuculline induction in CSPα-/- may not only, or solely, be due to a loss of the fast spiking interneuronal population. Lack of inducible activity could also be due to deficiency in the CSPα-/- neurons to increase their action potential frequency. Dynamin-1, synuclein triple (α, β, γ), CSPα, and Neuroligin-2 knockout mice, have shown presynaptic dysfunctions which have been associated with neuronal activity (Hayashi, Raimondi et al. 2008; Gibson, Huber et al. 2009; Burre, Sharma et al. 2010). In the case of the Dynamin-1, neuroligin-2 and CSPα knockout mice the dysfunctions have been selectively associated with fast-firing interneurons (Hayashi, Raimondi et al. 2008; Gibson, Huber et al. 2009; Burre, Sharma et al. 2010). This highlights the stress associated with neuronal activity, and in particular in neuronal cells with higher firing rates.

7.1.8 Synaptic dysfunction due to loss of CSPα

The synapses affected by the loss of CSPα all show adaptive specialisations to the core exocytosis and endocytosis mechanisms (Section 1.6). Lack of CSPα in mice and *Drosophila* has been shown to affect the Ca^{2+}- secretion coupling of the nmj synapse (Dawson-Scully, Bronk et al. 2000; Dawson-Scully, Lin et al. 2007; Ruiz, Casanas et al. 2008). The neuronal synapses that degenerate in the CSPα-/- mice; the calyx of Held synapse (Fernandez-Chacon, Wolfel et al. 2004), parvalbumin positive interneuron (Garcia-Junco-Clemente, Cantero et al. 2010) and retinal ribbon synapses (Schmitz, Tabares et al. 2006) have all been shown to have nanodomain Ca^{2+} domains to trigger synaptic vesicle release (Fedchyshyn and Wang 2005; Bucurenciu, Kulik et al. 2008; Jarsky, Tian et al. 2010). Furthermore, the mature nmj, which has also been shown to undergo degeneration in CSPα-/- mice has been shown to have tight Ca^{2+} - secretion coupling, not inhibited by EGTA the slow Ca^{2+} binding buffer (Rosato-Siri, Piriz et al. 2002). This contrasts to the glutamatergic layer 5 neocortical pyramidal cell synapses (Ohana and Sakmann 1998) which show micro-domain, loose Ca^{2+} -secretion coupling, and pyramidal cells in the hippocampus have been shown to not degenerate in the CSPα-/- mice (Garcia-Junco-Clemente, Cantero et al. 2010).

This tighter Ca^{2+}-secretion coupling in the more active neuronal synapses, likely reflects an advantage that aids efficient neurotransmitter release, and confers the ability to respond quickly after action potential activation, minimising the intracellular diffusional component of the synaptic delay (Bucurenciu, Kulik et al. 2008). Tighter coupling has also been shown to be important for increasing the ratio of synchronous to asynchronous release (Hefft and Jonas 2005). Tight coupling in the fast spiking GABAergic neurons is likely to enhance their signalling properties by increasing the speed and reliability of GABA release, important for the generation of fast network oscillations in interneuron networks (Bartos, Vida et al. 2007). Lack of parvalbumin interneuron activity leads to dysfunction in gamma oscillations (Fuchs, Zivkovic et al. 2007) and increased expression of GluR2 in interneurons, which normally express very low levels of GluR2 containing AMPA receptors, and is the determinant of relatively slow EPSCs in excitatory neurons (Section 1.5.1 and 1.6.7). This leads to slowing of interneuron EPSCs and dysfunction in gamma oscillation synchronicity (Fuchs, Doheny et al. 2001). This highlights the importance of the fast spiking activity in interneurons and how their dysfunction can lead to network-wide changes.

In CSPα-/- mice dysfunction may principally affect the neuronal cells that are involved in fast firing activities because these neurons rely on tight Ca^{2+} -secretion coupling that is dysfunctional in the absence of CSPα.

CSPα has also been shown to interact with synaptotagmin (Evans and Morgan 2002; Boal, Laguerre et al. 2010) as well as the SNARE proteins syntaxin and synaptobrevin (Leveque, Pupier et al. 1998; Boal, Zhang et al. 2004). SNARE complex assembly has also been shown to be unstable in CSPα-/- mice (Chandra, Gallardo et al. 2005). The synaptic vesicle localisation of CSPα, together with its documented interaction with SNARE proteins and the Ca^{2+} channels, places it an ideal place to couple Ca^{2+} entry through voltage-gated Ca^{2+} channels to the Ca^{2+} sensor synaptotagmin to SNARE complex formation. The differential reliance of different isoforms of synaptotagmin for fast vesicle exocytosis between glutamatergic and GABAergic hippocampal neurons (Kerr, Reisinger et al. 2008) may link to the different Ca^{2+} -secretion coupling observed at these synapses (Charvin, L'Eveque et al. 1997).

CSPα has been shown to interact with the chaperone protein Hsc70. Hsc70 is known to function at the synapse to remove the clathrin shell from clathrin coated vesicles after endocytosis (Jiang, Gao et al. 2000) (Section 1.4.1 and 1.4.2). CSPα has been shown to increase the ATPase of Hsc70 along with the co-chaperone SGT by 19 fold (Tobaben, Thakur et al. 2001; Tobaben, Varoqueaux et al. 2003), suggesting that CSPα may be important to localise the Hsc70-SGT chaperone complex to the synaptic vesicle for clathrin-uncoating. Synapses with high activity levels have been shown to be particularly reliant on clathrin-mediated endocytosis (Sun, Wu et al. 2002; Rea, Li et al. 2004; Hayashi, Raimondi et al. 2008) compared to less active glutamatergic neurons (Gandhi and Stevens 2003). Possibly, this could prevent clogging up the active site with non-functional vesicles. However, in the absence of CSPα this may lead to different endocytotic stresses in different synapse subtypes.

SGT can increase the ATPase activity of Hsc70 necessary of clathrin-uncoating by 5 fold, and in the absence of CSPα Hsc70 may still be recruited to the synaptic vesicles through its interaction with the adaptor protein AP-2. However, in highly active synapses the decreased ATPase activity of Hsc70 in the absence of CSPα may become rate limiting for vesicle uncoating and vesicle endocytosis. Indeed increased numbers of clathrin-coated vesicles were observed in the ribbon synapses of the photoreceptors in the absence of CSPα (Schmitz, Tabares et al. 2006).

The specialisations which adapt fast spiking and tonically active synapses to their functions may make them more prone to degeneration in the absence of CSPα, this could be because their function is compromised and/or because the normal stresses associated with synaptic transmission are overwhelming without the function of CSPα.

Future work could address the lack of induction observed in Arc:Arg3.1 levels in the CSPα-/- compared to the control (Figure 6.14). This could be due to a transient increase in Arc:Arg 3.1 before P28, Arc:Arg 3.1 mRNA levels have been suggested to be regulated by mRNA degradation by translation dependent mRNA decay (Giorgi, Yeo et al. 2007), which could regulate the level of Arc:Arg 3.1 protein, and action at the synapse, therefore changes in Arc:Arg 3.1 expression would be expected to be only transient. A time course of CSPα-/- mice could be used to assess if the Arc:Arg 3.1 induction was occurring earlier in the hippocampal network.

If a time period before and after Arc:Arg 3.1 induction was identified in mouse hippocampal samples, Hi-Spot cultures could then be used to assess if this related to network activity changes near the corresponding days *in vitro*. It would be expected that the time line would develop first with the dysfunction of fast spiking inhibitory neurons leading to increased basal excitatory activity, Arc:Arg 3:1 induction would then lead to synaptic down scaling through AMPA receptor internalisation and network activity would return to its set-point level. Alternatively the network activity could be dynamically regulated due to the progressive degeneration of the inhibitory neurons leading to progressive compensatory changes and no observable increase in network activity.

From the MEA results in figure 6.11 it could be predicted that since the activity level in the CSPα-/- cultures does not change during development (from *DIV 14* to *DIV 21*) or upon bicuculline addition that, firstly, the inhibitory neuronal dysfunction has already occurred at *DIV 14.* Secondly, that so has the Arc:Arg 3.1 induction and synaptic down-scaling, this relationship is summarised in a model in figure 6.15.

It would also be interesting to investigate other synapses known to have high activity stresses. In particular the cerebral granule cells have a high expression of the CSPα chaperone components and present a highly active neuronal subtype (Liu and Kaczmarek 1998; Tobaben, Thakur et al. 2001; Tobaben, Varoqueaux et al. 2003), investigation into the neuronal dysfunction at these synapses would provide further insight into the neuronal types susceptible to degeneration in the absence of CSPα, and further insight into the brain dysfunction occurring in the CSPα-/- mice leading to their premature death after 3 months.

7.2 Conclusion

In conclusion, this work has shown that Hi-Spot cultures can be formed from postnatal rat and mouse tissue and that these cultures contain maturing neurons and glial cells, which develop spontaneous network activity. The investigations have highlighted that different Hi-Spot cultures are not homologous in their level of basal spontaneous activity, or their bicuculline induced activity. This variability is not intrinsic to Hi-Spot cultures; other multielectrode array studies have highlighted the culture-to-culture variation in activity

levels and have concluded the importance of multiple repeats, and consistency with culturing conditions (Wagenaar, Pine et al. 2006).

We have shown that Hi-Spot cultures can be used to assess the network changes due to a molecular lesion and have shown a functional network phenotype for CSPα-/- tissue without overt degeneration. In the absence of CSPα the neuronal network has reduced capacity to increase activity levels when GABAergic inhibition is reduced. We infer from this data that, in the absence of CSPα there is either a selective loss of certain subclasses of inhibitory interneuron with a compensatory homeostatic down regulation of activity, or a reduced ability to produce high frequency synaptic activity. Both of these processes would be consistent with a key role for CSPα in high frequency synaptic transmission.

To test the Hi-Spots for a preferential loss of parvalbumin positive interneurons in CSPα-/- Hi-Spots the Hi-Spots could be assessed for their expression of the calcium binding protein parvalbumin and synaptobrevin 2 compared to calrectinin. Previous studies have shown that while interneurons expressing calrectinin are spared, parvalbumnin and synaptobrevin 2 containing interneurons are lost in CSPα-/- cultures and brains (Garcia-Junco-Clemente, Cantero et al. 2010). An enhancement to this would be to also test the Hi-Spots for the proteoglycan DSD-1-PG which is selectively expressed in the perineuronal net of parvalbumin positive neurons (Wintergerst, Faissner et al. 1996). Previous work assaying cultures for the interneuron marker parvabumin have been hindered because this protein is expressed in an activity depended fashion and only upregulated two weeks after birth (Garcia-Junco-Clemente, Cantero et al. 2010). Testing cultures for DSD-1-PG could provide an independent marker of the presence or absence of parvalbumin positive fast spiking cells.

Secondly, to test the CSPα-/- Hi-Spots for their ability to fire at high frequencies could be tested using 4 –Aminopyridine (4-AP). 4-AP is a potassium channel blocker and increasing the spiking activity of neuronal cells. CSPα+/+ and CSPα-/- Hi-Spots could be compared using 4-AP to assess if the two culture genotypes had the same high level of inducible activity.

8 -References

Abraham, C., H. Hutter, et al. (2006). "Synaptic tetraspan vesicle membrane proteins are conserved but not needed for synaptogenesis and neuronal function in Caenorhabditis elegans." Proc Natl Acad Sci U S A **103**(21): 8227-8232.

Ahmari, S. E., J. Buchanan, et al. (2000). "Assembly of presynaptic active zones from cytoplasmic transport packets." Nat Neurosci **3**(5): 445-451.

Ahnert-Hilger, G., U. Kutay, et al. (1996). "Synaptobrevin is essential for secretion but not for the development of synaptic processes." Eur J Cell Biol **70**(1): 1-11.

Alho, H., C. Ferrarese, et al. (1988). "Subsets of GABAergic neurons in dissociated cell cultures of neonatal rat cerebral cortex show co-localization with specific modulator peptides." Brain Res **467**(2): 193-204.

Almeida, C. G., D. Tampellini, et al. (2005). "Beta-amyloid accumulation in APP mutant neurons reduces PSD-95 and GluR1 in synapses." Neurobiol Dis **20**(2): 187-198.

Anderson, S. A., D. D. Eisenstat, et al. (1997). "Interneuron migration from basal forebrain to neocortex: dependence on Dlx genes." Science **278**(5337): 474-476.

Angulo, M. C., A. S. Kozlov, et al. (2004). "Glutamate released from glial cells synchronizes neuronal activity in the hippocampus." Journal of Neuroscience **24**(31): 6920-6927.

Annis, C. M., R. T. Robertson, et al. (1993). "Aspects of early postnatal development of cortical neurons that proceed independently of normally present extrinsic influences." J Neurobiol **24**(11): 1460-1480.

Antonopoulos, J., I. S. Pappas, et al. (1997). "Activation of the GABAA receptor inhibits the proliferative effects of bFGF in cortical progenitor cells." Eur J Neurosci **9**(2): 291-298.

Aptowicz, C. O., P. E. Kunkler, et al. (2004). "Homeostatic plasticity in hippocampal slice cultures involves changes in voltage-gated Na+ channel expression." Brain Res **998**(2): 155-163.

Araque, A., N. Li, et al. (2000). "SNARE protein-dependent glutamate release from astrocytes." J Neurosci **20**(2): 666-673.

Araque, A., V. Parpura, et al. (1998). "Glutamate-dependent astrocyte modulation of synaptic transmission between cultured hippocampal neurons." Eur J Neurosci **10**(6): 2129-2142.

Araque, A., V. Parpura, et al. (1999). "Tripartite synapses: glia, the unacknowledged partner." Trends Neurosci **22**(5): 208-215.

Araque, A., R. P. Sanzgiri, et al. (1998). "Calcium elevation in astrocytes causes an NMDA receptor-dependent increase in the frequency of miniature synaptic currents in cultured hippocampal neurons." Journal of Neuroscience **18**(17): 6822-6829.

Arnold, F. J., F. Hofmann, et al. (2005). "Microelectrode array recordings of cultured hippocampal networks reveal a simple model for transcription and protein synthesis-dependent plasticity." J Physiol **564**(Pt 1): 3-19.

Atluri, P. P. and W. G. Regehr (1998). "Delayed release of neurotransmitter from cerebellar granule cells." J Neurosci **18**(20): 8214-8227.

Attwell, D., B. Barbour, et al. (1993). "Nonvesicular release of neurotransmitter." Neuron **11**(3): 401-407.

Babb, T. L., W. R. Kupfer, et al. (1991). "Synaptic reorganization by mossy fibers in human epileptic fascia dentata." Neuroscience **42**(2): 351-363.

Babb, T. L., N. Mikuni, et al. (2005). "Pre- and postnatal expressions of NMDA receptors 1 and 2B subunit proteins in the normal rat cortex." Epilepsy Res **64**(1-2): 23-30.

Babcock, M., G. T. Macleod, et al. (2004). "Genetic analysis of soluble N-ethylmaleimide-sensitive factor attachment protein function in Drosophila reveals positive and negative secretory roles." J Neurosci **24**(16): 3964-3973.

Bacci, A., G. Sancini, et al. (2002). "Block of glutamate-glutamine cycle between astrocytes and neurons inhibits epileptiform activity in hippocampus." J Neurophysiol **88**(5): 2302-2310.

Bains, J. S., J. M. Longacher, et al. (1999). "Reciprocal interactions between CA3 network activity and strength of recurrent collateral synapses." Nat Neurosci **2**(8): 720-726.

Banks, M. I. and R. A. Pearce (2000). "Kinetic differences between synaptic and extrasynaptic GABA(A) receptors in CA1 pyramidal cells." J Neurosci **20**(3): 937-948.

Baraban, S. C. and M. K. Tallent (2004). "Interneuron Diversity series: Interneuronal neuropeptides--endogenous regulators of neuronal excitability." Trends Neurosci **27**(3): 135-142.

Bargmann, C. I. (1998). "Neurobiology of the Caenorhabditis elegans genome." Science **282**(5396): 2028-2033.

Barres, B. A. (2008). "The mystery and magic of glia: a perspective on their roles in health and disease." Neuron **60**(3): 430-440.

Barszczewski, M., J. J. Chua, et al. (2008). "A novel site of action for alpha-SNAP in the SNARE conformational cycle controlling membrane fusion." Mol Biol Cell **19**(3): 776-784.

Bartos, M., I. Vida, et al. (2001). "Rapid signaling at inhibitory synapses in a dentate gyrus interneuron network." J Neurosci **21**(8): 2687-2698.

Bartos, M., I. Vida, et al. (2002). "Fast synaptic inhibition promotes synchronized gamma oscillations in hippocampal interneuron networks." Proc Natl Acad Sci U S A **99**(20): 13222-13227.

Bartos, M., I. Vida, et al. (2007). "Synaptic mechanisms of synchronized gamma oscillations in inhibitory interneuron networks." Nat Rev Neurosci **8**(1): 45-56.

Ben-Ari, Y. (2001). "Developing networks play a similar melody." Trends Neurosci **24**(6): 353-360.

Ben-Ari, Y., J. L. Gaiarsa, et al. (2007). "GABA: a pioneer transmitter that excites immature neurons and generates primitive oscillations." Physiol Rev **87**(4): 1215-1284.

Ben-Ari, Y., R. Khazipov, et al. (1997). "GABAA, NMDA and AMPA receptors: a developmentally regulated 'menage a trois'." Trends Neurosci **20**(11): 523-529.

Benson, D. L., F. H. Watkins, et al. (1994). "Characterization of GABAergic neurons in hippocampal cell cultures." J Neurocytol **23**(5): 279-295.

Berke, J. D., V. Hetrick, et al. (2008). "Transient 23-30 Hz oscillations in mouse hippocampus during exploration of novel environments." Hippocampus **18**(5): 519-529.

Biederer, T., Y. Sara, et al. (2002). "SynCAM, a synaptic adhesion molecule that drives synapse assembly." Science **297**(5586): 1525-1531.

Blake, J. F., M. W. Brown, et al. (1988). "CNQX blocks acidic amino acid induced depolarizations and synaptic components mediated by non-NMDA receptors in rat hippocampal slices." Neurosci Lett **89**(2): 182-186.

Blomgren, K., C. Zhu, et al. (2001). "Synergistic activation of caspase-3 by m-calpain after neonatal hypoxia-ischemia: a mechanism of "pathological apoptosis"?" J Biol Chem **276**(13): 10191-10198.

Boal, F., M. Laguerre, et al. (2010). "A charged prominence in the linker domain of the cysteine-string protein Csp{alpha} mediates its regulated interaction with the calcium sensor synaptotagmin 9 during exocytosis." FASEB J.

Boal, F., H. Zhang, et al. (2004). "The variable C-terminus of cysteine string proteins modulates exocytosis and protein-protein interactions." Biochemistry **43**(51): 16212-16223.

Boehler, M. D., B. C. Wheeler, et al. (2007). "Added astroglia promote greater synapse density and higher activity in neuronal networks." Neuron Glia Biol **3**: 127-140.

Bollmann, J. H., B. Sakmann, et al. (2000). "Calcium sensitivity of glutamate release in a calyx-type terminal." Science **289**(5481): 953-957.

Borck, C. and J. G. Jefferys (1999). "Seizure-like events in disinhibited ventral slices of adult rat hippocampus." J Neurophysiol **82**(5): 2130-2142.

Braun, J. E., S. M. Wilbanks, et al. (1996). "The cysteine string secretory vesicle protein activates Hsc70 ATPase." J Biol Chem **271**(42): 25989-25993.

Brecht, M., W. Singer, et al. (1998). "Correlation analysis of corticotectal interactions in the cat visual system." J Neurophysiol **79**(5): 2394-2407.

Bredt, D. S. and R. A. Nicoll (2003). "AMPA receptor trafficking at excitatory synapses." Neuron **40**(2): 361-379.

Brewer, G. J. (1997). "Isolation and culture of adult rat hippocampal neurons." J Neurosci Methods **71**(2): 143-155.

Brickley, S. G., S. G. Cull-Candy, et al. (1996). "Development of a tonic form of synaptic inhibition in rat cerebellar granule cells resulting from persistent activation of GABAA receptors." J Physiol **497 (Pt 3)**: 753-759.

Brickley, S. G., S. G. Cull-Candy, et al. (1999). "Single-channel properties of synaptic and extrasynaptic GABAA receptors suggest differential targeting of receptor subtypes." J Neurosci **19**(8): 2960-2973.

Briggs, C. A. and D. G. McKenna (1996). "Effect of MK-801 at the human alpha 7 nicotinic acetylcholine receptor." Neuropharmacology **35**(4): 407-414.

Brodin, L., P. Low, et al. (2000). "Sequential steps in clathrin-mediated synaptic vesicle endocytosis." Curr Opin Neurobiol **10**(3): 312-320.

Bronk, P., J. J. Wenniger, et al. (2001). "Drosophila Hsc70-4 is critical for neurotransmitter exocytosis in vivo." Neuron **30**(2): 475-488.

Brose, N., A. G. Petrenko, et al. (1992). "Synaptotagmin: a calcium sensor on the synaptic vesicle surface." Science **256**(5059): 1021-1025.

Brown, H., O. Larsson, et al. (1998). "Cysteine string protein (CSP) is an insulin secretory granule-associated protein regulating beta-cell exocytosis." EMBO J **17**(17): 5048-5058.

Brusa, R., F. Zimmermann, et al. (1995). "Early-onset epilepsy and postnatal lethality associated with an editing-deficient GluR-B allele in mice." Science **270**(5242): 1677-1680.

Bucurenciu, I., A. Kulik, et al. (2008). "Nanodomain coupling between Ca2+ channels and Ca2+ sensors promotes fast and efficient transmitter release at a cortical GABAergic synapse." Neuron **57**(4): 536-545.

Budd, S. L. and D. G. Nicholls (1996). "Mitochondria, calcium regulation, and acute glutamate excitotoxicity in cultured cerebellar granule cells." J Neurochem **67**(6): 2282-2291.

Buhl, D. L., K. D. Harris, et al. (2003). "Selective impairment of hippocampal gamma oscillations in connexin-36 knock-out mouse in vivo." J Neurosci **23**(3): 1013-1018.

Buki, A., D. O. Okonkwo, et al. (2000). "Cytochrome c release and caspase activation in traumatic axonal injury." J Neurosci **20**(8): 2825-2834.

Burgoyne, R. D., J. W. Barclay, et al. (2009). "The functions of Munc18-1 in regulated exocytosis." Ann N Y Acad Sci **1152**: 76-86.

Burgoyne, R. D. and A. Morgan (1995). "Ca2+ and secretory-vesicle dynamics." Trends Neurosci **18**(4): 191-196.

Burre, J., M. Sharma, et al. (2010). "{alpha}-Synuclein Promotes SNARE-Complex Assembly in Vivo and in Vitro." Science.

Butovsky, O., A. E. Talpalar, et al. (2005). "Activation of microglia by aggregated beta-amyloid or lipopolysaccharide impairs MHC-II expression and renders them cytotoxic whereas IFN-gamma and IL-4 render them protective." Mol Cell Neurosci **29**(3): 381-393.

Buzsaki, G. (2002). "Theta oscillations in the hippocampus." Neuron **33**(3): 325-340.

Buzsaki, G. and J. J. Chrobak (1995). "Temporal structure in spatially organized neuronal ensembles: a role for interneuronal networks." Curr Opin Neurobiol **5**(4): 504-510.

Cantero, J. L., M. Atienza, et al. (2003). "Sleep-dependent theta oscillations in the human hippocampus and neocortex." J Neurosci **23**(34): 10897-10903.

Cardona, A. E., E. P. Pioro, et al. (2006). "Control of microglial neurotoxicity by the fractalkine receptor." Nat Neurosci **9**(7): 917-924.

Carlin, R. K., D. J. Grab, et al. (1980). "Isolation and characterization of postsynaptic densities from various brain regions: enrichment of different types of postsynaptic densities." J Cell Biol **86**(3): 831-845.

Castillo, P. E., R. C. Malenka, et al. (1997). "Kainate receptors mediate a slow postsynaptic current in hippocampal CA3 neurons." Nature **388**(6638): 182-186.

Cavara, N. A. and M. Hollmann (2008). "Shuffling the deck anew: how NR3 tweaks NMDA receptor function." Mol Neurobiol **38**(1): 16-26.

Cepeda, C., R. S. Hurst, et al. (2003). "Transient and progressive electrophysiological alterations in the corticostriatal pathway in a mouse model of Huntington's disease." J Neurosci **23**(3): 961-969.

Chad, J. E. and R. Eckert (1984). "Calcium domains associated with individual channels can account for anomalous voltage relations of CA-dependent responses." Biophys J **45**(5): 993-999.

Chamberlain, L. H. and R. D. Burgoyne (1997). "The molecular chaperone function of the secretory vesicle cysteine string proteins." J Biol Chem **272**(50): 31420-31426.

Chamberlain, L. H. and R. D. Burgoyne (1998). "The cysteine-string domain of the secretory vesicle cysteine-string protein is required for membrane targeting." Biochem J **335 (Pt 2)**: 205-209.

Chamberlain, L. H. and R. D. Burgoyne (1998). "Cysteine string protein functions directly in regulated exocytosis." Mol Biol Cell **9**(8): 2259-2267.

Chandra, S., G. Gallardo, et al. (2005). "Alpha-synuclein cooperates with CSPalpha in preventing neurodegeneration." Cell **123**(3): 383-396.

Chapman, E. R., P. I. Hanson, et al. (1995). "Ca2+ regulates the interaction between synaptotagmin and syntaxin 1." J Biol Chem **270**(40): 23667-23671.
Charvin, N., C. L'Eveque, et al. (1997). "Direct interaction of the calcium sensor protein synaptotagmin I with a cytoplasmic domain of the alpha1A subunit of the P/Q-type calcium channel." EMBO J **16**(15): 4591-4596.
Chatterton, J. E., M. Awobuluyi, et al. (2002). "Excitatory glycine receptors containing the NR3 family of NMDA receptor subunits." Nature **415**(6873): 793-798.
Chaudhry, F. A., R. J. Reimer, et al. (1998). "The vesicular GABA transporter, VGAT, localizes to synaptic vesicles in sets of glycinergic as well as GABAergic neurons." J Neurosci **18**(23): 9733-9750.
Chen, M., T. J. Lu, et al. (2008). "Differential roles of NMDA receptor subtypes in ischemic neuronal cell death and ischemic tolerance." Stroke **39**(11): 3042-3048.
Chen, X., D. R. Tomchick, et al. (2002). "Three-dimensional structure of the complexin/SNARE complex." Neuron **33**(3): 397-409.
Chen, Y. A., S. J. Scales, et al. (1999). "SNARE complex formation is triggered by Ca2+ and drives membrane fusion." Cell **97**(2): 165-174.
Chen, Y. A., S. J. Scales, et al. (2001). "Sequential SNARE assembly underlies priming and triggering of exocytosis." Neuron **30**(1): 161-170.
Chiappalone, M., M. Bove, et al. (2006). "Dissociated cortical networks show spontaneously correlated activity patterns during in vitro development." Brain Res **1093**(1): 41-53.
Chicurel, M. E. and K. M. Harris (1992). "Three-dimensional analysis of the structure and composition of CA3 branched dendritic spines and their synaptic relationships with mossy fiber boutons in the rat hippocampus." J Comp Neurol **325**(2): 169-182.
Chiel, H. J. and R. D. Beer (1997). "The brain has a body: adaptive behavior emerges from interactions of nervous system, body and environment." Trends Neurosci **20**(12): 553-557.
Chih, B., H. Engelman, et al. (2005). "Control of excitatory and inhibitory synapse formation by neuroligins." Science **307**(5713): 1324-1328.
Chittajallu, R., M. Vignes, et al. (1996). "Regulation of glutamate release by presynaptic kainate receptors in the hippocampus." Nature **379**(6560): 78-81.
Choi, D. W. (1985). "Glutamate neurotoxicity in cortical cell culture is calcium dependent." Neurosci Lett **58**(3): 293-297.
Choi, D. W., J. Y. Koh, et al. (1988). "Pharmacology of glutamate neurotoxicity in cortical cell culture: attenuation by NMDA antagonists." J Neurosci **8**(1): 185-196.
Choi, D. W., M. Maulucci-Gedde, et al. (1987). "Glutamate neurotoxicity in cortical cell culture." J Neurosci **7**(2): 357-368.
Chow, S. K., D. Yu, et al. (2009). "Amyloid-beta directly induces spontaneous calcium transients, delayed intercellular calcium waves, and gliosis in rat cortical astrocytes." ASN Neuro.
Chowdhury, S., J. D. Shepherd, et al. (2006). "Arc/Arg3.1 interacts with the endocytic machinery to regulate AMPA receptor trafficking." Neuron **52**(3): 445-459.
Christie, J. M. and C. E. Jahr (2006). "Multivesicular release at Schaffer collateral-CA1 hippocampal synapses." J Neurosci **26**(1): 210-216.
Christopherson, K. S., E. M. Ullian, et al. (2005). "Thrombospondins are astrocyte-secreted proteins that promote CNS synaptogenesis." Cell **120**(3): 421-433.

Chua, J. J., S. Kindler, et al. (2010). "The architecture of an excitatory synapse." J Cell Sci **123**(Pt 6): 819-823.
Chubykin, A. A., D. Atasoy, et al. (2007). "Activity-dependent validation of excitatory versus inhibitory synapses by neuroligin-1 versus neuroligin-2." Neuron **54**(6): 919-931.
Chudotvorova, I., A. Ivanov, et al. (2005). "Early expression of KCC2 in rat hippocampal cultures augments expression of functional GABA synapses." J Physiol **566**(Pt 3): 671-679.
Chuhma, N. and H. Ohmori (1998). "Postnatal development of phase-locked high-fidelity synaptic transmission in the medial nucleus of the trapezoid body of the rat." J Neurosci **18**(1): 512-520.
Chung, H. J., J. Xia, et al. (2000). "Phosphorylation of the AMPA receptor subunit GluR2 differentially regulates its interaction with PDZ domain-containing proteins." J Neurosci **20**(19): 7258-7267.
Clarke, V. R., B. A. Ballyk, et al. (1997). "A hippocampal GluR5 kainate receptor regulating inhibitory synaptic transmission." Nature **389**(6651): 599-603.
Clary, D. O., I. C. Griff, et al. (1990). "SNAPs, a family of NSF attachment proteins involved in intracellular membrane fusion in animals and yeast." Cell **61**(4): 709-721.
Cobb, S. R., E. H. Buhl, et al. (1995). "Synchronization of neuronal activity in hippocampus by individual GABAergic interneurons." Nature **378**(6552): 75-78.
Cobos, I., M. E. Calcagnotto, et al. (2005). "Mice lacking Dlx1 show subtype-specific loss of interneurons, reduced inhibition and epilepsy." Nat Neurosci **8**(8): 1059-1068.
Cohen, R., L. A. Elferink, et al. (2003). "The C2A domain of synaptotagmin alters the kinetics of voltage-gated Ca2+ channels Ca(v)1.2 (Lc-type) and Ca(v)2.3 (R-type)." J Biol Chem **278**(11): 9258-9266.
Coleman, P. D. and P. J. Yao (2003). "Synaptic slaughter in Alzheimer's disease." Neurobiol Aging **24**(8): 1023-1027.
Collin, T., M. Chat, et al. (2005). "Developmental changes in parvalbumin regulate presynaptic Ca2+ signaling." J Neurosci **25**(1): 96-107.
Cope, D. W., S. W. Hughes, et al. (2005). "GABAA receptor-mediated tonic inhibition in thalamic neurons." J Neurosci **25**(50): 11553-11563.
Cossart, R., R. Tyzio, et al. (2001). "Presynaptic kainate receptors that enhance the release of GABA on CA1 hippocampal interneurons." Neuron **29**(2): 497-508.
Crepel, V., D. Aronov, et al. (2007). "A parturition-associated nonsynaptic coherent activity pattern in the developing hippocampus." Neuron **54**(1): 105-120.
Csicsvari, J., H. Hirase, et al. (1999). "Oscillatory coupling of hippocampal pyramidal cells and interneurons in the behaving Rat." J Neurosci **19**(1): 274-287.
Csicsvari, J., H. Hirase, et al. (2000). "Ensemble patterns of hippocampal CA3-CA1 neurons during sharp wave-associated population events." Neuron **28**(2): 585-594.
Csicsvari, J., B. Jamieson, et al. (2003). "Mechanisms of gamma oscillations in the hippocampus of the behaving rat." Neuron **37**(2): 311-322.
Cukierman, E., R. Pankov, et al. (2001). "Taking cell-matrix adhesions to the third dimension." Science **294**(5547): 1708-1712.
Cunningham, C., R. Deacon, et al. (2003). "Synaptic changes characterize early behavioural signs in the ME7 model of murine prion disease." Eur J Neurosci **17**(10): 2147-2155.

Dahlhaus, R., R. M. Hines, et al. (2010). "Overexpression of the cell adhesion protein neuroligin-1 induces learning deficits and impairs synaptic plasticity by altering the ratio of excitation to inhibition in the hippocampus." Hippocampus **20**(2): 305-322.

Dai, H., O. H. Shin, et al. (2004). "Structural basis for the evolutionary inactivation of Ca2+ binding to synaptotagmin 4." Nat Struct Mol Biol **11**(9): 844-849.

Damoiseaux, J. G., E. A. Dopp, et al. (1994). "Rat macrophage lysosomal membrane antigen recognized by monoclonal antibody ED1." Immunology **83**(1): 140-147.

Danysz, W. and C. G. Parsons (2003). "The NMDA receptor antagonist memantine as a symptomatological and neuroprotective treatment for Alzheimer's disease: preclinical evidence." Int J Geriatr Psychiatry **18**(Suppl 1): S23-32.

Davis, A. F., J. Bai, et al. (1999). "Kinetics of synaptotagmin responses to Ca2+ and assembly with the core SNARE complex onto membranes." Neuron **24**(2): 363-376.

Dawson-Scully, K., P. Bronk, et al. (2000). "Cysteine-string protein increases the calcium sensitivity of neurotransmitter exocytosis in Drosophila." J Neurosci **20**(16): 6039-6047.

Dawson-Scully, K., Y. Lin, et al. (2007). "Morphological and functional effects of altered cysteine string protein at the Drosophila larval neuromuscular junction." Synapse **61**(1): 1-16.

Dawson, V. L., V. M. Kizushi, et al. (1996). "Resistance to neurotoxicity in cortical cultures from neuronal nitric oxide synthase-deficient mice." J Neurosci **16**(8): 2479-2487.

de Lecea, L., J. A. del Rio, et al. (1995). "Developmental expression of parvalbumin mRNA in the cerebral cortex and hippocampus of the rat." Brain Res Mol Brain Res **32**(1): 1-13.

de Wit, H. (2010). "Molecular mechanism of secretory vesicle docking." Biochem Soc Trans **38**(Pt 1): 192-198.

Deak, F., Y. Xu, et al. (2009). "Munc18-1 binding to the neuronal SNARE complex controls synaptic vesicle priming." J Cell Biol **184**(5): 751-764.

Dean, C., F. G. Scholl, et al. (2003). "Neurexin mediates the assembly of presynaptic terminals." Nat Neurosci **6**(7): 708-716.

Debanne, D., B. H. Gahwiler, et al. (1998). "Long-term synaptic plasticity between pairs of individual CA3 pyramidal cells in rat hippocampal slice cultures." J Physiol **507 (Pt 1)**: 237-247.

Debanne, D., N. C. Guerineau, et al. (1995). "Physiology and pharmacology of unitary synaptic connections between pairs of cells in areas CA3 and CA1 of rat hippocampal slice cultures." J Neurophysiol **73**(3): 1282-1294.

del Cerro, S., A. Arai, et al. (1994). "Stimulation of NMDA receptors activates calpain in cultured hippocampal slices." Neurosci Lett **167**(1-2): 149-152.

Demir, R., B. X. Gao, et al. (2002). "Interactions between multiple rhythm generators produce complex patterns of oscillation in the developing rat spinal cord." J Neurophysiol **87**(2): 1094-1105.

Dick, O., S. tom Dieck, et al. (2003). "The presynaptic active zone protein bassoon is essential for photoreceptor ribbon synapse formation in the retina." Neuron **37**(5): 775-786.

Dietrich, D., T. Kirschstein, et al. (2003). "Functional specialization of presynaptic Cav2.3 Ca2+ channels." Neuron **39**(3): 483-496.

Distler, P. G. and R. T. Robertson (1993). "Formation of synapses between basal forebrain afferents and cerebral cortex neurons: an electron microscopic study in organotypic slice cultures." J Neurocytol **22**(8): 627-643.

Dityatev, A., G. Dityateva, et al. (2000). "Synaptic strength as a function of post- versus presynaptic expression of the neural cell adhesion molecule NCAM." Neuron **26**(1): 207-217.

Doischer, D., J. A. Hosp, et al. (2008). "Postnatal differentiation of basket cells from slow to fast signaling devices." J Neurosci **28**(48): 12956-12968.

Dong, H., P. Zhang, et al. (1999). "Characterization of the glutamate receptor-interacting proteins GRIP1 and GRIP2." J Neurosci **19**(16): 6930-6941.

Dulubova, I., M. Khvotchev, et al. (2007). "Munc18-1 binds directly to the neuronal SNARE complex." Proc Natl Acad Sci U S A **104**(8): 2697-2702.

Dupree, J. L., J. L. Mason, et al. (2004). "Oligodendrocytes assist in the maintenance of sodium channel clusters independent of the myelin sheath." Neuron Glia Biol **1**(3): 179-192.

Dux, E., U. Oschlies, et al. (1996). "Serum prevents glutamate-induced mitochondrial calcium accumulation in primary neuronal cultures." Acta Neuropathol **92**(3): 264-272.

Egebjerg, J. and S. F. Heinemann (1993). "Ca2+ permeability of unedited and edited versions of the kainate selective glutamate receptor GluR6." Proc Natl Acad Sci U S A **90**(2): 755-759.

Egert, U., B. Schlosshauer, et al. (1998). "A novel organotypic long-term culture of the rat hippocampus on substrate-integrated multielectrode arrays." Brain Res Brain Res Protoc **2**(4): 229-242.

Elfant, D., B. Z. Pal, et al. (2008). "Specific inhibitory synapses shift the balance from feedforward to feedback inhibition of hippocampal CA1 pyramidal cells." Eur J Neurosci **27**(1): 104-113.

Eng, L. F., R. S. Ghirnikar, et al. (2000). "Glial fibrillary acidic protein: GFAP-thirty-one years (1969-2000)." Neurochem Res **25**(9-10): 1439-1451.

Esteban, J. A., S. H. Shi, et al. (2003). "PKA phosphorylation of AMPA receptor subunits controls synaptic trafficking underlying plasticity." Nat Neurosci **6**(2): 136-143.

Evans, G. J. and A. Morgan (2002). "Phosphorylation-dependent interaction of the synaptic vesicle proteins cysteine string protein and synaptotagmin I." Biochem J **364**(Pt 2): 343-347.

Evans, G. J., M. C. Wilkinson, et al. (2001). "Phosphorylation of cysteine string protein by protein kinase A. Implications for the modulation of exocytosis." J Biol Chem **276**(51): 47877-47885.

Fasshauer, D. (2003). "Structural insights into the SNARE mechanism." Biochim Biophys Acta **1641**(2-3): 87-97.

Fedchyshyn, M. J. and L. Y. Wang (2005). "Developmental transformation of the release modality at the calyx of Held synapse." J Neurosci **25**(16): 4131-4140.

Fellin, T., O. Pascual, et al. (2004). "Neuronal synchrony mediated by astrocytic glutamate through activation of extrasynaptic NMDA receptors." Neuron **43**(5): 729-743.

Fernandez-Chacon, R., A. Konigstorfer, et al. (2001). "Synaptotagmin I functions as a calcium regulator of release probability." Nature **410**(6824): 41-49.

Fernandez-Chacon, R. and T. C. Sudhof (1999). "Genetics of synaptic vesicle function: toward the complete functional anatomy of an organelle." Annu Rev Physiol **61**: 753-776.

Fernandez-Chacon, R., M. Wolfel, et al. (2004). "The synaptic vesicle protein CSP alpha prevents presynaptic degeneration." Neuron **42**(2): 237-251.
Flint, A. C., U. S. Maisch, et al. (1997). "NR2A subunit expression shortens NMDA receptor synaptic currents in developing neocortex." J Neurosci **17**(7): 2469-2476.
Foster, A. C. and E. H. Wong (1987). "The novel anticonvulsant MK-801 binds to the activated state of the N-methyl-D-aspartate receptor in rat brain." Br J Pharmacol **91**(2): 403-409.
Fox, M. A. and J. R. Sanes (2007). "Synaptotagmin I and II are present in distinct subsets of central synapses." J Comp Neurol **503**(2): 280-296.
Frassoni, C., F. Inverardi, et al. (2005). "Analysis of SNAP-25 immunoreactivity in hippocampal inhibitory neurons during development in culture and in situ." Neuroscience **131**(4): 813-823.
Frerking, M., J. Schulte, et al. (2005). "Spike timing in CA3 pyramidal cells during behavior: implications for synaptic transmission." J Neurophysiol **94**(2): 1528-1540.
Freund, T. F. and G. Buzsaki (1996). "Interneurons of the hippocampus." Hippocampus **6**(4): 347-470.
Frey, D., C. Schneider, et al. (2000). "Early and selective loss of neuromuscular synapse subtypes with low sprouting competence in motoneuron diseases." J Neurosci **20**(7): 2534-2542.
Fu, Z., P. Washbourne, et al. (2003). "Functional excitatory synapses in HEK293 cells expressing neuroligin and glutamate receptors." J Neurophysiol **90**(6): 3950-3957.
Fuchs, E. C., H. Doheny, et al. (2001). "Genetically altered AMPA-type glutamate receptor kinetics in interneurons disrupt long-range synchrony of gamma oscillation." Proc Natl Acad Sci U S A **98**(6): 3571-3576.
Fuchs, E. C., A. R. Zivkovic, et al. (2007). "Recruitment of parvalbumin-positive interneurons determines hippocampal function and associated behavior." Neuron **53**(4): 591-604.
Fuhrmann, M., G. Mitteregger, et al. (2007). "Dendritic pathology in prion disease starts at the synaptic spine." J Neurosci **27**(23): 6224-6233.
Fukuda, T. and T. Kosaka (2000). "Gap junctions linking the dendritic network of GABAergic interneurons in the hippocampus." J Neurosci **20**(4): 1519-1528.
Futai, K., M. J. Kim, et al. (2007). "Retrograde modulation of presynaptic release probability through signaling mediated by PSD-95-neuroligin." Nat Neurosci **10**(2): 186-195.
Gage, F. H., P. W. Coates, et al. (1995). "Survival and differentiation of adult neuronal progenitor cells transplanted to the adult brain." Proc Natl Acad Sci U S A **92**(25): 11879-11883.
Gahwiler, B. H., M. Capogna, et al. (1997). "Organotypic slice cultures: a technique has come of age." Trends Neurosci **20**(10): 471-477.
Galarreta, M. and S. Hestrin (2002). "Electrical and chemical synapses among parvalbumin fast-spiking GABAergic interneurons in adult mouse neocortex." Proc Natl Acad Sci U S A **99**(19): 12438-12443.
Galea, E., D. L. Feinstein, et al. (1992). "Induction of calcium-independent nitric oxide synthase activity in primary rat glial cultures." Proc Natl Acad Sci U S A **89**(22): 10945-10949.
Gandhi, S. P. and C. F. Stevens (2003). "Three modes of synaptic vesicular recycling revealed by single-vesicle imaging." Nature **423**(6940): 607-613.

Garcia-Junco-Clemente, P., G. Cantero, et al. (2010). "Cysteine string protein-alpha prevents activity-dependent degeneration in GABAergic synapses." J Neurosci **30**(21): 7377-7391.

Gauthier, S., Y. Wirth, et al. (2005). "Effects of memantine on behavioural symptoms in Alzheimer's disease patients: an analysis of the Neuropsychiatric Inventory (NPI) data of two randomised, controlled studies." Int J Geriatr Psychiatry **20**(5): 459-464.

Geiger, J. R., J. Lubke, et al. (1997). "Submillisecond AMPA receptor-mediated signaling at a principal neuron-interneuron synapse." Neuron **18**(6): 1009-1023.

Geiger, J. R., T. Melcher, et al. (1995). "Relative abundance of subunit mRNAs determines gating and Ca2+ permeability of AMPA receptors in principal neurons and interneurons in rat CNS." Neuron **15**(1): 193-204.

Gerber, S. H., J. C. Rah, et al. (2008). "Conformational switch of syntaxin-1 controls synaptic vesicle fusion." Science **321**(5895): 1507-1510.

Gerona, R. R., E. C. Larsen, et al. (2000). "The C terminus of SNAP25 is essential for Ca(2+)-dependent binding of synaptotagmin to SNARE complexes." J Biol Chem **275**(9): 6328-6336.

Ghosh, A. and M. E. Greenberg (1995). "Distinct roles for bFGF and NT-3 in the regulation of cortical neurogenesis." Neuron **15**(1): 89-103.

Ghoumari, A. M., C. Ibanez, et al. (2003). "Progesterone and its metabolites increase myelin basic protein expression in organotypic slice cultures of rat cerebellum." J Neurochem **86**(4): 848-859.

Gibson, J. R., K. M. Huber, et al. (2009). "Neuroligin-2 deletion selectively decreases inhibitory synaptic transmission originating from fast-spiking but not from somatostatin-positive interneurons." J Neurosci **29**(44): 13883-13897.

Giordana, M. T., A. Attanasio, et al. (1994). "Reactive cell proliferation and microglia following injury to the rat brain." Neuropathol Appl Neurobiol **20**(2): 163-174.

Giorgi, C., G. W. Yeo, et al. (2007). "The EJC factor eIF4AIII modulates synaptic strength and neuronal protein expression." Cell **130**(1): 179-191.

Giraudo, C. G., W. S. Eng, et al. (2006). "A clamping mechanism involved in SNARE-dependent exocytosis." Science **313**(5787): 676-680.

Goda, Y. and C. F. Stevens (1994). "Two components of transmitter release at a central synapse." Proc Natl Acad Sci U S A **91**(26): 12942-12946.

Gonzalez-Burgos, G., T. Hashimoto, et al. (2010). "Alterations of cortical GABA neurons and network oscillations in schizophrenia." Curr Psychiatry Rep **12**(4): 335-344.

Gonzalez-Burgos, G. and D. A. Lewis (2008). "GABA neurons and the mechanisms of network oscillations: implications for understanding cortical dysfunction in schizophrenia." Schizophr Bull **34**(5): 944-961.

Gorgulu, A., T. Kins, et al. (2000). "Reduction of edema and infarction by Memantine and MK-801 after focal cerebral ischaemia and reperfusion in rat." Acta Neurochir (Wien) **142**(11): 1287-1292.

Gottmann, K. (2008). "Transsynaptic modulation of the synaptic vesicle cycle by cell-adhesion molecules." J Neurosci Res **86**(2): 223-232.

Guan, R., H. Dai, et al. (2008). "Binding of the Munc13-1 MUN domain to membrane-anchored SNARE complexes." Biochemistry **47**(6): 1474-1481.

Gutierrez, R., V. Armand, et al. (1999). "Epileptiform activity induced by low Mg2+ in cultured rat hippocampal slices." Brain Res **815**(2): 294-303.

Gutierrez, R. and U. Heinemann (1999). "Synaptic reorganization in explanted cultures of rat hippocampus." Brain Res **815**(2): 304-316.
Gutierrez, R. C., J. Hung, et al. (2009). "Altered synchrony and connectivity in neuronal networks expressing an autism-related mutation of neuroligin 3." Neuroscience **162**(1): 208-221.
Hagler, D. J., Jr. and Y. Goda (2001). "Properties of synchronous and asynchronous release during pulse train depression in cultured hippocampal neurons." J Neurophysiol **85**(6): 2324-2334.
Halassa, M. M., T. Fellin, et al. (2007). "The tripartite synapse: roles for gliotransmission in health and disease." Trends Mol Med **13**(2): 54-63.
Hall, D. H. and R. L. Russell (1991). "The posterior nervous system of the nematode Caenorhabditis elegans: serial reconstruction of identified neurons and complete pattern of synaptic interactions." J Neurosci **11**(1): 1-22.
Hammarlund, M., M. T. Palfreyman, et al. (2007). "Open syntaxin docks synaptic vesicles." PLoS Biol **5**(8): e198.
Hanley, J. G. and J. M. Henley (2005). "PICK1 is a calcium-sensor for NMDA-induced AMPA receptor trafficking." EMBO J **24**(18): 3266-3278.
Hanley, L. J. and J. M. Henley (2010). "Differential roles of GRIP1a and GRIP1b in AMPA receptor trafficking." Neurosci Lett.
Hardingham, G. E., F. J. Arnold, et al. (2001). "Nuclear calcium signaling controls CREB-mediated gene expression triggered by synaptic activity." Nat Neurosci **4**(3): 261-267.
Hardingham, G. E. and H. Bading (2002). "Coupling of extrasynaptic NMDA receptors to a CREB shut-off pathway is developmentally regulated." Biochim Biophys Acta **1600**(1-2): 148-153.
Hardingham, G. E. and H. Bading (2010). "Synaptic versus extrasynaptic NMDA receptor signalling: implications for neurodegenerative disorders." Nat Rev Neurosci **11**(10): 682-696.
Hardingham, G. E., Y. Fukunaga, et al. (2002). "Extrasynaptic NMDARs oppose synaptic NMDARs by triggering CREB shut-off and cell death pathways." Nat Neurosci **5**(5): 405-414.
Hartley, D. M. and D. W. Choi (1989). "Delayed rescue of N-methyl-D-aspartate receptor-mediated neuronal injury in cortical culture." J Pharmacol Exp Ther **250**(2): 752-758.
Hata, Y., C. A. Slaughter, et al. (1993). "Synaptic vesicle fusion complex contains unc-18 homologue bound to syntaxin." Nature **366**(6453): 347-351.
Hatten, M. E., W. Q. Gao, et al. (1998). Chapter 16: The Cerebellum: Purification and Coculture of Identified Cell populations. Book Culturing nerve cells. Cambridge, Mass., MIT Press.
Hayashi, M., A. Raimondi, et al. (2008). "Cell- and stimulus-dependent heterogeneity of synaptic vesicle endocytic recycling mechanisms revealed by studies of dynamin 1-null neurons." Proc Natl Acad Sci U S A **105**(6): 2175-2180.
Hayman, M. W., K. H. Smith, et al. (2004). "Enhanced neurite outgrowth by human neurons grown on solid three-dimensional scaffolds." Biochem Biophys Res Commun **314**(2): 483-488.
Hayman, M. W., K. H. Smith, et al. (2005). "Growth of human stem cell-derived neurons on solid three-dimensional polymers." J Biochem Biophys Methods **62**(3): 231-240.

Heckmann, M., H. Adelsberger, et al. (1997). "Evoked transmitter release at neuromuscular junctions in wild type and cysteine string protein null mutant larvae of Drosophila." Neurosci Lett **228**(3): 167-170.

Hefft, S. and P. Jonas (2005). "Asynchronous GABA release generates long-lasting inhibition at a hippocampal interneuron-principal neuron synapse." Nat Neurosci **8**(10): 1319-1328.

Hermann, J., M. Pecka, et al. (2007). "Synaptic transmission at the calyx of Held under in vivo like activity levels." J Neurophysiol **98**(2): 807-820.

Hoek, R. M., S. R. Ruuls, et al. (2000). "Down-regulation of the macrophage lineage through interaction with OX2 (CD200)." Science **290**(5497): 1768-1771.

Hofmann, F. and H. Bading (2006). "Long term recordings with microelectrode arrays: studies of transcription-dependent neuronal plasticity and axonal regeneration." J Physiol Paris **99**(2-3): 125-132.

Holstein, S. E., H. Ungewickell, et al. (1996). "Mechanism of clathrin basket dissociation: separate functions of protein domains of the DnaJ homologue auxilin." J Cell Biol **135**(4): 925-937.

Honda, S., Y. Sasaki, et al. (2001). "Extracellular ATP or ADP induce chemotaxis of cultured microglia through Gi/o-coupled P2Y receptors." J Neurosci **21**(6): 1975-1982.

Hormuzdi, S. G., I. Pais, et al. (2001). "Impaired electrical signaling disrupts gamma frequency oscillations in connexin 36-deficient mice." Neuron **31**(3): 487-495.

Huettner, J. E. and R. W. Baughman (1986). "Primary culture of identified neurons from the visual cortex of postnatal rats." J Neurosci **6**(10): 3044-3060.

Hume, R. I., R. Dingledine, et al. (1991). "Identification of a site in glutamate receptor subunits that controls calcium permeability." Science **253**(5023): 1028-1031.

Hussman, J. P. (2001). "Suppressed GABAergic inhibition as a common factor in suspected etiologies of autism." J Autism Dev Disord **31**(2): 247-248.

Ichikawa, M., K. Muramoto, et al. (1993). "Formation and maturation of synapses in primary cultures of rat cerebral cortical cells: an electron microscopic study." Neurosci Res **16**(2): 95-103.

Iida, J., S. Hirabayashi, et al. (2004). "Synaptic scaffolding molecule is involved in the synaptic clustering of neuroligin." Mol Cell Neurosci **27**(4): 497-508.

Innocenti, B., V. Parpura, et al. (2000). "Imaging extracellular waves of glutamate during calcium signaling in cultured astrocytes." Journal of Neuroscience **20**(5): 1800-1808.

Isokawa, M., M. F. Levesque, et al. (1993). "Single mossy fiber axonal systems of human dentate granule cells studied in hippocampal slices from patients with temporal lobe epilepsy." J Neurosci **13**(4): 1511-1522.

Iwasaki, S., A. Momiyama, et al. (2000). "Developmental changes in calcium channel types mediating central synaptic transmission." J Neurosci **20**(1): 59-65.

Iwasaki, S. and T. Takahashi (1998). "Developmental changes in calcium channel types mediating synaptic transmission in rat auditory brainstem." J Physiol **509 (Pt 2)**: 419-423.

Jahn, R. and R. H. Scheller (2006). "SNAREs--engines for membrane fusion." Nat Rev Mol Cell Biol **7**(9): 631-643.

Janigro, D., S. Gasparini, et al. (1997). "Reduction of K+ uptake in glia prevents long-term depression maintenance and causes epileptiform activity." J Neurosci **17**(8): 2813-2824.

Jarsky, T., M. Tian, et al. (2010). "Nanodomain control of exocytosis is responsible for the signaling capability of a retinal ribbon synapse." J Neurosci **30**(36): 11885-11895.

Jaskolski, F., F. Coussen, et al. (2004). "Subunit composition and alternative splicing regulate membrane delivery of kainate receptors." J Neurosci **24**(10): 2506-2515.

Jeffrey, M., W. G. Halliday, et al. (2000). "Synapse loss associated with abnormal PrP precedes neuronal degeneration in the scrapie-infected murine hippocampus." Neuropathol Appl Neurobiol **26**(1): 41-54.

Jiang, R., B. Gao, et al. (2000). "Hsc70 chaperones clathrin and primes it to interact with vesicle membranes." J Biol Chem **275**(12): 8439-8447.

Jiang, R. F., T. Greener, et al. (1997). "Interaction of auxilin with the molecular chaperone, Hsc70." J Biol Chem **272**(10): 6141-6145.

Jimbo, Y., A. Kawana, et al. (2000). "The dynamics of a neuronal culture of dissociated cortical neurons of neonatal rats." Biol Cybern **83**(1): 1-20.

Jimbo, Y. and H. P. Robinson (2000). "Propagation of spontaneous synchronized activity in cortical slice cultures recorded by planar electrode arrays." Bioelectrochemistry **51**(2): 107-115.

Jin, H., H. Wu, et al. (2003). "Demonstration of functional coupling between gamma - aminobutyric acid (GABA) synthesis and vesicular GABA transport into synaptic vesicles." Proc Natl Acad Sci U S A **100**(7): 4293-4298.

Jonas, P., C. Racca, et al. (1994). "Differences in Ca2+ permeability of AMPA-type glutamate receptor channels in neocortical neurons caused by differential GluR-B subunit expression." Neuron **12**(6): 1281-1289.

Jones, M. W. (2010). "Errant ensembles: dysfunctional neuronal network dynamics in schizophrenia." Biochem Soc Trans **38**(2): 516-521.

Joshi, I., S. Shokralla, et al. (2004). "The role of AMPA receptor gating in the development of high-fidelity neurotransmission at the calyx of Held synapse." J Neurosci **24**(1): 183-196.

Jourdain, P., L. H. Bergersen, et al. (2007). "Glutamate exocytosis from astrocytes controls synaptic strength." Nat Neurosci **10**(3): 331-339.

Jugloff, D. G., B. P. Jung, et al. (2005). "Increased dendritic complexity and axonal length in cultured mouse cortical neurons overexpressing methyl-CpG-binding protein MeCP2." Neurobiol Dis **19**(1-2): 18-27.

Juhaszova, M., P. Church, et al. (2000). "Location of calcium transporters at presynaptic terminals." Eur J Neurosci **12**(3): 839-846.

Kamioka, H., E. Maeda, et al. (1996). "Spontaneous periodic synchronized bursting during formation of mature patterns of connections in cortical cultures." Neurosci Lett **206**(2-3): 109-112.

Kamioka, H., E. Maeda, et al. (1996). "Spontaneous periodic synchronized bursting during formation of mature patterns of connections in cortical cultures." Neuroscience Letters **206**(2-3): 109-112.

Kang, J., L. Jiang, et al. (1998). "Astrocyte-mediated potentiation of inhibitory synaptic transmission." Nat Neurosci **1**(8): 683-692.

Kang, Y., X. Zhang, et al. (2008). "Induction of GABAergic postsynaptic differentiation by alpha-neurexins." J Biol Chem **283**(4): 2323-2334.

Kassmann, C. M. and K. A. Nave (2008). "Oligodendroglial impact on axonal function and survival - a hypothesis." Curr Opin Neurol **21**(3): 235-241.

Kater, S. B. and L. R. Mills (1991). "Regulation of growth cone behavior by calcium." J Neurosci **11**(4): 891-899.

Katz, B. (1971). "Quantal mechanism of neural transmitter release." Science **173**(992): 123-126.
Kawaguchi, Y. and S. Kondo (2002). "Parvalbumin, somatostatin and cholecystokinin as chemical markers for specific GABAergic interneuron types in the rat frontal cortex." J Neurocytol **31**(3-5): 277-287.
Kawashima, T., H. Okuno, et al. (2009). "Synaptic activity-responsive element in the Arc/Arg3.1 promoter essential for synapse-to-nucleus signaling in activated neurons." Proc Natl Acad Sci U S A **106**(1): 316-321.
Kennedy, T. E. and M. Tessier-Lavigne (1995). "Guidance and induction of branch formation in developing axons by target-derived diffusible factors." Curr Opin Neurobiol **5**(1): 83-90.
Kerr, A. M., E. Reisinger, et al. (2008). "Differential dependence of phasic transmitter release on synaptotagmin 1 at GABAergic and glutamatergic hippocampal synapses." Proc Natl Acad Sci U S A **105**(40): 15581-15586.
Kim, D. K. and W. A. Catterall (1997). "Ca2+-dependent and -independent interactions of the isoforms of the alpha1A subunit of brain Ca2+ channels with presynaptic SNARE proteins." Proc Natl Acad Sci U S A **94**(26): 14782-14786.
Kim, M. J., A. W. Dunah, et al. (2005). "Differential roles of NR2A- and NR2B-containing NMDA receptors in Ras-ERK signaling and AMPA receptor trafficking." Neuron **46**(5): 745-760.
Kinney, J. W., C. N. Davis, et al. (2006). "A specific role for NR2A-containing NMDA receptors in the maintenance of parvalbumin and GAD67 immunoreactivity in cultured interneurons." J Neurosci **26**(5): 1604-1615.
Klausberger, T. (2009). "GABAergic interneurons targeting dendrites of pyramidal cells in the CA1 area of the hippocampus." Eur J Neurosci **30**(6): 947-957.
Klausberger, T., P. J. Magill, et al. (2003). "Brain-state- and cell-type-specific firing of hippocampal interneurons in vivo." Nature **421**(6925): 844-848.
Klausberger, T., J. D. Roberts, et al. (2002). "Cell type- and input-specific differences in the number and subtypes of synaptic GABA(A) receptors in the hippocampus." J Neurosci **22**(7): 2513-2521.
Klausberger, T. and P. Somogyi (2008). "Neuronal diversity and temporal dynamics: the unity of hippocampal circuit operations." Science **321**(5885): 53-57.
Koffie, R. M., M. Meyer-Luehmann, et al. (2009). "Oligomeric amyloid beta associates with postsynaptic densities and correlates with excitatory synapse loss near senile plaques." Proc Natl Acad Sci U S A **106**(10): 4012-4017.
Kofuji, P., M. Hofer, et al. (1996). "Functional analysis of the weaver mutant GIRK2 K+ channel and rescue of weaver granule cells." Neuron **16**(5): 941-952.
Koike-Tani, M., N. Saitoh, et al. (2005). "Mechanisms underlying developmental speeding in AMPA-EPSC decay time at the calyx of Held." J Neurosci **25**(1): 199-207.
Kudo, M., M. Aono, et al. (2001). "Effects of volatile anesthetics on N-methyl-D-aspartate excitotoxicity in primary rat neuronal-glial cultures." Anesthesiology **95**(3): 756-765.
Kunkler, P. E. and R. P. Kraig (1997). "Reactive astrocytosis from excitotoxic injury in hippocampal organ culture parallels that seen in vivo." J Cereb Blood Flow Metab **17**(1): 26-43.
Kuromi, H. and Y. Kidokoro (1998). "Two distinct pools of synaptic vesicles in single presynaptic boutons in a temperature-sensitive Drosophila mutant, shibire." Neuron **20**(5): 917-925.

Kurosinski, P. and J. Gotz (2002). "Glial cells under physiologic and pathologic conditions." Arch Neurol **59**(10): 1524-1528.

Kwak, S., T. Hideyama, et al. (2010). "AMPA receptor-mediated neuronal death in sporadic ALS." Neuropathology **30**(2): 182-188.

Lalancette-Hebert, M., G. Gowing, et al. (2007). "Selective ablation of proliferating microglial cells exacerbates ischemic injury in the brain." J Neurosci **27**(10): 2596-2605.

Lancelot, E. and M. F. Beal (1998). "Glutamate toxicity in chronic neurodegenerative disease." Prog Brain Res **116**: 331-347.

Larson, J., G. Lynch, et al. (1999). "Alterations in synaptic transmission and long-term potentiation in hippocampal slices from young and aged PDAPP mice." Brain Res **840**(1-2): 23-35.

Laurie, D. J., W. Wisden, et al. (1992). "The distribution of thirteen GABAA receptor subunit mRNAs in the rat brain. III. Embryonic and postnatal development." J Neurosci **12**(11): 4151-4172.

Lavoie, A. M., J. J. Tingey, et al. (1997). "Activation and deactivation rates of recombinant GABA(A) receptor channels are dependent on alpha-subunit isoform." Biophys J **73**(5): 2518-2526.

Leonard, A. S., M. A. Davare, et al. (1998). "SAP97 is associated with the alpha-amino-3-hydroxy-5-methylisoxazole-4-propionic acid receptor GluR1 subunit." J Biol Chem **273**(31): 19518-19524.

Leranth, C., Z. Szeidemann, et al. (1996). "AMPA receptors in the rat and primate hippocampus: a possible absence of GluR2/3 subunits in most interneurons." Neuroscience **70**(3): 631-652.

Lerma, J. (2006). "Kainate receptor physiology." Curr Opin Pharmacol **6**(1): 89-97.

Lerma, J., M. Morales, et al. (1997). "Glutamate receptors of the kainate type and synaptic transmission." Trends Neurosci **20**(1): 9-12.

Leveque, C., S. Pupier, et al. (1998). "Interaction of cysteine string proteins with the alpha1A subunit of the P/Q-type calcium channel." J Biol Chem **273**(22): 13488-13492.

Levitt, P., K. L. Eagleson, et al. (2004). "Regulation of neocortical interneuron development and the implications for neurodevelopmental disorders." Trends Neurosci **27**(7): 400-406.

Lewis, D. A., T. Hashimoto, et al. (2005). "Cortical inhibitory neurons and schizophrenia." Nat Rev Neurosci **6**(4): 312-324.

Li, B., N. Chen, et al. (2002). "Differential regulation of synaptic and extra-synaptic NMDA receptors." Nat Neurosci **5**(9): 833-834.

Li, X., W. Zhou, et al. (2007). "Long-term recording on multi-electrode array reveals degraded inhibitory connection in neuronal network development." Biosens Bioelectron **22**(7): 1538-1543.

Li, X. G., P. Somogyi, et al. (1994). "The hippocampal CA3 network: an in vivo intracellular labeling study." J Comp Neurol **339**(2): 181-208.

Liang, Y., L. L. Yuan, et al. (2002). "Calcium signaling at single mossy fiber presynaptic terminals in the rat hippocampus." J Neurophysiol **87**(2): 1132-1137.

Liao, D., R. H. Scannevin, et al. (2001). "Activation of silent synapses by rapid activity-dependent synaptic recruitment of AMPA receptors." J Neurosci **21**(16): 6008-6017.

Link, E., L. Edelmann, et al. (1992). "Tetanus toxin action: inhibition of neurotransmitter release linked to synaptobrevin proteolysis." Biochem Biophys Res Commun **189**(2): 1017-1023.

Lipton, S. A. and P. A. Rosenberg (1994). "Excitatory amino acids as a final common pathway for neurologic disorders." N Engl J Med **330**(9): 613-622.

Littleton, J. T., R. J. Barnard, et al. (2001). "SNARE-complex disassembly by NSF follows synaptic-vesicle fusion." Proc Natl Acad Sci U S A **98**(21): 12233-12238.

Liu, Q. S., Q. Xu, et al. (2004). "Astrocyte-mediated activation of neuronal kainate receptors." Proc Natl Acad Sci U S A **101**(9): 3172-3177.

Liu, S. J. and L. K. Kaczmarek (1998). "The expression of two splice variants of the Kv3.1 potassium channel gene is regulated by different signaling pathways." J Neurosci **18**(8): 2881-2890.

Liu, X. B., K. D. Murray, et al. (2004). "Switching of NMDA receptor 2A and 2B subunits at thalamic and cortical synapses during early postnatal development." J Neurosci **24**(40): 8885-8895.

Livet, J., T. A. Weissman, et al. (2007). "Transgenic strategies for combinatorial expression of fluorescent proteins in the nervous system." Nature **450**(7166): 56-62.

Llado, J., C. Haenggeli, et al. (2006). "Degeneration of respiratory motor neurons in the SOD1 G93A transgenic rat model of ALS." Neurobiol Dis **21**(1): 110-118.

Llobet, A., A. Cooke, et al. (2003). "Exocytosis at the ribbon synapse of retinal bipolar cells studied in patches of presynaptic membrane." J Neurosci **23**(7): 2706-2714.

Lonart, G. and T. C. Sudhof (2000). "Assembly of SNARE core complexes prior to neurotransmitter release sets the readily releasable pool of synaptic vesicles." J Biol Chem **275**(36): 27703-27707.

Lu, W., H. Man, et al. (2001). "Activation of synaptic NMDA receptors induces membrane insertion of new AMPA receptors and LTP in cultured hippocampal neurons." Neuron **29**(1): 243-254.

Ma, H. T., C. H. Wu, et al. (2004). "Initiation of spontaneous epileptiform events in the rat neocortex in vivo." J Neurophysiol **91**(2): 934-945.

Ma, J., M. Endres, et al. (1998). "Synergistic effects of caspase inhibitors and MK-801 in brain injury after transient focal cerebral ischaemia in mice." Br J Pharmacol **124**(4): 756-762.

Maeda, E., H. P. Robinson, et al. (1995). "The mechanisms of generation and propagation of synchronized bursting in developing networks of cortical neurons." J Neurosci **15**(10): 6834-6845.

Magga, J. M., S. E. Jarvis, et al. (2000). "Cysteine string protein regulates G protein modulation of N-type calcium channels." Neuron **28**(1): 195-204.

Maier, N., V. Nimmrich, et al. (2003). "Cellular and network mechanisms underlying spontaneous sharp wave-ripple complexes in mouse hippocampal slices." J Physiol **550**(Pt 3): 873-887.

Malinow, R. and R. C. Malenka (2002). "AMPA receptor trafficking and synaptic plasticity." Annu Rev Neurosci **25**: 103-126.

Mander, P. and G. C. Brown (2005). "Activation of microglial NADPH oxidase is synergistic with glial iNOS expression in inducing neuronal death: a dual-key mechanism of inflammatory neurodegeneration." J Neuroinflammation **2**: 20.

Mao, B. Q., F. Hamzei-Sichani, et al. (2001). "Dynamics of spontaneous activity in neocortical slices." Neuron **32**(5): 883-898.

Maragakis, N. J. and J. D. Rothstein (2006). "Mechanisms of Disease: astrocytes in neurodegenerative disease." Nat Clin Pract Neurol **2**(12): 679-689.
Markram, H., M. Toledo-Rodriguez, et al. (2004). "Interneurons of the neocortical inhibitory system." Nat Rev Neurosci **5**(10): 793-807.
Marks, J. D., J. E. Friedman, et al. (1996). "Vulnerability of CA1 neurons to glutamate is developmentally regulated." Brain Res Dev Brain Res **97**(2): 194-206.
Martinoia, S., L. Bonzano, et al. (2005). "In vitro cortical neuronal networks as a new high-sensitive system for biosensing applications." Biosens Bioelectron **20**(10): 2071-2078.
Masliah, E., M. Alford, et al. (1996). "Deficient glutamate transport is associated with neurodegeneration in Alzheimer's disease." Ann Neurol **40**(5): 759-766.
Massieu, L., A. Morales-Villagran, et al. (1995). "Accumulation of extracellular glutamate by inhibition of its uptake is not sufficient for inducing neuronal damage: an in vivo microdialysis study." J Neurochem **64**(5): 2262-2272.
Mastrogiacomo, A., S. M. Parsons, et al. (1994). "Cysteine string proteins: a potential link between synaptic vesicles and presynaptic Ca2+ channels." Science **263**(5149): 981-982.
Matthews, G. (2004). "Cycling the synapse: scenic versus direct routes for vesicles." Neuron **44**(2): 223-226.
May, A. P., S. W. Whiteheart, et al. (2001). "Unraveling the mechanism of the vesicle transport ATPase NSF, the N-ethylmaleimide-sensitive factor." J Biol Chem **276**(25): 21991-21994.
Mazzoleni, G., D. Di Lorenzo, et al. (2009). "Modelling tissues in 3D: the next future of pharmaco-toxicology and food research?" Genes Nutr **4**(1): 13-22.
McBain, C. J. and A. Fisahn (2001). "Interneurons unbound." Nat Rev Neurosci **2**(1): 11-23.
McTigue, D. M. and R. B. Tripathi (2008). "The life, death, and replacement of oligodendrocytes in the adult CNS." J Neurochem **107**(1): 1-19.
Meinrenken, C. J., J. G. Borst, et al. (2002). "Calcium secretion coupling at calyx of held governed by nonuniform channel-vesicle topography." J Neurosci **22**(5): 1648-1667.
Meinrenken, C. J., J. G. Borst, et al. (2003). "Local routes revisited: the space and time dependence of the Ca2+ signal for phasic transmitter release at the rat calyx of Held." J Physiol **547**(Pt 3): 665-689.
Melani, R., R. Rebaudo, et al. (2005). "Changes in extracellular action potential detect kainic acid and trimethyltin toxicity in hippocampal slice preparations earlier than do MAP2 density measurements." Altern Lab Anim **33**(4): 379-386.
Mennerick, S., J. Que, et al. (1995). "Passive and synaptic properties of hippocampal neurons grown in microcultures and in mass cultures." J Neurophysiol **73**(1): 320-332.
Miles, R., K. Toth, et al. (1996). "Differences between somatic and dendritic inhibition in the hippocampus." Neuron **16**(4): 815-823.
Milev, P., P. Maurel, et al. (1998). "Differential regulation of expression of hyaluronan-binding proteoglycans in developing brain: aggrecan, versican, neurocan, and brevican." Biochem Biophys Res Commun **247**(2): 207-212.
Miller, L. C., L. A. Swayne, et al. (2003). "Molecular determinants of cysteine string protein modulation of N-type calcium channels." J Cell Sci **116**(Pt 14): 2967-2974.

Mintz, I. M. and B. P. Bean (1993). "GABAB receptor inhibition of P-type Ca2+ channels in central neurons." Neuron **10**(5): 889-898.

Misura, K. M., R. H. Scheller, et al. (2000). "Three-dimensional structure of the neuronal-Sec1-syntaxin 1a complex." Nature **404**(6776): 355-362.

Mochida, S., C. T. Yokoyama, et al. (1998). "Evidence for a voltage-dependent enhancement of neurotransmitter release mediated via the synaptic protein interaction site of N-type Ca2+ channels." Proc Natl Acad Sci U S A **95**(24): 14523-14528.

Moga, D., P. R. Hof, et al. (2002). "Parvalbumin-containing interneurons in rat hippocampus have an AMPA receptor profile suggestive of vulnerability to excitotoxicity." J Chem Neuroanat **23**(4): 249-253.

Mohler, H. (2006). "GABA(A) receptor diversity and pharmacology." Cell Tissue Res **326**(2): 505-516.

Mohler, H. (2007). "Molecular regulation of cognitive functions and developmental plasticity: impact of GABAA receptors." J Neurochem **102**(1): 1-12.

Monnet-Tschudi, F., M. G. Zurich, et al. (2007). "Neurotoxicant-induced inflammatory response in three-dimensional brain cell cultures." Hum Exp Toxicol **26**(4): 339-346.

Monyer, H., P. H. Seeburg, et al. (1991). "Glutamate-operated channels: developmentally early and mature forms arise by alternative splicing." Neuron **6**(5): 799-810.

Morales, M., A. Ferrus, et al. (1999). "Presynaptic calcium-channel currents in normal and csp mutant Drosophila peptidergic terminals." Eur J Neurosci **11**(5): 1818-1826.

Mori, H., H. Masaki, et al. (1992). "Identification by mutagenesis of a Mg(2+)-block site of the NMDA receptor channel." Nature **358**(6388): 673-675.

Morrison, B., 3rd, A. K. Pringle, et al. (2002). "L-arginyl-3,4-spermidine is neuroprotective in several in vitro models of neurodegeneration and in vivo ischaemia without suppressing synaptic transmission." Br J Pharmacol **137**(8): 1255-1268.

Mosbacher, J., R. Schoepfer, et al. (1994). "A molecular determinant for submillisecond desensitization in glutamate receptors." Science **266**(5187): 1059-1062.

Moser, T. and D. Beutner (2000). "Kinetics of exocytosis and endocytosis at the cochlear inner hair cell afferent synapse of the mouse." Proc Natl Acad Sci U S A **97**(2): 883-888.

Mukai, Y., T. Shiina, et al. (2003). "Continuous monitoring of developmental activity changes in cultured cortical networks." Electrical Engineering in Japan **145**(4): 28-37.

Muramoto, K., M. Ichikawa, et al. (1993). "Frequency of synchronous oscillations of neuronal activity increases during development and is correlated to the number of synapses in cultured cortical neuron networks." Neurosci Lett **163**(2): 163-165.

Naisbitt, S., E. Kim, et al. (1999). "Shank, a novel family of postsynaptic density proteins that binds to the NMDA receptor/PSD-95/GKAP complex and cortactin." Neuron **23**(3): 569-582.

Natochin, M., T. N. Campbell, et al. (2005). "Characterization of the G alpha(s) regulator cysteine string protein." J Biol Chem **280**(34): 30236-30241.

Nave, K. A. and B. D. Trapp (2008). "Axon-glial signaling and the glial support of axon function." Annu Rev Neurosci **31**: 535-561.

Newman, E. A. (2003). "New roles for astrocytes: regulation of synaptic transmission." Trends Neurosci **26**(10): 536-542.
Nie, Z., R. Ranjan, et al. (1999). "Overexpression of cysteine-string proteins in Drosophila reveals interactions with syntaxin." J Neurosci **19**(23): 10270-10279.
Noraberg, J., B. W. Kristensen, et al. (1999). "Markers for neuronal degeneration in organotypic slice cultures." Brain Res Brain Res Protoc **3**(3): 278-290.
Nusser, Z., W. Sieghart, et al. (1998). "Segregation of different GABAA receptors to synaptic and extrasynaptic membranes of cerebellar granule cells." J Neurosci **18**(5): 1693-1703.
Nyiri, G., T. F. Freund, et al. (2001). "Input-dependent synaptic targeting of alpha(2)-subunit-containing GABA(A) receptors in synapses of hippocampal pyramidal cells of the rat." Eur J Neurosci **13**(3): 428-442.
Ohana, O. and B. Sakmann (1998). "Transmitter release modulation in nerve terminals of rat neocortical pyramidal cells by intracellular calcium buffers." J Physiol **513 (Pt 1)**: 135-148.
Opitz, T., A. D. De Lima, et al. (2002). "Spontaneous development of synchronous oscillatory activity during maturation of cortical networks in vitro." Journal of Neurophysiology **88**(5): 2196-2206.
Opitz, T., A. D. De Lima, et al. (2002). "Spontaneous development of synchronous oscillatory activity during maturation of cortical networks in vitro." J Neurophysiol **88**(5): 2196-2206.
Ozawa, S., H. Kamiya, et al. (1998). "Glutamate receptors in the mammalian central nervous system." Prog Neurobiol **54**(5): 581-618.
Paillart, C., J. Li, et al. (2003). "Endocytosis and vesicle recycling at a ribbon synapse." J Neurosci **23**(10): 4092-4099.
Palop, J. J., J. Chin, et al. (2007). "Aberrant excitatory neuronal activity and compensatory remodeling of inhibitory hippocampal circuits in mouse models of Alzheimer's disease." Neuron **55**(5): 697-711.
Pang, Z. P., J. Sun, et al. (2006). "Genetic analysis of synaptotagmin 2 in spontaneous and Ca2+-triggered neurotransmitter release." EMBO J **25**(10): 2039-2050.
Parri, H. R. and V. Crunelli (2001). "Pacemaker calcium oscillations in thalamic astrocytes in situ." Neuroreport **12**(18): 3897-3900.
Parri, H. R., T. M. Gould, et al. (2001). "Spontaneous astrocytic Ca2+ oscillations in situ drive NMDAR-mediated neuronal excitation." Nat Neurosci **4**(8): 803-812.
Pasti, L., M. Zonta, et al. (2001). "Cytosolic calcium oscillations in astrocytes may regulate exocytotic release of glutamate." J Neurosci **21**(2): 477-484.
Payne, J. A., C. Rivera, et al. (2003). "Cation-chloride co-transporters in neuronal communication, development and trauma." Trends Neurosci **26**(4): 199-206.
Peng, J., M. J. Kim, et al. (2004). "Semiquantitative proteomic analysis of rat forebrain postsynaptic density fractions by mass spectrometry." J Biol Chem **279**(20): 21003-21011.
Perea, G., M. Navarrete, et al. (2009). "Tripartite synapses: astrocytes process and control synaptic information." Trends Neurosci **32**(8): 421-431.
Platel, J.-C., K. A. Dave, et al. (2010). "NMDA Receptors Activated by Subventricular Zone Astrocytic Glutamate Are Critical for Neuroblast Survival Prior to Entering a Synaptic Network." Neuron **65**: 859-872.

Platel, J. C., K. A. Dave, et al. (2010). "NMDA receptors activated by subventricular zone astrocytic glutamate are critical for neuroblast survival prior to entering a synaptic network." Neuron **65**(6): 859-872.
Pobbati, A. V., A. Stein, et al. (2006). "N- to C-terminal SNARE complex assembly promotes rapid membrane fusion." Science **313**(5787): 673-676.
Powell, E. M., D. B. Campbell, et al. (2003). "Genetic disruption of cortical interneuron development causes region- and GABA cell type-specific deficits, epilepsy, and behavioral dysfunction." J Neurosci **23**(2): 622-631.
Prange, O., T. P. Wong, et al. (2004). "A balance between excitatory and inhibitory synapses is controlled by PSD-95 and neuroligin." Proc Natl Acad Sci U S A **101**(38): 13915-13920.
Prenosil, G. A., E. M. Schneider Gasser, et al. (2006). "Specific subtypes of GABAA receptors mediate phasic and tonic forms of inhibition in hippocampal pyramidal neurons." J Neurophysiol.
Qin, L., Y. Liu, et al. (2002). "Microglia enhance beta-amyloid peptide-induced toxicity in cortical and mesencephalic neurons by producing reactive oxygen species." J Neurochem **83**(4): 973-983.
Quinlan, J. J., L. L. Firestone, et al. (2000). "Mice lacking the long splice variant of the gamma 2 subunit of the GABA(A) receptor are more sensitive to benzodiazepines." Pharmacol Biochem Behav **66**(2): 371-374.
Ranjan, R., P. Bronk, et al. (1998). "Cysteine string protein is required for calcium secretion coupling of evoked neurotransmission in drosophila but not for vesicle recycling." J Neurosci **18**(3): 956-964.
Rao-Mirotznik, R., G. Buchsbaum, et al. (1998). "Transmitter concentration at a three-dimensional synapse." J Neurophysiol **80**(6): 3163-3172.
Rao, A., K. J. Harms, et al. (2000). "Neuroligation: building synapses around the neurexin-neuroligin link." Nat Neurosci **3**(8): 747-749.
Rappert, A., I. Bechmann, et al. (2004). "CXCR3-dependent microglial recruitment is essential for dendrite loss after brain lesion." J Neurosci **24**(39): 8500-8509.
Rea, R., J. Li, et al. (2004). "Streamlined synaptic vesicle cycle in cone photoreceptor terminals." Neuron **41**(5): 755-766.
Reim, K., M. Mansour, et al. (2001). "Complexins regulate a late step in Ca2+-dependent neurotransmitter release." Cell **104**(1): 71-81.
Remondes, M. and E. M. Schuman (2002). "Direct cortical input modulates plasticity and spiking in CA1 pyramidal neurons." Nature **416**(6882): 736-740.
Rheims, S., M. Minlebaev, et al. (2008). "Excitatory GABA in rodent developing neocortex in vitro." J Neurophysiol **100**(2): 609-619.
Rial Verde, E. M., J. Lee-Osbourne, et al. (2006). "Increased expression of the immediate-early gene arc/arg3.1 reduces AMPA receptor-mediated synaptic transmission." Neuron **52**(3): 461-474.
Ribak, C. E., R. Nitsch, et al. (1990). "Proportion of parvalbumin-positive basket cells in the GABAergic innervation of pyramidal and granule cells of the rat hippocampal formation." J Comp Neurol **300**(4): 449-461.
Ricotta, D., S. D. Conner, et al. (2002). "Phosphorylation of the AP2 mu subunit by AAK1 mediates high affinity binding to membrane protein sorting signals." J Cell Biol **156**(5): 791-795.
Rieke, F. and E. A. Schwartz (1996). "Asynchronous transmitter release: control of exocytosis and endocytosis at the salamander rod synapse." J Physiol **493 (Pt 1)**: 1-8.

Rizo, J. and C. Rosenmund (2008). "Synaptic vesicle fusion." Nat Struct Mol Biol **15**(7): 665-674.

Robinson, H. P., M. Kawahara, et al. (1993). "Periodic synchronized bursting and intracellular calcium transients elicited by low magnesium in cultured cortical neurons." J Neurophysiol **70**(4): 1606-1616.

Rodriguez-Contreras, A., J. S. van Hoeve, et al. (2008). "Dynamic development of the calyx of Held synapse." Proc Natl Acad Sci U S A **105**(14): 5603-5608.

Roselli, F., M. Tirard, et al. (2005). "Soluble beta-amyloid1-40 induces NMDA-dependent degradation of postsynaptic density-95 at glutamatergic synapses." J Neurosci **25**(48): 11061-11070.

Rosenberg, P. A. and E. Aizenman (1989). "Hundred-fold increase in neuronal vulnerability to glutamate toxicity in astrocyte-poor cultures of rat cerebral cortex." Neurosci Lett **103**(2): 162-168.

Rosenberg, P. A., S. Amin, et al. (1992). "Glutamate uptake disguises neurotoxic potency of glutamate agonists in cerebral cortex in dissociated cell culture." J Neurosci **12**(1): 56-61.

Rothstein, J. D., M. Dykes-Hoberg, et al. (1996). "Knockout of glutamate transporters reveals a major role for astroglial transport in excitotoxicity and clearance of glutamate." Neuron **16**(3): 675-686.

Rothstein, J. D., M. Van Kammen, et al. (1995). "Selective loss of glial glutamate transporter GLT-1 in amyotrophic lateral sclerosis." Ann Neurol **38**(1): 73-84.

Rubenstein, J. L. and M. M. Merzenich (2003). "Model of autism: increased ratio of excitation/inhibition in key neural systems." Genes Brain Behav **2**(5): 255-267.

Ruiz, R., J. J. Casanas, et al. (2008). "Cysteine string protein-alpha is essential for the high calcium sensitivity of exocytosis in a vertebrate synapse." Eur J Neurosci **27**(12): 3118-3131.

Sabatini, B. L. and W. G. Regehr (1996). "Timing of neurotransmission at fast synapses in the mammalian brain." Nature **384**(6605): 170-172.

Sakaba, T. and E. Neher (2003). "Direct modulation of synaptic vesicle priming by GABA(B) receptor activation at a glutamatergic synapse." Nature **424**(6950): 775-778.

Sakisaka, T., T. Meerlo, et al. (2002). "Rab-alphaGDI activity is regulated by a Hsp90 chaperone complex." EMBO J **21**(22): 6125-6135.

Sala, C., V. Piech, et al. (2001). "Regulation of dendritic spine morphology and synaptic function by Shank and Homer." Neuron **31**(1): 115-130.

Salinas, E. and T. J. Sejnowski (2001). "Correlated neuronal activity and the flow of neural information." Nat Rev Neurosci **2**(8): 539-550.

Salio, C., L. Lossi, et al. (2006). "Neuropeptides as synaptic transmitters." Cell Tissue Res **326**(2): 583-598.

Salter, M. W. and J. L. Hicks (1995). "ATP causes release of intracellular Ca2+ via the phospholipase C beta/IP3 pathway in astrocytes from the dorsal spinal cord." J Neurosci **15**(4): 2961-2971.

Sanchez-Vives, M. V. and D. A. McCormick (2000). "Cellular and network mechanisms of rhythmic recurrent activity in neocortex." Nat Neurosci **3**(10): 1027-1034.

Santhakumar, V. and I. Soltesz (2004). "Plasticity of interneuronal species diversity and parameter variance in neurological diseases." Trends Neurosci **27**(8): 504-510.

Sato, M., L. Lopez-Mascaraque, et al. (1994). "Action of a diffusible target-derived chemoattractant on cortical axon branch induction and directed growth." Neuron **13**(4): 791-803.
Sattler, R. and M. Tymianski (2001). "Molecular mechanisms of glutamate receptor-mediated excitotoxic neuronal cell death." Mol Neurobiol **24**(1-3): 107-129.
Sattler, R., Z. Xiong, et al. (1999). "Specific coupling of NMDA receptor activation to nitric oxide neurotoxicity by PSD-95 protein." Science **284**(5421): 1845-1848.
Satzler, K., L. F. Sohl, et al. (2002). "Three-dimensional reconstruction of a calyx of Held and its postsynaptic principal neuron in the medial nucleus of the trapezoid body." J Neurosci **22**(24): 10567-10579.
Schaub, J. R., X. Lu, et al. (2006). "Hemifusion arrest by complexin is relieved by Ca2+-synaptotagmin I." Nat Struct Mol Biol **13**(8): 748-750.
Scheiffele, P., J. Fan, et al. (2000). "Neuroligin expressed in nonneuronal cells triggers presynaptic development in contacting axons." Cell **101**(6): 657-669.
Schiavo, G., G. Stenbeck, et al. (1997). "Binding of the synaptic vesicle v-SNARE, synaptotagmin, to the plasma membrane t-SNARE, SNAP-25, can explain docked vesicles at neurotoxin-treated synapses." Proc Natl Acad Sci U S A **94**(3): 997-1001.
Schikorski, T. and C. F. Stevens (1997). "Quantitative ultrastructural analysis of hippocampal excitatory synapses." J Neurosci **17**(15): 5858-5867.
Schmid, D., A. Baici, et al. (1994). "Kinetics of molecular chaperone action." Science **263**(5149): 971-973.
Schmitz, F., L. Tabares, et al. (2006). "CSPalpha-deficiency causes massive and rapid photoreceptor degeneration." Proc Natl Acad Sci U S A **103**(8): 2926-2931.
Schoch, S., P. E. Castillo, et al. (2002). "RIM1alpha forms a protein scaffold for regulating neurotransmitter release at the active zone." Nature **415**(6869): 321-326.
Schubert, D. and D. Piasecki (2001). "Oxidative glutamate toxicity can be a component of the excitotoxicity cascade." J Neurosci **21**(19): 7455-7462.
Schummers, J., J. Marino, et al. (2002). "Synaptic integration by V1 neurons depends on location within the orientation map." Neuron **36**(5): 969-978.
Schuske, K., A. A. Beg, et al. (2004). "The GABA nervous system in C. elegans." Trends Neurosci **27**(7): 407-414.
Sederberg, P. B., M. J. Kahana, et al. (2003). "Theta and gamma oscillations during encoding predict subsequent recall." J Neurosci **23**(34): 10809-10814.
Sederberg, P. B., A. Schulze-Bonhage, et al. (2007). "Hippocampal and neocortical gamma oscillations predict memory formation in humans." Cereb Cortex **17**(5): 1190-1196.
Segev, R., Y. Shapira, et al. (2001). "Observations and modeling of synchronized bursting in two-dimensional neural networks." Phys Rev E Stat Nonlin Soft Matter Phys **64**(1 Pt 1): 011920.
Selkoe, D. J. (2002). "Alzheimer's disease is a synaptic failure." Science **298**(5594): 789-791.
Semyanov, A., M. C. Walker, et al. (2004). "Tonically active GABA A receptors: modulating gain and maintaining the tone." Trends Neurosci **27**(5): 262-269.
Sheng, Z. H., J. Rettig, et al. (1994). "Identification of a syntaxin-binding site on N-type calcium channels." Neuron **13**(6): 1303-1313.
Shepherd, J. D., G. Rumbaugh, et al. (2006). "Arc/Arg3.1 mediates homeostatic synaptic scaling of AMPA receptors." Neuron **52**(3): 475-484.

Shirataki, H., K. Kaibuchi, et al. (1993). "Rabphilin-3A, a putative target protein for smg p25A/rab3A p25 small GTP-binding protein related to synaptotagmin." Mol Cell Biol **13**(4): 2061-2068.

Siksou, L., F. Varoqueaux, et al. (2009). "A common molecular basis for membrane docking and functional priming of synaptic vesicles." Eur J Neurosci **30**(1): 49-56.

Siskova, Z., A. Page, et al. (2009). "Degenerating synaptic boutons in prion disease: microglia activation without synaptic stripping." Am J Pathol **175**(4): 1610-1621.

Sloviter, R. S. (1991). "Feedforward and feedback inhibition of hippocampal principal cell activity evoked by perforant path stimulation: GABA-mediated mechanisms that regulate excitability in vivo." Hippocampus **1**(1): 31-40.

So, E. C., Y. H. Chen, et al. (2010). "Sound exposure accelerates reflex emergence and development in young rats." Brain Res Bull **81**(4-5): 391-397.

Sohal, V. S., F. Zhang, et al. (2009). "Parvalbumin neurons and gamma rhythms enhance cortical circuit performance." Nature **459**(7247): 698-702.

Sollner, T., M. K. Bennett, et al. (1993). "A protein assembly-disassembly pathway in vitro that may correspond to sequential steps of synaptic vesicle docking, activation, and fusion." Cell **75**(3): 409-418.

Somogyi, P. and T. Klausberger (2005). "Defined types of cortical interneurone structure space and spike timing in the hippocampus." J Physiol **562**(Pt 1): 9-26.

Song, J. Y., K. Ichtchenko, et al. (1999). "Neuroligin 1 is a postsynaptic cell-adhesion molecule of excitatory synapses." Proc Natl Acad Sci U S A **96**(3): 1100-1105.

Sorensen, J. B. (2009). "Conflicting views on the membrane fusion machinery and the fusion pore." Annu Rev Cell Dev Biol **25**: 513-537.

Sorensen, J. B., K. Wiederhold, et al. (2006). "Sequential N- to C-terminal SNARE complex assembly drives priming and fusion of secretory vesicles." EMBO J **25**(5): 955-966.

Spencer, K. M., P. G. Nestor, et al. (2003). "Abnormal neural synchrony in schizophrenia." J Neurosci **23**(19): 7407-7411.

Sterling, P. and G. Matthews (2005). "Structure and function of ribbon synapses." Trends Neurosci **28**(1): 20-29.

Stevens, B., N. J. Allen, et al. (2007). "The classical complement cascade mediates CNS synapse elimination." Cell **131**(6): 1164-1178.

Stevens, C. F. and J. H. Williams (2000). ""Kiss and run" exocytosis at hippocampal synapses." Proc Natl Acad Sci U S A **97**(23): 12828-12833.

Steward, O., C. S. Wallace, et al. (1998). "Synaptic activation causes the mRNA for the IEG Arc to localize selectively near activated postsynaptic sites on dendrites." Neuron **21**(4): 741-751.

Stoppini, L., P. A. Buchs, et al. (1991). "A simple method for organotypic cultures of nervous tissue." J Neurosci Methods **37**(2): 173-182.

Sudhof, T. C. (2004). "The synaptic vesicle cycle." Annu Rev Neurosci **27**: 509-547.

Sun, J. Y., X. S. Wu, et al. (2002). "Single and multiple vesicle fusion induce different rates of endocytosis at a central synapse." Nature **417**(6888): 555-559.

Sutton, R. B., D. Fasshauer, et al. (1998). "Crystal structure of a SNARE complex involved in synaptic exocytosis at 2.4 A resolution." Nature **395**(6700): 347-353.

Swann, J. W., K. L. Smith, et al. (1993). "Localized excitatory synaptic interactions mediate the sustained depolarization of electrographic seizures in developing hippocampus." J Neurosci **13**(11): 4680-4689.

Swanson, G. T., D. Feldmeyer, et al. (1996). "Effect of RNA editing and subunit co-assembly single-channel properties of recombinant kainate receptors." J Physiol **492 (Pt 1)**: 129-142.

Swayne, L. A., K. E. Beck, et al. (2006). "The cysteine string protein multimeric complex." Biochem Biophys Res Commun **348**(1): 83-91.

Sytnyk, V., I. Leshchyns'ka, et al. (2002). "Neural cell adhesion molecule promotes accumulation of TGN organelles at sites of neuron-to-neuron contacts." J Cell Biol **159**(4): 649-661.

Sze, C. I., H. Bi, et al. (2000). "Selective regional loss of exocytotic presynaptic vesicle proteins in Alzheimer's disease brains." J Neurol Sci **175**(2): 81-90.

Sze, C. I., J. C. Troncoso, et al. (1997). "Loss of the presynaptic vesicle protein synaptophysin in hippocampus correlates with cognitive decline in Alzheimer disease." J Neuropathol Exp Neurol **56**(8): 933-944.

Tafoya, L. C., M. Mameli, et al. (2006). "Expression and function of SNAP-25 as a universal SNARE component in GABAergic neurons." J Neurosci **26**(30): 7826-7838.

Takahashi, H., I. Brasnjevic, et al. (2010). "Hippocampal interneuron loss in an APP/PS1 double mutant mouse and in Alzheimer's disease." Brain Struct Funct **214**(2-3): 145-160.

Takahashi, T. and A. Momiyama (1993). "Different types of calcium channels mediate central synaptic transmission." Nature **366**(6451): 156-158.

Tanaka, K., K. Watase, et al. (1997). "Epilepsy and exacerbation of brain injury in mice lacking the glutamate transporter GLT-1." Science **276**(5319): 1699-1702.

Tang, J., A. Maximov, et al. (2006). "A complexin/synaptotagmin 1 switch controls fast synaptic vesicle exocytosis." Cell **126**(6): 1175-1187.

Terry, R. D., E. Masliah, et al. (1991). "Physical basis of cognitive alterations in Alzheimer's disease: synapse loss is the major correlate of cognitive impairment." Ann Neurol **30**(4): 572-580.

Thompson, S. M., M. Capogna, et al. (1993). "Presynaptic inhibition in the hippocampus." Trends Neurosci **16**(6): 222-227.

Thoreson, W. B., K. Rabl, et al. (2004). "A highly Ca2+-sensitive pool of vesicles contributes to linearity at the rod photoreceptor ribbon synapse." Neuron **42**(4): 595-605.

Tobaben, S., P. Thakur, et al. (2001). "A trimeric protein complex functions as a synaptic chaperone machine." Neuron **31**(6): 987-999.

Tobaben, S., F. Varoqueaux, et al. (2003). "A brain-specific isoform of small glutamine-rich tetratricopeptide repeat-containing protein binds to Hsc70 and the cysteine string protein." J Biol Chem **278**(40): 38376-38383.

Tozuka, Y., S. Fukuda, et al. (2005). "GABAergic excitation promotes neuronal differentiation in adult hippocampal progenitor cells." Neuron **47**(6): 803-815.

Traub, R. D., N. Kopell, et al. (2001). "Gap junctions between interneuron dendrites can enhance synchrony of gamma oscillations in distributed networks." J Neurosci **21**(23): 9478-9486.

Tsien, J. Z., D. F. Chen, et al. (1996). "Subregion- and cell type-restricted gene knockout in mouse brain." Cell **87**(7): 1317-1326.

Tucker, W. C., T. Weber, et al. (2004). "Reconstitution of Ca2+-regulated membrane fusion by synaptotagmin and SNAREs." Science **304**(5669): 435-438.
Tymianski, M., M. P. Charlton, et al. (1993). "Source specificity of early calcium neurotoxicity in cultured embryonic spinal neurons." J Neurosci **13**(5): 2085-2104.
Tyzio, R., G. L. Holmes, et al. (2007). "Timing of the developmental switch in GABA(A) mediated signaling from excitation to inhibition in CA3 rat hippocampus using gramicidin perforated patch and extracellular recordings." Epilepsia **48 Suppl 5**: 96-105.
Ubach, J., X. Zhang, et al. (1998). "Ca2+ binding to synaptotagmin: how many Ca2+ ions bind to the tip of a C2-domain?" EMBO J **17**(14): 3921-3930.
Uchida, N., Y. Honjo, et al. (1996). "The catenin/cadherin adhesion system is localized in synaptic junctions bordering transmitter release zones." J Cell Biol **135**(3): 767-779.
Uesaka, N., S. Hirai, et al. (2005). "Activity dependence of cortical axon branch formation: a morphological and electrophysiological study using organotypic slice cultures." J Neurosci **25**(1): 1-9.
Ullian, E. M., K. S. Christopherson, et al. (2004). "Role for glia in synaptogenesis." Glia **47**(3): 209-216.
Ullian, E. M., K. S. Christopherson, et al. (2004). "Role for glia in synaptogenesis." Glia **47**(3): 209-216.
Ullian, E. M., S. K. Sapperstein, et al. (2001). "Control of synapse number by glia." Science **291**(5504): 657-661.
Ulrich, D. and B. Bettler (2007). "GABA(B) receptors: synaptic functions and mechanisms of diversity." Curr Opin Neurobiol **17**(3): 298-303.
Umbach, J. A. and C. B. Gundersen (1997). "Evidence that cysteine string proteins regulate an early step in the Ca2+-dependent secretion of neurotransmitter at Drosophila neuromuscular junctions." J Neurosci **17**(19): 7203-7209.
Umbach, J. A., K. E. Zinsmaier, et al. (1994). "Presynaptic dysfunction in Drosophila csp mutants." Neuron **13**(4): 899-907.
Ungewickell, E., H. Ungewickell, et al. (1995). "Role of auxilin in uncoating clathrin-coated vesicles." Nature **378**(6557): 632-635.
Uto, A., E. Dux, et al. (1994). "Effect of serum on intracellular calcium homeostasis and survival of primary cortical and hippocampal CA1 neurons following brief glutamate treatment." Metab Brain Dis **9**(4): 333-345.
Van Pelt, J., M. A. Corner, et al. (2004). "Longterm stability and developmental changes in spontaneous network burst firing patterns in dissociated rat cerebral cortex cell cultures on multielectrode arrays." Neurosci Lett **361**(1-3): 86-89.
van Pelt, J., I. Vajda, et al. (2005). "Dynamics and plasticity in developing neuronal networks in vitro." Prog Brain Res **147**: 173-188.
van Pelt, J., P. S. Wolters, et al. (2004). "Long-term characterization of firing dynamics of spontaneous bursts in cultured neural networks." IEEE Trans Biomed Eng **51**(11): 2051-2062.
van Vliet, E., L. Stoppini, et al. (2007). "Electrophysiological recording of re-aggregating brain cell cultures on multi-electrode arrays to detect acute neurotoxic effects." Neurotoxicology **28**(6): 1136-1146.
Varming, T., J. Drejer, et al. (1996). "Characterization of a chemical anoxia model in cerebellar granule neurons using sodium azide: protection by nifedipine and MK-801." J Neurosci Res **44**(1): 40-46.

Varoqueaux, F., G. Aramuni, et al. (2006). "Neuroligins determine synapse maturation and function." Neuron **51**(6): 741-754.
Varoqueaux, F., A. Sigler, et al. (2002). "Total arrest of spontaneous and evoked synaptic transmission but normal synaptogenesis in the absence of Munc13-mediated vesicle priming." Proc Natl Acad Sci U S A **99**(13): 9037-9042.
Verderio, C., A. Bacci, et al. (1999). "Astrocytes are required for the oscillatory activity in cultured hippocampal neurons." Eur J Neurosci **11**(8): 2793-2800.
Verderio, C., D. Pozzi, et al. (2004). "SNAP-25 modulation of calcium dynamics underlies differences in GABAergic and glutamatergic responsiveness to depolarization." Neuron **41**(4): 599-610.
Verhage, M. and J. B. Sorensen (2008). "Vesicle docking in regulated exocytosis." Traffic **9**(9): 1414-1424.
Vermeiren, C., M. Najimi, et al. (2005). "Acute up-regulation of glutamate uptake mediated by mGluR5a in reactive astrocytes." J Neurochem **94**(2): 405-416.
Vidal, L., B. Heller, et al. (1995). "Quantitation of dopaminergic neurons in 3-dimensional reaggregate tissue culture by computer-assisted image analysis." J Neurosci Methods **56**(1): 89-98.
Vissel, B., G. A. Royle, et al. (2001). "The role of RNA editing of kainate receptors in synaptic plasticity and seizures." Neuron **29**(1): 217-227.
Voets, T., R. F. Toonen, et al. (2001). "Munc18-1 promotes large dense-core vesicle docking." Neuron **31**(4): 581-591.
Voigt, T., H. Baier, et al. (1997). "Synchronization of neuronal activity promotes survival of individual rat neocortical neurons in early development." Eur J Neurosci **9**(5): 990-999.
Voigt, T., T. Opitz, et al. (2001). "Synchronous oscillatory activity in immature cortical network is driven by GABAergic preplate neurons." J Neurosci **21**(22): 8895-8905.
Voigt, T., T. Opitz, et al. (2005). "Activation of early silent synapses by spontaneous synchronous network activity limits the range of neocortical connections." J Neurosci **25**(18): 4605-4615.
Voisine, C., E. A. Craig, et al. (1999). "The protein import motor of mitochondria: unfolding and trapping of preproteins are distinct and separable functions of matrix Hsp70." Cell **97**(5): 565-574.
Volterra, A. and J. Meldolesi (2005). "Astrocytes, from brain glue to communication elements: the revolution continues." Nat Rev Neurosci **6**(8): 626-640.
von Gersdorff, H. and J. G. Borst (2002). "Short-term plasticity at the calyx of held." Nat Rev Neurosci **3**(1): 53-64.
von Gersdorff, H., E. Vardi, et al. (1996). "Evidence that vesicles on the synaptic ribbon of retinal bipolar neurons can be rapidly released." Neuron **16**(6): 1221-1227.
Wagenaar, D. A., J. Pine, et al. (2006). "An extremely rich repertoire of bursting patterns during the development of cortical cultures." BMC Neurosci **7**: 11.
Waites, C. L., A. M. Craig, et al. (2005). "Mechanisms of vertebrate synaptogenesis." Annu Rev Neurosci **28**: 251-274.
Wang, C., C. Shimizu-Okabe, et al. (2002). "Developmental changes in KCC1, KCC2, and NKCC1 mRNA expressions in the rat brain." Brain Res Dev Brain Res **139**(1): 59-66.
Wang, C. T., J. C. Lu, et al. (2003). "Different domains of synaptotagmin control the choice between kiss-and-run and full fusion." Nature **424**(6951): 943-947.

Wang, F., V. M. Weaver, et al. (1998). "Reciprocal interactions between beta1-integrin and epidermal growth factor receptor in three-dimensional basement membrane breast cultures: a different perspective in epithelial biology." Proc Natl Acad Sci U S A **95**(25): 14821-14826.

Wang, Y., M. Okamoto, et al. (1997). "Rim is a putative Rab3 effector in regulating synaptic-vesicle fusion." Nature **388**(6642): 593-598.

Washbourne, P., J. E. Bennett, et al. (2002). "Rapid recruitment of NMDA receptor transport packets to nascent synapses." Nat Neurosci **5**(8): 751-759.

Weaver, V. M., O. W. Petersen, et al. (1997). "Reversion of the malignant phenotype of human breast cells in three-dimensional culture and in vivo by integrin blocking antibodies." J Cell Biol **137**(1): 231-245.

Weber, T., B. V. Zemelman, et al. (1998). "SNAREpins: minimal machinery for membrane fusion." Cell **92**(6): 759-772.

Wei, W., N. Zhang, et al. (2003). "Perisynaptic localization of delta subunit-containing GABA(A) receptors and their activation by GABA spillover in the mouse dentate gyrus." J Neurosci **23**(33): 10650-10661.

Weimer, R. M., E. O. Gracheva, et al. (2006). "UNC-13 and UNC-10/rim localize synaptic vesicles to specific membrane domains." J Neurosci **26**(31): 8040-8047.

Weimer, R. M., J. E. Richmond, et al. (2003). "Defects in synaptic vesicle docking in unc-18 mutants." Nat Neurosci **6**(10): 1023-1030.

Weninger, K., M. E. Bowen, et al. (2008). "Accessory proteins stabilize the acceptor complex for synaptobrevin, the 1:1 syntaxin/SNAP-25 complex." Structure **16**(2): 308-320.

Westenbroek, R. E., L. Hoskins, et al. (1998). "Localization of Ca2+ channel subtypes on rat spinal motor neurons, interneurons, and nerve terminals." J Neurosci **18**(16): 6319-6330.

Wierenga, C. J., M. F. Walsh, et al. (2006). "Temporal regulation of the expression locus of homeostatic plasticity." J Neurophysiol **96**(4): 2127-2133.

Williams, K. (1993). "Ifenprodil discriminates subtypes of the N-methyl-D-aspartate receptor: selectivity and mechanisms at recombinant heteromeric receptors." Mol Pharmacol **44**(4): 851-859.

Wilson, N. R., J. Kang, et al. (2005). "Presynaptic regulation of quantal size by the vesicular glutamate transporter VGLUT1." J Neurosci **25**(26): 6221-6234.

Wintergerst, E. S., A. Faissner, et al. (1996). "The proteoglycan DSD-1-PG occurs in perineuronal nets around parvalbumin-immunoreactive interneurons of the rat cerebral cortex." Int J Dev Neurosci **14**(3): 249-255.

Wojcik, S. M., J. S. Rhee, et al. (2004). "An essential role for vesicular glutamate transporter 1 (VGLUT1) in postnatal development and control of quantal size." Proc Natl Acad Sci U S A **101**(18): 7158-7163.

Wu, M. N., T. Fergestad, et al. (1999). "Syntaxin 1A interacts with multiple exocytic proteins to regulate neurotransmitter release in vivo." Neuron **23**(3): 593-605.

Wulff, P., A. A. Ponomarenko, et al. (2009). "Hippocampal theta rhythm and its coupling with gamma oscillations require fast inhibition onto parvalbumin-positive interneurons." Proc Natl Acad Sci U S A **106**(9): 3561-3566.

Xia, Y. and G. W. Gross (2003). "Histiotypic electrophysiological responses of cultured neuronal networks to ethanol." Alcohol **30**(3): 167-174.

Xiang, G., L. Pan, et al. (2007). "Microelectrode array-based system for neuropharmacological applications with cortical neurons cultured in vitro." Biosens Bioelectron **22**(11): 2478-2484.

Xu, J., T. Mashimo, et al. (2007). "Synaptotagmin-1, -2, and -9: Ca(2+) sensors for fast release that specify distinct presynaptic properties in subsets of neurons." Neuron **54**(4): 567-581.

Xu, J., Y. Xu, et al. (2002). "Differential regulation of exocytosis by alpha- and beta-SNAPs." J Neurosci **22**(1): 53-61.

Yamashita, T., T. Hige, et al. (2005). "Vesicle endocytosis requires dynamin-dependent GTP hydrolysis at a fast CNS synapse." Science **307**(5706): 124-127.

Yao, J., A. Nowack, et al. (2010). "Cotrafficking of SV2 and synaptotagmin at the synapse." J Neurosci **30**(16): 5569-5578.

Yin, H., D. Turetsky, et al. (1994). "Cortical neurones with Ca2+ permeable AMPA/kainate channels display distinct receptor immunoreactivity and are GABAergic." Neurobiol Dis **1**(1-2): 43-49.

Ylinen, A., A. Bragin, et al. (1995). "Sharp wave-associated high-frequency oscillation (200 Hz) in the intact hippocampus: network and intracellular mechanisms." J Neurosci **15**(1 Pt 1): 30-46.

Ylinen, A., I. Soltesz, et al. (1995). "Intracellular correlates of hippocampal theta rhythm in identified pyramidal cells, granule cells, and basket cells." Hippocampus **5**(1): 78-90.

Yoshitaka Mukai, T. S. a. Y. J. (2003). "Continuous Monitoring of Developmental Activity Changes in Cultured Cortical Networks." Electrical Engineering in Japan **145**: 1481-1489.

Zamponi, G. W. (2003). "Regulation of presynaptic calcium channels by synaptic proteins." J Pharmacol Sci **92**(2): 79-83.

Zenisek, D., V. Davila, et al. (2003). "Imaging calcium entry sites and ribbon structures in two presynaptic cells." J Neurosci **23**(7): 2538-2548.

Zha, X. M., S. H. Green, et al. (2005). "Regulation of hippocampal synapse remodeling by epileptiform activity." Mol Cell Neurosci **29**(4): 494-506.

Zhang, H., W. L. Kelley, et al. (1999). "Mutational analysis of cysteine-string protein function in insulin exocytosis." J Cell Sci **112 (Pt 9)**: 1345-1351.

Zhang, H., W. L. Kelley, et al. (1998). "Cysteine-string proteins regulate exocytosis of insulin independent from transmembrane ion fluxes." FEBS Lett **437**(3): 267-272.

Zhang, X., M. J. Kim-Miller, et al. (2002). "Ca2+-dependent synaptotagmin binding to SNAP-25 is essential for Ca2+-triggered exocytosis." Neuron **34**(4): 599-611.

Zhang, X., J. Rizo, et al. (1998). "Mechanism of phospholipid binding by the C2A-domain of synaptotagmin I." Biochemistry **37**(36): 12395-12403.

Zhang, Z., J. Sun, et al. (2002). "A selective reduction in the relative density of parvalbumin-immunoreactive neurons in the hippocampus in schizophrenia patients." Chin Med J (Engl) **115**(6): 819-823.

Zhang, Z. J. and G. P. Reynolds (2002). "A selective decrease in the relative density of parvalbumin-immunoreactive neurons in the hippocampus in schizophrenia." Schizophr Res **55**(1-2): 1-10.

Zinsmaier, K. E., K. K. Eberle, et al. (1994). "Paralysis and early death in cysteine string protein mutants of Drosophila." Science **263**(5149): 977-980.

Zinsmaier, K. E., A. Hofbauer, et al. (1990). "A cysteine-string protein is expressed in retina and brain of Drosophila." J Neurogenet **7**(1): 15-29.

Zurich, M. G., C. Eskes, et al. (2002). "Maturation-dependent neurotoxicity of lead acetate in vitro: implication of glial reactions." J Neurosci Res **70**(1): 108-116.